

CLIC5A-Dependent Regulation of ERM Proteins Phosphorylation

by

Abass Mohammad Theeb Al-Momany

A thesis submitted in partial fulfillment of the requirements for the

degree of

Doctor of Philosophy

Department of Physiology

University of Alberta

© Abass Al-Momany, 2015

Abstract

The kidneys regulate total body fluid volume, acid-base status, and electrolyte composition through the filtration of large amounts of plasma by glomerular capillaries, followed by selective reabsorption of solutes and water by renal tubules. To sustain filtration, the hydraulic pressure within glomerular capillaries is much higher than in other systemic capillaries. While the glomerular capillary wall is extremely water permeable, it is nearly impermeable to larger plasma proteins. This “permselectivity” is attributed to the highly specialized nature of the glomerular capillary wall, which consists of three layers: glomerular endothelial cells, basement membrane and podocytes. The podocytes are specialized epithelial cells that wrap primary and secondary actin-based projections around the exterior of the glomerular capillary loops. They counteract the high intracapillary pressure, and they contribute significantly to the size-selective retention of plasma proteins in the capillary lumen. This thesis explores the role of CLIC5A (chloride intracellular channel 5A) in regulating the structure and function of podocytes.

Our laboratory previously reported that CLIC5A mRNA is nearly 800-fold more abundant in renal glomeruli than in other tissues. This level of enrichment suggested a specialized function of CLIC5A in glomeruli. CLIC5A belongs to a family of highly conserved proteins (CLICs) that associate reversibly with lipid bilayers. CLICs are often found in the same location as ERM (ezrin, radixin, moesin) proteins, and deletion of some CLICs can functionally mimic the deletion of specific ERM proteins. ERM proteins connect the cytoplasmic domain of integral membrane proteins to cortical actin, and consequently shape and control the cell cortex.

Even though a functional interaction between CLICs and ERM proteins had been

postulated, a mechanism had not been described. Studies underlying this thesis revealed that ectopic expression of CLIC5A in COS-7 and HeLa cells, which do not express CLIC5A at baseline, significantly increased ezrin and moesin phosphorylation and their association with the actin cytoskeleton. CLIC5A expression also induced the formation of apical membrane projections, accompanied by increased actin polymerization. Since ERM protein phosphorylation indicates ERM activation, I was able to conclude that CLIC5A expression results in ERM protein activation and consequent cell-surface remodeling.

ERM proteins can exist in an inactive, auto-inhibited form due to interactions between their N- and C-termini. PI(4,5)P₂ docking, which is a required first step in ERM activation, produces a conformational change that allows binding of the ERM N-terminus to integral membrane proteins and the C-terminus to F-actin. PI(4,5)P₂ docking also exposes a highly conserved Thr residue in the ERM C-terminus that is then phosphorylated, stabilizing the activated form.

I observed that ectopic expression of CLIC5A increased PI(4,5)P₂ production in clusters at the apical membrane and that silencing of endogenous PI4P5K α inhibited CLIC5A-dependent ERM protein activation. HA-PI4P5K α and - β as well as HA-PI5P4K α and - β were pulled from cell lysates by GST-CLIC5A, indicating that CLIC5A and PI(4,5)P₂ generating kinases can exist in the same complex.

In podocytes, *in vivo*, CLIC5A was localized to the apical domain of podocyte foot processes, and it co-localized strongly with ezrin, podocalyxin and NHERF2 in glomeruli. Ezrin was previously shown to couple podocalyxin to cortical F-actin, in part through the intermediary NHERF2. In CLIC5 deficient mice, ezrin phosphorylation and ezrin abundance in podocytes

were profoundly reduced, NHERF2 was uncoupled from the cytoskeleton, and podocalyxin abundance and electrophoretic mobility were altered. Furthermore, ultrastructural evaluation showed that podocyte foot processes were much broader and fewer in number in CLIC5 deficient mice when compared to wild-type mice. CLIC5 deficient mice also had microalbuminuria at baseline and they were more susceptible to Adriamycin-induced glomerular injury.

Thus, CLIC5A serves to activate ezrin at the apical domain of glomerular podocyte foot processes. Studies in COS-7 cells indicate that this CLIC5A effect is due to the localized production of PI(4,5)P₂ and involves activation of a PI4P5- or a PI5P4 kinase. In the absence of CLIC5A the podocyte Podocalyxin/NHERF2/Ezrin complex dissociates from cortical actin, associated with a reduction of the number of foot processes, microalbuminuria, and enhanced susceptibility to glomerular injury.

Preface

Author Contributions

Portions of chapter 3 and 4 has been published in *Journal of Cell Science*, 2014 **Abass Al-Momany**, Laiji Li, R. Todd Alexander and Barbara Ballermann, *Clustered PI4,5P2 accumulation and ezrin phosphorylation in response to CLIC5A*. J Cell Sci. 2014 Dec 15;127(24):5164-78.. Abass Al-Momany designed and performed all the experiments in chapter 3 and 4, and he prepared the first draft of the *Journal of Cell Science* paper for publication (including the figures and the legends). Dr Laiji Li prepared the different cDNA/Vector constructs of CLIC5A (including GFP-CLIC5A, CLIC5A mutants and GST-CLIC5A) used in this study, he provided the protocol for GST-Pulldown experiments and helped in data analysis. Dr R.Todd Alexander provided the PI(4,5)P2 reporter (GFP-and RFP-PH-PLC) and negative surface charge reporter (GFP-Kras). He also helped design and interpret PI(4,5)P2 and negative charge reporter assays. Dr Barbara J. Ballermann the principal investigator supervised the studies and prepared the final draft of the *Journal of Cell Science* paper for submission.

Portions of Chapter 5 have been published in a peer-reviewed journal: Binytha Wegner, **Abass Al-Momany**, Stephen C. Kulak, Kathy Kozlowski, Marya Obeidat, Nadia Jahroudi, John Paes, Mark Berryman, Barbara J. Ballermann, *CLIC5A, a component of the ezrin-podocalyxin complex in glomeruli, is a determinant of podocyte integrity*. American Journal of Physiology Renal Physiology (2010) 298:F1492-503. Abass Al-Momany performed all the experiments in chapter-4 of this thesis except figures (5.1, 5.2-B and 5.6). Figure 5.1-A and 5.1-B were prepared Mr Steve Kulak (laboratory technician), figure 5-2-B was done by the Ms Kathy Kozlowski (laboratory technician). Dr Mark Berryman prepared grid for TEM (Figure 5.1-C and 5-6 A and

C) and Dr Barbara Ballermann did the morphometric analysis (Figure 5.1-D and 5-6 B and D). Figure 5-6-E was done by Dr Binytha Wegner (Postdoctoral Fellow). Dr Barbara J. Ballermann, the principal investigator, designed the experiments, supervised the studies and prepared the final draft of the American Journal of Physiology paper for the submission.

Dedication

I lovingly dedicate this thesis to my big family who supported me each step of the way and without whose endless support none of this would be possible. I will always appreciate all you have done to me.

Acknowledgements

First, I would like to acknowledge my supervisor Dr. Barbara J Ballermann for giving me the chance to join her laboratory and make my dream come true. Thanks Dr. Ballermann for your help, guidance, patience, and support during the last six years. Dr. Ballermann has been perfect scientist for me to learn from. Since day one in her lab, Dr. Ballermann guided me through a variety of experiences, how to design and perform my experiment, analyze my results and she was always there to provide me with the feedback to promote excellence in my project. Special thanks for my Supervisory Committee members Dr. R. Todd Alexander and Dr. Sarah Hughes for their thoughtful mentoring, time and their helpful comments throughout my study.

My sincere thanks to my past and present colleagues in Ballermann Lab: Dr Laiji Li our Research Associate and Lab Manager for his friendship, support and guidance over the past 6 years, Mr. Steve Kulak our previous technician for being there for me whenever I needed you and your endless help and support especially during the first 2 years in lab. I would like also to thank Marya Obeidat (Ph.D. Candidate) and Mahtab Tavasoli (Ph.D. student) for their friendship and support.

I would like to acknowledge the financial support of the funding agencies that have supported my project: The Canadian Institutes For Health Research (CIHR), The Kidney Foundation of Canada, and the Division of Nephrology-University of Alberta

Finally, I am also grateful to my love Ensaf and my lovely kids Kareem and Nadeen. You supported me in pursuing challenges in my study unconditionally, and with that freedom to become who I would like to be. I truly appreciate your love, support and patience.

Table of Contents

Chapter 1. Literature Review, Hypothesis and Objectives.....	1
1- Introduction.....	2
1.1 Chloride Intracellular Channels (CLICs).....	2
1.1.1 CLIC1.....	4
1.1.2 CLIC2.....	6
1.1.3 CLIC3.....	6
1.1.4 CLIC4.....	7
1.1.5 CLIC5.....	9
1.1.6 CLIC6 (Parchorin).....	11
1.2 Band 4.1 superfamily.....	13
1.2.1 The ERM Protein Family.....	14
1.2.1.1 Structure and binding partners of ERM proteins.....	15
1.2.1.2 Regulation of ERM proteins activity.....	18
1.2.1.3 ERM proteins functions.....	22
1.2.1.3.1. ERM proteins maintains epithelial cell morphology and integrity.....	22
1.2.1.3.2. ERM proteins signaling pathways.....	23
1.2.1.3.3- Cell-matrix and cell-cell adhesion.....	24

1.3 Phosphoinositides.....	25
1.3.1 The PI4P5K family of enzymes.....	30
1.3.1.1 PI4P5K α	30
1.3.1.2 PI4P5K β	31
1.3.1.3 PI4P5K γ	31
1.3.2 Regulation of PI4P5K activity.....	33
1.4 The Kidney: Anatomy and Physiology.....	35
1.5 The Glomerular Capillary Wall.....	37
1.5.1 Fenestrated glomerular endothelium.....	38
1.5.2 The glomerular basement membrane (GBM)	41
1.5.2.1 Type IV collagen.....	41
1.5.2.2 Laminins.....	42
1.5.2.3 Heparan sulfate proteoglycans (HSPGs).....	42
1.5.2.4 Nidogen (Entactin).....	43
1.5.3 Podocytes.....	43
1.5.3.1 Protein complex defining the Podocyte–GBM interaction	44
1.5.3.1.1 α 3 β 1- integrin.....	44
1.5.3.1.2 Dystroglycan (DG).....	44

1.5.3.2 The podocyte slit diaphragm protein complex.....	47
1.5.3.2.1 Nephrin.....	47
1.5.3.2.2 Podocin.....	48
1.5.3.2.3 Neph proteins.....	48
1.5.3.2.4 FAT proteins.....	49
1.5.3.2.5 ZO-1.....	49
1.5.3.2.6 P-cadherin	50
1.5.3.2.7 CD2AP.....	50
1.5.3.3 The podocalyxin/NHERF2/ezrin complex at the apical domain of podocyte foot processes.....	51
1.5.3.4 The podocyte cytoskeleton.....	51
1.5.3.4.1 α -Actinin-4	52
1.5.3.4.2 Synaptopodin.....	52
1.6 Hypothesis and Objectives.....	54
Chapter 2. Materials And Methods.....	56
2.1 Cell culture, transfection and cell lysis	57
2.2 Reagents and antibodies	57
2.3 CLIC5A cloning.....	58
2.4 Cloning of CLIC5A mutants.....	59

2.5 Cytoskeleton preparation.....	60
2.6 Western blot (WB) analysis.....	60
2.7 Immunofluorescence microscopy and live cell imaging.....	61
2.8 Immunofluorescence microscopy of kidney sections	63
2.9 Scanning electron microscopy (SEM).....	64
2.10 siRNA knockdown.....	65
2.11 GST-CLIC5A construct, bacterial expression and protein purification.....	65
2.12 Staurosporine (SSP), Y-27632 and Calyculin A (CALA) treatment.....	66
2.13 Quantification of the rate of ERM protein de-phosphorylation	66
2.14 Treatment with the Cl ⁻ channel inhibitor (IAA-94) or the PLC activator m-3M3FBS	66
2.15 GST pull-down assay.....	67
2.16 Animal care.....	67
2.17 Isolation of mouse glomeruli and preparation of glomerular lysates	68
2.18 Immunoprecipitation.....	69
2.19 Transmission electron microscopy and morphometry.....	70
2.20 Adriamycin treatment.....	71

Chapter 3. CLIC5A enhances ERM proteins phosphorylation and association with the actin cytoskeleton.....	73
3.1 Introduction.....	74
3.2 Results.....	77
3.2.1 Increased ERM proteins phosphorylation in COS-7 cells expressing CLIC5A.....	77
3.2.2 Increased ERM proteins cytoskeletal association in COS-7 cells expressing CLIC5A.....	78
3.2.3 CLIC5A overexpression does not alter the half-life of ezrin in COS-7 cells.....	79
3.2.4 Actin polymerization and dorsal remodeling in CLIC5A-transfected COS-7 cells.....	79
3.2.5 CLIC5A N- and C-terminal deletion mutants fail to stimulate ERM proteins phosphorylation.....	80
3.2.6 CLIC1 and CLIC4 also enhance ERM protein phosphorylation.....	80
3.3 Discussion.....	82
3.4 Figures.....	87

Chapter 4. CLIC5A-stimulated ERM phosphorylation is mediated by dorsal phosphatidyl (4,5) bisphosphate clustering, a novel function independent of Cl^- channel activity.....95

4.1 Introduction.....	96
4.2 Results.....	99
4.2.1 PKC is the main kinase involved in ERM phosphorylation in COS-7 cells.....	99
4.2.2 CLIC5A does not alter the abundance of phosphorylated PKC.....	99
4.2.3 CLIC5A does not inhibit ERM phosphatases.....	100
4.2.4 The Cl^- channel inhibitor IAA-94 does not block CLIC5A-stimulated ERM phosphorylation.....	100
4.2.5 Re-organization of the plasma membrane surface charge distribution in COS-7 cells expressing CLIC5A.....	101
4.2.6 CLIC5A increases the abundance of PI(4,5)P2 in dorsal plasma membrane clusters.....	101
4.2.7 CLIC5A-stimulated ERM phosphorylation is mediated by PI(4,5)P2.....	102
4.2.8 Silencing of endogenous PI4P5K α reduces CLIC5A-stimulated ERM phosphorylation.....	103
4.2.9 PLC activation reduces CLIC5A and PI(4,5)P2 reporter association with the dorsal plasma membrane.....	104
4.2.10 CLIC5A co-localizes with PI4P5K α at the dorsal plasma membrane....	104

4.2.11 CLIC5A interacts with PI(4,5)P2 kinases <i>in vitro</i>	105
4.2.12 CLIC5A N- And C-terminal deletion mutants abrogate its membrane localization and PI(4,5)P2 clustering at the dorsal membrane.....	106
4.3 Discussion.....	107
4.4 Figures.....	116
Chapter 5. CLIC5A maintains the ezrin-dependent podocyte architecture <i>in vivo</i>.....	127
5.1 Introduction.....	129
5.2 Results.....	134
5.2.1 Localization of CLIC5A protein in glomerular podocytes and endothelial cells (ECs).....	134
5.2.2 Glomerular CLIC5A is a component of the ezrin-NHERF2-podocalyxin complex.....	134
5.2.3 Molecular abnormalities in glomeruli of CLIC5-deficient mice.....	135
5.2.3.1 Reduced phospho- and total ezrin abundance in glomeruli of CLIC5 ^{-/-} mice.....	135
5.2.3.2 Reduced association of NHERF2 with the cytoskeletal fraction in CLIC5 ^{-/-} mice.....	136
5.2.3.3 Reduced abundance and altered mobility of glomerular podocalyxin from CLIC5 ^{-/-} mice.....	137

5.2.4 Ultrastructural and functional abnormalities in Glomeruli of CLIC5 ^{-/-} mice.....	137
5.2.5 Increased susceptibility of CLIC5 ^{-/-} mice to Adriamycin-induced glomerular injury.....	138
5.2.5.1 Histological and ultrastructural characterization of Adriamycin nephropathy in CLIC5 ^{-/-} mice	138
5.2.5.2 Functional characterization of Adriamycin nephropathy in CLIC5 ^{-/-} mice	139
5.3 Discussion.....	140
5.4 Figures.....	146
Chapter 6. General discussion and future directions.....	155
6.1 General discussion.....	156
6.2 Future directions.....	159
6.2.1 Explore the nature of molecular and functional interaction between CLIC5A and PI(4,5)P2 generating kinases	159
6.2.2 The potential role of CLIC1, CLIC4 and CLIC5 in the mechanism for ERM protein phosphorylation in glomerular endothelial cells ,.....	162
6.2.3 Mechanism(s) regulating the CLIC5A-plasma membrane association	163
References.....	166

Appendices.....	231
1. Predicted phosphorylation sites for CLIC5A	231
2. Ethics approval for animal use protocol.....	232
3. Ethics approval for the use of human samples	233

List of tables

Table 1.1 Summary of CLIC family member distribution and protein partners.....	12
Table 3.1 Primer sequences used in the cloning of different CLIC5A constructs	59

Figures

<i>Figure 1.1. Structural domains and domain homology of the Merlin/ERM proteins</i>	17
<i>Figure 1.2. ERM protein regulation</i>	21
<i>Figure 1.3. Overview of PI(4,5)P2 functions</i>	28
<i>Figure 1.4. The network of interconversions between phosphoinositides</i>	29
<i>Figure 1.5. Regulation of PI(4,5)P2 and PIP3 Synthesis</i>	34
<i>Figure 1.6. Glomerular Filtration System</i>	40
<i>Figure 1.7. Anatomy of podocyte foot processes</i>	46
<i>Figure 3.1. Increased abundance of P-ERM in COS-7 and HeLa cells transfected with CLIC5A</i>	87
<i>Figure 3.2. Redistribution P-ERM in COS-7 cells transfected with CLIC5A</i>	88
<i>Figure 3.3. CLIC5A overexpression enhances ERM association with cytoskeleton</i>	89
<i>Figure 3.4. CLIC5A overexpression did not alter ezrin stability in COS-7 cells</i>	90
<i>Figure 3.5. Transfection of CLIC5A enhances the formation of actin based membrane projections</i>	91
<i>Figure 3.6. CLIC5A mutants fail to augment ERM phosphorylation</i>	93
<i>Figure 3.7. CLIC1 and CLIC4 overexpression also enhance ERM phosphorylation</i>	94

Figure 4.1. PKC is the main kinases involved in ERM phosphorylation in COS-7 cells and CLIC5A does not enhance PKC activity.....	116
Figure 4.2. CLIC5A does not block P-ERM protein dephosphorylation.....	117
Figure 4.3. The Cl ⁻ channel inhibitor IAA-94 does not alter CLIC5A-dependent ERM phosphorylation.....	118
Figure 4.4. Clustered dorsal PI(4,5)P ₂ accumulation in the presence of CLIC5A.....	119
Figure 4.5. Co-localization of the PI(4,5)P ₂ biosensor RFP-PH-PLC with GFP-CLIC5A.....	120
Figure 4.6. Abrogation of CLIC5A-dependent ERM phosphorylation by the PLC activator m-3M3FBS.....	121
Figure 4.7. PI4P5K α silencing abrogates CLIC5A-dependent ERM phosphorylation.....	122
Figure 4.8. Time-dependent loss of PI(4,5)P ₂ clusters and GFP-CLIC5A from the dorsal plasma membrane in response to m-3M3FBS treatment.....	123
Figure 4.9. Co-localization of CLIC5A with PI4P5K α	124
Figure 4.10. PI(4,5)P ₂ generating enzymes associate with CLIC5A.....	125
Figure 4.11. The effect of CLIC5A on ERM phosphorylation is abrogated by disruption of CLIC5A membrane association.....	126
Figure 5.1. CLIC5 protein expression in glomeruli.....	146
Figure 5.2. Glomerular CLIC5A is a component of the Ezrin-NHERF2-Podocalyxin complex.....	147

Figure 5.3. *Reduced P-ERM and total ezrin abundance in glomeruli podocytes of CLIC5^{-/-} mice*.....148

Figure 5.4. *CLIC5 deletion reduces NHERF2 association with actin cytoskeletal fraction.*.....149

Figure 5.5. *CLIC5 deletion reduces and alters podocalyxin migration*.....150

Figure 5.6. *Abnormal glomerular ultrastructure and function in CLIC5^{-/-} mice*.....151

Figure 5.7. *CLIC5 deletions enhance susceptibility to glomerular injury as a result of ADR administration*.....152

Figure 5.8. *CLIC5 deletion enhances susceptibility to glomerular injury*153

Figure 5.9. *Schematic model of CLIC5A function in glomerular podocytes*.....154

Figure 6.1. *Schematic model of the mechanism of CLIC5A-stimulated ERM phosphorylation.*158

Abbreviations and Symbols

aa	Amino Acid
AJ	Adherens Junctions
ARF	ADP-ribosylation factor
BSA	Bovine Serum Albumin
Cal A	Calyculin A
cDNA	Complementary DNA
CLIC	Chloride Intracellular Channel
CLIC5A	Chloride Intracellular Channel 5A
DAG	Diacylglycerol
Dmoesin	<i>D. melanogaster</i> moesin
EBP50	ERM Binding Protein 50
EC	Endothelial Cell
ERM	Ezrin/Radixin/Moesin protein
NHERF2	Sodium-hydrogen exchange regulatory cofactor
ERMAD	ERM Association Domain
FERM	Four-point-one, Ezrin, Radixin, Moesin

FAK	Focal Adhesion Kinase
F-actin	Filamentous Actin
GBM	Glomerular Basement Membrane
GFP	Green Fluorescent Protein
GFB	Glomerular Filtration Barrier
GST	Glutathione-S-Transferase
GPCR	G-protein Coupled Receptor
IAA-94	Indanyloxy Acetic Acid 94
IP3	Inositol 3,4,5 Trisphosphate
IP	Immunoprecipitation
IF	Immunofluorescence
KO	Knock Out
Kras	Kirsten rat sarcoma viral oncogene homolog
Merlin	Moesin, Ezrin, Radixin-like Protein
NF2	Neurofibromatosis 2
PA	Phosphatidic Acid
PBS	Phosphate Buffered Saline

PECAM-1	Platelet Endothelial Cell Adhesion Molecule-1
P-ERM	Phosphorylated ERM (on C-terminal Thr)
PH	Plextrin Homology domain
PI(4)P	Phosphatidylinositol 4, phosphate
PI(4,5)P2	Phosphatidylinositol 4,5 bisphosphate
PI(3,4,5)P3	Phosphatidylinositol 3,4,5 trisphosphate
PI4P5K	Phosphatidylinositol 4 phosphate 5 kinase
PI5P4K	Phosphatidylinositol 5 phosphate 4 kinase
PLC	Phospholipase C
PKA	Protein kinase A
PKC	Protein Kinase C
PLD	Phospholipase D
PM	Plasma Membrane
PTP	Protein Trosine Phosphatase
RFP	Red Fluorescent Protein
ROCK	Rho Associated Kinase
RPE	Retinal Pigment Epithelium

SAGE	Serial Analysis of Gene Expression
SEM	Scanning Electron Microscopy
siRNA	Small Interfering Ribo-Nucleic Acid
SSP	Staurosporine
TCA	Trichloroacetic Acid
T-Ezrin	Total Ezrin
TEM	Transmission Electron Microcopy
TGF- β 1	Transforming Growth Factor beta 1
VEGF	Vascular Endothelial Cell Growth Factor
WT	Wild Type

Prefixes

K	kilo (10^3)
m	milli (10^{-3})
μ	micro (10^{-6})
n	nano (10^{-9})

Units

L	liter
gm	gram
kDa	Kilo dalton
$^{\circ}\text{C}$	degree Celsius

Symbols

α	alpha
β	beta
γ	gamma

Chapter 1

Literature Review, Hypothesis

And Objectives

Chapter 1

1. Introduction

The function of differentiated cells *in vivo* almost always requires the development and dynamic maintenance of a very specific structure. For example, neurons send out axons and dendrites for cell-to-cell signal transfer, and renal proximal epithelial cells are covered on their apical surface by a dense array of microvilli, forming a large surface area for salt and water reabsorption. Glomerular podocytes develop complex actin-based projections that wrap around the exterior of glomerular capillaries, counteracting the physical force of the high intracapillary filtration pressure, while at the same time allowing for permselective filtration between the projections. The formation of specialized surface structures that protrude from the cell generally involves the organization of cortical actin and its attachment to integral membrane proteins by ERM (Ezrin, Radixin, Moesin) proteins. While the activation of ERM proteins is partially understood, how they become organized at very specific locations to shape the plasma membrane is still unclear. This thesis describes a novel role of the CLIC5A protein in the activation and apical clustering of ezrin in renal glomerular podocytes.

1.1 Chloride Intracellular Channels (CLICs)

The name “chloride intracellular channel” was first given to p64 when it was isolated from bovine kidney cortex, based on its affinity for IAA-94, a chloride channel inhibitor. There are 6 mammalian CLIC genes that produce 6 CLIC isoforms, and p64 is the CLIC5B isoform. The CLICs have ion conducting properties when they are inserted into artificial lipid bilayers, but their overall structures and inhibitor sensitivities differ markedly from the other classes of Cl⁻

channels. CLIC proteins are structural homologues of glutathione S-transferases (1), and are redox sensitive. The members of the CLIC family are expressed in most body tissues and cells. In cells, CLICs function both in the plasma membranes and in intracellular organelles. (1,2). CLICs also exist in invertebrates, for instance DmCLIC in *Drosophila melanogaster*, EXC4 and EXL1 in *Caenorhabditis elegans* (3,4) and AtDHAR1-4 in the plant *Arabidopsis thaliana* (5).

The CLIC family members display high degree of identity with aa sequence conservation among them of 67-88%. The C-termini of CLICs are highly conserved, while the N-termini of the proteins are different in both length and sequence (6,7). The CLIC proteins lack signal peptide sequences, but hydrophobic domains at the N- and C-termini mediate spontaneous association of the CLICs with lipid bilayers resulting in Cl⁻ channel activity (8,9). Metamorphic proteins can adapt more than one well-defined three-dimensional structure. In this regard, CLICs are considered metamorphic proteins, since they are redox-sensitive (10,11), and can change their three-dimensional structure under reduced and oxidized conditions. (12,13).

The CLICs are believed to function as intracellular Cl⁻ channels though the sequences of CLIC proteins do not look like the classical ion channel proteins which usually possess several membrane spanning domains. The primary structure of CLICs and the presence of single trans-membrane domain of their tertiary structure make them different from the classical ion channels. Whether CLICs normally function as bona fide Cl⁻ channels or perturb lipid bilayer to increase ion conductance *in vivo*, or whether they modify the activity of other Cl⁻ channels is still controversial (2,14)

The CLIC proteins can spontaneously associate with artificial lipid bilayers similar to bacterial pore forming toxins (15), annexins and the apoptotic proteins Bcl-2 family (16). Surface plasmon resonance (SPR) showed that the association to membrane between human

CLIC1 (4) and CLIC4 (17) and invertebrate CLIC-like proteins (Exc-4 and DmCLIC (4) is concentration dependent. Furthermore, the acidic pH and oxidizing conditions enhance membrane binding of these CLICs and CLIC-like proteins (18). When overexpressed in cells, CLIC proteins CLIC2 (19), CLIC4 (20,21), CLIC5A (22), CLIC5B (23,24) can also confer channel activity. Integration of CLICs to lipid bilayers is also dependent on membrane lipid composition. For instance, CLIC1 and CLIC4 can integrate and localize in cholesterol-rich region like caveolae (25).

The first identified CLIC p64 (CLIC5B) was isolated from kidney cortex microsomal membrane fractions using chloride channel inhibitor indanyloxy acetic acid 94 (IAA94) (23,26). CLIC5B was purified and found to mediate a Cl⁻ flux upon reconstitution in vesicles (27). Though this family is called a Cl⁻ channel, their ion selectivity is strongly divergent. Electrophysiological characterization of recombinant CLIC1, CLIC4 and CLIC5 by reconstituting them in artificial bilayers showed that they are either poorly selective for anions like CLIC1 (11), completely non-selective for anions, like CLIC4 (21) and CLIC5 (22), or that they cannot even differentiate between cations and anions, as observed for CLIC5 (11,21,22). Several members of CLIC family interact with cytoskeletal components (25,28) and their ion channel activity can be inhibited by cytoskeletal F-actin. In this regard, the ion conductance of CLIC1 and CLIC5 are completely inhibited by polymerized F-actin, while that of CLIC4 was unaffected (22).

1.1.1 CLIC1

The CLIC1 (NCC27) was initially identified by Breit and coworkers. Overexpression of CLIC1 in CHO-K1 cells resulted in Cl⁻ channel activity in plasma and nuclear membranes (29). Purified recombinant CLIC1 can function also as Cl⁻ channel *in vitro* (30). The expression and

activity of CLIC1 varied with the cell cycle, indicating that it is involved in the regulation of cell-volume and the passage through cell cycle (31). CLIC1 expression and activity is highly up-regulated during cell cycle and cell treatment with Cl⁻ channel inhibitor IAA-94 arrests the cells cycle (32), indicating the importance of CLIC1 in cell cycle regulation.

CLIC1 is widely expressed and localized at the apical domain of simple columnar epithelia including the glandular stomach, small intestine, colon, bile ducts, pancreatic ducts, airway, epididymis and renal proximal tubule. CLIC1 expression shows also a non-polarized distribution in the basal epithelial cell layer of stratified squamous epithelium of the upper gastrointestinal tract and the basal cells of the epididymis, and is present diffusely in skeletal muscles cells (33). CLIC1 is also expressed in luminal and glandular epithelium of human endometrium and its distribution is altered in the proliferative and secretory phase (34). In Alzheimer's disease, brain β -amyloid protein stimulates the translocation of CLIC1 from cytoplasm to plasma membrane and induces a Cl⁻ channel activity in microglia (35). CLIC1 expression was also significantly increased in human glioblastomas relative to normal brain tissues and lower CLIC1 expression was associated with better survival (36). Also, CLIC1 is highly expressed in macrophages and CLIC1^{-/-} animals exhibit impaired phagosomal acidification of about 0.2 pH units, similar to the effect of a Cl⁻ channel inhibitor observed in the macrophages of wild-type animals (37). These findings were interpreted to indicate that CLIC1 might play an important role in the acidification process of phagosomes.

Despite the fact that CLIC1 is widely expressed and distributed in body tissues, CLIC1 deficient animals (CLIC1^{-/-}) are viable although they have a mild bleeding disorder (38), suggesting a potential functional redundancy between the different members of the CLIC family.

1.1.2 CLIC2

CLIC2 is highly expressed in cardiac and skeletal muscle. Several studies show that CLIC2 binds directly and enhances the activity of the main calcium-release channels of sarcoplasmic reticulum (SR), known as Ryanodine Receptors 1 and 2 (RyR1 and RyR2) (39). The effect of CLIC2 on RyR1 and RyR2 can be inhibited by using CLIC2 antibodies (2). CLICs are redox sensitive, and the interaction of CLIC2 with RyR1 and RyR2 is altered by the redox state of CLIC2 (39), suggesting that the redox state of the cell is involved in controlling the release of Ca^{+2} and hence muscle contraction.

The CLIC2 gene is located on chromosome region Xq28 (40,41). Mutation in this region is associated with mental retardation and X-linked epilepsy. Mutation in CLIC2 results in hyperstimulation of RyR channels; with the channels remaining open for longer times and subsequently increasing Ca^{+2} release and signals dependent on RyR channel activity. The excessively active RyRs causes abnormal cardiac function and potentiates post-synaptic pathways and neurotransmitter release. This is associated with X-linked intellectual disability (ID), atrial fibrillation, cardiomegaly, congestive heart failure (CHF), and seizures (42)

1.1.3 CLIC3

CLIC3 was initially identified based on its ability to bind with the COOH tail of extracellular signal-regulated kinase7 (ERK7) using a two-hybrid screen. Northern blot analysis suggests that CLIC3 is highly expressed in placenta and somewhat less in lung and heart, whereas skeletal muscle, kidney, and pancreas show a minimal expression (8). When overexpressed in COS, CV-1, or A2780 human ovarian cancer cells, CLIC3 localized in nuclei, endosomes, and lysosomes (8,43). Electrophysiological characterization showed that overexpression of CLIC3 in LTK cultured fibroblast cells induced Cl^- channel activity (8).

CLIC3 is involved in endosome trafficking and recycling of cell surface receptor proteins. The Small GTPase, Rab25 plays an important role in priming the endosome containing active $\alpha 5\beta 1$ integrin. In cells expressing Rab25, CLIC3 up-regulation resulted in the acidification of endosomes, a process that is necessary for recycling of $\alpha 5\beta 1$ integrin containing endosomes to the plasma membrane (43). Furthermore, CLIC3 is necessary for phagosome-lysosome fusion; a process that is necessary for killing pathogens (44). CLIC3 is also required for cell migration and knockdown of CLIC3 in A2780 cell line stably expressing either Rab25 (A2780-Rab25) or a control vector (A2780-DNA3) reduces the migration rate relative to control cells.

CLIC3 was detected in several types of ovarian tumors including serous, endometrioid, clear cells and mucinous carcinoma and in pancreatic ductal adenocarcinoma. Interestingly, CLIC3 knock down reduces the invasiveness of Rab25 expressing A2780 cells into Matrigel (43), suggesting a potential role for CLIC3 in cancer metastasis.

1.1.4 CLIC4

CLIC4 was the first homologue of a bovine kidney intracellular chloride channel (p64) discovered (45). It is widely expressed in several body tissues including lung, brain, liver, kidney, and skin (46). CLIC4 localized to different cellular organelles including Golgi apparatus in pancreatic cells, endoplasmic reticulum (ER) in rat hippocampal HT-4 cells, and large dense core vesicles in neurosecretory cells (20,40,47). In addition to being associated with intracellular organelles, CLIC4 is also associated with dynamic actin-based membrane projection like membrane ruffles and lamellipodia and it interacts with dynamin I, actin, tubulin, and 14-3-3 proteins in neuronal cells (25).

The CLIC4 is involved in many biological processes. For instance, the invertebrate CLIC

homologue EXC4 plays a role in the formation of the excretory cell of *C. elegans*, potentially by enhancing the fusion and acidification of vacuoles involved in tube formation. The mutation in EXC4 results in the formation of large cyst instead of an excretory canal (3). Furthermore, CLIC4 regulates endothelial cell proliferation and morphogenesis and it is up-regulated during capillary network formation, sprouting and lumen formation in HUVECs (48)

In cultured endothelial cells, CLIC4 is up-regulated during tube formation (49), indicating that CLIC4 is directly involved in this process, and knockdown of CLIC4 greatly reduced the ability of these cells to form tubes (48). In CLIC4 deficient animals (CLIC4^{-/-}), the ability to form new blood vessels was significantly decreased relative to WT control. In cultured endothelial cells from CLIC4^{-/-} there was defective vacuolization and accumulation of unfused vacuoles. A similar phenotype was observed by treating the cells with the Cl⁻ channel inhibitor IAA-94 or proton pump inhibitor Bafilomycin. In CLIC4^{-/-}-derived endothelial cells there was impaired acidification of intracellular vacuoles indicating the importance of CLIC4 in the acidification process of the vacuoles (48).

CLIC4 is also involved in apoptosis; overexpression of CLIC4 caused changes in membrane potential, release of cytochrome C and caspase activation (50). TGF-β1 treatment stimulates nuclear localization of CLIC4 and the process appears to be important for the pro-apoptotic role of CLIC4 (51). Furthermore, CLIC4 is involved in the formation and maintenance of the integrity of apical cortex in epithelial cells. CLIC4 is highly expressed and co-localizes with ERM protein ezrin in the apical microvilli of retinal pigment epithelium (RPE) and suppressing the expression of CLIC4 in rat retina results in loss of apical microvilli, reduced retinal adhesion, epithelial-mesenchymal transition and severe dysplasia in neighboring neuronal retinas (52). In kidney, CLIC4 is highly expressed in renal proximal tubule cells, glomerular

endothelial cells and peritubular capillaries. CLIC4^{-/-} mice are small in size and they have smaller kidneys with fewer glomeruli and less dense peritubular capillary networks relative to the WT. Functionally, CLIC4^{-/-} show increased proteinuria and increased vulnerability to folic acid-induced acute kidney injury (53), suggesting the crucial role of CLIC4 in maintain the structural and functional integrity of kidney.

1.1.5 CLIC5

CLIC5 is transcribed from two alternative exons 1 (A and B) producing 32 KDa CLIC5A (251 aa) and the 49 KDa isoform CLIC5B (410 aa). CLIC5A was initially identified in GST-pull-down assay from extracts of placental microvilli using ERM protein ezrin COOH domain as bait. (28). CLIC5A is widely expressed in body tissues. In this regard, Northern blot analysis showed that CLIC5A is expressed in heart, skeletal muscles, kidney, lungs and placenta (28), whereas CLIC5B was found in avian osteoclast (54,55). When CLIC5A was overexpressed it localized to microvilli and a substantial portion became resistant to detergent extraction and remained associated with actin cytoskeleton (56).

The electrophysiological characterization of CLIC5A showed that it can induce Cl⁻ channel activity, and this activity is inhibited by F-actin and by the Cl⁻ channel inhibitor IAA-94 (22). In wild-type mice, CLIC5 is highly expressed and co-localized with the ERM protein radixin in both cochlear and vestibular hair cell stereocilia, where it plays a role in maintaining the interaction between actin cytoskeleton and plasma membrane proteins. Similarly, in hair cells of the chicken utricle, CLIC5 is expressed with radixin at 1:1 ratio (57).

CLIC5 deficient mice (CLIC5^{-/-}) (also called jitterbug) result from a spontaneous recessive mutation of the CLIC5 gene. In the inner ear hair cells of CLIC5^{-/-} mice, radixin abundance is reduced compared to that observed in wild-type mice, and the stereocilia progressively degenerate

leading to impaired hearing and deafness by 7 months of age (57). Interestingly, a similar phenotype is associated with mutations leading to radixin deficiency (58).

In human, a homozygous nonsense mutation of CLIC5 is also associated with autosomal recessive hearing impairment (arNSHI). Mutation analysis of CLIC5 revealed a homozygous nonsense mutation c.96T4A (p.(Cys32Ter)) that segregated with the hearing loss. Similar to CLIC5^{-/-} mice, the hearing loss in affected patients starts in early childhood and proceeds from mild to severe before the second decade. This impaired hearing is also accompanied by vestibular areflexia and with mild renal dysfunction (59).

In kidneys, CLIC5A is highly expressed in podocyte and endothelial cells of renal glomeruli (60). Each podocyte forms several actin based extensions called foot processes, spanning between these processes is a nephrin based filtration slit diaphragm. The slit diaphragm along with the glomerular basement membrane and glomerular endothelial cells form the glomerular filtration barrier, which prevents large molecular weight compounds from diffusing into urine (61).

The sialoglycoprotein podocalyxin is localized at the podocyte apical membrane where it interacts with the actin cytoskeleton via ERM protein ezrin and the scaffolding protein NHERF2. The CLIC5A, podocalyxin, NHERF2 and ezrin localize to the podocyte foot processes and are essential for keeping normal permselectivity function of the kidney. The CLIC5^{-/-} mice show baseline micro-albuminuria and they are more susceptible to kidney injury than wild-type mice. TEM examination reveals broadened podocytes and vacuolization of endothelial cells in CLIC5^{-/-} mice indicating that CLIC5 plays a crucial role in maintaining both structure and function of glomerular capillary wall (60,62).

Several reports have confirmed the importance of Chloride Intracellular Channel 5B

(CLIC5B) in bone resorption by osteoclasts (54,55). CLIC5B knock-down using antisense oligonucleotides resulted in decreased bone resorption in differentiating osteoclasts and the membrane vesicles from cells in which CLIC5B had been suppressed showed an acidification defect, postulated to reflect decreased Cl^- influx. CLIC5B can be phosphorylated by Src-family tyrosine kinases and this phosphorylation activates the channel activity of CLIC5B (63). Suppression of c-Src in differentiating osteoclast abrogates the co-localization of CLIC5B with the H-ATPase (54).

1.1.6 CLIC6 (Parchorin)

CLIC6 is the longest identified member of the CLIC family with 704 amino acid residues. CLIC6 has two different isoforms: CLIC6A and CLIC6B encoding 704 and 687 amino acids respectively. Both of these forms have a single trans-membrane domain. Northern blot examination showed that CLIC6 is expressed in the lung, stomach, heart, muscle, brain, kidney testis and eyes. Immunofluorescence microscopy showed that overexpressed GFP-CLIC6 localizes in the cytoplasm and in the perinuclear area in COS-7 and MDCK cells (64). A yeast two-hybrid screen of a rat brain cDNA library found that CLIC6 interacts with the COOH tail of dopamine receptors D2R, D3R and D4R. GST-pull down assay showed that CLIC6 interacts with GST-D3R but not with the control GST (65).

CLIC6 can form a multimeric complex with G-protein coupled receptor (GPCR) and localize in water and hormone secreting cells (65). In the gastric mucosa, the content of parchorin increased after weaning, since the acid-secreting ability of the mammalian stomach is limited after birth until weaning, and subsequently is significantly increases after weaning (6). Similar to CLIC6, the H^+ -K-ATPase activity follows the same pattern of increased acid secretion in the rabbit stomach (66). In the mammary gland, the level of parchorin expression was

increased during the lactating period relative to the pregnant period. These data suggests a regulatory role for CLIC6 in water and hormone secretion, and the level of parchorin expression is correlated with the secretory ability of the exocrine glands.

CLIC Family Member	Subcellular Distribution	Protein Partners
CLIC1	Nuclear membrane, Cytoplasm, Plasma Membrane	ERM, Rac2 and RhoA
CLIC2	Membrane of the sarcoplasmic reticulum (SR)	Ryanodine Receptors 1 and 2
CLIC3	Nucleus, Endosomes, Lysosomes	Extracellular signal-regulated kinase7 (ERK7)
CLIC4	Nucleus, Mitochondria, Golgi, ER, Membrane Projections, Secretory vesicles	Ezrin, Dynamin I, Actin, Tubulin, and 14-3-3
CLIC5A	Cytoplasm, Membrane Projections	ERM
CLIC5B	Cytoplasm, intracellular membranes	Co-localize with H-ATPase
CLIC6/Parchorin	Cytoplasm and perinuclear area	Dopamine receptors (D2R), (D3R) and (D4R)

Table 1. Summary of CLIC family members distribution and protein partners.

1.2 Band 4.1 superfamily

The band 4.1 superfamily is a group of proteins characterized by the presence of a conserved FERM (Four-point-one, Ezrin, Radixin, Moesin) domain, which is about 300 amino acid in length, hydrophobic cysteine-rich, (67) and takes on a globular configuration (68).

The original prototype of this superfamily is the band 4.1 protein, which was originally identified as an 80 kDa constituent of red blood cell (RBCs) membranes and cytoskeleton. The band 4.1 protein interacts with the actin and spectrin cytoskeletal network in RBC, providing mechanical strength and plasticity crucial for the maintenance of shape and integrity of RBCs (69). Deficiency of band 4.1 protein results the clinical condition hereditary elliptocytosis in which the shape of RBC is abnormal (70), leading to congenital hemolytic anemia (71). The band 4.1R protein is also expressed in cerebellum granular cells and in the dentate gyrus of the hippocampus (72). Band 4.1R-deficient mice show impaired balance and coordination, consistent with cerebellar dysfunction, and insufficiencies in spatial learning and memory, that might be related to impaired function of the hippocampus (73).

The crystal structure of moesin and radixin suggests that FERM domains contain three lobes F1, F2 and F3 (74,75). FERM domains are located at the N-terminus of most proteins in the band 4.1 superfamily, including DAL-1, the ERMs (Ezrin, Radixin and Moesin), merlin, protein tyrosine phosphatases, the Janus Kinases, focal adhesion kinase, guanidine exchange factors and talin. FERM domains are also present at the C-terminus of the unconventional myosins VIIa and X. FERM domains can interact with several plasma membrane molecules including inositol containing membrane phospholipids, glycoporphins, CD44, ICAM-2 and the C-terminal domain of FERM-containing proteins (68) as well as actin (76,77).

The Band 4.1 superfamily members are usually distributed at the inner leaflet of the plasma

membrane of dynamic cell surface protrusion structure such as membrane ruffles, filopodia, lamellipodia and neurite extensions, where they are directly involved in the formation and stability of these cellular protrusion by controlling cytoskeleton dynamics. Furthermore, the FERM domain proteins also exist at cell-cell and cell-matrix adhesion points, where they modulate the signaling pathways involved in cell growth and differentiation (78).

1.2.1 ERM Protein Family

The ERM protein family belongs to the band 4.1 superfamily (79). In human ezrin, radixin and moesin are encoded by genes located on chromosome 6, 11 and 10 respectively (80). Many cultured cells express all three ERM proteins ezrin, radixin and moesin (81-83). However, *in vivo* ezrin is predominantly expressed in epithelial cells (81), radixin in hepatocytes (84), and cochlear stereocilia (85), while moesin is expressed in endothelial cells and leukocytes (86) .

The ERM proteins are involved in the formation of actin-dependent cell membrane protrusions such as microvilli, filopodia and lamellipodia by mediating the interaction between the cortical actin cytoskeleton and plasma membrane proteins. ERM proteins are critical for several physiological and morphological processes in cells including maintenance of cell-shape, regulation of membrane protein function, mitosis, epithelial morphogenesis and integrity, cell-extracellular matrix interactions, cell-cell communication, membrane transport and signal transduction. Furthermore, cell adhesion, transformation of cells and malignancy, as well as signal transduction events may depend on ERM proteins (87-90).

The ERM proteins are widely distributed in body tissues, and each family member exhibits distinctive distribution in different tissues. Ezrin was originally purified from intestinal microvilli. It is highly expressed in the placenta, stomach, lung and kidney and to lesser extent in the spleen. Ezrin is mainly localized in the dynamic structure of actin-rich membrane projections

of epithelial cells (81), while in Schwann cells ezrin is concentrated at the paranodal microvilli that extend into the Node of Ranvier (91). Ezrin knockout mice are viable, but they show a defect in villus morphogenesis and epithelial organization in the developing gastrointestinal tract leading to achlorhydria, failure to thrive past weaning and death at the age of 3 weeks (92).

Radixin was originally isolated from adherens junctions (AJ) in liver (84). It is widely distributed and highly expressed in body tissues including liver, kidney, ovary and bone marrow. Lower levels of expression are also observed in skin, colon, thymus and lung (93). Several reports showed that radixin is localized to AJ in the liver (84), microvilli (94), contractile rings (95), focal contacts and cleavage furrows in dividing cells (96). Radixin knockout mice are viable and look normal but they develop deafness and suffer from mild liver dysfunction characterized by hyperbilirubinemia (97,98).

Moesin was originally isolated from bovine uterine cells (99). Similar to ezrin and radixin, moesin is highly expressed in lung and spleen with lower levels of expression in the kidney (81). Moesin is also detected in macrophages and lymphocytes, as well as fibroblastic, endothelial, epithelial and neuronal cell lines. Immuno-fluorescence analysis shows that moesin is localized to cellular protrusions like filopodia, microvilli, and retraction fibers (100). Moesin knockout mice appear normal and are viable (101), suggesting a potential functional redundancy between the different members of ERM proteins family when they are co-expressed. This is most likely due to high level of similarities between their sequences and three-dimensional structures.

1.2.1.1 Structure and the binding partners of ERM proteins

The ERM protein family members have a high degree of sequence and structural identities. They share an N-terminal FERM domain, a central alpha-helical domain and a C-terminal domain that contains an actin-binding motif. The C-terminal domain comprises the last 34

amino acids, is highly conserved among the different members of ERM proteins and interacts with F-Actin directly (Figure 1.1) (102), suggesting a cross linker function between F-actin and plasma membrane protein.

The FERM domain of ERM proteins can directly bind to inositol-containing plasma membrane lipids, mainly phosphatidylinositol-4,5-bisphosphate (PI(4,5)P2) (103), and the cytoplasmic tail of membrane proteins like CD44 (104-106), CD43 (107-109), ICAM-1 and ICAM-2 (109-112), as well as the sodium-hydrogen exchanger 1/NHE1 (113). Furthermore, the FERM domain of ERM proteins can interact with membrane proteins indirectly through PDZ domain-containing scaffolding proteins EBP50 (ERM binding protein of 50 kDa, also known as NHERF1) and NHE3 kinase A regulatory protein (E3KARP, or NHERF2) (114-117).

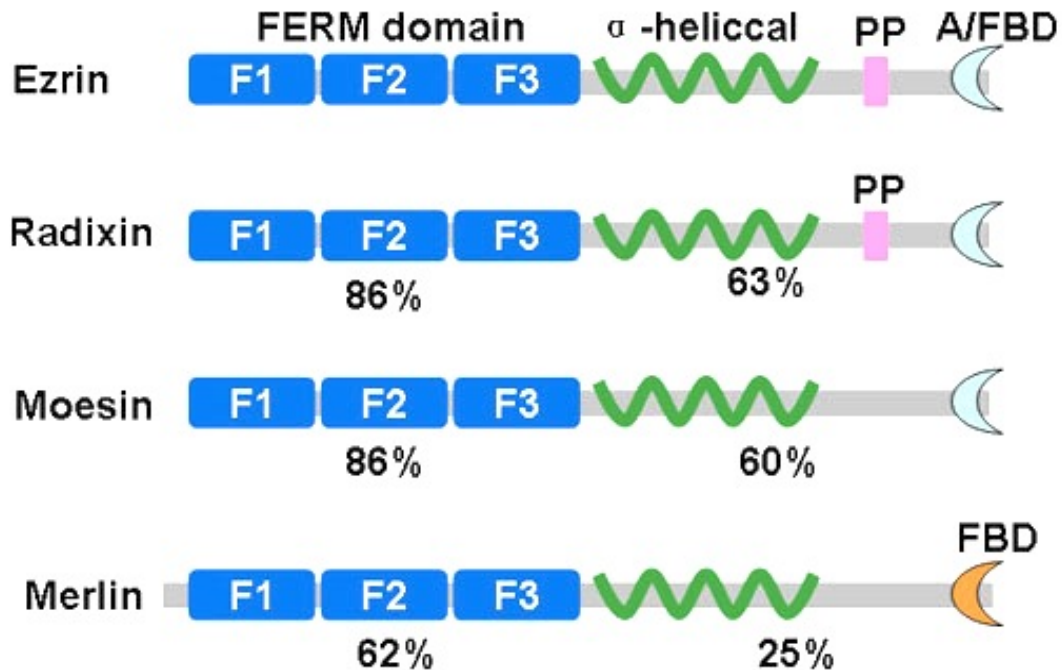


Figure 1.1 Structural domains and domain homology of the Merlin/ERM proteins.

The amino acid sequence-based domain structure of ERM proteins shows a high degree of similarity, whereas Merlin is more divergent. ERM proteins share a C-terminal F-actin binding domain (A/FBD: actin/FERM binding domain), but Merlin does not. The domain between the FERM domain and C-terminal ERM association domains (C-ERMAD) form an alpha-helical coiled-coil (green). Ezrin and Radixin have a proline-rich region (PP). (From Yu H1, Zhang Y, Ye L, Jiang WG. *Front Biosci (Landmark Ed)*. 2011 Jan 1;16:1536-50).

1.2.1.2 Regulation of ERM proteins activity

The ERM proteins can exhibit two different conformations: the closed, inactive (or dormant) conformation that results from intra- or inter-molecular association between N- and C-terminal ERM association domains (ERMAD). This interaction masks the binding sites for plasma membrane proteins at the N-terminal FERM domain, and the F-actin binding site at the C-terminus. By contrast, in the open, active conformation, binding motifs for plasma membrane protein and F-actin, at the N-terminal FERM and C-termini respectively are exposed (90).

The change between the active and inactive conformation of the ERM proteins is regulated by PI(4,5)P2 and by phosphorylation of C-terminal threonine (Figure 1.2). Several reports show that the FERM domain of ERM protein binds to PI(4,5)P2 (103). The interaction of ezrin with PI(4,5)P2 enhances its binding to the cytoplasmic tail of CD44 (105), ICAM-1 and ICAM-2 (112), and the interaction of moesin with PI(4,5)P2 enhances its binding to CD93 (118). Site-directed mutagenesis of the basic amino acid lysine at K63, K64, K253, K254, K262 and K263 in the FERM domain of ezrin abrogates PI(4,5)P2 binding and plasma membrane localization (119). Conversely, overexpression of PI4P5 kinases, which generate PI(4,5)P2, results in increased ERM phosphorylation, cytoskeletal association and the formation of membrane projections (120). Depletion of PI(4,5)P2 by phospholipase C (PLC), by the PLC activator m-3M3FBS, reduced the abundance and association of ERM proteins with actin cytoskeleton (121,122). Taken together, these findings suggest that the interaction of ERM protein with PI(4,5)P2 is required for their association with their protein partners.

The binding of PI(4,5)P2 to the FERM domain most likely reduces its affinity for the ERM C-terminus. In this regard, phosphorylation of ezrin at Thr567 must be preceded by PI(4,5)P2 binding to the FERM domain, implying that PI(4,5)P2 binding and Thr phosphorylation steps act

in a sequential manner to activate ezrin (123). Osmotic cell shrinkage activates ERM proteins through a shrinkage-induced increase in membrane PI(4,5)P₂ levels (124). Phosphorylation of the C-terminus of ERM proteins at the conserved Thr residue in the actin binding site (T567 in ezrin, T564 in radixin, T558 in moesin) results in the localization of these proteins to the actin-rich membrane extensions (125-128), and increase in their association with the cytoskeletal fraction (129,130). Overexpression of phospho-mimic ezrin Thr567D mutant induces the formation of actin based cellular projections like lamellopodia, membrane ruffles and microvilli. In contrast, the un-phosphorylatable mutant of ezrin (Thr567A) is poorly associated with the cytoskeleton (129). Similarly the translocation of ezrin from membrane to cytoplasm and collapse of microvilli in response anoxia or Fas ligand mediated apoptosis is associated with its dephosphorylation (131,132). These findings suggest that regulated dephosphorylation of ERM proteins can also define their activity and their association with the cytoskeletal fraction.

Several kinases, including Rho kinase (133,134), PKC α (135), PKC θ (136,137), AKT (138), Nck-interacting kinase (NIK) (139), lymphocyte-oriented kinase (LOK) (140), and Mammalian STE-20 like kinase 4 (MST4) (141) can phosphorylate the ERM protein C-terminal Thr residue. This phosphorylation step is very important to stabilize the active/open conformation of the ERM protein and allows the interaction with their partners (137). ERM proteins can also be phosphorylated at other sites. For example, pRb-mediated senescence by cyclin dependent kinase 5 (cdk5) phosphorylates ezrin at Thr235 (142). Ezrin is also phosphorylated at tyrosine residues by the tyrosine kinase p56lck upon T lymphocytes activation (143), while EGF and HGF treatment of A431 carcinoma cell line and LLC-PK1 Kidney derived cell line phosphorylate ezrin at Tyr 145 and Tyr 353 respectively, inducing its redistribution to membrane ruffles and microvilli (144-146). In *D. melanogaster*, the Ste20-like

kinase (Slik) phosphorylates fly ERM ortholog, Dmoesin at Thr559 (147-149).

ERM protein dephosphorylation in response to anoxia and apoptosis also results in the collapse of microvilli and redistribution of ERM protein toward cytoplasm (150). The phosphatases involved in ERM dephosphorylation include myosin light chain phosphatase, which interacts with moesin through its myosin binding subunit (151), and potentially protein phosphatase 2C (PP2C), which can dephosphorylate purified Thr558 moesin (152).

Inactivation of ezrin also occurs by calpain-mediated cleavage in leukocytes upon stimulation with phorbol 12-myristate 13-acetate (PMA) (153,154) and leads to the dissociation of ezrin from its associated plasma membrane binding partner(s) and from the actin cytoskeleton.

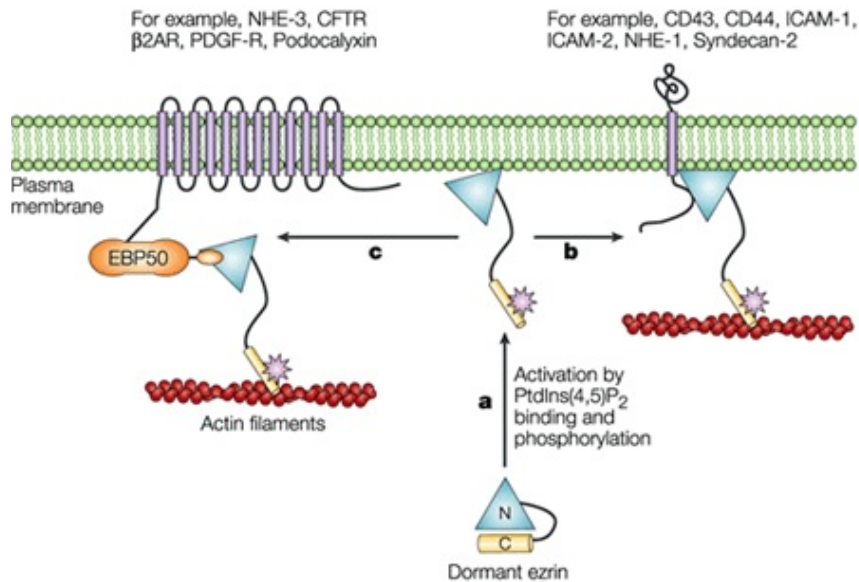


Figure 1.2 *ERM protein regulation.* In the dormant state, the N- and C-termini associate with one another to form an auto-inhibited conformation. PI(4,5)P₂ binding to the N-terminus releases this inhibitory interaction resulting in activation. (From Anthony Bretscher, Kevin Edwards and Richard G. Fehon, *Nature Reviews Molecular Cell Biology* **3**, 586-599, 2002, with permission).

1.2.1.3 ERM proteins functions

1.2.1.3.1. *ERM proteins maintain epithelial cell morphology and integrity*

The localization of ERM proteins at the apical domain of actin-based cellular projection suggests an important role in maintaining cell morphology and integrity. *In vivo* studies showed that Dmoesin is crucial for maintaining the integrity of the developing wing disc epithelium in *D. melanogaster*. Dmoesin loss of function mutants disrupt the morphology and integrity of epithelial cells which failed to express the epithelial marker for intercellular junctions, the apical basal polarity was lost and they were more susceptible to epithelial to mesenchymal transition (155,156). Similarly, during mitosis, Dmoesin is necessary for cortical stiffness to promote cell rounding, and loss of Dmoesin function in S2 cells results in several mitotic abnormalities in cell shape, mitotic spindle deformation, chromosome misalignment and delay of anaphase onset. These cells fail to undergo cortical retraction and show membrane blebbing. A similar phenotype is observed in depletion of SLIK, the kinase that phosphorylates Dmoesin, indicating the importance of phosphorylated Dmoesin in cortical contraction during mitosis (147,157).

The *C. elegans* ERM ortholog ERM-1 localizes to the luminal membrane of epithelial cells. Loss of the ERM-1 results in defects in the integrity of the developing intestinal epithelium leading to the formation of a cyst-like structure (158,159), indicating the critical role of ERM-1 in lumen morphogenesis *in vivo*. In mammals, the ezrin knock out results in abnormal fusion of intestinal villi (92), suggesting the role of ezrin in intestinal epithelial morphogenesis. In thymoma cells, ERM protein suppression by antisense oligonucleotide causes microvilli to disappear from the cell surface (160). Similarly ezrin knockdown in primary retinal pigment epithelium (PRE) results in complete disappearance of microvilli (161).

1.2.1.3.2. ERM proteins signaling pathways

Several studies have highlighted the role of ERM protein in Rho-GTPase signaling pathways and associated several cellular processes. RhoA stimulates Rho kinase (ROCK) to phosphorylate ERM proteins, causing their redistribution to the apical membrane of actin rich structure (128). For instance, in neurons Rho kinase (ROCK) phosphorylates ERM and induces the formation of filopodia associated with neurite growth (162). Rac 1, another member of Rho GTPase family is activated by phosphorylated ezrin leading to E-cadherin-dependent AJ assembly (163). Interestingly, ezrin localization to N-cadherin containing AJ is also regulated by Rac1 through PI4P5K activity. The relationship between ERM protein and Rho-GTPase family is bidirectional, since ERM also acts as upstream regulator of Rho GTPase by binding and inhibiting Rho-GDI, which inhibits the formation of active Rho-GTP (164). In another study, Speck *et al* showed that moesin negatively regulate the Rho signaling pathway involved in regulating epithelial polarity and integrity *Drosophila* flies (155).

The ERM protein have also been found to be involved in signaling pathways associated with cancer and tumor metastasis. Many studies have shown increased expression and/or activity of ERM proteins in metastatic tumors like osteosarcomas and rhabdomyosarcomas (165). It has been suggested that the increased expression and/or activation of ERM protein in metastatic tumors could be explained by the activation of the survival signal from the PI3K/AKT pathway and negative regulation of apoptosis. Ezrin is known to interact with the regulatory subunit of PI3K and the activation of PI3K/AKT signaling pathway requires ezrin phosphorylation on Tyr353 (166). On the other hand, ezrin acts as a negative regulator of Fas induced apoptosis (167). In addition ezrin and moesin (but not radixin) are involved in signaling pathways related to immunological synapse (IS) formation in leukocytes. The recognition of antigen-presenting

cells by T-cells is associated with the breakdown of microvilli, movement of CD43 away from, and recruitment of T-cell receptor to the IS site, steps that all are coordinated by ERM proteins (168-170).

1.2.1.3.3- Cell-matrix and cell-cell adhesion

The enrichment of ERM proteins at the cell-matrix and cell-cell adhesion sites suggest their potential role in the formation and maintaining these sites (96). Inhibition of ERM protein expression by antisense oligonucleotides resulted in reduced cell-matrix and cell-cell adhesion in thymoma and mouse epithelial cells (160). A similar phenotype was observed when ezrin expression was suppressed in human colorectal epithelial tumor cell lines (171). In contrast, overexpression of ezrin in insect cells SF9 increased cell adhesion to plastic or glass substratum (172). The initiation and assembly of focal adhesions is associated with recruitment of many membrane-linked protein like paxillin, vinculin, talin and alpha-actinin, and this step is associated with Rho-stimulated contractility and PI(4,5)P2 activation (173).

The importance of ERM protein in cell-cell and cell-matrix adhesion could be explained by the interaction between different members of ERM protein family and adhesion molecules. For instance, the ERM protein ezrin binds directly to a tumor suppressor hamartin that is involved in cell-matrix adhesion in Swiss 3T3 fibroblasts (174). Likewise, ICAM-1 and -2 (112), ICAM-3 (175), CD43 (176) and the hyaluronan receptor CD44 (104) that mediate cell-cell and cell-matrix adhesions, binds directly to the ERM proteins in several cells lines. The role of ERM protein in cell-matrix adhesion could be due to positive regulation of Rho-GTPase by ERM protein, which may enhance the Rho-mediated formation of focal adhesion (177).

1.3 Phosphoinositides

The phosphoinositides are inositol-containing membrane phospholipids. Differential phosphorylation of hydroxyl (OH) groups of the inositol ring of the phosphatidylinositol lipid (PI) produces distinct phosphoinositides, enriched in the inner leaflet of the plasma membrane which function as localized second messengers (178). In eukaryotic cells, phosphoinositide lipids represent about 10% of the total phospholipid pool. Phosphoinositide signaling pathways control several major cellular functions including cell growth, cytoskeleton rearrangements, proliferation, protein trafficking, focal adhesion formation, motility and pre-mRNA splicing (179-183). Abnormalities in phosphoinositide-dependent signals have been reported in several pathological disorders like cancer, diabetes and channelopathies (184-186). Furthermore, the phosphoinositide PI(4,5)P₂ plays a key role in gating of ion channels (187,188), exocytosis (189,190), and apoptosis (191,192) (Figure 1.3). PI(4,5)P₂ also is the main phospholipid involved in regulating the actin cytoskeleton. PI(4,5)P₂ enhances plasma membrane protein-actin interactions by activating ERM proteins. It also stimulates actin polymerization by enhancing the activity of WASP and WAVE family proteins that promote Arp2/3-mediated actin filament assembly, by inhibiting the actin filament barbed end capping proteins gelsolin and heterodimeric capping protein, and finally by inhibiting ADF/cofilin and twinfilin, which cause actin filament disassembly and actin monomer sequestering (193).

The phosphoinositide lipids localize to distinct sites within the cell, depending on their specific function. PI(4,5)P₂ is enriched in the plasma membrane, while PI(3)P is found on early endosomes. PI(3,5)P₂ is found on late endocytic organelles, while PI(4)P is in the trans Golgi network. PI(3,4,5)P₃ is normally not seen in quiescent cells, but becomes abundant in the plasma membrane upon stimulation with extracellular agonists (179). PI(4)P and PI(4,5)P₂

constitute about 1% and 0.25-0.5% of the phosphorylated phosphoinositides, respectively (194,195). The inter-conversion of phosphoinositide lipids is regulated by many phosphatases and kinases and it is known as canonical phosphoinositide cycle. During this cycle PI is phosphorylated by phosphatidylinositol 4-kinase (PI4K) at the 4th –OH group to become PI(4)P. This PI(4)P is the substrate for phosphatidylinositol 4, 5 bisphosphate-kinases (PI4P5K) that phosphorylate the 5th –OH group to produce PI(4,5)P₂. The PI(4,5)P₂ can also be produced by the action of PI(5)P₄ kinases that phosphorylate PI(5)P at the 4th –OH group (196-198). However, since PI(4)P is much more abundant than PI(5)P, it is believed that most of the PI(4,5)P₂ in the plasma membrane is produced by PI4P5K from PI(4)P (199).

Several enzymes dephosphorylate, and therefore regulate the cellular level of P(4,5)P₂. Phospholipase C (PLC) cleaves PI(4,5)P₂ forming the second messengers inositol 1,4,5-triphosphate (IP₃) and diacyl glycerol (DAG). IP₃ binds to specific receptors in the smooth endoplasmic reticulum (ER) increasing cytoplasmic Ca⁺² through the release of Ca⁺². Increased Ca⁺² and DAG lead to protein kinase C (PKC) activation. Ca⁺²-sensitive DAG kinase then phosphorylates DAG to produce phosphatidic acid (PA), resulting in a positive feedback loop, since PA enhances the activity of PIP5K generating PI(4,5)P₂, completing the cycle (200,201). PI(4,5)P₂ is also regulated by synaptojanin, which is a 5-phosphatase that hydrolyzes the 5-phosphate of PI(4,5)P₂, to produce PI(4)P (202) (Figure 1.4).

Accumulating evidence suggest that PI(4,5)P₂ itself can act as a second messenger by binding to-, and regulating the activity of many proteins and enzymes involved in signal transduction pathways. PI(4,5)P₂ is involved in actin cytoskeleton polymerization by interaction with cofilin and gelsolin and inhibits their actin severing activity and uncapping of actin filament barbed ends by binding to actin capping proteins (203). The PI(4,5)P₂ can also induce

conformational change and activation of the ERM proteins by binding to their N- terminal, hence, supports the interaction between F-actin and the cytoplasmic tail of PM proteins.

Depleting cellular PI(4,5)P2 by either microinjection of PI(4,5)P2 antibodies or overexpression of the PI(4,5)P2 hydrolyzing enzyme like synaptojanin, or enhancing the activity of PLC in cells results in reduced membrane ruffling, disorganization of actin stress fibers and dephosphorylation of ERM protein. In contrast, increasing PI(4,5)P2 levels promotes actin polymerization and microvillus formation and increased ERM protein phosphorylation (204,205)

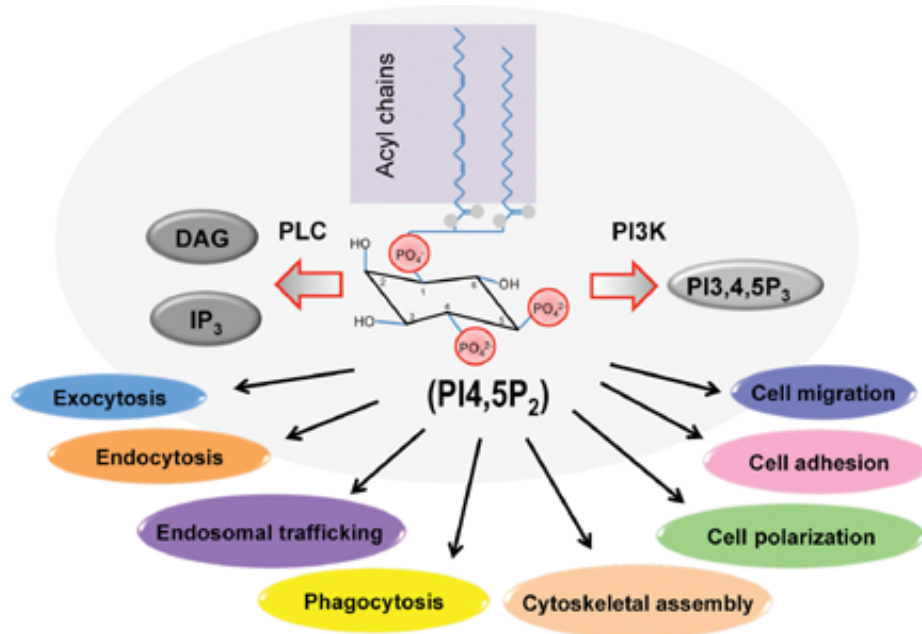


Figure 1.3 Overview of $PI(4,5)P_2$ functions. By enhancing actin cytoskeleton re-arrangements and plasma membrane protein-actin cytoskeleton interactions, $PI(4,5)P_2$ controls several cellular activities like shape, motility, membrane transport and attachment to the extracellular matrix and other cells. (From Yue Sun, Narendra Thapa, Andrew C. Hedman and Richard A. Anderson. *BioEssays* Volume 35, Issue 6, pages 513–522, 2013, with permission)

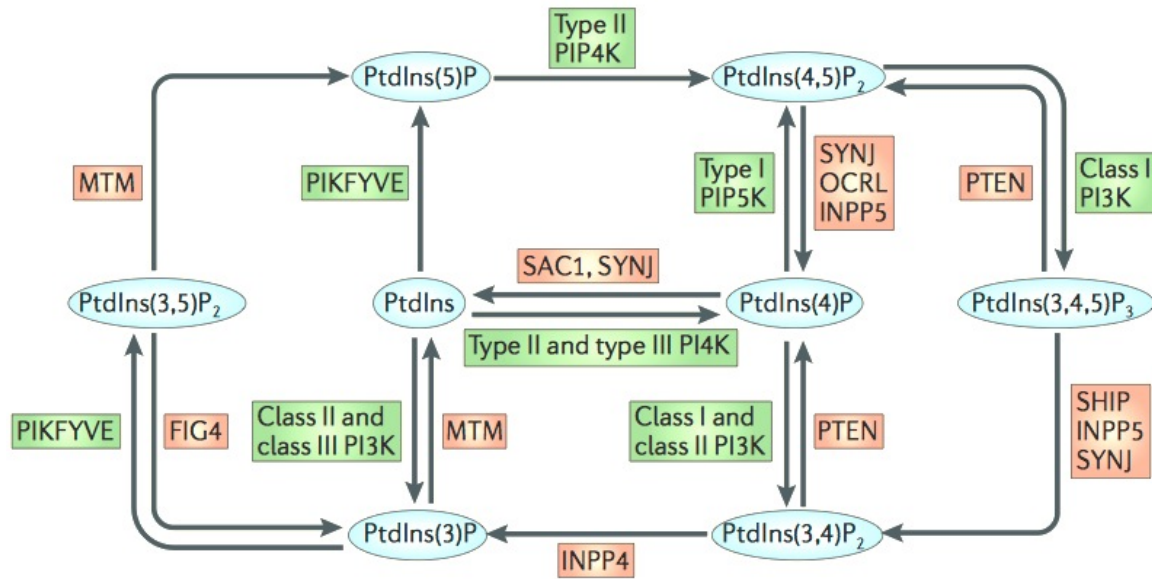


Figure 1.4 The network of interconversions between phosphoinositides. Several kinases and phosphatases regulate the inter-conversion between the different Phosphoinositides. Phosphorylation of phosphatidylinositol can give rise to seven different phosphoinositide. Most forms can also be generated through the action of specific phosphatase. (From Steve Jean and Amy A. Kiger. *Nature Reviews Molecular Cell Biology* **13**, 463-470, 2012, with permission)

1.3.1 The PI4P5K family of enzymes

The main pathway for PI(4,5)P₂ synthesis in mammalian cells is controlled by PI4P5 kinases that phosphorylate the inositol ring of PI(4)P at the 5th –OH group. The PI4P5K isoforms are encoded by three different genes α , β , and γ , and the γ isoform consists of several splicing variants: γ 87, γ 90 and γ 93 (206-210). The PI4P5 kinases share a highly conserved central catalytic domain of approximately 400 residues, but their N- and C- terminus are highly variable. The structural differences in N- and C- terminals of PI4P5K family determine their tissue distribution and subcellular localization and most likely the specific function carried out by each isoform. PIP5K α is highly expressed in skeletal muscles, while PI4P5K β is mostly found in the heart, and PI4P5K γ is abundant in the brain, suggesting at least some non-overlapping functions between the different members of the PI4P5K family (211,212).

1.3.1.1- PI4P5K α

The PI4P5K α consists of 549 aa with a molecular weight around 68 kDa (208,213). Endogenous PI4P5K α is found in several subcellular locations. It is very abundant in membrane ruffles, and induces the membrane ruffle formation in a Rac-dependent fashion upon PDGF stimulation (214). The PI4P5K α also exist in cytosol and in nuclear speckles where it controls the activity of Star-poly(A) polymerase (215). The PI4P5K α also plays a crucial role in phagocytosis, and overexpression of a kinase-dead mutant of PI4P5K α suppresses phagocytosis (216). On the other hand, overexpression of PI4P5K α in 293T cells results in formation of large vesicles and impaired endosomal trafficking (217). The PI4P5K α is also known to increase phospholipase D2 (PLD2) activity (218). While PI4P5K α deficient (PI4P5K α ^{-/-}) mice are viable, they are less fertile than wild-type mice. Bone marrow derived mast cells from the PI4P5K α ^{-/-} mice display fewer cortical F-actin filaments when compared to cells from wild-type

mice, as well as increased degranulation, increased intracellular Ca^{+2} signaling and cytokine production as well as hyperphosphorylation of many signaling proteins in response to high-affinity IgE receptor (FC ϵ RI) stimulation (219). Also, in PI4P5K $\alpha^{-/-}$ mice, thrombin- and thromboxane-induced platelet aggregation is defective, baseline PI(4,5)P2 abundance is reduced, and PI(4,5)P2 formation is blunted upon stimulation (220).

1.3.1.2- PI4P5K β

Endogenous PI4P5K β is localized to cytosolic vesicular structures in the perinuclear region in MG-63 human osteosarcoma fibroblasts (221). The PI4P5K β is involved in the regulation of several cellular activities, including receptor endocytosis by clathrin-coated vesicles. Suppression of PI4P5K β by specific siRNA reduced the pool of PI(4,5)P2 involved in receptor-mediated endocytosis in CV-1 and HeLa cells (222). Furthermore, PI4P5K β seems to be involved in neutrophil polarity and it localizes at the uropod of polarized, differentiated HL60 cells and knockdown of PI4P5K β by RNAi prevented the development of HL60 cells (223). The PI4P5K β is also involved in oxidative stress induced apoptosis, and cytoskeletal remodeling (191,224). The PI4P5K β deficient mice (PI4P5K $\beta^{-/-}$) are viable, fertile and show no histological abnormalities as compared to wild type mice (225), suggesting a potential functional redundancy between PI4P5K β and PI4P5K α .

1.3.1.3 PI4P5K γ

Several splice variants of PI4P5K γ have been identified in mammals including, γ 87 (635aa), γ 90 (661aa), γ 93 (687aa), PI4P5K γ 700aa and PI4PK γ 707aa (226). Each splice variant shows a distinct cellular localization. Exogenously expressed PI4P5K γ 87 has been observed in the cytosol (226), PI4P5K γ 90 localizes to focal adhesions (227,228), while PI4P5K γ 700 is

found the nucleus and PI4P5K γ 707 in punctate structures in the cytosol (226). The main splice variants of PI4P5K γ are PI4P5K γ 87 and PI4P5K γ 90 (229). The PI4P5K γ 87 is involved in the synthesis of PI(4,5)P2 in HeLa and mast cells (230,231) and is involved in phospholipase D2 stimulated integrin-mediated adhesion of HeLa cells (232), and in regulating actin dynamics to promote clustering of Fc γ receptors during phagocytosis (225). The PI4P5K γ 90 plays a crucial role in the formation of focal adhesions (227,228). In epithelial cells, PI4P5K γ 90 localizes to AJ and plays a role in cell-cell contact (233). In the brain, the PI4P5K γ 90 is enriched at the neuronal synapse and focal adhesions, where it is involved in the regulation of synaptic transmission, membrane trafficking, actin dynamics and focal adhesion formation (228,234), as well as in synaptic vesicle endocytosis (235,236).

The PI4P5K γ ^{-/-} mice have been generated by two different groups. One reported that PI4P5K γ ^{-/-} mice are smaller and suffer from cardiovascular defects, resulting in embryonic lethality at E9.5 (237). The other reported that PI4P5K γ ^{-/-} mice die within 24 hours of birth, possibly due to neuronal defects that and a failure to feed (238). In humans, a missense mutation in the PI4P5K γ catalytic domain causes the lethal contractural syndrome type 3 (LCCS3) characterized by joint contractures, micrognathia and anterior-horn spinal cord atrophy (239). Therefore, while the distinct PI4P5 kinases all serve to generate PI(4,5)P2, their functions in cells are only partially overlapping. From the KO data it seems likely that PI4P5k α and PI4P5k β can substitute for one another, while PI4P5K γ functions are more unique.

1.3.2 Regulation of PI4P5K activity

Many studies have highlighted the role of small GTPases of the Rho family, namely Rho, Rac and Cdc42 in controlling actin remodeling (240,241). The product of PI4P5K, PI(4,5)P₂ regulates actin rearrangements, and PI4P5K is proposed to be a downstream effector of Rho activation, suggesting a possible link between the two pathways (205). RhoA binds to PI4P5K and its kinase activity is enhanced in the presence of activated RhoA. The likely mechanism by which RhoA activates PI4P5K is through activation of the Rho associated kinase (ROCK) (242,243). In addition, Rac plays a role in targeting and localizing overexpressed PI4P5K to the plasma membrane through interaction with all isoforms of PI4P5K (244). The ADP-ribosylation factors (ARFs) are a family of small GTPases involved in membrane trafficking and actin cytoskeletal dynamics (245). ARF1 and ARF6 bind to and enhance the catalytic activity of PI4P5K in the presence of phosphatidic acid in HeLa cells and HL60 cells, respectively. Overexpression of ARF6 increases the abundance of PI(4,5)P₂ at the plasma membrane (246,247). Interestingly, overexpression of a constitutively active mutant of ARF6 (Q67L) results in the formation of large internal vesicle structures, similar to the vesicles formed by PI4P5K overexpression (245)

Phosphorylation is another mechanism that regulates PI4P5K activity. All PI4P5K isoforms are capable of autophosphorylation, resulting in inhibition of PI4P5K activity (248). A PKA-mediated phosphorylation of PI4P5K β also reduces, and dephosphorylation enhances its activity. The phosphorylation of PI4P5K γ 90 by Src increases its affinity for talin and enhances its localization to focal adhesions (249). Phosphatidic acid also stimulates PI4P5K activity, most likely by enhancing the affinity of PI4P5K for PI(4)P (250,251). (Figure 1.5)

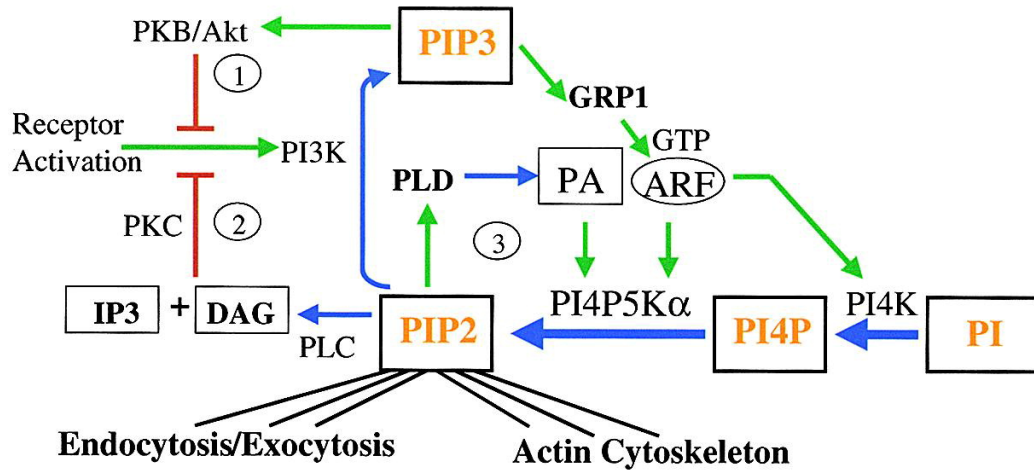


Figure 1.5 Regulation of PI(4,5)P2 and PIP3 Synthesis. (From Michael P Czech. *Cell*. 2000 17;100:603-606, 2000, with permission).

1.4 The Kidney: Anatomy and Physiology

The principal function of mammalian kidneys is to re-process the body's extracellular fluid, to maintain fluid and electrolyte homeostasis. Kidneys are paired organs located below the diaphragm, in retroperitoneum. Each kidney weighs 125-170 gm in adult men and 115-155 gm in adult women (252). The kidneys are perfused with blood via renal arteries, which arise directly from the abdominal aorta, at the rate of about 1 – 1.5 L/min. The renal arteries split into successively smaller arteries and arterioles, and finally into afferent arterioles, which empty into glomerular capillaries. Glomerular capillaries are exquisitely adapted for the filtration of plasma. They form a nearly protein-free filtrate consisting of water and small solutes at a rate of about 125ml/min (or about 150L/day). At their efferent end, the capillaries coalesce and blood flows from them into efferent arterioles. This anatomical arrangement permits fine regulation of the glomerular capillary pressure and flow rate, because the vascular tone of both the pre- and post-glomerular arterioles is controlled physiologically. The efferent arterioles then split again into peritubular capillaries, which surround the renal tubules and pick up reabsorbed fluid, which then return to the body via the renal veins.

When the kidney is cut longitudinally, two different regions are easily distinguished, namely the paler outer cortex which contains most of the glomeruli, proximal and distal tubules, and the darker inner medulla, which contains the loops of Henle and the collecting duct (252).

The basic structural and functional unit of the kidney is a nephron, and each human kidney contains approximately one million nephrons (253) . The nephron consists of the glomerulus, a tuft of capillaries already described above, which is surrounded by Bowman's space. The glomerular filtrate flows across the glomerular capillary wall into Bowman's space and into the proximal tubule. Depending on the extracellular volume status, anywhere from 70 to 95% of the

glomerular reabsorbed isotonicly by proximal tubules. The remaining tubular fluid then flows into the descending limb of Henle's loop, which dips deep into the renal medulla. Since the interstitium of the medulla is extremely concentrated, water moves out of the descending limb of Henle, causing the tubular fluid to become very concentrated. The nephron then takes a sharp turn upward forming the ascending limb of Henle's loop, which brings the fluid back into outer medulla and then the cortex. The ascending limb of Henle's loop is impermeable to water, but as the fluid moves up towards the cortex, it is diluted through active removal of NaCl and other ions. The ascending limb of Henle's loop touches the afferent and efferent arterioles of the glomerulus, sending signals to regulate their vascular tone so that the filtration can be matched to tubule function. Fluid in the ascending limb then flows into the distal tubule where it is made more dilute, and then empties into the collecting duct. The collecting duct again dips into the renal medulla. The collecting duct permeability to water depends on the osmolarity of the interstitial fluid, and the level of antidiuretic hormone (ADH). When ADH levels are high, water moves out of the collecting duct into hypertonic medullary interstitium, causing the urine to be very concentrated, and less water to be excreted. By contrast, in the absence of ADH, the urine remains diluted, allowing excess water to be excreted. The final urine is formed in the collecting duct of the nephron and empties into renal papilla, then into the ureter, from where it flows into the bladder for excretion.

By selective re-absorption and secretion of ions and many other molecules in the distinct sections of the nephron, the kidneys execute several physiological functions: they function to excrete metabolic end-product like creatinine, urea and uric acid, they control acid-base homeostasis by the regulated secretion of H^+ , and reabsorption of HCO_3^- , they regulate body osmolarity by differential excretion or reabsorption of water. They also regulate the

concentration of such critical ions as potassium, calcium and magnesium (252).

Finally, the kidneys also have endocrine functions: they secrete erythropoietin in response to hypoxemia, which in turn regulates red blood cell formation; they secrete renin in response to low blood pressure and nerve stimulation, which in turn regulates blood volume and blood vessel contraction, and promotes the secretion of aldosterone from the adrenal gland, and they regulate bone growth and density by activating vitamin D3 through di-hydroxylation forming 1,25-dihydroxyvitamine D3 (253) .

1.5 The Glomerular Capillary Wall

Each glomerulus is composed of 5-7 capillary branches originating from the afferent arterioles. Each capillary branch has several loops, formed by mesangial cells. Endothelial cells cover the inner surface of the capillaries, and specialized epithelial cells, the podocytes, cover the outer surface of the glomerular loops. A trilaminar basement membrane lies between the glomerular capillary endothelial cells and the podocytes and is manufactured and maintained by both cell types. Together, the glomerular endothelial cells, the basement membrane and the podocytes form the glomerular capillary wall. The capillary loop structure is maintained by mesangial cells and their extracellular matrix. Mesangial cells are pericyte-like cells that are actually located inside the capillary compartment. Mesangial cells are tethered to the capillary basement membrane from the inside; helping to give the capillary loops their shape (254-256).

Filtration across the glomerular capillary wall depends on a high hydraulic pressure gradient across the glomerular capillary wall, a high glomerular capillary plasma flow rate, and the permeability characteristics of the glomerular capillary wall. Usually, water and low molecular weight molecules can pass freely through the glomerular capillary wall (figure 1.6), but higher molecular weight proteins like albumin and immunoglobulins, as well as platelets and

red blood cells cannot move across. The components of the glomerular capillary wall that hinder the loss of protein and cells into the urine are called Glomerular Filtration Barrier (GFB). The GFB consists of three layers: a). the fenestrated glomerular endothelium with its glycocalyx; b). the glomerular basement membrane (GBM); and c. the podocyte foot processes with their slit diaphragms and negatively charged glycocalyx. The differential permeability of the glomerular capillary wall favoring filtration of water and small molecules over larger molecular weight substances is called permselectivity. In adult humans, glomerular filtration results in the formation of up to 180 liters/day of protein-free primary urine.. Preventing the loss of proteins like albumin into the primary urine is an essential function of glomerular capillaries. In fact, even a small amount of albumin in the urine is a sign of glomerular capillary injury or disease.

1.5.1 Fenestrated glomerular endothelium

Glomerular endothelial cells are much more permeable to water and small, dissolved molecules than other capillary endothelial cells, owing to the fact they are very flat and contain thousands of trans-cellular pores, called fenestrae. Fenestrae are plasma membrane lined pores, each ringed by cortical actin, measuring 70-100 nm in diameter (257,258). The fenestrae are almost 100 fold larger in diameter than dissolved globular albumin, but plasma albumin does not seem to enter the fenestrae despite the high rate of water flow through them. This seems to be due to the fact that endothelial cells and their fenestrae are covered by a thick coat consisting of glycoproteins, glycosaminoglycans and proteoglycans, which confer a negative charge to the endothelial cell surface. Associated with this endothelial cell-anchored coat is the endothelial cell surface layer, which consists of other proteins, some produced by the endothelial cell themselves and some derived from plasma, that are bound to the endothelial cell anchored proteins. Together, the endothelial-anchored glycoproteins and the endothelial surface layer form a

negatively charged glycocalyx. The presence of the negative charges in the endothelial glycocalyx contributes to the permselective properties of the glomerular filtration barrier (259)

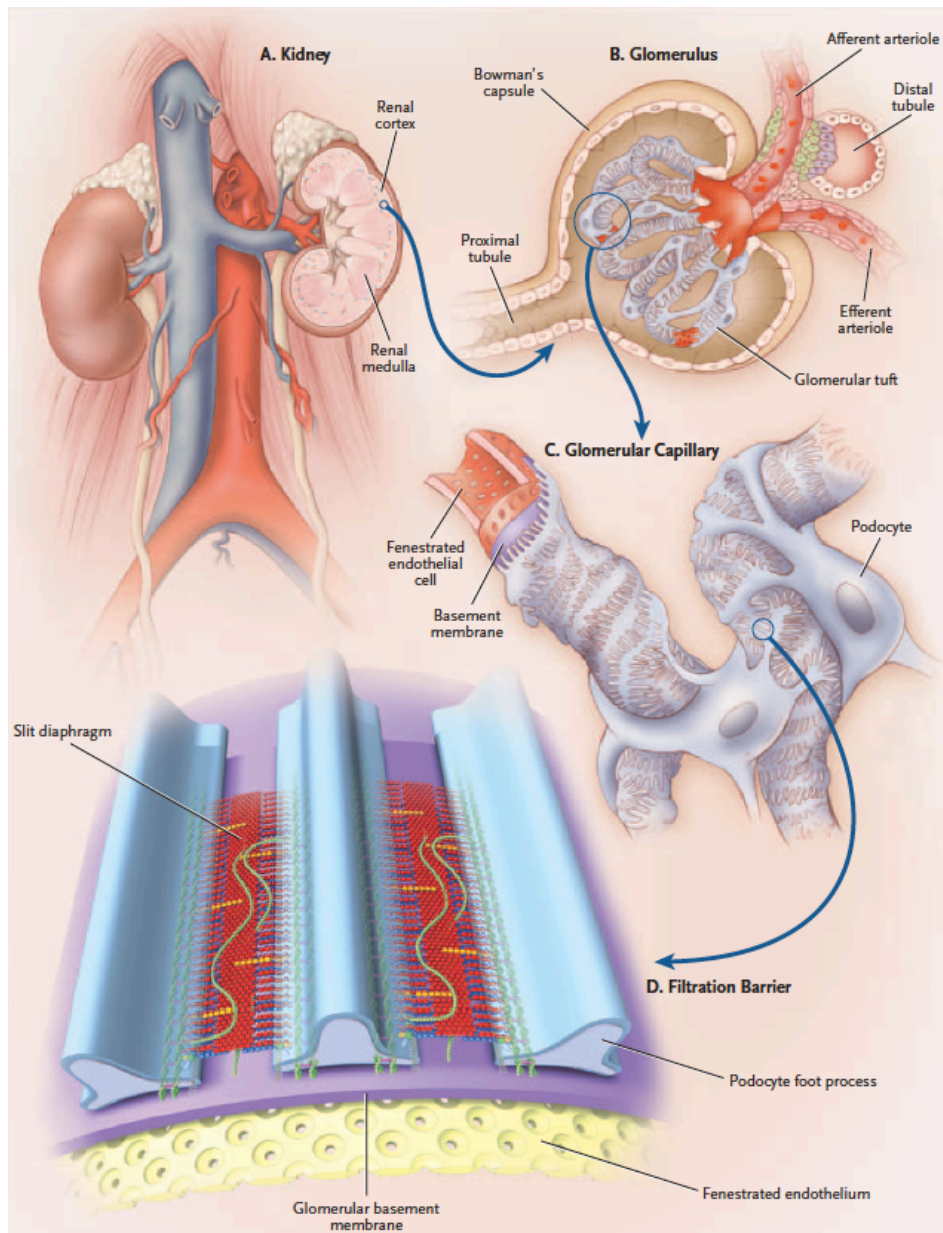


Figure 1.6 *Glomerular Filtration System.* A-The blood reaches the kidney through the renal arteries. B-The functional unit of the kidney is the nephron. The nephron consists of glomerulus and renal tubule. C-Filtration of the blood occurs across the glomerular capillary wall known as glomerular filtration barrier (GFB). D-The GFB is made up of three layers, fenestrated endothelium, glomerular basement membrane and podocyte foot processes with slit diaphragms. (Reproduced with permission from, Tryggvason and Patrakka, *N Engl J Med.* 354:1387-401, 2006, Copyright Massachusetts Medical Society).

1.5.2 The Glomerular Basement Membrane (GBM)

The glomerular basement membrane (GBM) forms the middle layer of glomerular capillary wall and separates the inner fenestrated endothelial cells from the outer podocytes. The GBM is produced by epithelial and endothelial cells. Ultrastructural examination shows that the GBM is made up of three layers, *ie* a central lamina densa, and laminae rara interna and externa (260). The GBM average thickness is approximately 300 nm (261).

The major components of GBM are the collagens (type IV, V and VI), several glycoproteins (laminin, fibronectin, entactin/nidogen), and proteoglycans (agrin, perlecan) (262). The Proteoglycans have anionic sites on their heparan sulfate and chondroitin sulfate side chains (263,264) and contributing to the charge-selectivity of the glomerular filtration barrier (265).

1.5.2.1 Type IV collagen

Collagen IV, a major component of the GBM, is a trimeric extracellular matrix protein made up of α chains that are rich in Glycine (266,267). Six different collagen subunits of collagen IV have been identified, termed $\alpha 1$ - $\alpha 6$, which are encoded by different genes COL4A1-A6 (260,261,268). In the early stages of glomerulogenesis, type IV collagen trimers are composed mainly of $\alpha 2/\alpha 1$ chains, which are substituted later at capillary loop stage by $\alpha 3/\alpha 4/\alpha 5$ produced by podocytes (269). The importance of collagen IV in renal function has been manifested by hereditary diseases associated with mutations in collagen IV. Mutations in any of the $\alpha 3$, $\alpha 4$ or $\alpha 5$ genes are usually associated with glomerular diseases. Alport syndrome is a X-linked hereditary basement membrane disease, resulting from a mutation in the $\alpha 5$ chain. This disease is characterized with progressive glomerulopathy that leads to renal failure; The Alport syndrome is also associated with deafness and ocular abnormalities. The Goodpasture syndrome, is an autoimmune disease, that is mediated by antibodies against the type IV collagen $\alpha 3$ chain

and characterized by glomerulonephritis and lung hemorrhage (266).

1.5.2.2 Laminins

The Laminins are trimeric molecules composed of α , β , and γ chains, which combine with each other to form at least 15 different heterotrimers (270,271). The laminin trimer composition undergoes developmental changes during glomerular formation. At early stage laminin is formed as LM-111 and later as LM-511, finally to LM-521 (271-273). In the adult, both endothelial cells and podocytes produce laminins. Laminin binds to agrin and associates with podocyte α -dystroglycan and integrins (268,274). The importance of laminin in GBM structure and renal function is confirmed with hereditary diseases associated with genetic mutations in laminin genes. The Pierson syndrome which is caused by a mutation in laminin β 2 gene is characterized by congenital nephrotic syndrome as well as ocular and neurological symptoms (275). Laminin β 2 knockout mice develop proteinuria and fusion of foot processes, resembling minimal change nephropathy (275). Hypomorphic mutations of laminin α 5 in mice result in glomerular proteinuria, hematuria, and cystic kidneys, indicating the importance the gene dosage of the laminin α 5 chain for the maintenance of the GBM (266).

1.5.2.3 Heparan sulfate proteoglycans (HSPGs)

Agrin and perlecan are the most abundant glomerular heparan sulfate proteoglycans (HSPGs) (276,277). Their negatively charge contributes to the permselectivity of the glomerular capillary wall (278,279). Several reports indicated that HSPGs are involved in transmembrane signaling by cells (268,276,280). In diabetic nephropathy, the agrin staining is reduced, suggesting a potential role in the pathogenesis of diabetic glomerular nephropathy (281). In the kidney perlecan is found in Bowman's capsule, in the mesangial matrix, and in the GBM

(282,283). Perlecan helps maintain of normal function of glomerular filtration barrier by binding other molecules in the glomerular basement membrane (268,280).

1.5.2.4 Nidogen (Entactin)

The nidogens-1 and -2 (entactin-1 and entactin-2) are widely expressed basement membrane glycoproteins. Their molecular weight is ~150 kDa and they consists of three globular domains (G1, G2 and G3). Nidogen-1 regulates the structure of the GBM by binding laminin via the G1 short arm (284) and type IV collagen via G2 (285,286).

1.5.3 Podocytes

The Podocytes form the outmost layer of the glomerular capillary wall. They are highly polarized epithelial cells that are characterized by a very unique structure. The podocytes cell body gives rise to long primary processes which branch further into numerous smaller secondary processes that extend around glomerular capillary loop. The secondary processes are generally known as foot processes. Podocyte foot processes play a crucial role in maintaining the strength of the glomerular capillary wall by counteracting the high intracapillary pressure, therefore preventing distension of the capillary loops (287-289). Podocytes are also involved in the production of glomerular basement membrane components and in the synthesis of vascular endothelial growth factor (VEGF). The VEGF is involved in the induction and maintenance of the fenestrae in glomerular capillary endothelial cells (290) The podocyte foot processes attach to the GBM via adhesion molecules including $\alpha 3\beta 1$ -integrin and α - and β -dystroglycans (280,291-293). The apical domain of the podocyte foot processes faces the urinary space and is negatively charged due to profoundly glycosylated podocalyxin (294). Foot processes from adjacent podocytes interdigitate, forming the filtration slit between them. A specialized cell

junction termed the slit diaphragm that is about a 40-nm-wide slit bridges the filtration slit between adjacent foot processes. The slit diaphragm is a zipper-like structure with pores whose dimensions are almost the same as the size of albumin (295). (Figure 1.7)

1.5.3.1 Protein complexes defining the Podocyte-GBM Interaction

In the basal domain integrin- and dystroglycan-based protein complexes anchor podocyte foot processes to the GBM, regulate intracellular signaling and are crucial in maintaining normal glomerular filtration. The main proteins involved in Podocyte- GBM interaction include:

1.5.3.1.1 $\alpha3\beta1$ -integrin

Integrins are heterodimeric adhesion receptors composed of distinct α and β chains that bind extracellular matrix type VI collagens, laminins, fibronectin and nidogen (296). In mature podocytes, the $\alpha3\beta1$ -integrin is most abundant and plays a significant role in the development and maintenance of podocyte foot processes (296,297). Integrin $\alpha3$ deficient mice lack podocyte foot processes, have fewer than normal glomerular capillary loops and die within 24 hours of birth(298). Similarly, podocyte-targeted integrin $\beta1$ deficiency in mice causes massive proteinuria, abnormal capillary morphogenesis, podocyte foot process effacement and podocyte apoptosis (299,300). Mutations in the human ITGA3 gene, which encodes $\alpha3$ integrin; results in the congenital nephrotic syndrome and severe GBM abnormalities (301). Hence, the $\alpha3\beta1$ integrin is critical for the development and maintenance of a normal glomerular filtration barrier.

1.5.3.1.2 Dystroglycans

Dystrophin–glycoprotein complexes composed of α - and β -dystroglycans, utrophin, and dystrophin are located at the basal domain of podocyte foot processes, where they bind to GBM

laminin, agrin, and perlecan. Dystroglycan expression is reduced in human minimal change disease and in several mouse models of glomerular disease (280,293). Nonetheless, the role of dystroglycans in podocytes is unclear since their deletion from podocytes in mice does not result in a glomerular phenotype or an increased susceptibility to injury. It therefore seems likely that integrins are the main adhesion molecules between podocytes and GBM (302).

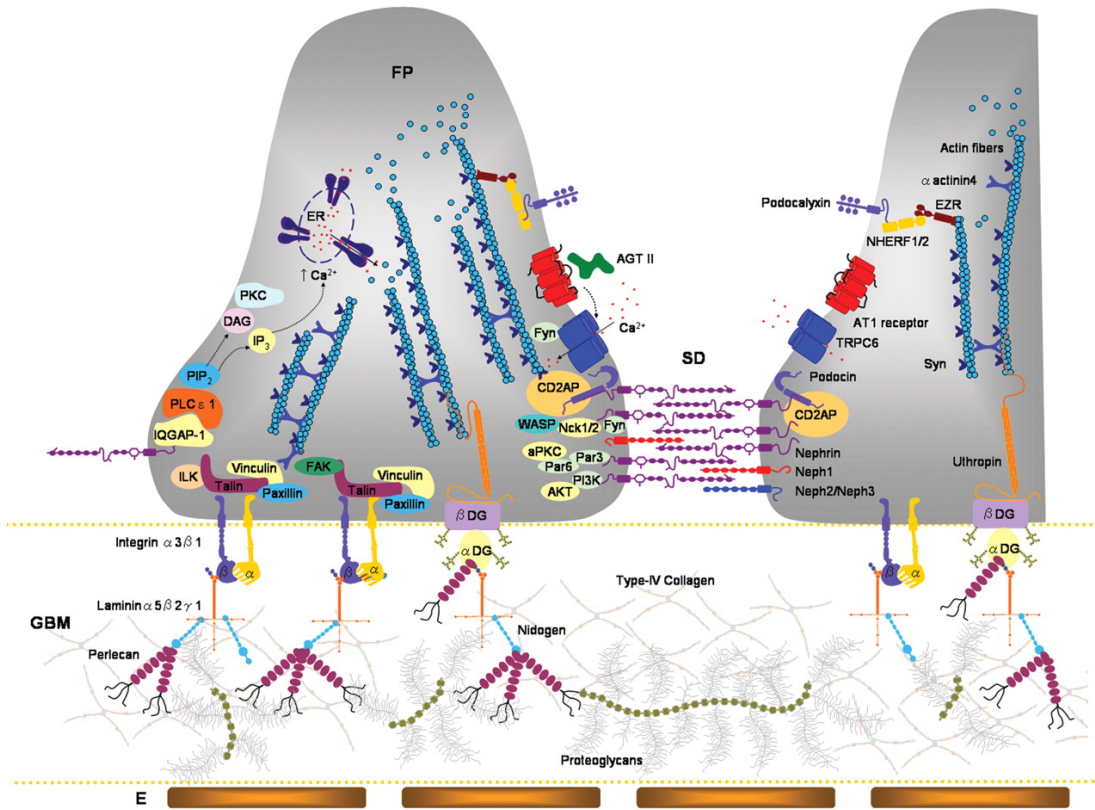


Figure 1.7 Anatomy of Podocyte Foot Processes. Podocyte foot process consists of three distinct domains: a). at the basal domain dystroglycan and integrins link the cytoskeleton to the GBM, b). at the lateral domain the filtration slit diaphragm, a modified adherens junction composed of nephrin, podocin, P-cadherin, FAT and CD2AP, also couples to the actin cytoskeleton, and c). at the apical domain the podocalyxin-NHERF2-ezrin protein complex interacts with cortical actin .
(from Machuca E et al. Hum. Mol. Genet. 18:R185-R194,2009, with permission)

1.5.3.2. The podocyte slit diaphragm protein complex

The slit diaphragm protein complex spans the space between adjacent podocyte foot processes and connects them with each other. The slit diaphragm protein complex connects with the foot process cytoskeleton. The slit diaphragm protein complex is composed of many proteins including nephrin, podocin, CD2AP, Neph, FAT and ZO-1 (303-307) (Figure 1.7). In 1974 Rodewald and Karnovsky described the slit diaphragm as rod-like units connected in the center to a linear bar forming a zipper-like pattern with pores. Due to the size of these pores ($40 \text{ \AA} \times 140 \text{ \AA}$), the slit-diaphragm is considered to be the main size-selective molecular sieve to plasma proteins in the kidney (278,308). The importance of the slit diaphragm in maintaining normal permselective glomerular filtration is highlighted by the fact that mutations in the genes for many of its components cause the nephrotic syndrome characterized by massive proteinuria.

1.5.3.2.1 Nephrin

Nephrin is a transmembrane protein of the immunoglobulin (Ig) superfamily, encoded by the NPHS1 gene, that forms the main component of slit diaphragm (309,310). The nephrin gene NPHS1 was identified in 1998 (311). The extracellular domains of nephrin from adjacent foot processes interact in the center of the slit to form the zipper-like structure of the slit diaphragm (312). Mutations in the NPHS1 gene result in congenital nephrotic syndrome of the Finnish type, (311) highlighting the role of Nephrin in the permselective barrier function of the glomerular capillary wall (313). Congenital nephrotic syndrome of the Finnish type is characterized by heavy proteinuria in utero, massive edema, premature birth and is lethal in human infants (314,315). The microscopic examination of the affected patients reveals increased glomerular size and number (316-319). The EM analysis shows effacement and fusion of podocyte foot processes, and an absent slit diaphragm (320-322). In mice, a similar phenotype is observed with

in response to inactivation of the nephrin gene (323,324). In addition to its role in maintaining the structure of the podocyte slit diaphragm, nephrin regulates several signaling pathways that control the organization of the foot process actin cytoskeleton (325). Nephrin function is furthermore controlled by phosphorylation. In this regard, phosphorylation of tyrosine residues on the cytoplasmic tail of nephrin by the Src family member Fyn leads to inhibition of apoptosis (326), elevation in cytosolic calcium levels (327) and raft-mediated endocytosis of nephrin (328).

1.5.3.2.2 Podocin

Podocin, encoded by the NPHS2 gene, interacts with other podocyte proteins including nephrin and mediates the interaction between plasma membrane proteins at the lateral domain of foot processes and the cytoskeleton (329). The NPHS2 gene is mutated in some forms of steroid-resistant nephrotic syndrome (329) characterized by early childhood proteinuria, focal and segmental glomerulosclerosis and progression to end-stage renal disease (329,330). Podocin-deficient mice have fused podocyte foot processes and lack slit diaphragms (331). These mice develop massive proteinuria antenatally and die a few days after birth, suggesting a critical role for podocin in the maintenance of the glomerular filtration barrier.

1.5.3.2.3 Neph Proteins

Neph1, Neph2, and Neph3 are transmembrane proteins with multiple immunoglobulin-like domains that resemble nephrin. The Neph proteins interact with nephrin and podocin through their extracellular domains (332). Similar to the nephrin and podocin knockout mice, mutations of Neph1 in mice results in massive proteinuria and perinatal lethality, but the phenotype is less striking than that observed in nephrin knockout mice, indicating the importance of nephrin to maintain the slit diaphragm structure and podocyte function. Disruption of Neph2 expression in

zebrafish also causes podocyte foot process effacement, a lack of slit diaphragms and an abnormally permeable glomerular filtration barrier (333). The disruption of Neph3 expression in zebrafish results in altered glomerular morphology and expanded pronephric tubules, suggesting that Neph3 is involved in the regulation of glomerular development (334).

1.5.3.2.4 FAT proteins

The FAT are transmembrane proteins belonging to the cadherin superfamily. They are composed of a short intracellular domain, a single transmembrane spanning domain and an extracellular domain with five Immunoglobulin-like motifs (335,336). In mammals, three FAT proteins, FAT1, FAT2, and FAT3 are expressed and localized to the podocyte slit diaphragm (332,337-339). FAT1 plays important role in cell–cell interaction between podocytes (340), and in the normal development of podocyte foot processes (341,342). FAT1 deficient mice show proteinuria and glomerular abnormalities characterized by effacement of podocyte foot processes, a lack of slit diaphragms and they usually die within 48 hours after birth (341).

1.5.3.2.5 ZO-1

ZO-1 is a member of the membrane-associated guanylate kinase (MAGUK) protein family. ZO-1 is widely expressed in body tissues and located at the cytoplasmic face of the junctional complexes of colon, kidney, and testis (343). In polarized epithelial cells, ZO-1 is located in the tight junctions that define the apical and basal lateral membrane domains. In kidney podocytes, ZO-1 is concentrated at the cytoplasmic face of podocyte foot processes in the slit diaphragm region where it acts as adaptor protein linking the slit diaphragm protein complex to the actin cytoskeleton (344,345).

1.5.3.2.6 P-cadherin

P-cadherin is a transmembrane protein that is expressed in podocytes foot processes where it colocalizes with ZO-1 (346). The extracellular domain of P-cadherin contributes to slit diaphragm formation, while its cytoplasmic tail connects the slit diaphragm complex to the actin cytoskeleton via α -catenin and ZO-1. P-cadherin and ZO-1 are co-expressed in cultured podocytes at in areas where slit diaphragms form (346). P-cadherin deficient mice are viable and the female are fertile despite the fact that P-cadherin is highly expressed in placenta (347).

1.5.3.2.7 CD2AP

CD2AP is an SH3-containing protein of T-lymphocytes that interacts with the cytoplasmic domain of CD2 is involved in enhancing T-lymphocyte adhesion to antigen-presenting cells (348). In the kidney, CD2AP is expressed in glomerular podocytes, collecting duct and in proximal tubule epithelial cells (349). In podocytes, CD2AP interacts with nephrin and serves as an adaptor protein involved in connecting the slit diaphragm complex to the actin cytoskeleton (350,351). Furthermore, CD2AP seems to be associated with endocytosis of plasma membrane proteins (352) and activation of PI3K/AKT signaling pathway (353,354).

In CD2AP-deficient mice foot processes are effaced in some glomeruli at birth and by the age of 2 weeks almost all glomeruli are affected. These mice develop proteinuria and progressive renal failure resulting in death by the age of 6-7 weeks (355). In humans, CD2AP mutations have been found in a few patients with FSGS (352), indicating the importance of CD2AP in the maintenance of the glomerular filtration barrier function.

1.5.3.3 The podocalyxin/NHERF2/ezrin complex at the apical domain of podocyte foot processes

Podocalyxin is a CD34-related integral membrane protein that is highly expressed by podocytes, mesothelial cells, vascular endothelial cells, hematopoietic stem cells, and platelets. Podocalyxin is a sialomucin protein with N- and O-linked carbohydrates, both of which are sialylated and sulfated (356). The negative charge of podocalyxin helps maintain the filtration slit open by repelling adjacent foot processes away from each other. (357,358).

Podocalyxin is localized at the apical domain of podocyte foot processes. Podocalyxin regulates podocyte foot processes cytoskeleton by the activation of the small Rho-GTPases. Podocalyxin forms a complex with ezrin and the adaptor protein NHERF2, which link the cytoplasmic tail of podocalyxin to the foot process actin cytoskeleton. This interaction plays a key role in maintaining the specialized podocyte foot process architecture (359), and the disruption of the podocalyxin-ezrin-actin interaction results in the nephrotic syndrome (133,359,360). Podocalyxin deficient mice die within 24 hours of birth due to renal failure. Ultrastructural analysis of glomeruli from podocalyxin deficient mice shows absence of podocyte foot processes. In these mice, the cell-cell junctions between the neighboring foot processes are replaced by impermeable tight junctions (361).

1.5.3.4 The podocyte cytoskeleton

The specialized morphology of the podocyte cell body and its primary processes is determined by microtubules and intermediate filaments vimentin, desmin, and nestin, while the shape of the foot processes is determined mainly by the actin cytoskeleton (362).

Several distinct adapter proteins link the foot process cytoskeleton to the basal, lateral and apical domains. The podocytes foot processes cytoskeleton is responsible for maintaining the

interaction between podocytes and GBM as well as the three dimensional shape of foot processes, both of these functions are crucial for maintaining normal GFB function, (figure 1.7). The cytoskeleton also serves as a stage for transmitting signals from the extracellular environment and adjacent podocytes, and provides mechanical strength to counteract the high glomerular capillary pressure stability (362). The main proteins involved in podocyte foot process cytoskeleton formation include:

1.5.3.4.1 α -Actinin-4

α -Actinin-4, encoded by ACTN4 gene, is mainly expressed in the podocyte foot processes where it cross-links F-actin filaments (363). α -Actinin-4 regulates the actin cytoskeleton and cellular plasticity to respond to glomerular hydrostatic pressure (364). It serves as an adaptor that mediates the interaction between the cytoskeleton and integrins to maintain the attachment of podocyte to GBM. Mutations in ACTN4 cause familial focal segmental glomerulosclerosis (FSGS) and α -actinin-4 deficient mice develop proteinuria, glomerulosclerosis, and podocyte foot processes effacement (365), indicating the importance of α -Actinin-4 in maintaining the normal permselectivity function of GFB.

1.5.3.4.2 Synaptopodin

Synaptopodin is an actin binding protein that is highly expressed in podocytes (366). It regulates podocyte foot process cytoskeleton dynamics by controlling the activity of small Rho GTPases (367). At baseline, glomerular function of synaptopodin-deficient mice is normal, but they develop more proteinuria, and show delayed recovery and podocyte foot process effacement after lipopolysaccharide (LPS) and protamine sulfate-induced injury, when compared to wild type mice (368). PKA and CaMKII can phosphorylate synaptopodin, enhancing its affinity for

the 14-3-3 protein and its stability, compared to dephosphorylated synaptopodin. It is therefore likely that phosphorylation-dependent regulation of synaptopodin plays a role in controlling podocyte function in vivo (369).

1.6 Hypothesis and Objectives

Rationale

This thesis focuses on the role of CLIC5A in regulating ezrin activation. The CLIC5A protein is expressed at extremely high levels in glomerular podocytes, and it localizes in a highly polarized fashion to the apical domain of podocyte foot processes. CLIC5A was first identified as a cytoskeleton-associated protein that interacts with ezrin in microvilli of placental epithelial cells. Unlike the more ubiquitous CLIC1 and CLIC4, expression of CLIC5A is extremely restricted. In the inner ear, CLIC5A concentrates in F-actin rich sensory microvilli of cochlear and vestibular hair cells, where it associates with the ERM protein radixin. That CLIC5 is functionally important was shown in CLIC5 deficient mice, where the number of hair-cell stereocilia is reduced, and radixin protein levels are lower than in wild-type mice. In the CLIC5^{-/-} mice the sensory stereocilia progressively deteriorate resulting in vestibular dysfunction that is evident soon after birth, and complete deafness by the age of 7 months.

This laboratory previously reported that CLIC5A mRNA levels are ~800-fold higher in glomeruli relative to pooled non-glomerular tissues and cells. Immunofluorescence microscopy showed that the CLIC5A protein is extremely abundant in glomerular podocytes and is not detected in tubule epithelial cells. Several studies have suggested a functional and molecular relationship between the CLIC and ERM proteins, but the nature of this relationship is unclear. In glomerular podocytes, we know that ezrin links apical podocalyxin to cortical actin in podocyte foot processes, but the potential involvement of any CLIC protein was not previously recognized. The experimental work that forms the foundation of this thesis explored the nature of the molecular and functional interaction between CLIC5A and ezrin, and sought to define the

role of CLIC5A in maintaining the unique structure and integrity of glomerular podocytes.

Hypothesis

CLIC5A regulates ezrin activation, and its association with the actin cytoskeleton in actin-based membrane projections. The absence of CLIC5A results in an increased susceptibility of ezrin to degradation and perturbs ezrin-dependent, actin-based cellular projections. In glomerular podocytes, CLIC5A is a member of the podocalyxin/NHERF2/Ezrin complex that links apically located podocalyxin to cortical actin in podocyte foot processes. Loss of CLIC5A perturbs the molecular stability of this complex, impairing the specialized three-dimensional structure of podocyte foot processes and consequently glomerular function.

Objectives

- 1. Explore the effect of CLIC5A on ERM protein activation**
- 2. Explore the effect of CLIC5A cell morphology.**
- 3. Define the signaling pathway(s) involved in CLIC5A-mediated ERM protein phosphorylation**
- 4. Define the relationship between CLIC5A and the ezrin/NHERF2/podocalyxin complex in glomerular podocytes.**
- 5. Explore the molecular abnormalities in the ezrin/podocalyxin/NHERF2/actin complex associated with CLIC5A deficiency**
- 6. Determine whether the absence of CLIC5A confers vulnerability to kidney injury.**

Chapter 2

Materials And Methods

2.1 Cell culture, transfection and cells lysis:

COS-7 and HeLa cells were maintained in Dulbecco's Modified Eagles Medium (DMEM) supplemented with 10% (V/V) Fetal Bovine Serum (FBS) (Life technologies, Burlington, ON) in a 37°C and 5% CO₂ humidified incubator. Cells in 6-well plates or P35 dishes were transfected with 4 µg of specific plasmid construct in 4 µl of either LipofectamineTM 2000 (Life Technologies) for COS-7 cells, or LipofectamineTM LTX (Life Technologies) for HeLa cells, both in OPTI-MEM reduced serum medium according to the manufacturer's instruction. Two days after transfection, the cells were washed twice with ice-cold PBS, and harvested in Triton X-100 lysis buffer (TX-100 0.5%; HEPES 10 mM; NaCl 0.1 M; 2-Mercaptoethanol 14 mM; EGTA 2.5mM; MgCl 5 mM; Cal-A 100 nM , and 1x PhosStop, pH= 7.4). To each P35 dish 500 µl of lysis buffer were added. For total cellular lysate (TCL), 100 µl of the lysate were diluted with 100 µl 4X Lammeli buffer and boiled for 5 minutes. To prepare detergent insoluble fractions (Pellet), the remaining 400 µl were centrifuged at 18,000 X G for 30 minutes at 4 °C, the supernatant was removed and the insoluble fraction was re-suspended in 100 µl 2X Laemmli buffer and boiled for 5 minutes. The resulting lysates were kept at -80 °C until the time of use.

2.2 Reagents and antibodies:

All chemicals were of reagent grade and purchased from Sigma (Oakville, ON, Canada) unless otherwise noted. Rabbit anti-phospho-Thr567 ezrin antibodies were purchased from Signalway Antibody LLC (SAB) (Maryland, USA), and mouse anti-Phospho-Thr567 ezrin antibodies were from BD Biosciences (Franklin Lakes, USA). Since the Phospho-Thr567 ezrin antibodies cross-react with phosphorylated radixin and moesin, we refer to signals obtained with them as phosphorylated ERM (P-ERM). Rabbit anti-ezrin antibodies were from Cell Signaling

(Danvers, USA), rabbit anti-CLIC5 antibodies from Aviva System Biology (San Diego, CA, USA), mouse anti- β -tubulin and anti- β -actin antibodies were from Millipore (Billerica, MA, USA) and Sigma (Oakville, ON, Canada) respectively. PI4P5KI α was purchased antibody from Cell Signaling 9693S, phospho-PKC antibody was purchased from Santa Cruz Biotechnology, Inc (CA, USA).

2.3 CLIC5A cloning:

A cDNA for CLIC5A encoding the complete open reading frame (ORF) (GenBankTM # DQ679794), was PCR-amplified from human kidney cDNA. In the forward primer a Kozak consensus sequence (bold) was added to enhance expression in mammalian cells and 6xHis tag sequence (italic) was integrated for subsequent detection. The PCR product was directly cloned into pCDNA3.1/V5-his-TOPO vector (Life Technologies). This construct is designated pcDNA3.1-CLIC5A, or CLIC5A in the figure legends.

The GFP-CLIC5A construct was generated by PCR-amplification of human CLIC5A full coding region from pcDNA3.1-CLIC5A, and cloning into Xho I/BamHI site of pEGFP-C1 vector (Clontech, Mountain View, CA, USA). Restriction enzyme digestion and full insert sequencing verified the DNA sequence orientation and fidelity.

The constructs of the PI(4,5)P₂ reporters (GFP-PH-PLC and RFP-PH-PLC) and negative charge biosensor (GFP-Kras) were originally obtained from S. Grinstein (University of Toronto). Constructs for the HA-PI(4,5)P kinases (PI4P5 α , PI4P5K β , PI5P4K α and PI5P4k β) were provided by Dr. Greg Longmore (Washington University- School of Medicine, USA) and the YFP-actin construct by Dr. Allan Murray (University of Alberta).

2.4 Cloning of CLIC5A mutants:

Xpress-tagged CLIC5A wild-type (WT) (1-251) and truncation deletion cDNAs (22-251 first β -pleated sheet deletion, 55-251 first β -pleated sheet and putative trans-membrane domain deletion and 1-232 (Helix #9 deletion) were PCR-amplified from pCDNA3.1-CLIC5A. Followed by cloning into pTARGET vector (Promega, Madison, WI, USA). Restriction enzyme digestion and full insert sequencing verified the DNA sequence orientation and fidelity.

CLIC5A cDNA		Primer Sequence
hCLIC5A (1-251)		
	Forward	5'CGCACTCGAGACCATGGGGCATCATCATCATCATACAGACTCGGGCAGCTAAC-3'
	Reverse	5'-CCGGGATCCTCAGGATCGGCTGAGGCGTTTGGC- 3'.
GFP-CLIC5A (1-251)		
	Forward	5'-CGCACTCGAGCCATGACAGACTCGGGCAGACTAAC-3'
	Reverse	5'-CCGGGATCCTCAGGATCGGCTGAGGCGTTTGGC-3'
Xpress-CLIC5A (1-251)		
	Forward	5'AGCTTCATGGGGGATCTGTACGACGATGACGATAAGACAGACTCGGGCAGCTAACGGG-3'
	Reverse	5'-CCGGGATC CTCAGGATCGGCTGAGGCGTTTGGC-3'
Xpress-CLIC5A (1-232)		
	Forward	5'AGCTTCATGGGGGATCTGTACGACGATGACGATAAGACAGACTCGGGCAGCTAACGGG-3'
	Reverse	5'-CCGGGATCCTCATGCACAGGTGTTGGTGAATCATC-3'
Xpress-CLIC5A (22-251)		
	Forward	5'GCTTCATGGGGGATCTGTACGACGATGACGATAAGGCTGGAATCGATGAGAAAGCATC-3'
	Reverse	5'-CCGGGATC CTCAGGATCGGCTGAGGCGTTTGGC-3'
Xpress-CLIC5A (55-251)		
	Forward	5'AGCTTCATGGGGGATCTGTACGACGATGACGATAAGGATCTGAAAAGAAGCCAGCTGAC-3'
	Reverse	5'-CCGGGATC CTCAGGATCGGCTGAGGCGTTTGGC-3'

Table 2.1 The sequence of different primers used in cloning the different constructs of CLIC5A.

2.5 Cytoskeleton preparation:

Cell cytoskeletal preparations were made as described by Berryman (56). Cells in P35 dishes were transfected with either CLIC5A-cDNA or empty vector. Two days post transfection cells were placed on ice and gently washed twice with cold PBS containing 5.0 nM of phosphatase inhibitor Cal-A, and then incubated at room temperature (RT) for 5 minutes in 500 μ L PBS containing 0.5% Triton X-100, 100 nM Cal-A, PhosStop (Roche, 1 tablet/10 ml) and complete proteinase inhibitor. The supernatant was removed and the cells were washed gently twice with cold PBS to remove solubilized material. The remaining cytoskeletons were collected in 200 μ L Laemmli buffer, boiled for 5 minutes and stored in -80 °C until the time of use.

2.6 Western blot (WB) analysis:

Boiled, denatured total cellular lysate (TCL), detergent insoluble fractions (Pellet) and cytoskeletal samples were loaded onto 10-12% SDS-PAGE and subjected to electrophoresis at 30 mA in the presence of running buffer containing (25 mM Tris-HCl, 192 mM Glycine and 7 mM SDS, pH 8.5). The separated proteins in the gel were then transferred onto the PVDF membranes at 100-115 Volt for 1 hour in the presence of a transfer buffer containing PH-7.5 (25 mM Tris-HCl, 192 mM Glycine and 20% Methanol, pH 8.5). After transfer, membranes were incubated in blocking solution (Sigma) for one hour at room temperature and then with primary antibody at the following dilutions: Rabbit anti Phospho-ERM 1:6000, Rabbit anti ezrin 1:4000, Rabbit anti CLIC5A 1: 6000, Mouse anti tubulin 1:10000, Mouse anti actin 1:10000. Goat anti NHERF2 1: 250, Rat anti HA 1:4000, Goat anti-podocalyxin 1:5000. All antibodies were diluted in blocking solution.

The membranes were washed three times for 30 minutes each with Tris-Buffered Saline and Tween 20 (TBST) containing (20 mM Tris-HCL, 150 mM NaCl and 0.1% Tween20, pH 7.5) at room temperature (RT), followed by incubation with the appropriate horse radish peroxidase (HRP)-conjugated secondary antibodies at the appropriate dilution (1:10,000) again in blocking solution for one hour at RT. Finally, the membranes were washed three times for 30 minutes each, in TBST and incubated with Enhanced Chemiluminescence (ECL; GE Amersham; Baie d'Urfe, QC, Canada) for 2 minutes. Images of the chemiluminescence on the membranes were captured by exposure to X-Ray film (Fuji Medical X-Ray Film Super Rx; Fujifilm) for several time-point followed by film development.

2.7 Immunofluorescence microscopy and live cell imaging:

To evaluate the abundance of phospho-ERM (P-ERM) in cultured cells, COS-7 cells grown on glass coverslips and transfected with pCDNA3.1/CLIC5A, its pCDNA3.1 vector control, pGFP-CLIC5A or its pGFP vector control were washed with cold PBS on ice and fixed with 10% Trichloroacetic Acid (TCA) for 15 min at room temperature (RT). TCA fixation was previously shown to preserve ERM phosphorylation (125). Cells were then permeabilized with 0.05 % TX-100 in PBS for 15 min, blocked with 5% goat serum in PBS and incubated with specific primary antibodies overnight at 4°C. The cells were then washed 4-6 times with PBS containing 30 mM glycine (G-PBS) and incubated with secondary antibodies for 1 hr at RT followed by three G-PBS washes and mounting in ProLong Antifade (Life Technologies).

For actin staining, COS-7 cells transfected with GFP-CLIC5A or pGFP vector were fixed with freshly prepared 4% paraformaldehyde in PBS for 15 min at RT, washed three times with PBS and blocked with 5% goat serum in PBS for 1.0 hour at RT. Cells were then incubated with Rhodamine-phalloidin for 30 min at RT, washed with PBS and mounted in ProLong Antifade.

To assess actin polymerization, COS-7 cells were grown on 25-mm glass coverslips and co-transfected with CLIC5A and YFP-actin or with pCDNA3.1 vector and YFP-actin. A ratio of 10:1 CLIC5A cDNA or pCDNA3.1 : YFP-actin cDNA was used to maximize the probability that YFP fluorescent cells were indeed co-transfected with CLIC5 or vector cDNA. Two days post transfection; the coverslips containing the transfected cells were mounted in a live cell-imaging chamber (37°C, 5% CO₂) of an Olympus spinning-disk fluorescence microscope (Olympus IX-81) for image acquisition. X-Z sections and final images were created using Volocity software (Improvision; UK).

For live cell imaging, COS-7 cells grown on 25-mm glass coverslips were transfected with the appropriate constructs at a ratio of 10:1 (CLIC5A, CLIC5A mutant or Vector : GFP-PH-PLC or GFP-Kras. Twenty-four hours after co-transfection cells were transferred to the live cell imaging chamber at 37°C and 5% CO₂ of an Olympus spinning-disk fluorescence microscope (Olympus IX-81), and image acquisition was performed with Volocity (Improvision) software.

To test the co-localization between HA-PI4P5K1 α and different mutants of CLIC5A, COS-7 cells grown on glass cover slip were co-transfected with HA- PI4P5K1 α and full length CLIC5A or CLIC5A deletion mutants. Two days post transfection, cells were washed with cold PBS on ice and fixed with 10% Trichloroacetic Acid (10% TCA) for 15 minutes on ice. Cells were then permeabilized with 0.05 % TX-100 in PBS for 15 min, blocked with 5% goat serum in PBS and incubated with primary antibodies (rabbit anti CLIC5A and rat anti -HA) overnight at 4°C. The cells were then washed 4-6 times with PBS containing 30 mM glycine (G-PBS) and incubated with secondary antibodies for 1 hour at room temperature followed by three G-PBS washes and mounting in ProLong Antifade (Life Technologies).

2.8 Immunofluorescence microscopy of kidney sections

Kidney cortex (~0.5-cm³ cubes) was incubated in 30% sucrose at 4°C overnight, frozen in optimal cutting temperature (OCT, Sakura Finetek, Torrance, CA), and stored at -80°C. Frozen sections (~5 µm thick) were thaw-mounted on SuperFrost Microscope slides (Micom International, Kalamazoo, MI), air-dried, and fixed for 10 min in acetone at 4°C. Slides were washed in PBS (3 × 5 min) at room temperature and blocked for 30 min with 3% bovine serum albumin (BSA) in PBS, followed by incubation with the primary antibodies in 3% BSA-PBS overnight at 4°C. The slides were then washed (3 × 5 min) in PBS and incubated for 1 h in the dark with 1:500 dilutions of the appropriate Alexa fluor 594- or 488-conjugated secondary antibodies (Molecular Probes, Eugene, OR) in 3% BSA-PBS. Slides were washed three times in PBS, mounted with ProLong Gold Antifade (Molecular Probes), and viewed on a Zeiss Axioplan 2 microscope and a Zeiss LSM 510 laser-scanning confocal microscope (Zeiss, Toronto, ON, Canada) at ×20, ×40, or ×100 magnification. Antibodies against Tie-2 (mouse, 1:100 dilution; Upstate Biotechnology, Lake Placid, NY), synaptopodin (mouse, undiluted; Biodesign International, Saco, ME), ezrin (rabbit, 1:2,000 dilution; Cell Signaling, Danvers, MA), NHERF2 (goat, 1:200 dilution, no. S1506; Santa Cruz Biotechnology, Santa Cruz, CA), podocalyxin (goat, 1:10,000 dilution, no. AF1556; R & D Systems) and CLIC5 (mouse, 1:2,000 dilution; no. H00053405-M03, Abnova, Taipei City, Taiwan) were used to define the expression and colocalization of CLIC5A in glomeruli.

To study the co-localization between Podocalyxin, Podocin, PECAM and P-ERM in CLIC5^{+/+} and CLIC5^{-/-}, kidney cortex from both genotypes was fixed in 10 % Trichloroacetic Acid (TCA) for 1 hour on ice to preserve ERM phosphorylation (125). Fixed tissues were embedded in OCT (Sakura Finetek, CA, USA). Frozen kidney section (4-5 µM) were

permeabilized with 0.05 % Triton X-100 in PBS for 15 min, blocked in 5% goat serum and incubated with the following primary antibodies overnight at the cold room: rabbit anti P-Ezrin (phospho-Thr567) (Signalway Antibody LLC (SAB), Maryland, USA) goat anti-podocalyxin (1:10,000 dilution, no. AF1556; R & D Systems). The goat anti-platelet endothelial cell adhesion molecule-1 (PECAM-1; 1:200 dilution, no. S1506; Santa Cruz Biotechnology, Santa Cruz, CA) was used as endothelial cell marker and goat anti-podocin (1:200 dilution, no. A11058; Santa Cruz Biotechnology) as the podocyte marker. The sections were then washed 4-6 times with PBS containing 30 mM Glycine (G-PBS) and incubated with the secondary antibodies for 1 hour (RT) followed by G-PBS washing and mounting in ProLong Antifade (Life Technologies). All immunofluorescence studies were repeated at least three times using distinct samples.

2.9 Scanning electron microscopy (SEM):

To examine the morphological changes associated with CLIC5A overexpression, COS-7 cells transfected with CLIC5A or vector were fixed with 2% glutaraldehyde for 15 min. After fixation, the cells were washed twice with PBS and dehydrated in a graded series of ethanol (30%, 50%, 70%, 95% and 100%). The cells were then passed through serial dilutions of Hexamethyldisilazane (HMDS) in ethanol (75% Ethanol: 25% HMDS), (50% Ethanol: 50% HMDS), (25% Ethanol: 75% HMDS), and 100% HMDS. The cells were then left to dry, mounted on SEM stubs and sputter-coated with Gold-palladium (Au/Pd). Samples were imaged with a Philips/FEI (XL30) scanning electron microscope (Dept. of Biological Sciences - University of Alberta).

2.10 siRNA knockdown.

Transfection with siRNA was performed using Lipofectamine 2000 (Life Technologies). Control siRNA (Scramble, cat # sc-37007), PI4P5KI α siRNA (cat # sc-36232) were purchased from Santa Cruz Biotechnology. Briefly COS-7 or HeLa cells were plated in 35 mm culture dishes at ~60% confluence the day prior to transfection. The DMEM medium was replaced with 1.0 ml DMEM without antibiotics just before transfection. Two-three μ g CLIC5A or vector plasmid with 60 pM Scramble or PI4P5KI α kinase siRNA (Mix A), and 4 μ l Lipofectamine 2000 (Mix B) were each suspended in 100 μ l Opti-MEM I medium (Life Technologies) respectively. Mix A and B were combined and incubated for 30-45 min (RT). The combined mix was then added them to the cells. After 5-7 hrs 1.0 ml DMEM containing 20% FBS was added to the cells. On the evening prior to lysis, the medium was changed to DMEM without serum followed by overnight incubation. Cells were lysed 48 hrs after initiation of transfection.

2.11 GST-CLIC5A construct, bacterial expression and protein purification.

The full coding region of human CLIC5A was PCR-amplified from pCDNA3.1-CLIC5A with the primers:

GST-CLIC5A		Primer Sequence
	Forward	5'CGTGGGATCCCCATGACAGACTCGGCGACAGCTAAC-3'
	Reverse	5'-CCGGAATTCTCAGGATCGGCTGAGGCGTTTGGC-3'

The PCR-derived CLIC5A was cloned into pGEX-3 (GE Healthcare, Piscataway, USA). DNA sequence fidelity was verified by sequencing. *E. Coli* BL21 Gold (DE3) bacteria (Agilent Technologies, Santa Clara, USA) were then transformed with pGEX-3 or pGEX-CLIC5A constructs, induced with 0.2 mM IPTG and grown at 37°C for 4 hrs. Bacteria were harvested in

PBS containing 1x proteinase inhibitor cocktail (Roche Diagnostics, Indianapolis, US) followed by sonication and addition of Triton X-100 to a final concentration of 1%. GST and GST-CLIC5A proteins were purified by affinity chromatography on Glutathione Sepharose 4B (GE Healthcare) according to the manufacturer's protocol.

2.12 Staurosporine (SSP), Y-27632 and Calyculin A (Cal-A) treatment.

Confluent COS-7 cells plated in 6 well plates were treated with 100 nM SSP or 15 μ M Y-27632 for 1 hour or with 100 nM Cal-A for 15 minutes. Cells were washed twice with cold PBS, and harvested in Triton X-100 lysis buffer (0.5% TX-100, 10 mM HEPES pH 7.5, 0.1M NaCl, 14 mM 2-mercaptoethanol, 2.5 mM EGTA, 5 mM MgCl, 100 nM Cal-A, 1xPhosStop).

2.13 Quantification of the rate of ERM protein de-phosphorylation.

Confluent COS-7 cells in P35 well plates were transfected with CLIC5A or vector cDNA. Two days after transfection the cells were treated with 100 nM SSP for 0, 1, 3 or 5 minutes. At the appropriate time points, cells were washed twice with cold PBS and then harvested in Triton X-100 lysis buffer (0.5% TX-100, 10 mM HEPES pH 7.5, 0.1 M NaCl, 14 mM 2-mercaptoethanol, 2.5 mM EGTA, 5 mM MgCl, 100 nM Cal-A, 1xPhosStop), mixed with 4X Laemmli buffer, boiled for 5 minutes and frozen at -80°C until WB analysis.

2.14 Treatment with the Cl⁻ channel inhibitor (IAA-94) or the PLC activator m-3M3FBS.

COS-7 cells were plated in P35 transfected with CLIC5A or vector cDNA were treated with 50 μ M of the Cl⁻ channel inhibitor IAA-94 or with 800 μ M of the PLC activator m-3M3FBS. At the appropriate time points cells were washed twice with cold PBS and harvested in Triton X-100 lysis buffer (0.5% TX-100, 10 mM HEPES pH 7.5, 0.1 M NaCl, 14 mM 2-

mercaptoethanol, 2.5 mM EGTA, 5 mM MgCl₂, 100 nM Cal-A, 1xPhosStop), mixed with 4X Laemmli buffer, boiled for 5 minutes and stored at -80°C until WB analysis.

2.15 GST-pull down assay.

COS-7 cells transfected with a HA-PI4P5K α , HA-PI4P5K β , HA-PI5P4K α or HA-PI5P4K β cDNA were scraped into lysis buffer (1.0% TX-100, 20 mM HEPES pH 7.4, 0.6 M KCl and 1mM EDTA), 48 hours after transfection. The lysate was incubated at RT for 20 min., followed by centrifugation for 30 min. at 14,000 RPM. The supernatant was diluted 1:5 (V:V) in buffer containing 20 mM HEPES pH 7.4, 10 mM MgCl₂, 1.0 mM ATP, 1x Proteinase inhibitor complex and PhosStop. One hundred μ l were reserved to define protein input, and the rest was used for the GST- pull down. The GST or GST-CLIC5A immobilized on glutathione beads was incubated with the diluted supernatant on a rotator for 3 hr. (RT). The beads were washed for five times, three min. each, with a wash buffer (20 mM HEPES pH 7.4, 100 mM NaCl and 0.1% TX-100) Bound proteins were eluted with 2x Laemmli buffer followed by WB analysis.

2.16 Animal care.

The CLIC5^{-/-} mutant mice were discovered in The Jackson Laboratory (Bar Harbor, MN, USA) due to their head-bobbing and circling behavior, which is characteristic for abnormalities in the vestibular apparatus. This strain of mice, initially on the C3H/HeJ background was therefore given the name “jitterbug”. Through positional cloning they were discovered to have a spontaneous 97-bp deletion in the CLIC5 gene (87 bp at the 3' end of exon 5 plus 10 bp in the adjacent intron) that leads to skipping of exon 5 and a translational frame shift producing a premature stop codon (57). They were back-crossed in our laboratory for > 15 generations onto the C57BL/6J background. For the studies reported here, offspring were derived by breeding

wild-type CLIC5^{+/+} or heterozygous CLIC5^{+/-} females with CLIC5^{-/-} homozygous male mice, first on the C3H/HeJ and later on the C57BL/6J background. Mice were housed in the animal facility at University of Alberta and all procedures using mice were approved by the University of Alberta Animal Care and Use Committee. The use of human samples was approved by Health Research Ethics Board of the University of Alberta (see appendices)

2.17 Isolation of mouse glomeruli and preparation of glomerular lysates.

Mouse glomeruli were isolated by differential sieving as previously reported (370), with modifications. Kidneys were freshly harvested from C57BL/6J-CLIC5^{+/+} and CLIC5^{-/-} mice. The kidney capsules were removed, followed by the separation and collection of kidney cortex under dissecting microscope with a sharp scalpel blade. For each glomerular isolation, the kidney cortex from three 8-month old C57BL/6J CLIC5^{+/+} or CLIC5^{-/-} mice was pooled according to genotype and carefully minced. The material was then suspended in RPMI 1640 medium (Sigma) containing 1.0 mg/ml Collagenase IV (Worthington, Lakewood NJ USA) and 10 nM Cal-A and digested at 37°C for 1.0 hr. The digested tissue suspensions were passed through stacked 100 µm, 70 µm and 40 µm cell strainers (BD Falcon, Durham NC USA) using gentle pressure with cell lifter on the 100 µm strainer. The glomeruli that accumulated on the surface of 40 µm cell strainer were collected and placed into 100 mm tissue culture plates in 15 ml RPMI 1640 media containing 0.5% FBS (Life Technologies) and 10 nM Cal-A and incubated in a cell culture incubator at 37°C in 5% CO₂/air for 10 min. Contaminating tubules, but not glomeruli, rapidly adhere to cell culture plastic under these conditions. After 10 min. of incubation, the medium containing the non-adherent glomeruli gently transferred to a new culture dish. This procedure was repeated twice. Glomerular preparations were evaluated for purity by light microscopy and were consistently free of tubules.

The glomeruli were harvested by centrifugation at 4°C at 4,500 rpm for 5 min, and were washed once with cold PBS. They were then resuspended in 250 µl lysis buffer (50 mM Tris-HCl pH 7.5, 150 mM NaCl, 1% Nonidet P40, 0.5% sodium deoxycholate, 1x proteinase, 1x PhosStop and 100 nM Cal-A), and incubated on ice for 15 min. To lyse the cells, they were passed through a 28 ½ Gauge needle three times, and centrifuged for 10 min at 18,000 X G. The supernatant (detergent soluble fraction) and pellet (detergent insoluble fraction) were subjected to WB analysis using rabbit anti-P-ERM (anti phospho-Thr567 ezrin, Signalway Antibody LLC, Maryland, USA), rabbit anti-ezrin (Cell Signaling, Danvers, USA), rabbit anti-CLIC5 (Aviva System Biology, San Diego, CA, USA), goat anti-podocalyxin (R&D Systems, Minneapolis, MN USA), mouse anti-β-tubulin (Millipore, Billerica, MA, USA) and mouse anti-β-actin (Sigma, Oakville, ON, Canada) antibodies.

2.18 Immunoprecipitation.

To determine whether CLIC5A is found in the same complex as podocalyxin, co-immunoprecipitation was performed as described by Takeda *et al.* (360). Briefly, glomeruli were homogenized with a Dounce homogenizer in RIPA buffer (0.1% SDS, 1% sodium deoxycholate, 1% Triton X-100, 150 mM NaCl, 2 mM EDTA, 25 mM Tris, pH=7.4) containing complete protease inhibitors (Roche, Laval, QC, Canada). The glomerular lysate was passed through a 26-G needle, and then sonicated. After sedimentation of insoluble material, podocalyxin or CLIC5 was immunoprecipitated in immunoprecipitation (IP) buffer (50 mM Tris, pH=7.4, 150 mM NaCl, 1% NP-40, 0.5% sodium deoxycholate, and complete protease inhibitors). 100 µl of lysate was brought to a volume of 1,000 µl in IP buffer and precleared for 30 min with 10 µl agarose beads [either protein A-Sepharose (Sigma-Aldrich, St. Louis, MO) for CLIC5 IP or protein G plus/protein A-Agarose (Calbiochem, San Diego, CA) for podocalyxin IP]. Lysates

were then incubated overnight at 4°C with 5 µl of affinity-purified anti-CLIC5 polyclonal rabbit antiserum (B132 serum), 5 µg of rat anti-podocalyxin antibody, (R & D Systems, Minneapolis, MN), or the corresponding rabbit preimmune serum or normal rat IgG (Jackson ImmunoResearch Laboratories, West Grove, PA). The B132 monospecific polyclonal rabbit antiserum was prepared by Mark Berrynann (28). Lysates were then incubated with 50 µl of appropriate protein A or protein G beads for 6 h (RT). Bead complexes were washed six times for 2 min each at room temperature. Protein complexes were eluted by boiling for 10 min at 95°C in 2× Laemmli buffer. Precipitated proteins were separated by SDS-PAGE, transferred to Immobilon membranes, and blotted with goat anti-podocalyxin (R & D Systems) and mouse anti-CLIC5 (Abnova, Taipei, Taiwan) antibodies. Blots of whole lysate served as “input controls.” All IPs were repeated three or more times using tissue from different mice.

2.19 Transmission electron microscopy and morphometry.

For immunogold transmission electron microscopy (TEM), kidney cortex from wild-type adult mice was fixed with 0.1% glutaraldehyde and 4% formaldehyde, treated with 50 mM ammonium chloride, postfixed with 2% uranyl acetate, and dehydrated with acetone before embedding in LR Gold resin, as described previously. Sections were incubated with affinity-purified rabbit antibody specific for CLIC5 followed by gold-conjugated goat anti-rabbit IgG (10 nm, Ted Pella) and then counterstained with 2% osmium tetroxide and lead citrate (28).

For conventional TEM, kidneys were removed without perfusion, cortex was cut to produce ~5 × 5 mm cubes, and specimens were prefixed in 2.5% glutaraldehyde in Millonig's buffer solution (pH=7.2) for 1.5 h at room temperature. They were then washed and postfixed with 1% osmium tetroxide in Millonig's buffer solution for 1.5 h. After a brief wash in distilled

water, samples were dehydrated in a graded ethanol series (50%, 70%, 90%, 100%, and 100%, 10 min each). Samples were then embedded in Araldite resin and cured at 60°C for 36 h. Thick sections (1–2 μm) were stained with methylene blue to locate glomeruli by light microscopy. Ultrathin sections were stained with 4% uranyl acetate for 30 min and lead citrate for 5 min and viewed with a Hitachi transmission electron microscope H-7000 (Tokyo, Japan). All glomeruli in a given section were photographed in a blinded fashion. Morphometry was performed by point counting, using a grid with points at 1- μm intervals on one complete glomerular cross-section from each of four CLIC5^{+/+} and four CLIC5^{-/-} mice, 8 months of age. For each image, the complete length of GBM was also quantified by tracing and digitization, and glomerular EC vacuoles were counted. Data were similarly obtained for one CLIC5^{+/+} and one CLIC5^{-/-} mouse aged 3 mo. For immunogold TEM, the density of gold particles associated with specific cells was quantified for glomeruli, peritubular capillaries, and renal arterioles at $\times 24,000$ magnification. The area represented by each cell type was determined by point counting, with grid points spaced at 200-nm intervals. Data were obtained for 10–12 images from each of three separate sections of renal cortex. Statistical analysis was by one-way analysis of variance followed by multiple comparison between groups using the Bonferroni method.

2.20 Adriamycin treatment

Male 12- to 13-week old CLIC5^{+/+} or CLIC5^{-/-} mice were anesthetized with isoflurane inhalation. Adriamycin (10 mg/kg, doxorubicin hydrochloride; Alexis Biochemicals, San Diego, CA) prepared in 200 μl of 0.9% NaCl was then injected via the jugular vein. Mice were allowed to recover, and then water and chow were provided ad libitum. Urine was collected from conscious mice 5 times/week. Spontaneous voiding was stimulated by stroking the suprapubic area. The creatinine concentration in urine was measured with the Creatinine Enzymatic Assay

Kit (DZ072B; Diazyme, San Diego, CA). Urine creatinine was adjusted to 20 mg/dl with distilled water and then diluted 3:1 (vol/vol) in 4X Laemmli buffer and boiled. For mice not treated with adriamycin, the equivalent of 10 μ l of urine was subjected to SDS-PAGE followed by WB analysis with goat anti-mouse albumin antibodies (Bethyl Laboratories, Montgomery, TX). For mice treated with adriamycin, the equivalent of 0.25 μ l of urine (1:40 dilution) was subjected to SDS-PAGE. Urinary albumin was quantified by densitometry of western blots against a standard curve of mouse albumin on the same blots. Statistical comparison of albuminuria after adriamycin treatment was by Student's *t*-test.

Chapter 3

CLIC5A enhances ERM proteins phosphorylation
and association with the actin cytoskeleton

Chapter 3

CLIC5A enhances ERM proteins phosphorylation and association with the actin cytoskeleton¹

3.1 Introduction

The recognition that CLICs associate with ERM proteins began with the identification of CLIC5A in a complex with actin, ezrin, gelsolin, IQGAP1 and α -actinin in a pull-down assay from placental microvilli extract using the ezrin C-ERMAD domain as bait. Confocal imaging showed that CLIC5A immunofluorescence co-localized with ezrin at the apical surface of placental microvilli (28) and also in JEG-3 choriocarcinoma cells transfected with CLIC5A (56).

Positional cloning then identified a deletion in the CLIC5 gene as the disease-causing mutation in Jitterbug mice (jgb/jgb) that showed spontaneous abnormalities in vestibular and cochlear function. In wild-type mice, the CLIC5A isoform was highly concentrated at the base of actin bundles that form sensory stereocilia in cochlear and vestibular hair cells, where it co-localized with the ERM protein radixin. Similarly, CLIC5A is expressed with radixin at a 1:1 ratio in chicken utricle hair cells. In CLIC5^{-/-} mice, CLIC5A was not detected in cochlear and vestibular hair cells, radixin levels were reduced, and progressive stereocilia degeneration was observed, leading to vestibular dysfunction and deafness by 7 months of age (57). It is noteworthy that radixin deficiency similarly causes deafness associated with progressive

¹ Portions of this chapter has been published in a peer-reviewed journal:

Abass Al-Momany, Laiji Li, R. Todd Alexander and Barbara J. Ballermann. *Clustered PI(4,5)P2 accumulation and ezrin phosphorylation in response to CLIC5A*. J Cell Sci. 2014 Dec 15;127(24):5164-78

degeneration of cochlear hair cell stereocilia in mice (98). The genetic mutation in the human radixin gene is also associated with nonsyndromic hearing loss (58). Given that CLIC5 loss results in a defect in mice that is a phenocopy of the radixin deficiency, and that CLIC5A is very abundant in hair cell stereocilia where it co-localizes with radixin, it seems likely that CLIC5A plays a role in preserving radixin levels, and the normal structure and function of stereocilia.

Similarly, CLIC4 is highly expressed, and co-localizes with ezrin in the retinal pigment epithelium (RPE) of the eye. Previous studies showed that suppression of CLIC4 expression in rat RPE results in the loss of apical microvilli, reduced retinal adhesion and epithelial-mesenchymal transition (52). Interestingly, ezrin knockdown in cells, and ezrin deficient mice show a similar phenotype (161,371), suggesting a potential functional and molecular relationship between the two molecules in RPE cells.

Macrophages normally ingest pathogens, foreign particulates and apoptotic cells by phagocytosis. In macrophages, CLIC1 and ezrin co-localize and are coordinately redistributed from cytoplasm to the lipid bilayer of phagosomes during phagocytosis (37). The formation of the macrophage phagosome is regulated by Rho GTPases and ERM proteins (372), and in macrophages from CLIC1 deficient mice phagosome function is impaired (37), suggesting a functional relationship between CLIC1 and ezrin in macrophages.

In the nematode, *C. elegans*, disruption of CLIC homologue Exc-4 results in a cystic enlargement of the excretory cell canal, similar to the morphogenesis defect observed when the ERM homologue ERM-1 is deleted (158,159). These findings in an invertebrate suggest that the postulated functional relationship between CLIC and ERM proteins is evolutionarily conserved.

ERM proteins are key determinants of cortical cell morphology. This function is due to the

ability of ERM proteins to link several integral plasma membrane proteins to cortical F-actin. This process involves distinct interactions between the ERM N-terminus with cell membrane proteins, and the ERM C-terminus with F-actin. Several studies have shown that ERM proteins are enriched in actin-based cellular projections like microvilli, filopodia, uropods, membrane ruffles, and in areas where actin is associated with the plasma membrane such as retraction fibers, and cell adhesion (82,83,96,100,175). Suppression of ERM protein expression abolishes microvillus formation as well as cell-to-cell and cell-to-substrate adhesion in cultured fibroblasts and epithelial cells (160). On the other hand, overexpression of full-length ERM proteins seems to enhance cell adhesion, while overexpression of the ERM C-terminus alone perturbs cell surface morphology and inhibits cytokinesis (95,172). Further, overexpression of the ezrin N-terminal domain prevents microvilli formation (144). Several conditions, for instance anoxia and apoptosis, can cause ezrin to dissociate from the actin cytoskeleton (131,132). Oxidative stress also induces dissociation of ezrin from plasma membrane proteins, actin or both, and the dissociated (inactive) form of ezrin is susceptible to proteasomal degradation (373),.

Considering the body of evidence showing a potential functional relationship between ERM and CLIC proteins in general, and the specific findings that CLIC5A, in conjunction with radixin, plays a role in organizing and maintaining actin-based sensory stereocilia in the inner ear, the first set of objectives I pursued was as follows:

- 1. Explore the effect of CLIC5A on ERM protein phosphorylation and association with actin cytoskeleton**
- 2. Explore the effect of CLIC5A on cell morphology.**

3.2 Results

3.2.1 Increased ERM proteins phosphorylation in COS-7 cells expressing CLIC5A.

Since the inactive (dephosphorylated) form of ERM proteins may be susceptible to degradation (373) and the level of ERM protein radixin in the inner ear of stereocilia of CLIC5^{-/-} mice is reduced, I postulated that CLIC5A might regulate ERM protein phosphorylation and stability. I took advantage of the fact that CLIC5A is not expressed in most cell types, allowing me to study the function of ectopically expressed CLIC5A. I used COS-7 cells, which lack detectable endogenous CLIC5A and transfected them transiently with pcDNA3.1-CLIC5A or empty vector and evaluated ERM phosphorylation. Western Blot (WB) analysis showed that, total ezrin levels were similar in total cell lysates prepared from CLIC5A- and vector-transfected cells, but the abundance of phosphorylated ERM (P-ERM) proteins was significantly greater in cells expressing CLIC5A than in vector-transfected cells (Figure 3.1.A). Two P-ERM protein bands corresponding to P-Ezrin and P-Moesin, based on their respective molecular mass of 81 kDa and 80 kDa, were observed in COS-7 cells, and both were hyperphosphorylated in the presence of CLIC5A. Densitometric quantification showed that the ratio of P-ERM to total ezrin increased approximately three-fold in COS-7 cells expressing ectopic CLIC5A, compared to vector transfected cells (Figure 3.1-B). Similar result was observed in HeLa cells transfected with CLIC5A (Figure 3.1-C). These data indicate that expression of CLIC5A in COS-7 and in HeLa cells results in enhanced phosphorylation of ezrin and moesin.

To evaluate ERM phosphorylation, I also used confocal immunofluorescence (IF) microscopy, and observed that P-ERM immunofluorescence was greater in COS-7 cells transfected with CLIC5A compared to cells in the same monolayer that remained un-transfected

(Figure 3.2.A). Similar results were observed when COS-7 cells were transfected with naturally fluorescent GFP-CLIC5A (Figure 3.2.B). These data indicate that ectopic CLIC5A and GFP-CLIC5A expression in COS-7 cells results in enhanced ERM phosphorylation.

3.2.2 Increased ERM proteins cytoskeletal association in COS-7 cells expressing CLIC5A.

Several previous studies have shown that phosphorylated ERM proteins associate with F-actin (79,374). Since ectopic expression of CLIC5A significantly increased the level of P-ERM in total cellular lysates, I determined whether CLIC5A also alters the association of the ERM protein ezrin with the Triton X-100 insoluble cytoskeletal fraction. WB analysis showed that the level of total ezrin and P-ERM associated in the cytoskeletal fraction of COS-7 cells was much greater when the cells were transfected with CLIC5A, compared to vector-transfected control cells (Figure 3.3.A). Densitometric quantification showed that there was approximately four-fold more P-ERM in the detergent insoluble fraction of cells over-expressing CLIC5A than in cells transfected with vector alone (Figure 3.3.B).

Similarly, when cytoskeletons were prepared by removing detergent-soluble material from attached cells, a highly significant increase in total ezrin and P-ERM was observed in the cytoskeletons of CLIC5A transfected COS-7 cells compared to cells transfected with vector alone (Figure 3.3.C). Densitometric quantification showed approximately six-fold more P-ERM associated with cytoskeletons of cells over-expressing CLIC5A than in cells transfected with vector alone (Figure 3.3D.). Since total ezrin abundance in whole cell lysates was unchanged when CLIC5A was expressed (Figure 3.1.A), the results indicate that a greater fraction of ezrin is phosphorylated and associated with the cytoskeleton, in the presence of CLIC5A.

3.2.3 CLIC5A overexpression does not alter the half-life of ezrin in COS-7 cells.

Ezrin is a long-lived protein with a half-life much greater than 24 hrs. Ezrin degradation occurs through the proteasomal pathway (373). Previous reports showed that the inactive form of ezrin is more susceptible to degradation than activated ezrin. Since there was a significant reduction in the level of the ERM protein radixin in the inner ear stereocilia of CLIC5^{-/-} mice than in wild-type mice, it seemed logical to postulate that CLIC5A might enhance the stability of ERM proteins by maintaining them in the active, phosphorylated state. To explore the effect of CLIC5A on ezrin half-life, COS-7 cells were transfected with either CLIC5A or empty vector. Two days after transfection the cells were treated with 50 mg/ml cyclohexamide (CHX) for 24, 48 and 72 hours to inhibit new protein synthesis. WB analysis of total cellular lysate for ezrin, tubulin and CLIC5A showed that overexpression of CLIC5A did not change the rate of the decline of total ezrin abundance in total cell lysates relative to the control cells transfected with vector alone (Figure 3.4). It was also of note that the abundance of CLIC5A declined significantly during the 72 hours of cycloheximide treatment.

3.2.4 Actin polymerization and dorsal remodeling in CLIC5A-transfected COS-7 Cells

It is well established that ezrin phosphorylation can induce the formation of actin-rich apical protrusions (82,83,96,100,175). We therefore determined whether ectopic CLIC5A expression in COS-7 cells, which enhances ERM phosphorylation, also alters actin polymerization and the dorsal cell architecture. COS-7 cells were co-transfected with YFP-actin and CLIC5A or with YFP-actin and empty vector. To increase the probability of co-transfection, cells were transfected at a ratio of 10:1, CLIC5A (or empty vector) : YFP actin cDNA. Cells were examined by live cell confocal microscopy 48 hours later. Substantially more YFP-actin had organized into long filaments in CLIC5A transfected, than in control vector transfected cells

(Figure 3.5.A). In agreement with the live cell imaging data, scanning electron microscopy (SEM) showed many cell-surface ruffles in CLIC5A, but not in vector-transfected cells (Figure 3.5.B). The rhodamine phalloidin staining similarly showed an increase in polymerized actin in CLIC5A-, compared to vector-transfected cells (Figure 3.5.C). These data indicate that CLIC5A overexpression increases actin polymerization and remodeling of the dorsal cell surface, characterized by the formation of actin-based apical projections.

3.2.5 CLIC5A N- and C-terminal deletion mutants fail to stimulate ERM proteins phosphorylation

We next determined whether CLIC5A N- or C-terminal deletions would alter the functional effect on ERM phosphorylation. Three mutant forms of CLIC5A cDNA were produced using PCR: CLIC5A²²⁻²⁵¹, in which the first β -pleated sheet is deleted; CLIC5A⁵⁵⁻²⁵¹ in which the first β -pleated sheet along with the putative membrane-spanning domain are deleted; and CLIC5A¹⁻²³² in which the N-terminal 9th α -helix is were deleted. The CLIC5A mutant proteins were expressed in COS-7 cells followed by western blot analysis.

In contrast to wild-type CLIC5A, none of the deletion mutants supported enhanced ERM phosphorylation in COS-7 cells (Figure 3.6). The mutant CLIC5A proteins also did not achieve the level of expression obtained for full-length CLIC5A (Figure 3.6), leaving open the possibility the functional defect is related, in part, to low levels of expression. It is also possible that the CLIC5A mutants are more susceptible to degradation compared to full-length CLIC5A.

3.2.6 CLIC1 and CLIC4 also enhance ERM phosphorylation.

CLIC proteins are highly homologous, and all can associate with phospholipid bilayers. We therefore wondered whether other CLIC proteins could facilitate ERM protein

phosphorylation. Both CLIC1 and CLIC4 proteins are expressed at baseline in COS-7 cells. Overexpression of either CLIC1 or CLIC4 enhanced ERM phosphorylation (Figure 3.7), albeit to a lesser extent than that observed with CLIC5A. Nonetheless, the data raise the possibility that CLIC5A, CLIC1 and CLIC4 all share a similar mechanism of action in regulating ERM phosphorylation.

3.3 Discussion

In this component of the work, I showed several lines of evidence that all support the concept that CLIC5A stimulates ERM protein activation. CLIC5A expression led to increased ERM protein phosphorylation, increased ERM protein association with the cytoskeleton, increased actin polymerization and the formation of cell-surface ruffles. These functions were observed for CLIC5A, and the findings that CLIC1 and CLIC4 overexpression also enhanced ERM protein phosphorylation suggest that ERM protein activation may be a function shared generally by CLIC proteins. Several previous reports had highlighted the association between CLIC and ERM proteins (28,37,52,56), but a functional interaction between them was not previously demonstrated.

The CLIC5A mRNA and protein are extremely abundant in renal glomeruli. Ezrin is the most abundant ERM protein in glomerular podocytes. It localizes to the apical domain of podocyte foot processes where it couples podocalyxin to cortical F-actin. In endothelial cells, moesin is the predominant ERM protein (81). Moesin is required for the maintenance of the endothelial cell barrier (375) and it couples adhesion molecules to cortical actin (376). In mammalian endothelial cells CLIC4 is required for hollowing of capillaries *in vitro* (48), and in endothelial cells derived from CLIC4 deficient mice, lumen formation is impaired (377). CLIC1 plays a role in branching morphogenesis during vascular development (378). Chalothorn *et al* (379) reported that the vascular density is reduced in CLIC4, but not CLIC1 deficient mice, and that a compensatory increase in endothelial cell CLIC1 expression seems to compensate for the lack of CLIC4 in CLIC4^{-/-} mice (379). Thus, both ERM and CLIC proteins play a role in defining endothelial cell morphogenesis.

My data showed that similar to CLIC5A, CLIC1 and CLIC4 overexpression in COS-7 cells enhanced ERM phosphorylation (Figure 3.7). Cultured bovine glomerular endothelial cells express CLIC5A at levels ~30 fold higher than aortic endothelial cells (380). In order to determine whether CLIC1, CLIC4 or CLIC5A can enhance phosphorylation of moesin in glomerular endothelial cells, the expression of CLIC1, CLIC4 and CLIC5A will need to be silenced or deleted individually or in combination followed by evaluation of moesin activation.

The hypothesis that CLIC5A regulates ERM phosphorylation was based on the previous finding that CLIC5A co-localizes with the ERM protein radixin in the sensory stereocilia of cochlear and vestibular hair cells, and that the absence of CLIC5A in CLIC5^{-/-} mice was accompanied by reduced levels of radixin and morphological as well as functional changes, including a reduced number of stereocilia and progressive hearing loss and deafness (57), identical to those previously observed in radixin deficient mice (98). Also, a previous study showed that while ezrin has a relatively long half-life, its inactive, dephosphorylated form is more susceptible to degradation than the active, phosphorylated form (373). Therefore, it seemed plausible that the reduction of radixin abundance in sensory stereocilia of CLIC5 deficient mice reflects increased degradation of inactive radixin. However, whereas ectopic CLIC5A expression in COS-7 cells leads to a substantial, and highly reproducible increase of ERM protein phosphorylation and association with the cytoskeletal fraction (Figure 3.3), the overall ezrin abundance (Figure 3.1), and the rate of ezrin degradation did not appear to change in the presence of CLIC5A (Figure 3.4). It therefore seems that the degree of ezrin phosphorylation in cells is not the only factor controlling its degradation rate. A possible explanation for the findings in figure 3.4 is that the pool of inactive ezrin in cultured cells is much larger than the pool of active, phosphorylated ezrin, even in the presence of CLIC5A. If

this were the case, then any change in the rate of degradation of total ezrin might not be detectable. A more likely explanation is that cycloheximide treatment also led to a significant, time-dependent decline in CLIC5A protein abundance. In fact, ezrin seemed to be more stable than CLIC5A when new protein synthesis was inhibited. The decline in CLIC5A abundance during protein synthesis inhibition would be expected to abrogate any effect of CLIC5A on ezrin phosphorylation and stability. Finally, it is also possible that forty eight hours of CLIC5A expression and seventy two hours of protein synthesis inhibition are not long enough to recapitulate the *in vivo* findings showing that CLIC5A deficiency leads to a progressive reduction of ERM abundance.

The activity of ERM proteins is regulated by phosphorylation-dephosphorylation cycles. It is known that activation of ERM proteins is a stepwise process which requires initial binding of the ERM N-terminus to membrane PI(4,5)P₂, followed by phosphorylation of conserved threonine residues in the ERM C-terminus. The interaction with PI(4,5)P₂ exposes the binding site for plasma membrane proteins at the ERM N-terminus and for actin at the ERM C-terminus. Phosphorylation of the ERM protein seems to stabilize the interaction with F-actin. Previous experiments showed that dephosphorylated, inactive ezrin did not co-precipitate with any proteins from gastric gland lysate (381), while phosphorylation of ezrin at T567 increased F-actin binding and enhanced membrane protein binding (382). Similar results were also observed with the other members of ERM protein family radixin and moesin. The T558D mutant of moesin, mimicking the phosphorylated protein, binds to F-actin more strongly than non-phosphorylated wild-type moesin *in vitro* (75,130,133,152,383,384). Experiments in this study showing a significant increase in ERM protein phosphorylation and a concomitant increase in P-

ERM and ezrin association with the cytoskeleton (Figure 3.3) are consistent with such prior work, and indicate that CLIC5A, in some way leads to increased ERM protein activation.

Several studies have shown that the active, phosphorylated ERM proteins localize to lipid membranes (123,385), and that activation of ERM proteins is associated with a reorganization of the cell cortex. In agreement with the published data, confocal immunofluorescence showed that CLIC5A overexpression resulted in the redistribution of P-ERM into clusters that also contained CLIC5A, likely representing cellular projection. By contrast, P-ERM in vector-transfected cells (Figure 3.2) was much less abundant and few P-ERM clusters were observed in the absence of CLIC5A. Zhu *et al* showed that overexpression of the phospho-mimic T567D ezrin mutant in cultured primary renal tubule epithelial cells resulted in the formation of long, cell-surface structures that accumulated where the T567D mutant was localized (386). Similar to the ezrin T567D mutant, overexpression of CLIC5A in COS-7 cells induced the formation of surface projections, as determined by SEM. The P-ERM and F-actin co-localized with CLIC5A in these projections (Figures 3.2 and 3.5.C), suggesting an active process of actin polymerization and remodeling of the cell surface.

The formation of actin-based cellular extensions such as microvilli, pseudopods and lamellipodia depends mainly on rapid polymerization of actin (387-389). Several actin-binding proteins regulate the formation of F-actin for mechanical support, and rapid turnover of actin polymerization-depolymerization cycles is needed for physiological processes that require cell motility (390-392). The members of band 4.1 superfamily like talin, vinculin and the ERM proteins all are actin binding proteins that interact directly with actin and with PI(4,5)P₂. It is important to note that all of these proteins thought to be involved in regulating the assembly of actin on membrane projections bind PI(4,5)P₂ (103,204,393,394). In a similar fashion, the ERM

proteins are essential for actin assembly by phagosomes (395). Furthermore, ezrin can accelerate pyrene-stimulated actin assembly *in vitro* (396-398). In this assay, actin assembly and ezrin binding to actin was prevented by an anti-ezrin antibody. Also, N-terminal (13–30) and C-terminal (534–586) ezrin deletion mutants do not support actin polymerization and both of the mutants block *in vitro* ezrin–F–actin interactions (77,398) and inhibit the formation of cellular projections (144). Similar to ezrin, an antibody against moesin also partially inhibited actin assembly by phagosomes (398).

In this study, I observed that CLIC5A expression led to increased YFP-actin assembly, in live cell imaging experiments, and increased actin polymerization based on phalloidin staining of F-actin. These findings suggest that CLIC5A may play an important role in actin assembly or at least in the stability of F-actin. Since CLIC5A also stimulated phosphorylation of ERM proteins, it seems likely that the effect of CLIC5A on actin polymerization is due to CLIC5A-stimulated ERM protein activation. Several previous reports would also support this interpretation. First, CLIC5A and ERM proteins are enriched and colocalized in sites where the process of actin polymerization occurs, such as placental microvilli and the stereocilia of inner ear hair cells. Second, the absence of CLIC5A results in a reduced number of stereocilia in inner ear hair cells (28,57). However, the data leave open the following question: Through what mechanism(s) does CLIC5A regulate the activity of ERM proteins, and consequently the formation of membrane projections? This question will be explored in detail in the next chapter.

3.4 Figures

Figure 3.1

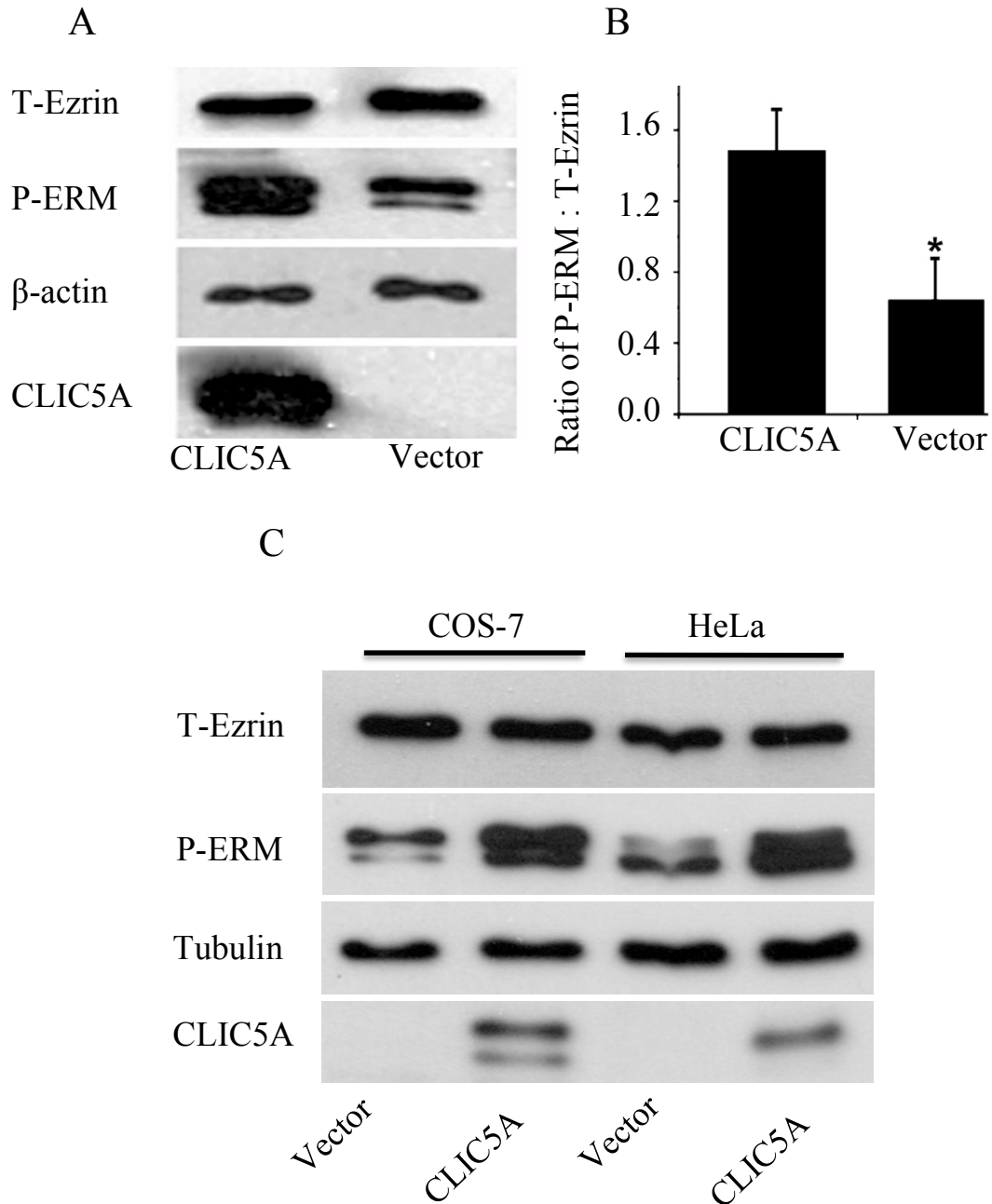
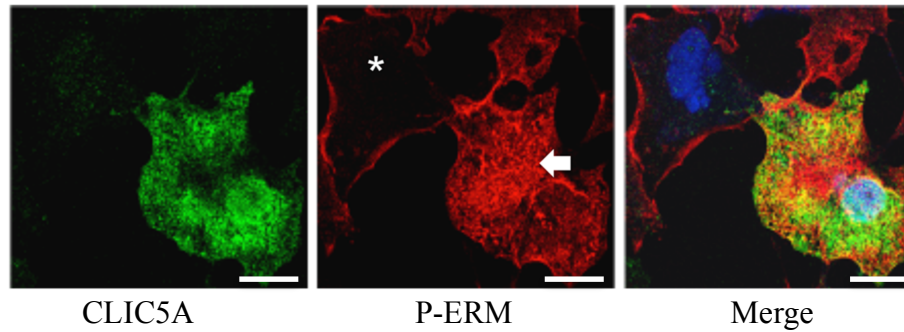


Figure 3.1. Increased abundance of P-ERM in COS-7 and HeLa cells transfected with CLIC5A. **A-** Western Blot (WB) analysis of total ezrin and P-ERM in COS-7 cells transfected with either CLIC5A or empty vector. **B-** Densitometric analysis of P-ERM in CLIC5A or empty vector transfected COS-7 cells (means \pm S.E.M; n=3, p=0.036). **C-** WB analysis of total ezrin and P-ERM in COS-7 and HeLa cells transfected with either CLIC5A or empty vector.

Figure 3.2

A



B

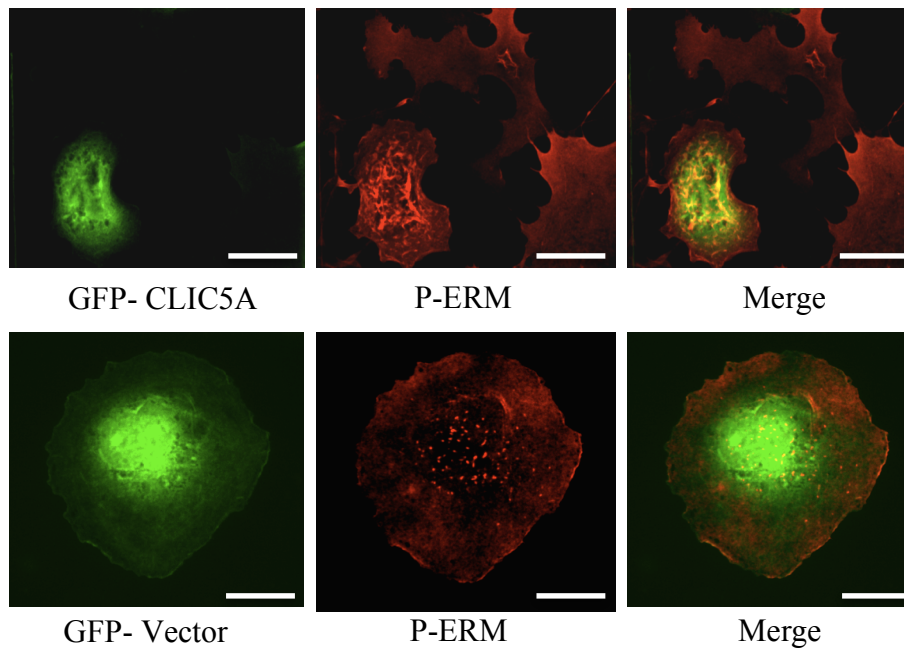


Figure 3.2. *Redistribution P-ERM in COS-7 cells transfected with CLIC5A.* **A-** Confocal Immuno-fluorescence of COS-7 cells transfected with CLIC5A. CLIC5A and P-ERM were detected by rabbit anti-CLIC5A or mouse anti-P-ERM antibodies. **B-** Natural fluorescence of GFP (green) was used to detect GFP-CLIC5A and GFP-vector. The arrow in A shows enhanced P-ERM proteins (red) in CLIC5A transfected cells relative to non-transfected cells (star). Scale bar =10 μ m

Figure 3.3

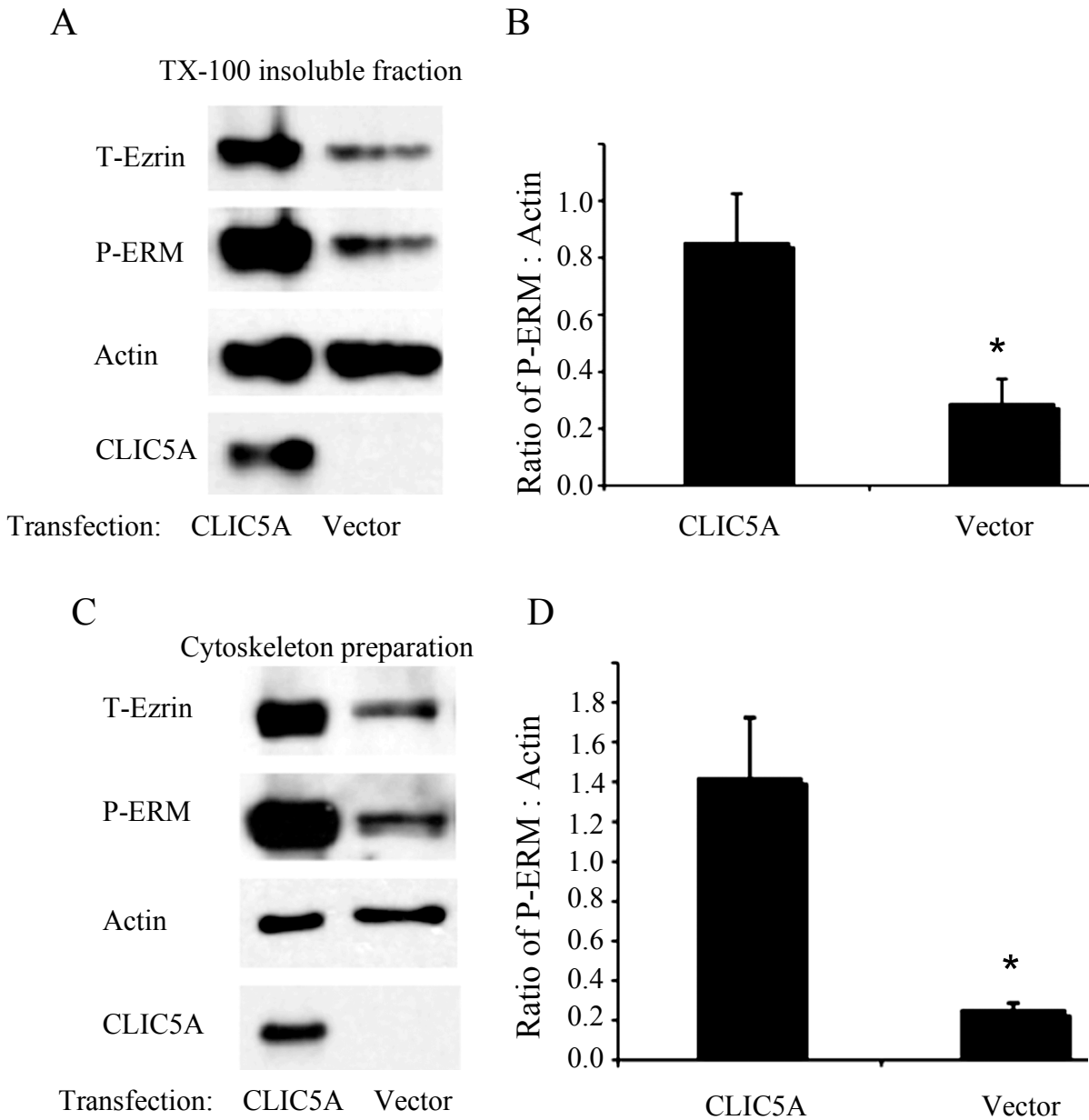


Figure 3.3. *CLIC5A* overexpression enhances *ERM* association with cytoskeleton. **A-** Western Blot (WB) analysis of total ezrin (T-Ezrin) and P-ERM in TX-100 insoluble fraction of COS-7 cells transfected with either *CLIC5A* or empty vector. **B-** Densitometric analysis of P-ERM in *CLIC5A* or empty vector transfected COS-7 cells (means \pm S.E.M; n=4, P=0.024). **C-** WB analysis of total ezrin and P-ERM in cytoskeleton preparation of COS-7 cells transfected with either *CLIC5A* or empty vector. **D-** Densitometric analysis of P-ERM in *CLIC5A* or empty vector transfected COS-7 cells (means \pm S.E.M; n=3, P=0.018).

Figure 3.4

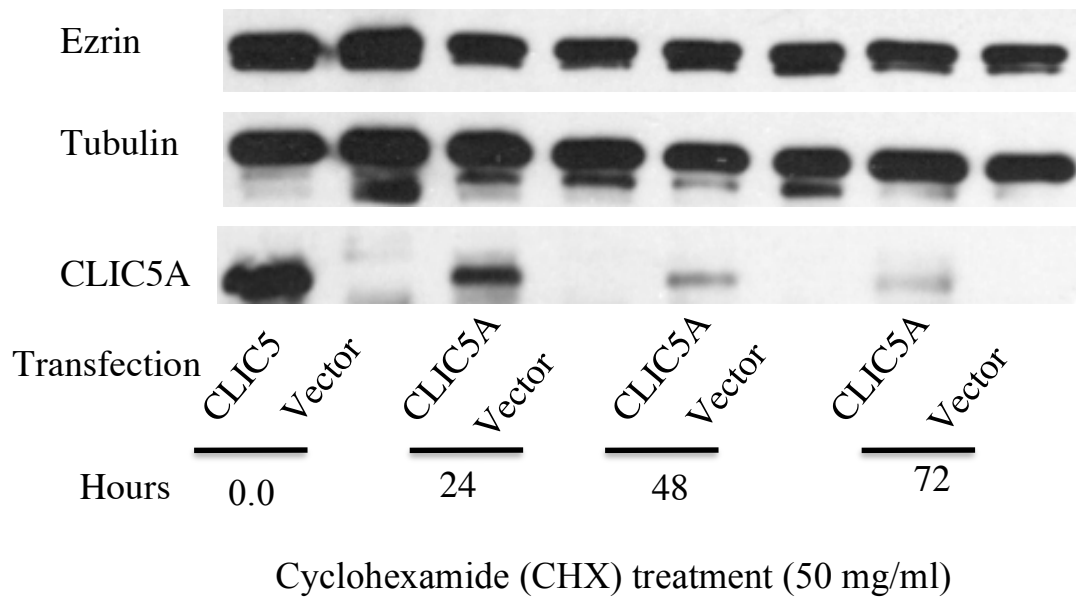


Figure 3.4. *CLIC5A* overexpression did not alter ezrin stability in COS-7 cells. WB analysis of total cellular lysate from cells transfected with either CLIC5A or empty vector. Two days after transfection, cells were treated with Cyclohexamide (CHX) 50mg/ml for several time points.

Figure 3.5

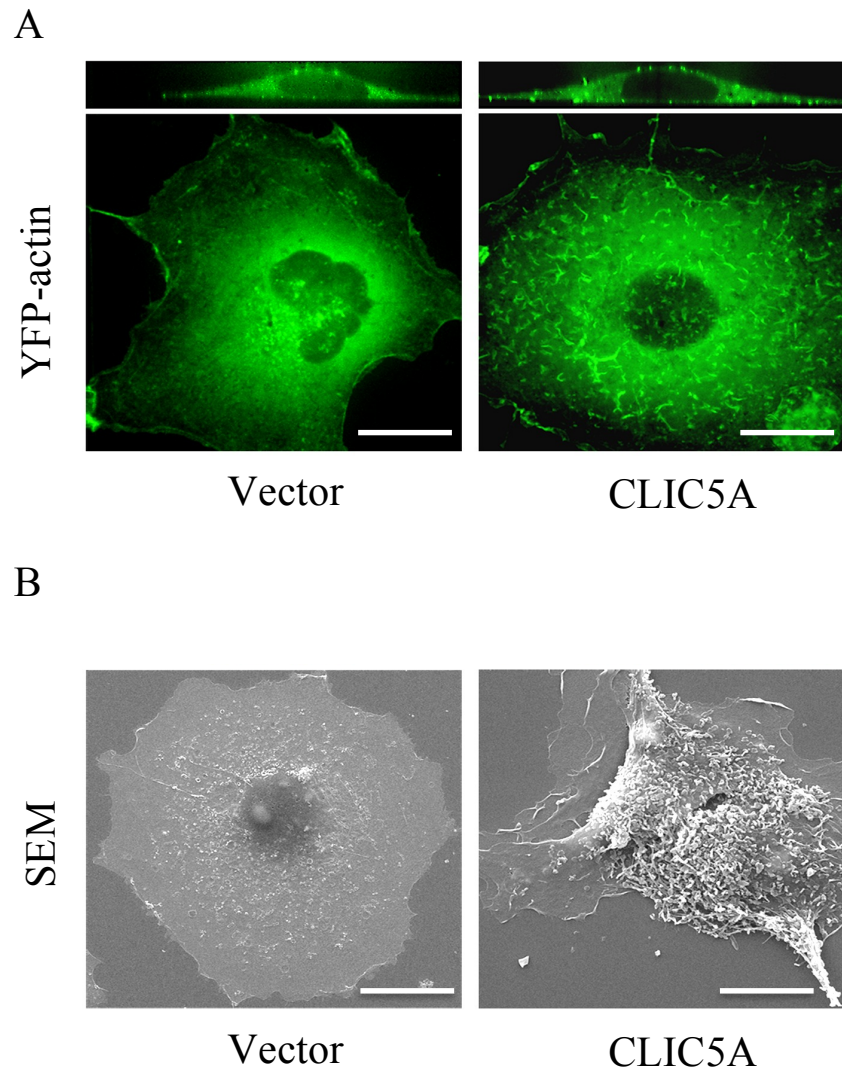


Figure 3.5. *Transfection of CLIC5A enhances the formation of actin based membrane projections.* (A) COS-7 cells were co-transfected with YFP-actin and either CLIC5A or vector. Actin-based membrane projections were visualized by natural YFP using Confocal live cell imaging. (B) Scanning Electron Microscopy (SEM) images for the COS-7 cells transfected with either CLIC5A or vector alone. Scale bar = 10 μ m

C

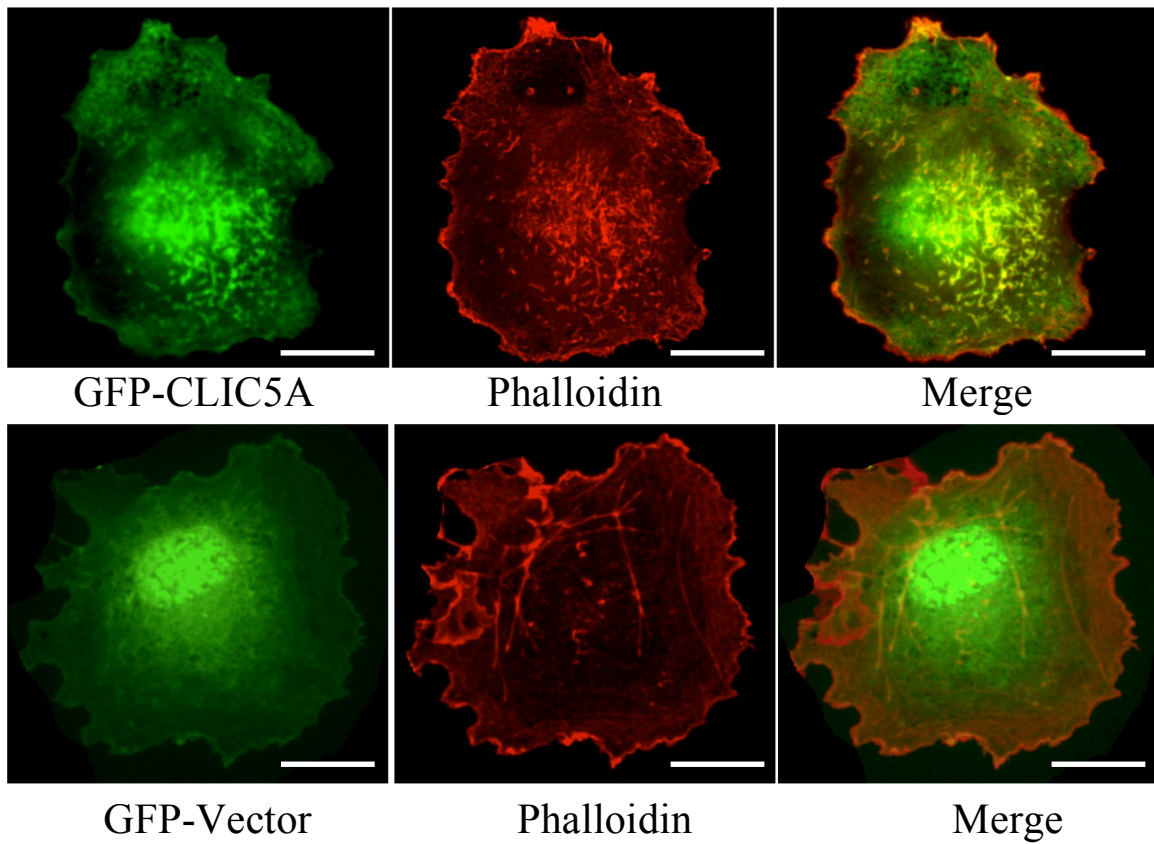


Figure 3.5 Transfection of *CLIC5A* enhances the formation of actin based membrane projections. (C) Confocal microscopy analysis for the COS-7 cells transfected with either GFP-*CLIC5A* or GFP-vector alone and stained with rhodamin-phalloidin.

Figure 3.6

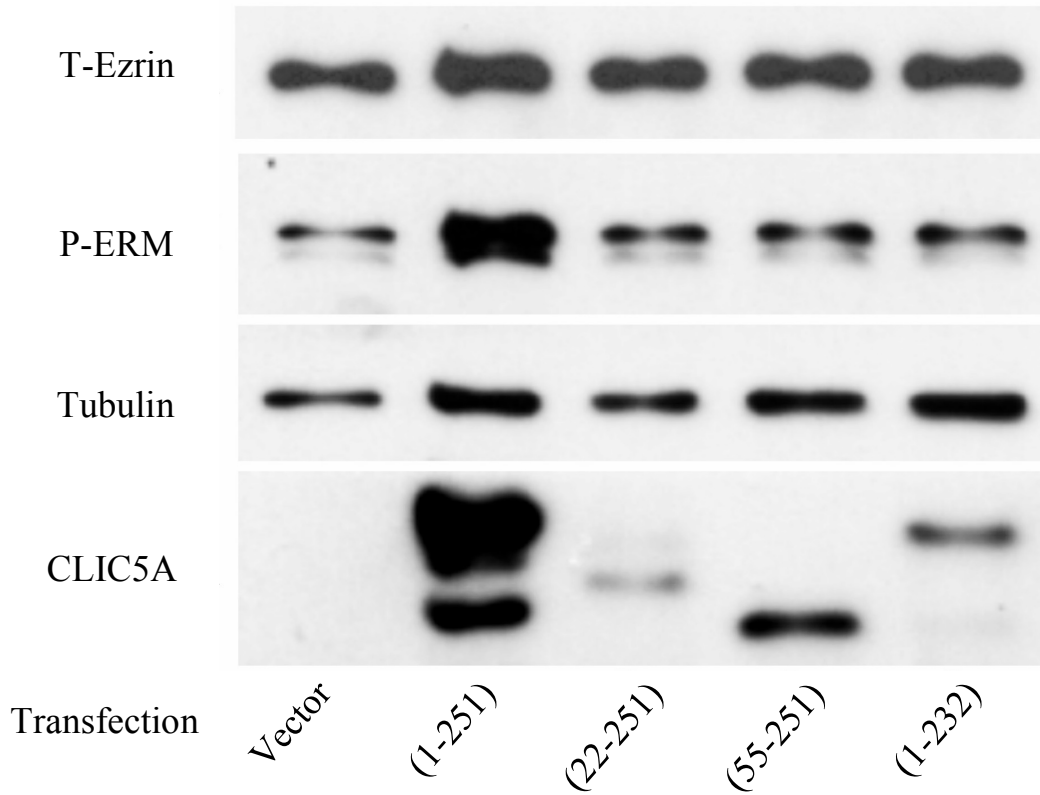


Figure 3.6. *CLIC5A* mutants fail to augment *ERM* phosphorylation. COS-7 cells were transfected with full-length wild-type *CLIC5A* (1-251) or *CLIC5A* mutants in which the first β -pleated sheet (22-251), the first β -pleated sheet and the putative trans-membrane domain (55-251) or the 9th α -helical domain (1-232) had been deleted, Western blot analysis of SDS-solubilized COS-7 cells performed 48 hours after transfection with full-length wild-type *CLIC5A* or *CLIC5A* mutants. Full-length *CLIC5A* induced *ERM* phosphorylation, but the *CLIC5A* deletion mutants did not.

Figure 3.7

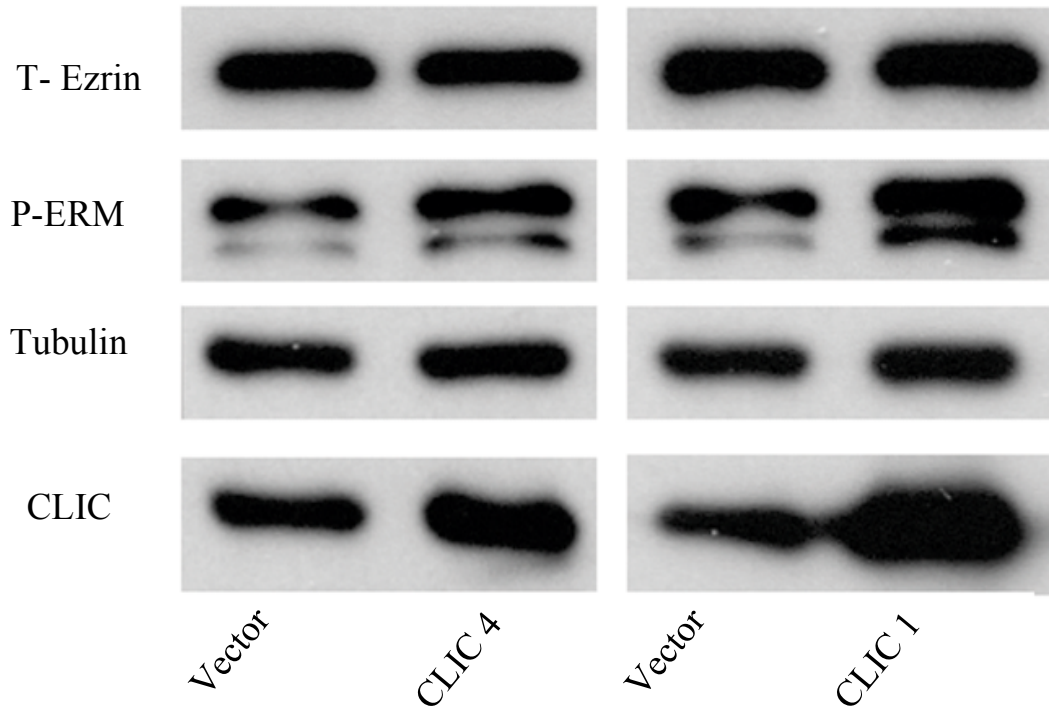


Figure 3.7. *CLIC1 and CLIC4 overexpression also enhance ERM phosphorylation.* WB analysis of P-ERM in total cellular lysate of COS-7 cells transfected with either CLIC 1 or CLIC 4 shows both CLIC1 and CLIC4 proteins are expressed at baseline in COS-7 cells and overexpression of either CLIC1 or CLIC4 enhances ERM phosphorylation.

Chapter 4

CLIC5A-stimulated ERM phosphorylation is mediated by dorsal phosphatidyl (4,5) bisphosphate clustering, a novel function independent of CL^- channel activity

Chapter 4

CLIC5A-stimulated ERM phosphorylation is mediated by dorsal phosphatidyl (4,5) bisphosphate clustering, a novel function independent of CL^- channel activity²

4.1 Introduction.

It is well established that ERM proteins function to link integral membrane proteins to cortical F-actin, and that this process is controlled by ERM protein activation. ERM protein activation requires the release of an auto-inhibitory interaction between the N-terminal FERM domain and the C-terminus of the ERM proteins, freeing the N-ERMAD and C-ERMAD (N- and C-terminal ERM association domains) so that they can interact with their respective binding partners (Figure 1.2). The conformational change that leads to the release of the N-ERMAD and C-ERMAD is regulated by two molecular events: docking of the ERM protein N-terminus on PI(4,5)P₂, and subsequent phosphorylation of a critical C-terminal Thr residue.

Several studies have highlighted the importance of PI(4,5)P₂ in the functional activation of ERM proteins (105,119,120). The role of phospholipid in ERM regulation arose from a study that indicated that the N-ERMAD of ezrin binds the phospholipid PI(4,5)P₂ and that this binding increases its interaction with plasma membrane proteins (103). The isolated N-ERMAD domain of ezrin was found to bind the cytoplasmic tail of CD44 in the absence of PI(4,5)P₂, but binding of full-length ezrin to CD44 required PI(4,5)P₂, suggesting that a PI(4,5)P₂-dependent conformational change facilitates the ezrin-CD44 interaction (105). Likewise, PI(4,5)P₂ also

² Portions of this chapter has been published in a peer-reviewed journal:

Abass Al-Momany, Laiji Li, R. Todd Alexander and Barbara J. Ballermann. *Clustered PI(4,5)P₂ accumulation and ezrin phosphorylation in response to CLIC5A*. J Cell Sci. 2014 Dec 15;127(24):5164-78

induces and enhances the interaction of ezrin with the cytoplasmic domains of ICAM-1 and ICAM-2 (112), and PI(4,5)P2 enhances the binding of moesin to CD93 (118). It has also been reported that an increase in the production of PI(4,5)P2 as a result of over-expression of PI4P5K enhanced ERM phosphorylation at the conserved C-terminal Thr. Conversely, downward titration of PI(4,5)P2 levels by microinjection of the aminoglycoside neomycin, results in ERM dephosphorylation, its translocation away from microvilli to the cytoplasm, and loss of cell-surface microvilli (120). The binding site for PI(4,5)P2 has been mapped to the lysine residues K63, K64, K253, K254, K262 and K263 in the N-FERM domain of ezrin and site-directed mutagenesis of these sites showed that they are required for PI(4,5)P2 binding and proper sub-cellular localization of ezrin to the membrane (119).

The ERM are phosphoproteins that can be phosphorylated at serine/threonine or tyrosine residues in response to different stimuli in many cell types. The activating phosphorylation of the highly conserved C-terminal Thr residue in all ERM proteins (Ezrin Thr567, Radixin Thr564 and Moesin Thr558) can be phosphorylated both *in vivo* and *in vitro* by numerous kinases including Rho kinase (133,134), PKC α (135), PKC θ (136,137), NIK/Nck-interacting kinase (139), LOK/lymphocyte-oriented kinase (140), MST4/Mammalian STE-20 like kinase 4 (141) and AKT2 (138). Phosphorylation of this critical C-terminal Thr residue reduces the affinity of the ERM C-terminal domain for the FERM domain (133,137), thereby preventing the head-to-tail auto-inhibitory interaction that makes ERM proteins inactive. The initial interaction between the FERM domain of ERM and PI(4,5)P2 unmask the C-terminal phosphorylation site and indicates that PI(4,5)P2 binding and Thr phosphorylation act in a sequential manner to activate ezrin (123). The C-terminal phosphorylation of ERM proteins is associated with their redistribution from the cytoplasm to cell membranes and enhanced binding to F-actin. Several

studies have shown that the ability of ERM to induce cell surface projections and to interact with plasma membrane proteins as well as cytoskeleton is controlled by ERM activation. For instance, RhoA activation in 3T3 fibroblasts results in C-terminal radixin phosphorylation by Rho associated kinase (ROCK) and relocalization of radixin to apical microvilli-like structures (128,133). Also, in activated platelets, the ERM protein moesin is phosphorylated by PKC at the C-terminal Thr558, and this phosphorylated moesin co-localizes with actin filaments in filopodia that form during platelet activation (399). Thus, a two-step model was proposed for ERM activation involving recruitment of ERM to the membrane by PI(4,5)P2 followed by subsequent phosphorylation of the conserved threonine residue in the C-ERMAD (123,400).

ERM proteins are also phosphorylated at other residues. For example, ERM protein can be phosphorylated on Tyr residues in response to hepatocyte growth factor (HGF) and epidermal growth factor (EGF), resulting in recruitment of ezrin to membrane ruffles and microvilli and increased cellular motility. The findings that the HGF-induced cell motility response is suppressed by site-directed mutagenesis of ezrin replacing Tyr145 and Tyr353 with Phe (144-146) suggest that Tyr phosphorylation may also activate ezrin. Ezrin is also phosphorylated at Thr235 in response to pRb-induced senescence by cyclin dependent kinase 5 (cdk5) (142), but the functional significance of this phosphorylation is unclear.

Results shown in chapter 3 clearly demonstrate that ectopic expression of CLIC5A in COS-7 cells stimulates ERM protein phosphorylation and association with actin cytoskeleton. Experiments in this chapter are designed to accomplish the following objective:

To elucidate the signaling pathway(s) that is (are) involved in CLIC5A mediated ERM protein phosphorylation.

4.2 Results

4.2.1 PKC is the main kinase involved in ERM phosphorylation in COS-7 cells.

It was previously reported that both PKC and ROCK can phosphorylate ERM proteins on their conserved C-terminal Thr residue (374). To explore which kinase(s) is (are) involved in ERM phosphorylation in COS-7 cells, untransfected COS-7 cells were treated with the PKC inhibitor Staurosporine (SSP), the ROCK inhibitor Y27632, and with the protein phosphatase 1 inhibitor Calyculin A (Cal-A). WB analysis of total cellular lysate (TCL) (Figure 4.1-A) and cytoskeleton preparations (Figure 4.1-B) showed that in the presence of Cal-A, P-ERM abundance increased substantially, indicating that Cal-A sensitive phosphatases actively dephosphorylate ERM proteins in COS-7 cells. Conversely, SSP rapidly and significantly reduced ERM phosphorylation, while Y27632 was essentially without effect. These results indicate that PKC is the principal kinase phosphorylating ERM proteins in COS-7 cells, at least under the conditions evaluated in these studies.

4.2.2 CLIC5A does not alter the abundance of phosphorylated PKC.

The previous experiment shows that PKC is the main kinase involved in ERM protein phosphorylation in COS-7 cells. Activation of PKC requires a priming phosphorylation on Ser660, which dissociate it from actin cytoskelton. The primed, dissociated form of PKC re-distributes from cytoplasm to plasma membrane during its activation by Ca^{+2} and diacyl glycerol (DAG) (401). Here, I evaluated the effect of CLIC5A on PKC Ser660 phosphorylation. WB analysis of total cellular lysates prepared from COS-7 cells transfected with CLIC5A or empty vector did not detect any difference in the level of P-PKC between CLIC5A- and vector transfected cells (Figure 4.1-C). This finding indicates that the effect of CLIC5A on ERM

phosphorylation is not explained by enhanced PKC phosphorylation, but this fact does not exclude a potential role for CLIC5A in the final step of activation.

4.2.3 CLIC5A does not inhibit ERM phosphatases

To determine whether the increase in ERM phosphorylation in response to CLIC5A could be due to the inhibition of ERM phosphatases, I evaluated the rate of ERM dephosphorylation during PKC inhibition. WB analysis of TCL showed that the abundance of P-ERM in total cellular lysate declined rapidly in both CLIC5A and vector-transfected cells treated with SSP, without change in total ezrin abundance (Figure 4.2-A). The ratio of P-ERM to total ezrin, was quantified by densitometry and expressed as the fraction remaining as a function of time after SSP addition. This analysis showed that the rate of ERM dephosphorylation did not differ between COS-7 cells expressing CLIC5A and those transfected with vector alone (Figure 4.2-B). These findings suggest that the increase in ERM phosphorylation in cells expressing CLIC5A cannot be attributed to inhibition of ERM phosphatase(s) by CLIC5A. Interestingly, the abundance of the CLIC5A immunoreactive band also declined upon SSP addition. This finding implies either that CLIC5A is very rapidly degraded during SSP treatment, and/or that it undergoes a conformational change that reduces the antibody reactivity upon PKC inhibition.

4.2.4 The Cl^- channel inhibitor IAA-94 does not block CLIC5A-stimulated ERM phosphorylation

Since the ion conductance of phospholipid bilayer-associated CLIC5A is inhibited by IAA-94 (56), we next determined whether IAA-94 alters ERM phosphorylation in COS-7 cells expressing CLIC5A. COS-7 cells were transfected with CLIC5A or empty vector and then treated with 50 mM IAA-94 for 30 min. Total cell lysates (Figure 4.3-A) and cytoskeletal

fractions (Figure 4.3-B) were then evaluated by WB. Densitometric analysis of WB of total cellular lysate (Figure 4.3-C) and cytoskeletal fraction (Figure 4.3-D) shows that IAA-94 did not inhibit the increase in P-ERM abundance observed in response to CLIC5A expression. This observation suggests that the CLIC5A effect on ERM phosphorylation is independent of its putative ion channel activity.

4.2.5 Re-organization of the plasma membrane surface charge distribution in COS-7 cells expressing CLIC5A

I next determined whether ectopic expression of CLIC5A alters the negative surface potential of the inner leaflet of the plasma membrane in COS-7 cells by co-transfecting the cells with the surface potential reporter GFP-Kras (402) and CLIC5A or empty vector. Live cell imaging revealed that the surface potential biosensor GFP-Kras was evenly distributed along the dorsal and basal plasma membrane in the absence of CLIC5A. By contrast, there was a dramatic redistribution of GFP-Kras into dorsal membrane clusters in the presence of CLIC5A (Figure 4.4-A). It seems plausible that the marked change in the surface potential in cells expressing CLIC5A could be due to change in PI(4,5)P2 abundance in the apical plasma membrane, or potentially to the binding of GFP-Kras to the negative foot loop of membrane-associated CLIC5A.

4.2.6 CLIC5A increases the Abundance of PI(4,5)P2 in dorsal plasma membrane clusters

The head of PI(4,5)P2 is negatively charged and it is well-established that PI(4,5)P2 is required for ezrin binding to plasma membrane (103). PI(4,5)P2 induces a conformational change in ERM proteins that frees the ERM C-terminus from auto-inhibition, and this conformational change is required for actin binding and phosphorylation of the critical C-

terminal Thr (103,119,403). I therefore investigated whether CLIC5A alters the abundance or distribution of PI(4,5)P2 in COS-7 cells, by co-transfecting the cells with the PI(4,5)P2 reporter GFP-PH-PLC and CLIC5A or vector alone. Live cell imaging showed that the PI(4,5)P2 reporter localized to dorsal membrane patches that extend vertically from the COS-7 cell surface (Figure 4.4-B), and that these sites of PI(4,5)P2 accumulation were more abundant in CLIC5A- than in vector-transfected cells. Furthermore, the dorsal plasma membrane : cytoplasm GFP-PH-PLC ratio was significantly greater in CLIC5A than in vector transfected cells (Figure 4.4-C), indicating that plasma membrane PI(4,5)P2 abundance increased in CLIC5A expressing cells.

When COS-7 cells were co-transfected with RFP-PH-PLC and GFP-CLIC5A, there was substantial co-localization of GFP-CLIC5A with the PI(4,5)P2 reporter at the dorsal plasma membrane (Figure 4-5, X-Z). In control cells expressing only GFP, the green fluorescence remained cytoplasmic and did not co-localize with the PI(4,5)P2 reporter. Examination of Z-stacks revealed the PI(4,5)P2 reporter to be organized in surface ruffles, and the density of these ruffles was much greater in cells transfected with CLIC5A, compared to cells transfected with vector alone. These experiments suggest strongly that the re-organization of the dorsal plasma membrane in COS-7 cells transfected with CLIC5A is accompanied by a polarized accumulation of PI(4,5)P2 in clusters containing CLIC5A.

4.2.7 CLIC5A-stimulated ERM phosphorylation is mediated by PI(4,5)P2.

PI(4,5)P2 is required as a membrane docking site for ERM protein activation (123). PI(4,5)P2 also is a substrate for PLC, and activation of PLC can deplete plasma membranes of PI(4,5)P2. I reasoned if the increase in ERM phosphorylation in response to CLIC5A is mediated by a localized increase in PI(4,5)P2 then cleavage of PI(4,5)P2 should eliminate CLIC5A-dependent ERM phosphorylation. I therefore examined whether activation of PLC

would alter CLIC5A-induced ERM phosphorylation. COS-7 cells transfected with CLIC5A or vector alone were treated with 800 μ M of the PLC activator m-3M3FBS. WB analysis revealed as early as 5 min after initiation of m-3M3FBS treatment, ERM phosphorylation decreased in CLIC5A and vector transfected cells (Figure 4.6-A). The abundance of CLIC5A also declined in response to m-3M3FBS (Figure 4.6-A). Densitometric analysis of 4 independent experiments revealed that ERM phosphorylation decreased significantly in total cellular lysate of both, CLIC5A and vector transfected cells and the reduction level was almost identical in CLIC5A and vector transfected cells relative to control untreated cells (Figure 4.6-B). Identical results were obtained in HeLa cells transfected with CLIC5A or vector and then treated with m-3M3FBS. These findings suggest that CLIC5A-mediated ERM phosphorylation is PI(4,5)P₂-dependent and this effect is abrogated in response to PI(4,5)P₂ depletion.

4.2.8 Silencing of endogenous PI4P5K α reduces CLIC5A-stimulated ERM phosphorylation

PI(4,5)P₂ is produced from its substrate PI4P by PI4P5 kinases. If PI(4,5)P₂ in fact mediates the CLIC5A-dependent phosphorylation of ERM protein in COS-7 cells, then the effect should be blunted when PI4P5 kinase(s) are silenced. Endogenous PI4P5K α was therefore depleted using specific siRNA in COS-7 and HeLa cells. The PI4P5K α -specific, but not the nonspecific siRNA significantly inhibited PI4P5K α protein expression. Furthermore, WB analysis of cellular lysate showed that CLIC5A-mediated ERM phosphorylation was profoundly reduced by silencing PI4P5K α in both COS-7 and HeLa cells (Figure 4.7). Similar to PLC activator results, these findings are consistent with a mechanism whereby CLIC5A-dependent ERM phosphorylation is mediated by PI(4,5)P₂.

4.2.9 PLC activation reduces PI(4,5)P2 and CLIC5A in the dorsal plasma membrane

Live cell imaging revealed that apical membrane clusters bearing the PI(4,5)P2 reporter RFP-PH-PLC were reduced in a time dependent fashion upon PLC activation. While a loss of PI(4,5)P2 was expected, we also observed that CLIC5A was rapidly lost from the dorsal plasma membrane and re-distributed to the cytosol in the presence of m-3M3FBS (Figure 4.8). These findings suggest that CLIC5A-dependent ERM phosphorylation, abrogated in response to PI(4,5)P2 depletion may reflect both, reduced PI(4,5)P2 and reduced CLIC5A in the plasma membrane. The findings are consistent with the possibility that the alteration in the distribution of GFP-KRas (Figure 4.4-A) and GFP-PH-PLC (Figure 4.4-B) in CLIC5A transfected cells results from changes in PI(4,5)P2 abundance in the dorsal plasma membrane, though it is still possible that CLIC5A itself serves as the docking site for the two reporters and for ezrin. The finding that m-3M3FBS also reduced CLIC5A association with the dorsal plasma membrane and resulted in a decline of CLIC5A abundance, suggests that the association of CLIC5A with the dorsal plasma membrane of cells is itself dependent on PI(4,5)P2.

4.2.10 CLIC5A co-localizes with PI4P5K α at the dorsal plasma membrane.

The PI(4,5)P2 in phospholipid bilayers is produced from PI4P by PI4P5K, and to a lesser degree from PI5P by PI5P4K (404). All isoforms of these PI(4,5)P2 generating kinases contain surface cationic residues conferring a positive charge that allow them to bind negatively charged phospholipids in the inner leaflet of the plasma membrane (405). I therefore studied whether CLIC5A and PI(4,5)P2 generating kinases are in close proximity in the dorsal plasma membrane. To this end, COS-7 cells were co-transfected with HA-PI4P5K α and GFP-CLIC5A or GFP-vector. Confocal-IF showed a considerable co-localization of GFP-CLIC5A with PI4P5K α at the

dorsal plasma membrane (Figure 3.9-A, X-Z), but not with GFP-vector in control cells, suggesting that CLIC5A and PI4P5K α are in a close proximity in the plasma membrane.

Similar to localization at the plasma membrane, occasionally overexpression of CLIC5A or the combination of CLIC5A/HA-PI4P5K α resulted in the formation of very large vacuoles in COS-7 cells. Such vacuoles were not observed in vector-transfected cells. CLIC5A and HA-PI4P5K α were found to co-localize in the membrane of such vacuoles (Figure 4.9-B) as well. In vacuolated cells transfected only with CLIC5A, the PI(4,5)P2 reporter GFP-PH-PLC also localized to the vacuolar membranes (Figure 4.9-C). These data also support the concept that CLIC5A co-localizes with HA-PI4P5K α at sites of PI(4,5)P2 production.

4.2.11 CLIC5A interacts with PI(4,5)P2 kinases *in vitro*.

To further probe whether CLIC5A may interact with PI(4,5)P2 generating kinases, COS-7 cells were transfected with HA-tagged PI4P5K α , PI4P5K β , PI5P4K α and PI5P4K β cDNA constructs. Lysates from transfected cells were then incubated with recombinant, GST-CLIC5A or GST immobilized on glutathione sepharose beads. Western blot analysis of the proteins eluted from GST- and GST-CLIC5A beads showed that HA-PI4P5K α (Figure 4.10-A), HA-PI4P5K β (Figure 4.10-B), PI5P4K α (Figure 4.10-C), and PI5P4K β (Figure 4.10-D), bound to GST-CLIC5A but not to GST. These results suggest that CLIC5A and different PI(4,5)P2 kinases can interact with one another, either directly or indirectly, and is consistent with the concept that they are members of the same protein complex in the plasma membrane.

4.2.12 CLIC5A N- And C-terminal deletion mutants abrogate its membrane localization and PI(4,5)P2 clustering at the dorsal membrane

My previous experiment showed that N- and C- terminal deletions abrogated CLIC5A-mediated ERM phosphorylation (Figure 3.6). To explore whether CLIC5A N- or C-terminal deletions would alter their targeting to the apical membrane and colocalization with PIP5K1 α , the CLIC5A mutants (CLIC5A²²⁻²⁵¹, CLIC5A⁵⁵⁻²⁵¹ and CLIC5A¹⁻²³²) were co-expressed with HA-PIP5K1 α in COS-7 followed by confocal microscopy analysis. In contrast to wild-type CLIC5A which was localized at the dorsal plasma membrane, the mutant CLIC5A proteins were observed in the cell cytoplasm but failed to localize to the plasma membrane, and consequently did not co-localize with HA-PI4P5K α at the cell membrane (Figure 3.11.A). Similarly, live cell imaging of COS-7 cells co-transfected with specific CLIC5A deletion mutants and the PI(4,5)P2 reporter GFP-PH-PLC showed that the three CLIC5A mutants also failed to induce clustered plasma membrane PI(4,5)P2 accumulation (Figure 4.11-B). These findings suggest that both N- and C-termini are required for the localization, and potentially also for the stabilization of the CLIC5A protein in the dorsal plasma membrane. Furthermore, the dorsal membrane localization of PI4P5K α appears to be independent of CLIC5A. Nonetheless, I observed that increased PI(4,5)P2 accumulation at the dorsal plasma membrane of COS-7 cells stimulated by full-length CLIC5A, is not substituted by PIP5K1 α . This finding implies that CLIC5A is not required for the recruitment of PI4P5K α to the plasma membrane, but that it is required for localized PI4P5 and/or PI5P4 kinase activation.

4.3 Discussion

The activity of ERM proteins involves phosphorylation-dephosphorylation cycles and the two main molecular events that are involved in generating and/or maintaining the active form of ERM proteins are PI(4,5)P₂ binding to their N-terminal domains and phosphorylation of their C-terminal Thr residue. Phosphorylation of ERM proteins is stimulated by PKC, ROCK (374) and AKT2 (138), while dephosphorylation is catalyzed by myosin phosphatase and protein phosphatase 2C (PP2C) (374). I found that in COS-7 cells, inhibition of PKC, but not ROCK inhibited ERM phosphorylation (Figure 4.1-A&B). These results are consistent with the previous report showing no effect of the potent RhoA kinase inhibitor C3 transferase on ERM phosphorylation in various kidney derived epithelial cells (120). While ERM protein phosphorylation was much greater in the presence of CLIC5A the rate of ERM dephosphorylation during PKC inhibition was essentially the same in the presence or absence of CLIC5A (Figure 4.2), suggesting that the effect of CLIC5A on ERM phosphorylation is not explained by inhibition of ERM phosphatases. Also, enhanced phosphorylation of PKC in COS-7 cells expressing CLIC5A was not observed (Figure 4.1-C). It is still possible that enhanced production of PI_{4,5}P₂ in cells expressing CLIC5A contributes to the final step of PKC activation (406,407), given that PI(4,5)P₂ is the substrate for PLC-mediated IP₃ and DAG synthesis. Further studies determining whether CLIC5A stimulates IP₃ and DAG generation, as well as PKC translocation to the plasma membrane will be needed to rule out this possibility. Interestingly, I observed a consistent, rapid decline in CLIC5A abundance upon treatment of COS-7 cells with PKC inhibitor staurosporine. The cause for the reduction in CLIC5A abundance is not yet clear, but given that staurosporine rapidly induces apoptosis in cells, it is conceivable that CLIC5A is subject to caspase-mediated cleavage. Alternatively, it is also

possible that CLIC5A itself is phosphorylated by PKC and that inhibition of PKC induces a conformational change altering antibody reactivity. Similarly, the tyrosine phosphatase inhibitor Phenylarsine oxide (PAO) also increased association of CLIC5A with the detergent insoluble fraction (Unpublished data), suggesting that CLIC5A association with the ezrin-containing plasma membrane complex may be regulated by tyrosine phosphorylation.

Analysis of the predicted phosphorylation sites (NetPhos 2) of CLIC5A suggests that it may be phosphorylated on serine (S), threonine (T) and tyrosine (Y) residues (see appendices). To determine whether CLIC5A association with the plasma membrane is regulated by PKC, site-directed mutations of serine and threonine residues might be useful, followed by expression of the resulting mutants in COS-7 cells and evaluation of the effect of the mutations on membrane association. It would also be interesting to determine whether CLIC5A is tyrosine phosphorylated and whether activation of tyrosine phosphorylation cascades, for instance with growth factors, might cause CLIC5A to dissociate from the plasma membrane. Analysis of COS-7 cells expressing the various CLIC5A mutants for the abundance of P-ERM in cellular lysates and in the cytoskeleton would then allow us to define whether regulated phosphorylation of CLIC5A, in turn regulates ERM protein phosphorylation.

The CLIC proteins are redox sensitive and spontaneously partition into lipid bilayers upon oxidation (17,408-410), where they have ion-conducting properties that are blocked by the partially selective Cl⁻ channel inhibitor IAA-94, but not by the more specific inhibitors SIDS or DIDS (14). Indeed, bovine CLIC5B (p64) was first isolated from kidney by affinity-purification with IAA-94 (27,411). In keeping with CLIC-mediated Cl⁻ ion conductance, a role in vacuolar/vesicular acidification has been reported for CLIC5B in osteoclasts (54), for CLIC1 in macrophages (37) and for CLIC4 in endothelial cells (377). Here, we observed that the effect of

CLIC5A on ERM phosphorylation was not inhibited by IAA-94 (Figure 4.3-A&-B). While the experiment does not exclude the possibility that CLIC5A might form ion-conducting pores when expressed in COS-7 cells, the data indicate that the effect of CLIC5A on ERM phosphorylation is not due to IAA-94 sensitive ion conductance. Given that CLIC5A expression leads to actin polymerization, and the previous report that F-actin inhibits CLIC-mediated ion conductance (22), it seems likely that CLIC5A expressed in COS-7 cells does not function as a Cl⁻ channel in the dorsal plasma membrane.

Activation of ERM proteins requires initial binding of the ERM N-terminus to PI(4,5)P₂, prompting a conformational change that then facilitates C-terminal actin binding and phosphorylation of a highly conserved threonine residue at the C-terminus (79,374). PI(4,5)P₂ therefore plays an essential role in ERM phosphorylation (103,119,403). The PI(4,5)P₂ molecules are produced by the action of PI(4,5)P₂ generating kinases: PI4P5Ks and PI5P4Ks. Previous report showed that all isoforms of PI(4,5)P₂ generating kinases contain a positively charged domain that interacts with negatively charged phospholipids in the inner leaflet of plasma membranes. Hence the location and abundance of the substrate (PI4P) as well as the product (PI(4,5)P₂) of PI4P5Ks regulate their recruitment from cytoplasm to plasma membrane (412,413). In addition, it is known that CLICs all possess a highly negatively charged “foot loop”, which could potentially serve to recruit PI(4,5)P₂ generating enzymes. To evaluate what happens to the negative surface charge distribution on the inner leaflet of COS-7 cells when CLIC5A is expressed, I co-transfected the cells with the membrane potential reporter GFP-Kras, which is the poly cationic tail of the small GTP-ase Kras (402). Confocal live cell imaging showed a smooth and even distribution of GFP-Kras in cells transfected with empty vector while there was a dramatic clustering of the reporter at the apical plasma membrane in cells transfected

with CLIC5A (Figure 4.4-A). This negative charge clustering could represent remodeling of the apical plasma membrane, a redistribution of negative charged lipids, and/or binding of the reporter to the acidic foot loop (414,415) of membrane-associated CLIC5A.

To test whether generation of PI(4,5)P2 might be involved in CLIC5A-mediated ERM phosphorylation, I looked for the distribution of PI(4,5)P2 reporter GFP-PH-PLC in cells transfected with CLIC5A or empty vector. Live cell imaging revealed that ectopic expression of CLIC5A was associated with clustered accumulation of the PI(4,5)P2 reporter GFP-PH-PLC at the dorsal membrane of COS-7 cells. Furthermore, the ratio of membrane:cytosolic PI(4,5)P2 reporter increased significantly in response to CLIC5A expression (Figure 4.4-B & -C), which suggests enhanced PI(4,5)P2 production at the plasma membrane in the presence of CLIC5A, or binding of the reporter to membrane associated CLIC5A. To confirm that the effect of CLIC5A on ERM protein phosphorylation is mediated by PI(4,5)P2 and to exclude the possibility that CLIC5A could functionally mimic PI(4,5)P2, binding the PI(4,5)P2 reporter and directly supporting the conformational change in ezrin that then leads to its phosphorylation, I depleted the cells of PI(4,5)P2 by stimulating PLC activity. The PLC hydrolyzes PI(4,5)P2 to form inositol trisphosphate (IP3) and diacylglycerol (DAG), reducing PI(4,5)P2 level in cells. Previous reports had shown that the PLC activator m-3M3FBS accelerates the hydrolysis of PI(4,5)P2, and reduces the level of ERM phosphorylation in HeLa (121) and Jurkat T cells (122). In my studies, m-3M3FBS largely abolished the increased ERM phosphorylation in the presence of CLIC5A (Figure 4.6-A&-B), suggesting that the effect of CLIC5A is mediated by PI(4,5)P2. This result is consistent with previous study showed that increased production of PI(4,5)P2 by overexpression of PI4P5K α is also associated with enhanced ERM phosphorylation (120,126). However, in addition to abolishing effect of CLIC5A on ERM phosphorylation, PLC activation

also resulted in the redistribution of GFP-CLIC5A to the cytosol (Figure 4.8), suggesting that its localization to the plasma membrane is dependent on the plasma membrane phospholipid composition. Since CLIC5A was no longer membrane associated after PI(4,5)P2 depletion, the possibility that the acidic foot loop of CLIC5A can mimic PI(4,5)P2, binding ezrin and facilitating its phosphorylation still remains open.

A previous report showed that the basic lysine residues K63, K64, K253, K254, K262 and K263 of ezrin are required for PI(4,5)P2 binding to the ezrin FERM domain, and site-directed mutagenesis of these sites abrogated the PI(4,5)P2 binding and localization of ezrin to the plasma membrane (119). The CLIC5A sequence contains 23 lysine residues. To determine whether CLIC5A association with the plasma membrane is due to association of a cationic domain with PI(4,5)P2, analysis of the crystal structure and evaluation of potential clustering of lysines would be useful, followed by site-directed mutation of key lysine (K) residues and expression of the mutated CLIC5A in COS-7 cells. If membrane localization of such mutated CLIC5A were changed, and the effect of CLIC5A on the distribution of the membrane potential and PI(4,5)P2 reporters were abrogated, then it might be possible to conclude that the association of CLIC5A with phospholipid bilayers is mediated, in part, by charge. If mutation of CLIC5A lysine residues blocked its association with the plasma membrane, PI(4,5)P2 generation and ERM phosphorylation was abrogated we would conclude that the charge-based CLIC5A interaction with the plasma is critical for its molecular actions at the plasma membrane

PI4P5 generating kinases (PI4P5K α , β and γ) phosphorylate the 5th position on the inositol ring of PI4P, producing the majority of PI(4,5)P2 at the plasma membrane. The PI5P4 generating kinases also exist as α , β and γ isoforms and catalyze phosphorylation of the 4th position on the inositol ring of PI5P to produce PI(4,5)P2 (416). Indeed, recruitment of PI4P5- and/or PI5P4

kinases to the plasma membrane is necessary for PI(4,5)P₂ production. Confocal IF imaging showed that PI4P5K α co-localizes with CLIC5A at the dorsal plasma membrane of COS-7 cells (Figure 4.9-A), suggesting that CLIC5A and PI4P5K α are in a close proximity or exist in the same complex. In addition, HA-tagged PI4P5K and PI5P4K α and β isoforms were all pulled down from cell lysates by GST-CLIC5A (Figure 4.10) indicating that CLIC5A and PI(4,5)P₂ generating kinases associate in cells. These findings are consistent with a yeast two-hybrid screen that has suggested a possible direct interaction between the C-terminal region of PI4P5K β and both CLIC1 and CLIC4 (<http://www.signaling-gateway.org>). Nonetheless, proof of a direct interaction between CLIC5A and PI(4,5)P₂ generating kinases is still lacking, and the mechanism by which CLIC5A might direct PI(4,5)P₂ accumulation to sites where ERM proteins can then dock remains unclear.

The best way to determine whether CLIC5A directly binds PI(4,5)P₂ generating kinases, would be to perform a GST-Pull down with recombinant purified GST-CLIC5A immobilized on glutathione-sepharose beads and incubating these with purified, recombinant PI(4,5)P₂ generating kinases. If the PI4P5- and PI5P4 kinases bound to GST-CLIC5A, but not to GST, this would be taken as evidence for a direct interaction. If there was a direct interaction, it would then be of great interest to determine whether this results in activation of the kinases. This can be tested by determining the phosphorylation of the substrate PI4P, *in vitro*.

Previous studies have shown that all isoforms of PI4P5 generating kinases contain a positively charged domain necessary for their recruitment to, and association with negatively charged regions of the plasma membrane (405). X-ray crystallography analysis of CLIC1 showed that CLIC1 has polyanionic foot loop located between helices 5 and 6 and this foot loop is believed to function in protein-protein interaction. Similar to CLIC1 all other members of

CLIC family share a polyanionic “foot loop”(417-420), which may serve to bind directly or creating a localized cluster of PI4P5Ks. To determine whether the acidic foot loop of CLIC5A plays a role in CLIC5A interaction with PI(4,5)P2 generating kinases. GST-Pull down assay using recombinant GST-CLIC5A with mutated acidic aa incubated with the different isoforms of PI(4,5)P2 generating kinases followed by WB analysis of the eluted protein would highlight the importance of the acidic foot loop in the interaction between CLIC5A and PI(4,5)P2 generating kinases. Similarly, to test the role of the acidic foot loop in subcellular localization of CLIC5A with mutated acidic aa, COS-7 cells can be co-transfected with the mutated CLIC5A and HA-PI4P5Ks followed by confocal immunofluorescence microscopy. If CLIC5A with a mutated acidic foot loop still associates with the plasma membrane, it would be important to determine whether the mutation abrogates co-localization of CLIC5A and the PI4P5K α . Furthermore, such studies can determine whether the acidic foot loop of CLIC5A plays a functional role in CLIC5A-mediated ERM protein phosphorylation. In addition to ERM phosphorylation, the effect of CLIC5A with mutated foot loop on the distribution of the membrane potential and PI(4,5)P2 abundance at the plasma membrane would need to be evaluated by live cell imaging using negative charge reporter GFP-Kras and PI(4,5)P2 reporter GFP-PH-PLC respectively.

In my studies reported here, siRNA mediated depletion of the endogenous PI4P5K1 α abrogated the CLIC5A-dependent ERM phosphorylation (Figure 4.7). This result strongly supports the concept that CLIC5A-mediated ERM phosphorylation is PI(4,5)P2 dependent, and is consistent with the previous report showing that TNF α mediated ERM phosphorylation is abolished by PI4P5K1 α depletion in endothelial cells (421). Some cells in cultures transfected with CLIC5A developed large intracellular vacuoles similar to those previously described in cells overexpressing PI4P5K α (120). These vacuoles were observed whether CLIC5A was

expressed with, or without exogenous HA-PI4P5K α , but never in vector-transfected cells. I observed that CLIC5A and HA-PI4P5K α co-localized at the membrane of these large vacuoles (Figure 4.9-B). Similarly, live cell imaging of cells co-transfected with CLIC5A and the PI(4,5)P2 reporter GFP-PH-PLC showed that PI(4,5)P2 is accumulated in the membranes lining these vacuoles (Figure 4.9-C). Therefore, there appears to be a close association of CLIC5A with PI4P5K α at locations of enhanced PI(4,5)P2 generation in CLIC5A transfected cells.

The PI(4,5)P2 generating kinases have been found in the nucleus (422,423), in focal adhesions (227), in adherens junctions, and endosomes (233). In my studies, exogenously expressed HA-PI4P5K α localized to the dorsal plasma membrane of COS-7 cells even in the absence of CLIC5A and HA-PI4P5K α was also found at the dorsal plasma membrane in the presence of CLIC5A truncation mutants (22-251, 55-251 and 1-232) that remained cytosolic (Figure 4.11-A). These findings essentially rule out the possibility that the CLICs are required for the recruitment of PI4P5K α to a plasma membrane location. Nonetheless, even though overexpressed PI4P5K α was observed at the plasma membrane in the absence of CLIC5A, and in the presence of the CLIC5A mutants, we only observed enhanced, clustered PI(4,5)P2 accumulation (Figure 4.11-B) in the presence of full-length CLIC5A. Hence, PI4P5K α membrane association did not depend on CLIC5A, but the generation of PI(4,5)P2 and its downstream effect on ERM phosphorylation did. This finding is most consistent with a model in which CLIC5A increases the localized activity of PI(4,5)P2 generating enzymes, rather than simply recruiting them to the plasma membrane. Phosphatidic acid, which is produced by PLD, can also stimulate PI4P5K activity, most likely by the localized additional anionic charges that increase the affinity of PI4P5K to the membrane (218,232). Since the abundance of endogenous PI(4,5)P2 generating enzymes was too low for detection by co-immunoprecipitation or co-

localization in this study, it remains unclear whether CLIC5A associates with, and activates a specific isoform.

4.4 Figures

Figure 4.1

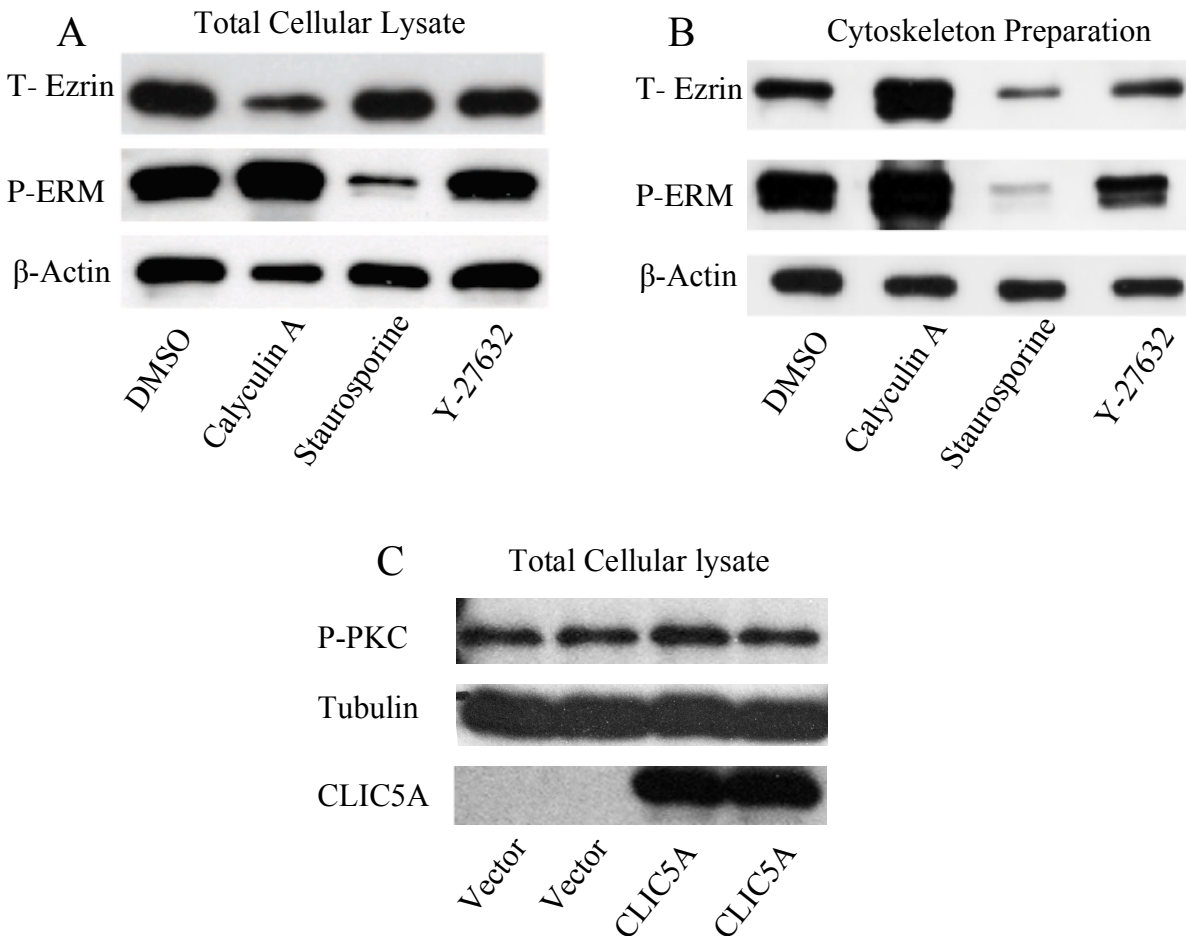
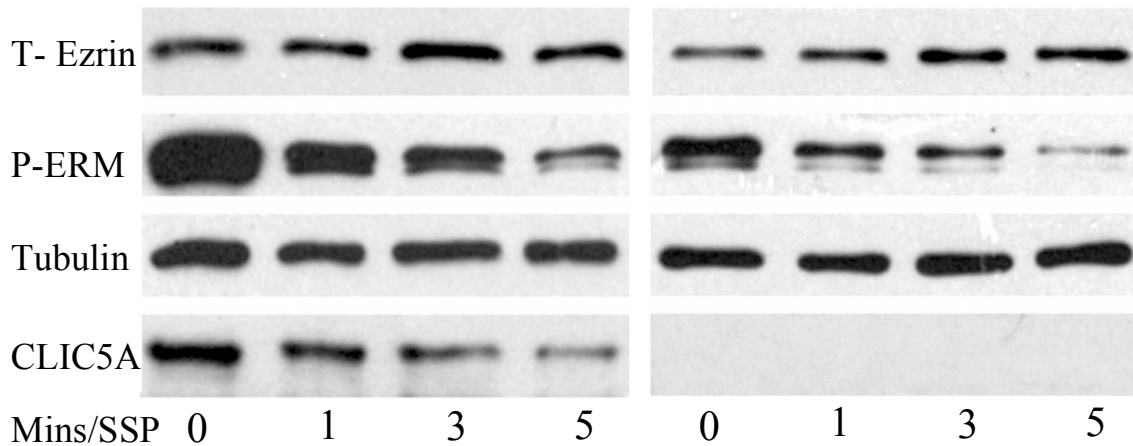


Figure 4.1. PKC is the main kinase involved in ERM phosphorylation in COS-7 cells and CLIC5A does not enhance P-PKC. **A-** WB analysis of total ezrin and P-ERM in COS-7 cells treated with either DMSO, PKC inhibitor Staurosporine or ROCK inhibitor Y-27632 for 1 hour and phosphatase inhibitor Calyculin A for 15 minutes. **B-** WB analysis of cytoskeletal preparation from COS-7 cells treated as previous. **C-** WB analysis of phospho-PKC (P-PKC) at Ser660 in COS-7 cells transfected with CLIC5A or empty vector.

Figure 4.2

A



B

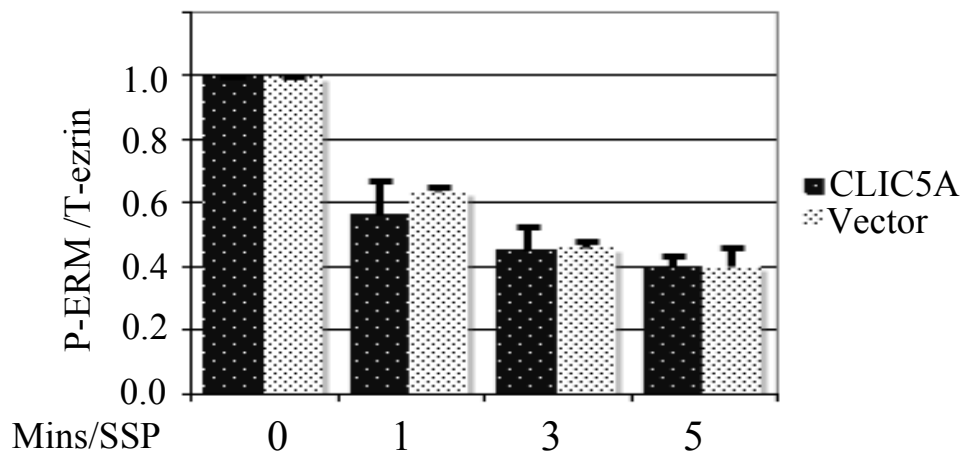
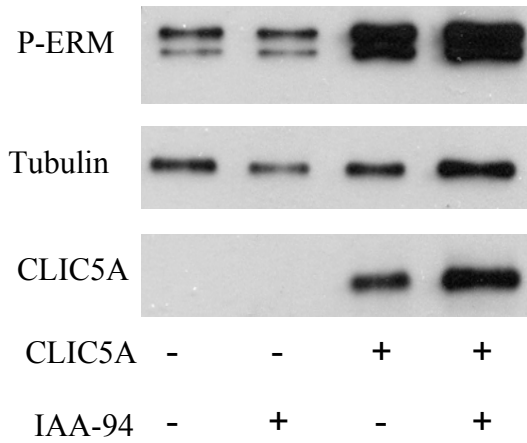


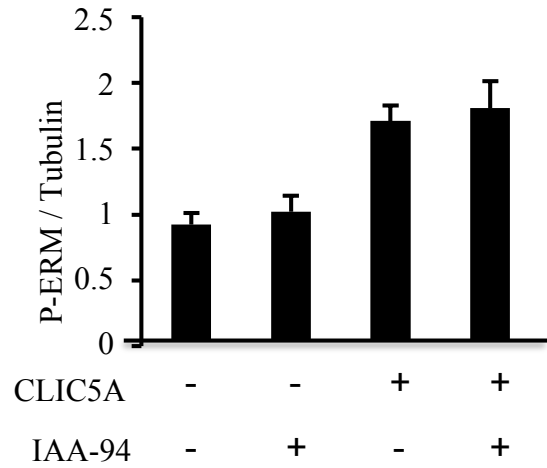
Figure 4.2. *CLIC5A does not block P-ERM protein dephosphorylation.* **A.** Western blot analysis of COS-7 cell lysates transiently transfected with CLIC5A cDNA or vector, and treated with Staurosporine (100 nM) for 1, 3, or 5 min. Control cells (t = 0) were not treated with Staurosporine. **B.** Densitometric analysis (mean P-ERM : T-Ezrin ratio relative to t = 0, n = 3 independent experiments). Though P-ERM was greater at t=0 in CLIC5A- than in vector-transfected cells, the rate of P-ERM de-phosphorylation was similar in CLIC5A and vector transfected cells.

Figure 4.3

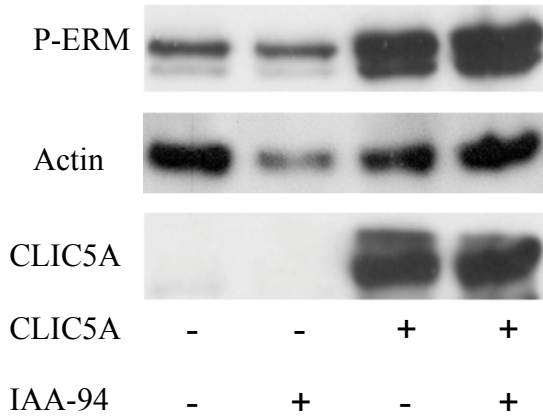
A



B



C



D

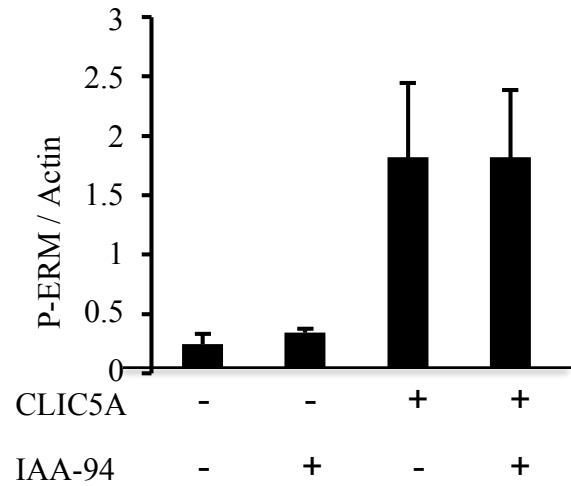
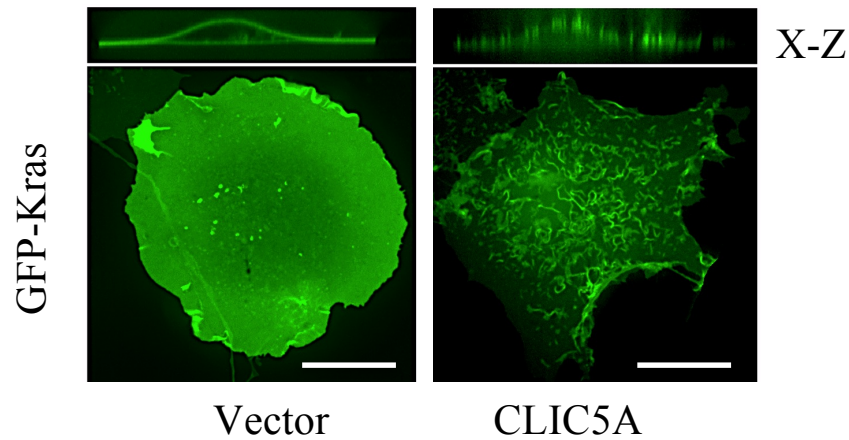


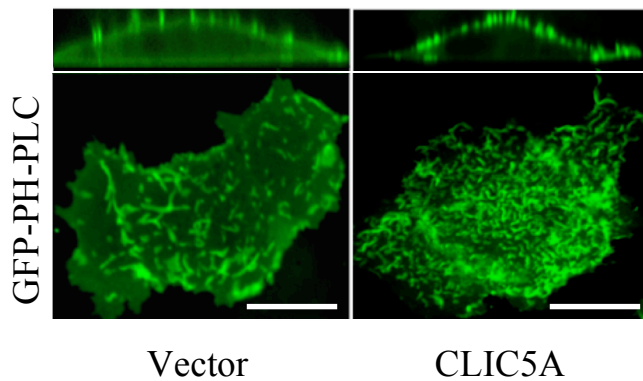
Figure 4.3. The Cl channel inhibitor IAA-94 does not alter CLIC5A-dependent ERM phosphorylation. WB analysis of SDS-soluble lysates (A) and SDS-insoluble fraction (C) of COS-7 cells transfected with CLIC5A or vector. 48 hours later, cells were treated with IAA-94 (50 μ M, 30 minutes). Densitometric analysis from 3 independent experiments shows that IAA-94 (50 μ M, 30 min) does not alter CLIC5A-dependent ERM phosphorylation in TCL (B) or cytoskeletal fraction (D).

Figure 4.4

A



B



C

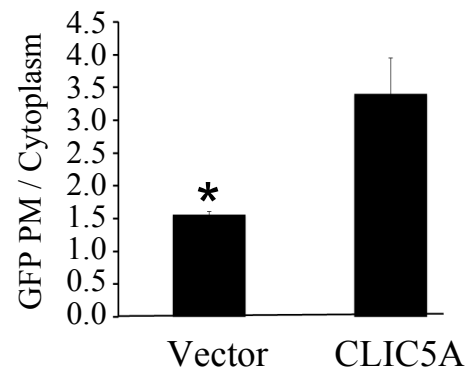


Figure 4.4. Clustered dorsal PI(4,5)P2 accumulation in the presence of CLIC5A. **A.** CLIC5A dependent re-distribution of plasma membrane negative surface potential. COS-7 cells were co-transfected with the surface potential biosensor GFP-Kras and CLIC5A or vector. In vector-transfected cells, GFP-Kras distributed uniformly along dorsal and basal cell membrane. In CLIC5A transfected cells, GFP-Kras was concentrated in dorsal clusters that appeared to project from the cell surface in the stacked image. **B.** CLIC5A-dependent accumulation of PI(4,5)P2 in the dorsal plasma membrane. COS-7 cells were co-transfected with CLIC5A or vector and the PI(4,5)P2 biosensor GFP-PH-PLC. In vector-transfected cells, clusters of GFP-PH-PLC at the apical cell membrane and diffuse GFP fluorescence in the cytoplasm are observed. In CLIC5A transfected cells, significantly more GFP-PH-PLC is observed in dorsal membrane clusters than in vector-transfected cells, and cytoplasmic GFP fluorescence is reduced. **C.** The ratio of dorsal membrane : cytoplasmic GFP-PH-PLC fluorescence is significantly greater in CLIC5A- than in vector transfected cells. (n = 10 cells/experiment, 3 independent experiments, mean \pm SEM, $p < 0.01$). Scale bar = 10 μ m

Figure 4.5

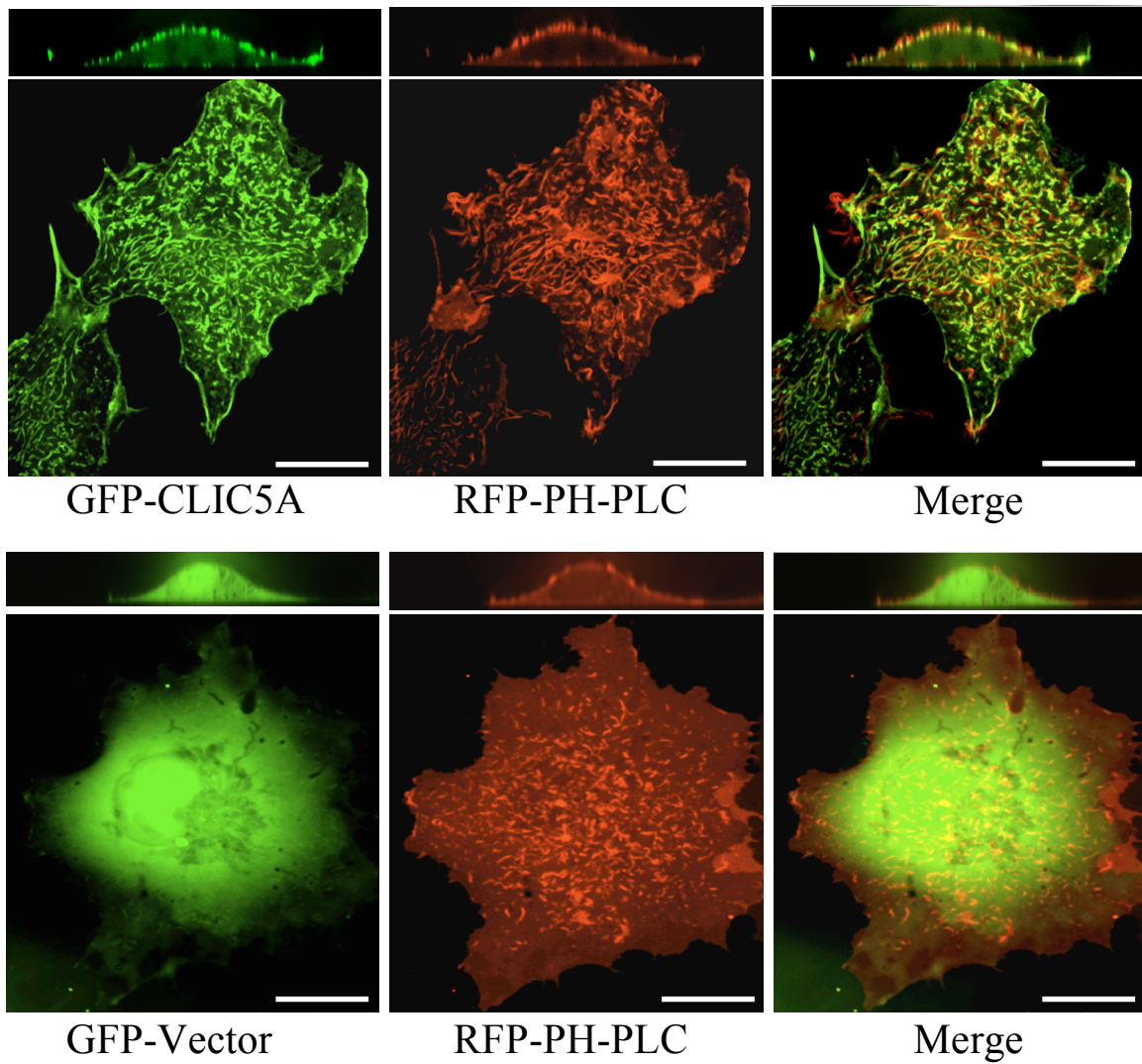
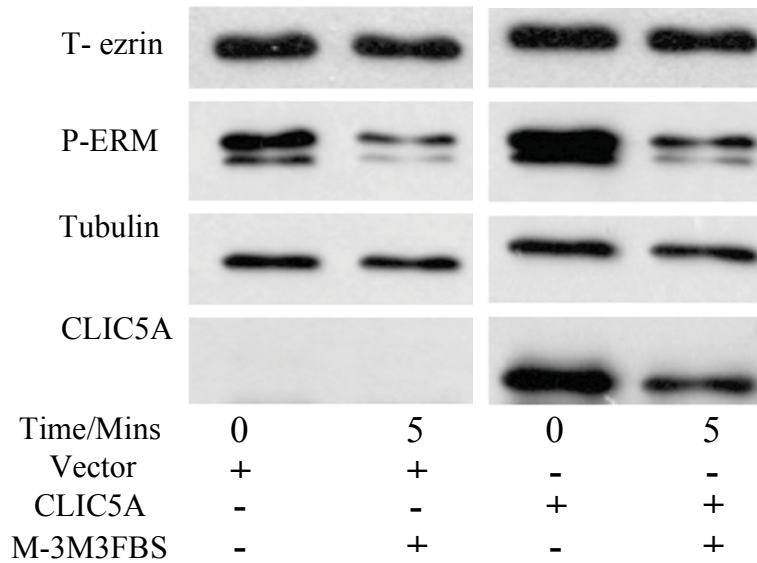


Figure 4.5. Co-localization of the PI(4,5)P2 biosensor RFP-PH-PLC with GFP-CLIC5A. COS-7 cells were co-transfected with the PI(4,5)P2 biosensor RFP-PH-PLC and GFP-CLIC5A (top) or GFP-Vector (bottom). GFP and RFP were visualized by spinning-disk confocal microscopy in living cells. The RFP-PH-PLC co-localized with GFP-CLIC5A, but not GFP, at the dorsal plasma membrane (X-Z). Scale bar = 10 μ m

Figure 4.6

A



B

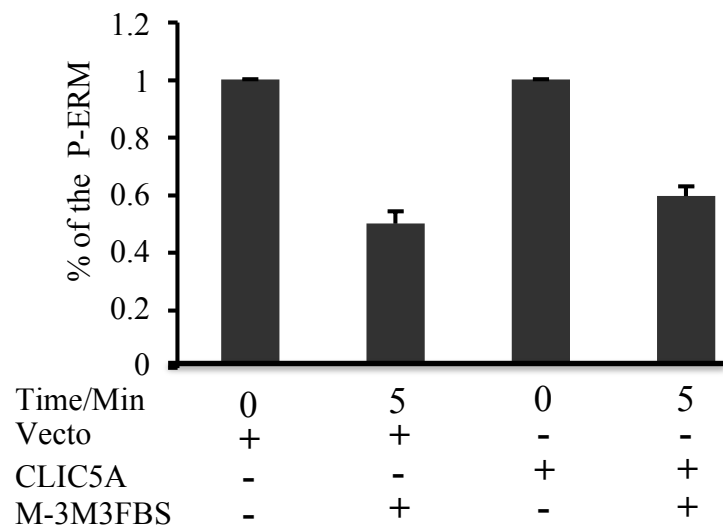


Figure 4.6. Abrogation of CLIC5A-dependent ERM phosphorylation by PLC activator *m-3M3FBS*. **A-** Western blots analysis of SDS-solubilized COS-7 cells transfected with CLIC5A cDNA or vector, and treated with the PLC activator *m-3M3FBS* (800 μ M) for 5 min. Treatment with *m-3M3FBS* reduced ERM phosphorylation in CLIC5A- and vector transfected cells. **B-** Densitometric analysis shows that the magnitude of the *m-3M3FBS* -mediated P-ERM dephosphorylation is similar in the presence and absence of CLIC5A.

Figure 4.7

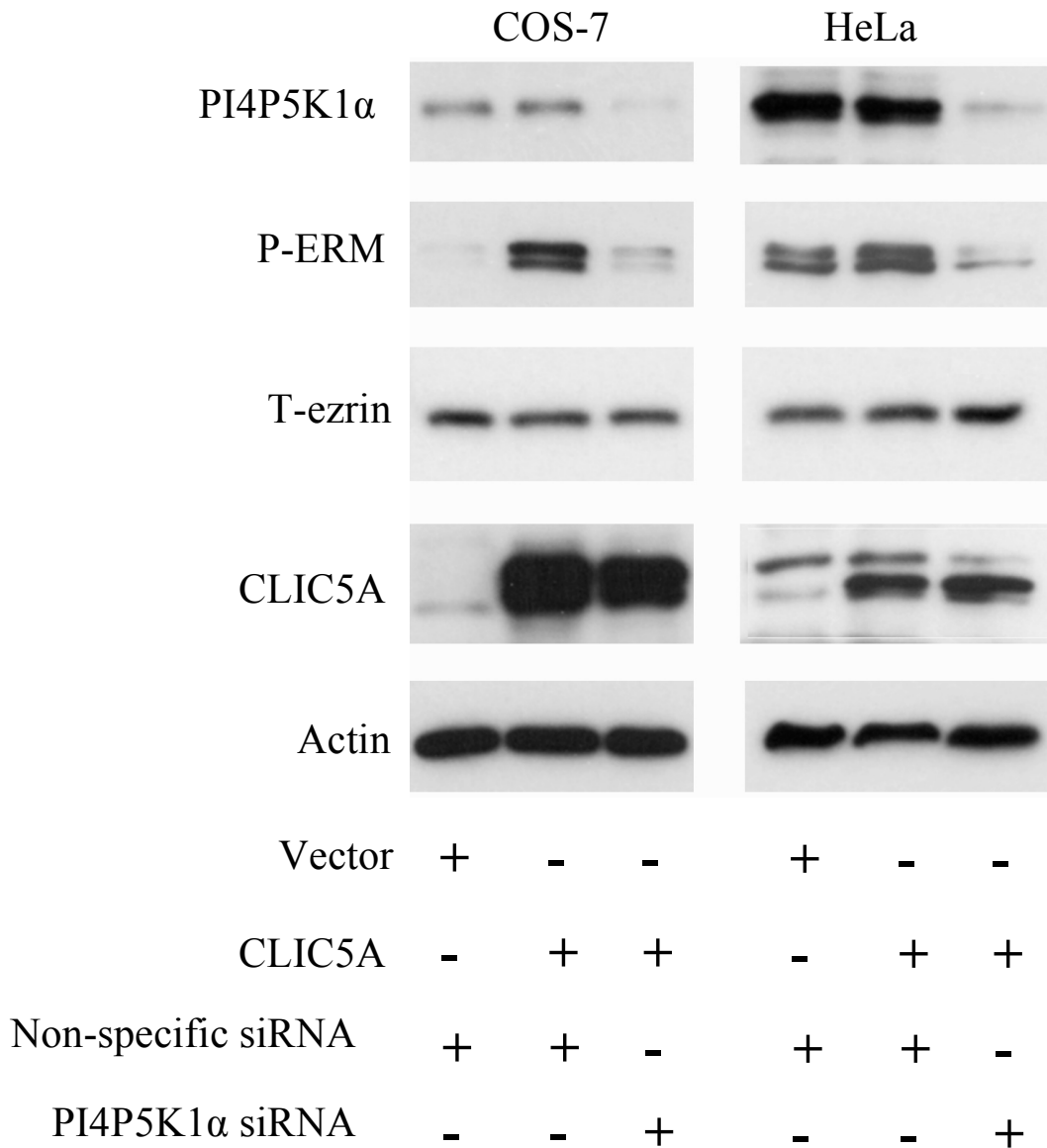


Figure 4.7. *PI4P5K α silencing abrogated CLIC5A-dependent ERM phosphorylation.* Western blots analysis of SDS-solubilized COS-7 and HeLa cells co-transfected with CLIC5A cDNA/vector and PI4P5K1 α siRNA/ non-specific siRNA, PI4P5K1 α silencing reduced ERM phosphorylation in CLIC5A and vector transfected cells, but not the non-specific siRNA.

Figure 4.8

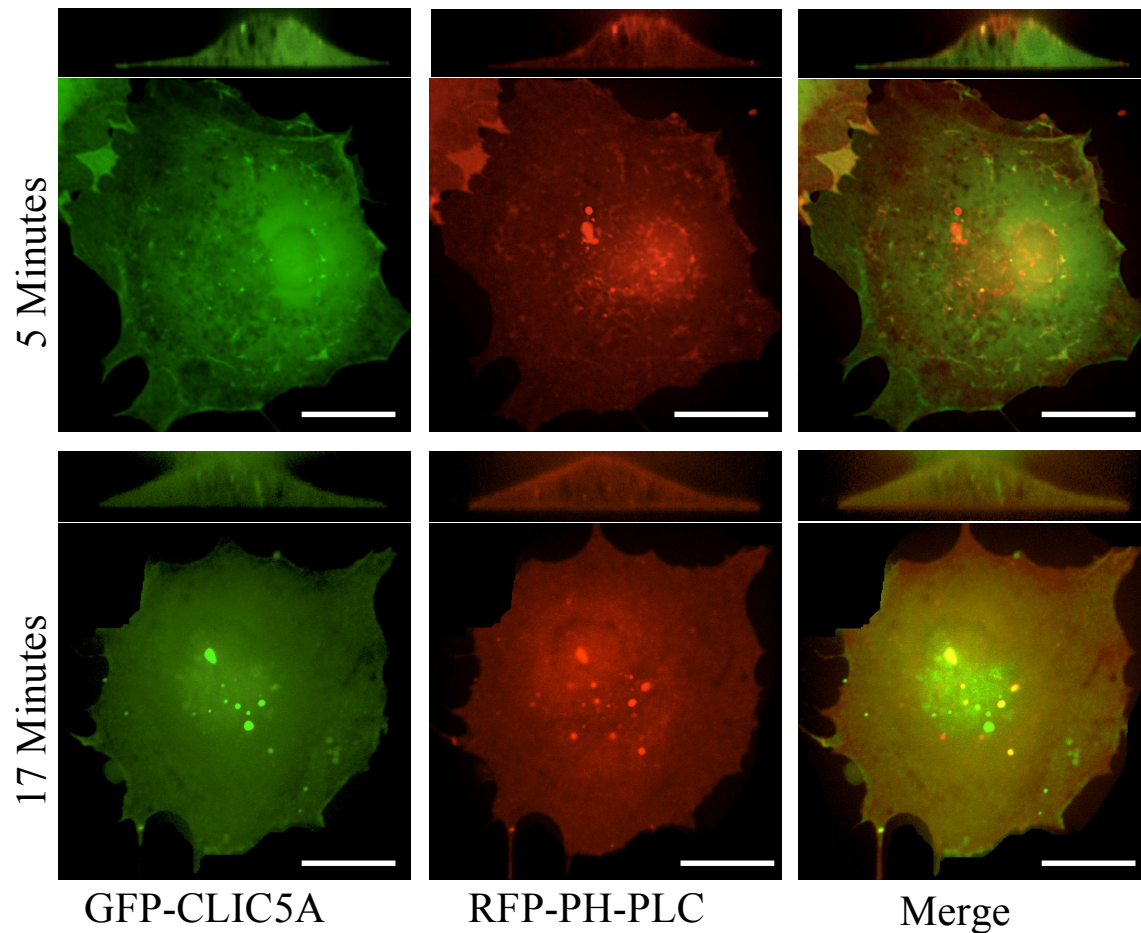
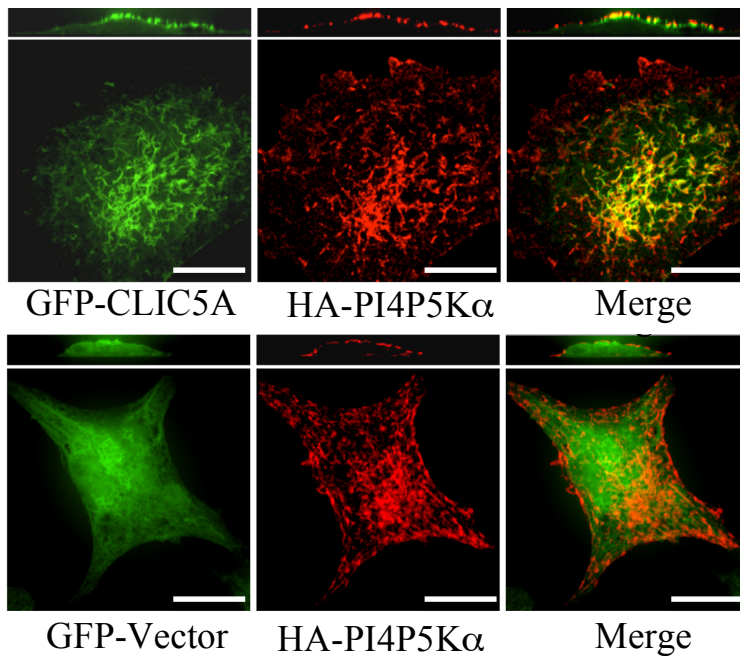


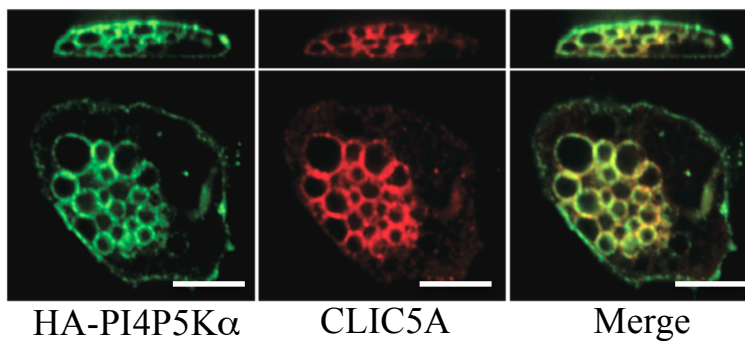
Figure 4.8. Time-dependent loss of PI(4,5)P₂ clusters and GFP-CLIC5A from the dorsal plasma membrane in response to m-3M3FBS treatment. COS-7 cells co-transfected with CLIC5A cDNA and RFP-PH-PLC were treated with the PLC activator m-3M3FBS (800 μ M) for 5-17 min followed by live cell imaging using spinning-disk confocal microscopy. A time-dependent loss of dorsal membrane CLIC5A/RFP-PH-PLC clusters was observed, and substantial CLIC5A redistributed into the cytosol. Scale bar = 10 μ m

Figure 4.9

A



B



C

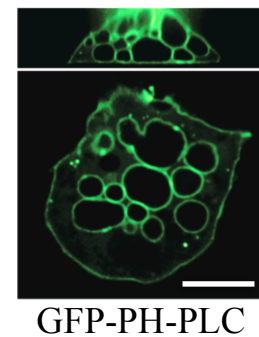


Figure 4.9. Co-localization of *CLIC5A* with *PI4P5K α* . **A-** COS-7 cells were co-transfected with HA-PI4P5K α and GFP-CLIC5A or GFP. Co-localization of GFP-CLIC5A and HA-PI4P5K α is observed at the dorsal plasma membrane (X-Z) (top panel), and in cellular ruffles (stacked image), but not GFP transfected cells (bottom panel). **B-** Co-localization of CLIC5A and PI4P5K α on vacuolar membranes. In cultures of COS-7 cells transfected with CLIC5A and HA-PI4P5K α , occasional cells developed large intracellular vacuoles. HA-PI4P5K α and CLIC5A co-localized on the vacuolar membranes in such cells. Vacuoles were not observed in vector-transfected cells. **C-** Confocal microscopy of living COS-7 cells co-transfected with CLIC5A cDNA and the PI(4,5)P2 biosensor GFP-PH-PLC (10:1, CLIC5A cDNA : GFP-PH-PLC cDNA) In cells that developed large vacuoles after transfection CLIC5A, the PI(4,5)P2 reporter also localized to the vacuolar membranes, even in the absence of HA-PI4P5K α . Scale bar = 10 μ m

Figure 4.10

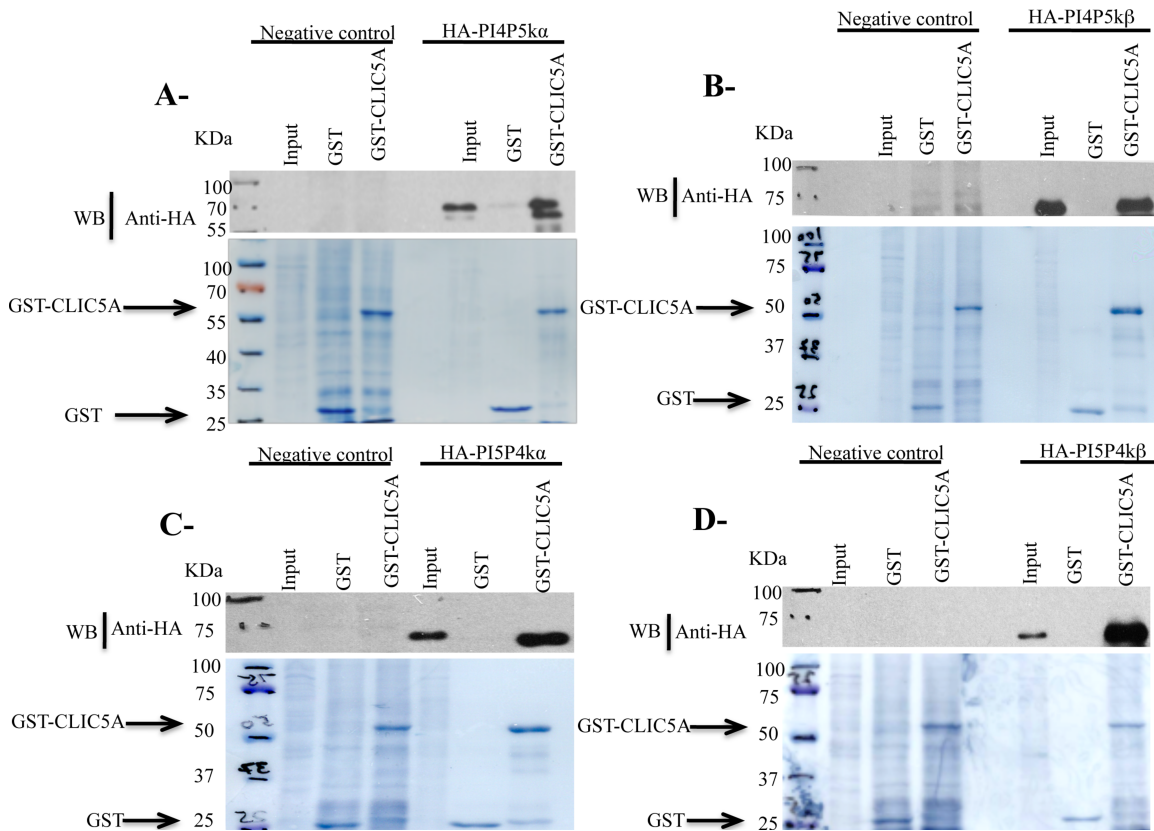


Figure 4.10. PI(4,5)P₂ generating enzymes associate with CLIC5A. Total cell lysates were prepared from COS-7 cells that had been transfected with HA-PI4P5K α (A), HA-PI4P5K β (B), HA-PI5P4K α (C) and HA-PI5P4K β (D). Cell lysates prepared with Triton X-100 lysis buffer were incubated with recombinant GST or GST-CLIC5A immobilized on glutathione sepharose beads. The beads were precipitated, washed exhaustively, and bound proteins eluted and evaluated by western blot analysis. Lysate served as the “input” control for each transfection and Amido black staining of the membranes show total (Input) and eluted proteins (GST, GST-CLIC5A). HA-PI4PK5 α (A), HA-PI4P5K β (B), HA-PI5P4K α (C) and HA-PI5P4K β (D) were all precipitated with immobilized GST-CLIC5A, but not GST.

Figure 4.11

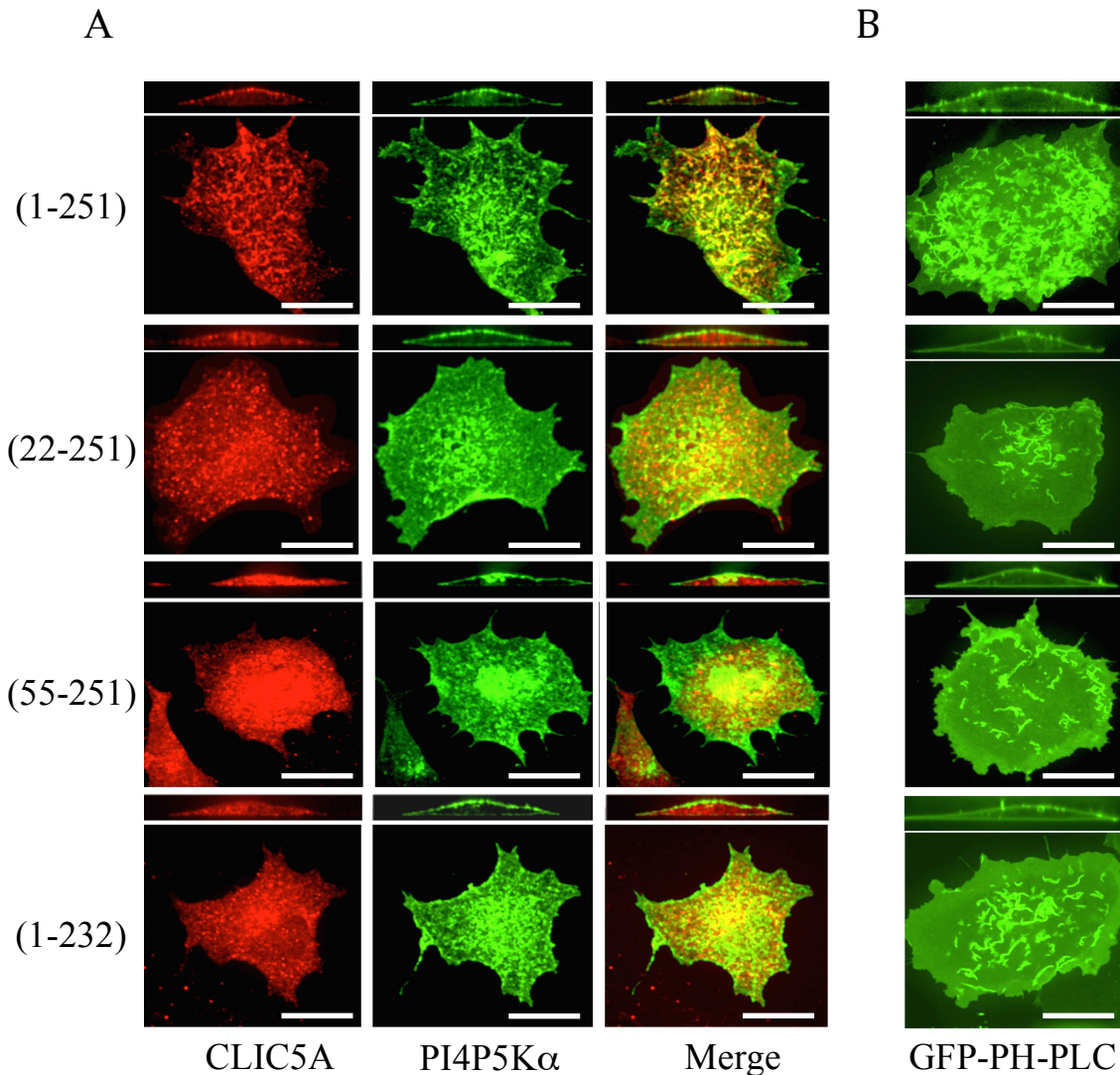


Figure 3.11. The effect of CLIC5A on ERM phosphorylation is abrogated by disruption of CLIC5A membrane association. **A.** CLIC5A mutants do not associate with the dorsal plasma membrane. COS-7 cells were co-transfected with HA-PI4P5K α and full-length CLIC5A (1-251) or CLIC5A mutants as in (figure 3.6). Confocal-IF showed that full-length CLIC5A localized to the plasma membrane and co-localized partially with HA-PI4P5K α . The CLIC5A mutants failed to localize to the plasma membrane and did not co-localize with HA-PI4P5K α . **B.** CLIC5A mutants do not increase apical PI(4,5)P2 accumulation. COS-7 cells were co-transfected with GFP-PH-PLC and full-length CLIC5A or CLIC5A mutants as in A (10:1, CLIC5A cDNA : GFP-PH-PLC cDNA), followed by evaluation of living cells for GFP fluorescence with confocal microscopy. Substantially more PI(4,5)P2 reporter localized to the dorsal plasma membrane in cells transfected with full-length CLIC5A than in cells transfected with CLIC5A mutants. Scale bar = 10 μ m

Chapter 5

CLIC5A maintains the ezrin-dependent
podocyte architecture *in vivo*

Chapter 5

CLIC5A maintains the ezrin-dependent podocyte architecture *in vivo*³

5.1 Introduction

Renal glomeruli are spherical capillary bundles specifically designed for high-volume, permselective filtration. Glomerular capillaries lie between two arterioles that control the intracapillary pressure and plasma flow rate. Glomeruli contain three cell types: endothelial cells that cover inside, and podocytes that cover the outside of each capillary, and mesangial cells that form a supporting interstitium between the capillary loops. The glomerular capillary basement membrane (GBM) lies between glomerular endothelial cells and podocytes. Together, glomerular endothelial cells, podocytes and GBM form the glomerular capillary wall, which functions as a selective filter that allows the rapid flow of water and small molecules but restricts the passage of cells and large plasma proteins (61,346,362,424,425).

Glomerular endothelial cells are perforated by hundreds of trans-endothelial cell pores, the fenestrae, which appear like a sieve under the scanning electron microscope (257,258). On the exterior of the capillary wall, podocytes extend regularly spaced projections from primary extensions that look like tongs of a comb, the foot processes (426). The foot processes from

³ Portions of this chapter has been published in a peer-reviewed journal:

Binytha Wegner, **Abass Al-Momany**, Stephen C. Kulak, Kathy Kozlowski, Marya Obeidat, Nadia Jahroudi, John Paes, Mark Berryman, Barbara J. Ballermann. *CLIC5A, a component of the ezrin-podocalyxin complex in glomerulai, is a determinant of podocyte integrity*. American Journal of Physiology- Renal physiology, 2010 Jun;298(6):F1492-503

adjacent cells interdigitate very precisely with each other, forming a space between them that is about 40 nm wide and is referred to as the filtration slit. Glomerular filtrate passes through the fenestrae, then through the GBM and then through the filtration slits. Together, the high density and relatively large open area of glomerular capillary fenestrae and podocyte filtration slits are responsible for the high permeability of the glomerular capillary wall to water and small solutes. The physical dimensions of glomerular endothelial cell fenestrae, about 70 -100 nm in diameter, and podocyte filtration slits, approximately 40 nm wide, predict that they would not restrict the filtration of plasma albumin, globular albumin being at least 10 fold smaller in diameter (albumin Stokes radius = 3.55 nm). Nonetheless, albumin does not pass through the glomerular capillary wall, so that the albumin concentration in plasma is nearly 10,000 fold greater than in the glomerular filtrate. This indicates that the glomerular capillary wall is an extremely effective barrier to albumin filtration. This glomerular filtration barrier (GFB) has several components. A thick layer of negatively charged proteins that includes heparan sulfate proteoglycans (HSPGs) like syndecan-1 and glypican-1 and as well as sialoglycoproteins like podocalyxin and endomucin cover the apical surface of glomerular endothelial cells and the inner surface of their fenestrae. Since albumin is itself negatively charged, it is restricted from penetrating this glycocalyx. A similar negatively charged glycocalyx made up, in part, of a very high density of the sialoglycoprotein podocalyxin and of the HSPG syndecan-4, covers the apical surface of podocytes. In addition, the HSPGs perlecan, agrin, nidogen and collagen XVIII in the GBM, most of which are produced by podocytes, contribute negative charges in the GBM (427,428). Alterations of the endothelial glycocalyx may directly contribute to increased permeability to albumin and lead to proteinuria (305,429), and a general elimination of anionic HSPGs using heparanases reduces the glomerular permselectivity for ferritin, in keeping with a role for HSPGs

in determining the glomerular charge selectivity (430). However, studies in mice lacking podocyte-derived agrin and perlecan heparan sulfate side chains revealed that these animals do not develop proteinuria (427), and collagen XVIII deficient mice only develop mesangial expansion and mild renal insufficiency, suggesting that the HSPGs in the GBM are not critical in determining the charge selectivity of the glomerular protein barrier (428).

In addition to the charge selectivity the glomerular capillary wall also restricts protein filtration by size. The filtration slit diaphragm, composed of the transmembrane spanning proteins nephrin, Nephs, FATs and P-cadherin that are coupled to intracellular podocin, ZO-1 and α -actinin, among others, spans the space between podocyte foot processes and seems to be the most important size-selective component of the glomerular filtration barrier. This conclusion is strongly supported by the finding that the deletion of nephrin (311) as well as Neph1 and Neph2 (333) results in massive proteinuria, the nephrotic syndrome, and perinatal mortality. In addition, the network of type IV collagens, heterotrimeric laminins and HSPGs of the GBM, to which glomerular endothelial cells and podocytes are attached, was long believed to contribute significantly to the size-selectivity of glomerular basement membrane (431), through ordered packing and varying degrees of compression of these matrix proteins. Supporting the role of the GBM in protein size selectivity are the observations that abnormalities in laminin 521, the $\alpha 5\beta 2\gamma 1$ heterotrimer, result in massive proteinuria. For instance, the human Pierson's syndrome, which is due to laminin $\beta 2$ mutations is characterized by perinatal massive proteinuria (432), and laminin $\beta 2$ deficient mice have massive proteinuria (275). However, mutations in the type IV collagen genes result in Alport's syndrome, is characterized by hematuria and progressive renal disease (266), without massive proteinuria. Modeling of the filtration barrier suggests that GBM matrix proteins contribute relatively little to its size-selectivity (433), and proteinuria due to

mutations is probably explained by associated podocyte abnormalities (434).

Podocytes consists of three morphologically and functionally distinct parts: a prominent cell body, large projections termed major processes, and actin-rich thin processes termed foot processes (435). The foot processes are functionally defined by three membrane domains: the apical membrane domain, the modified adherens junction domain anchoring the filtration slit diaphragm protein complex (346), and the basal membrane domain, which is associated with the GBM (436,437). The foot processes are anchored in the underlying GBM *via* integrins and dystroglycans and these are coupled to the basal actin cytoskeleton (61,346,362,424-426). The 25-60 nm filtration slits between adjacent foot processes are bridged by the zipper-like slit diaphragm composed of nephrin, nephs and FATs, that is largely responsible for the size-selectivity of the glomerular filtration barrier (61,346,362,424,425). The slit diaphragm proteins are also anchored to cortical actin by several intracellular proteins, including podocin, CD2AP and α -actinin. The apical domain of the foot processes forms a dome that is covered by a dense glycocalyx containing HSPGs and a high concentration of podocalyxin. These negatively charged proteins tend to repel adjacent foot processes, leaving a space between them. Podocalyxin, in turn, is anchored to cortical actin by NHERF2 and ezrin (359,360)

The distinct foot process domains are physically and functionally interconnected by the intracellular actin cytoskeleton, establishing structural integrity (426,436-438). The foot process cytoskeleton is composed of well-organized actin bundles that run parallel to the longitudinal axis of foot processes (426). Alterations in any of the three foot process domains leads to an active reorganization of the actin cytoskeleton (359,360) from parallel contractile bundles into a flat network, leading to foot process effacement and proteinuria (436). Hence, proteins involved in the dynamic regulation of the podocyte actin cytoskeleton are of critical importance for the

maintenance of normal glomerular function.

CLIC5A was recently identified as an actin-associated protein. . In our laboratory, Serial Analysis of Gene Expression (SAGE) revealed that the transcript for (CLIC5) is enriched ~800-fold in human glomeruli compared with non-glomerular tissues and cells (439). The glomerular CLIC5 transcript was subsequently shown to represent the CLIC5A isoform. A similar enrichment of the CLIC5 transcript is also obvious in a human glomerular SAGE library that was compared with libraries from microdissected nephron segments (440), and the CLIC5 transcript is enriched in a mouse glomerular expressed sequence tag library compared with whole kidney (441). Enrichment of the CLIC5 transcript in glomeruli, which is similar to that observed for transcripts of other podocyte-specific proteins like podocin and nephrin (439), suggests that CLIC5 might play an important role in glomerular function.

CLIC5A was first purified from human placenta microvilli using an ezrin peptide as bait, and was part of a complex containing actin, and several other actin-associated proteins (28). Ezrin is a member of the ERM protein family involved in coupling plasma membrane proteins to the cortical actin (80). CLIC5A colocalizes with ezrin at the apical surface of placental epithelium in tissue sections (28) and also in transfected placental epithelial cells expressing a CLIC5A fusion protein (56). CLIC5A is also essential for hearing and balance in mice. It is concentrated in stereocilia of mechanosensory hair cells of the cochlear and vestibular organs. In these highly specialized epithelial cells, CLIC5A concentrates at the base of the stereocilia bundle, a distinct morphological domain of the stereocilia where the ERM protein radixin is also concentrated (57,85). In CLIC5^{-/-} mice, CLIC5A protein is absent from the cochlear and vestibular hair cells, radixin protein levels are reduced, and stereocilia begin to degenerate soon after birth, leading to vestibular dysfunction and complete deafness by 7 months of age (57). The

fact that radixin deficiency also results in deafness associated with progressive degeneration of cochlear hair cell stereocilia in mice (98), and that mutations in the human radixin gene are associated with nonsyndromic hearing loss (58), suggests strongly that radixin and CLIC5A are part of a functionally important unit.

Since CLIC5A is highly expressed in glomeruli, and since I have established that CLIC5A activates ezrin in COS-7 cells, and taking into account previous reports showing that the podocyte apical domain contains abundant ezrin that connects the cytoplasmic tail of podocalyxin to the actin cytoskeleton (360,442) via the adaptor protein NHERF2, it seemed logical to postulate that CLIC5 regulates ezrin function in podocytes. I therefore undertook the following steps to test this hypothesis:

- 1- Define the molecular interaction between CLIC5A and the ERM protein ezrin/NHERF2/podocalyxin protein complex in glomerulus.**
- 2- Explore the molecular abnormalities in the ezrin/Podocalyxin/NHERF2 and actin complex, associated with CLIC5A deficiency.**
- 3- Determine whether the absence of CLIC5A confers vulnerability to kidney injury.**

5.2 Results

5.2.1 Localization of CLIC5A protein in glomerular podocytes and endothelial cells (ECs).

Expression of the CLIC5A protein in glomerular cells was evaluated with confocal immunofluorescence microscopy (IF). Frozen kidney sections from bovine and human kidneys were co-stained with antibodies against CLIC5A and the endothelial cell marker Tie-2 or the podocyte marker synaptopodin. Immunofluorescence microscopy showed that CLIC5A co-localized with the endothelial cell marker Tie-2 (Figure 5.1-A) and with the podocyte marker synaptopodin (Figure 5.1-B), suggesting that CLIC5 is expressed in both cell types. In negative control, where the primary antibodies were omitted, no immuno reactivity was observed.

To define the subcellular distribution of glomerular CLIC5A in greater detail, immunogold TEM was performed with affinity-purified CLIC5A-specific polyclonal antiserum. In podocyte foot processes, CLIC5A-reactive immunogold particles were found in close proximity to the apical plasma membrane and not at the filtration slit diaphragm or at the basal surface facing the GBM. In glomerular endothelial cells, CLIC5A was observed in both the fenestrated and nonfenestrated regions (Figure 5.1-C). The density of immunogold labeling was quantified by morphometric analysis and showed that CLIC5A labeling was greatest in podocytes and glomerular endothelial cells, in keeping with the mRNA expression data (Figure 5.1-D).

5.2.2 Glomerular CLIC5A is a component of the ezrin-NHERF2-podocalyxin complex

Several previous studies have shown that ezrin connects podocalyxin directly or via NHERF2 to the apical cytoskeleton of podocyte foot processes (359,360,442). In addition, ezrin affinity chromatography was used in the original isolation and identification of CLIC5A as a

cytoskeletal-associated protein (28). Given that the immunogold labeling of CLIC5A in podocytes observed here is very similar to that described for ezrin and podocalyxin (442), we next examined the possibility that CLIC5A may be part of the ezrin/NHERF2/podocalyxin complex. Using confocal immunofluorescence microscopy, I observed a considerable colocalization of CLIC5A immunoreactivity with podocalyxin, ezrin and NHERF2 in glomeruli (Figure 5.2-A). Furthermore, podocalyxin was co-immunoprecipitated with CLIC5A from lysates of mouse glomeruli (Figure 5.2-B). These results are consistent with the hypothesis that in glomeruli CLIC5A is part of the podocalyxin/NHERF2/ezrin complex.

5.2.3 Molecular abnormalities in glomeruli of CLIC5-deficient mice

5.2.3.1 Reduced phospho- and total ezrin abundance in glomeruli of CLIC5^{-/-} mic..

A Previous study had revealed that the ERM protein radixin is reduced in stereocilia of CLIC5^{-/-} mice (57). In addition, the previous finding that the dephosphorylated (inactive) form of ERM protein is more susceptible to proteasomal degradation (373), led me to compare the localization of P-ERM immunoreactivity in glomeruli of CLIC5^{+/+} and CLIC5^{-/-}. To preserve ERM phosphorylation, tissue was rapidly fixed in trichloroacetic acid (125). The COOH-terminal phosphorylation site is highly conserved among the ERM proteins; consequently, phospho-specific antibodies do not distinguish between them. Since CLIC5A is expressed in glomerular endothelial cells, and moesin is the predominant ERM in endothelial cells (81), P-ERM colocalization with the endothelial cell marker PECAM-1 was evaluated. Immunofluorescence labeling for P-ERM was observed as dual bands along glomerular capillary loops in CLIC5^{+/+} mice. One of the P-ERM bands strongly co-localized with PECAM-1. Interestingly, in glomeruli from age-matched CLIC5^{-/-} mutant mice, the P-ERM band co-

localizing with PECAM-1 was preserved, whereas labeling for P-ERM presumably associated with podocytes was markedly reduced (Figure 5.3-A). CLIC5A is also expressed in podocytes where ezrin is the main ERM protein. As shown in figure 5.3-B P-ERM labeling was observed in glomeruli of wild-type mice and overlapped with the podocyte marker podocin. In glomeruli of CLIC5^{-/-} mice, P-ERM staining was much less intense, and colocalization with podocin was reduced compared with the appearance in wild-type mice.

I next looked at the level of ezrin in glomeruli from CLIC5^{+/+} mice and CLIC5^{-/-} mutant mice. Glomeruli were collected as described in the materials and methods section (81,131). Western blot analysis showed that much less ezrin and P-ERM are associated with the detergent soluble and insoluble (pellet) fractions of glomeruli from CLIC5^{-/-}, compared to CLIC5^{+/+} mice. As expected, CLIC5A protein was detected on western blots of glomerular lysates from CLIC5^{+/+}, but not from CLIC5^{-/-} mutant mice (Figure 5.3-C). Taken together with the observation that P-ezrin and total ezrin abundance in glomeruli are reduced, the data suggest strongly that CLIC5 is crucial for maintaining the P-ERM protein ezrin, hence total ezrin in glomerular podocytes.

5.2.3.2- Reduced NHERF2 association with the cytoskeletal fraction in CLIC5^{-/-} mice.

In glomerular podocytes, P-Ezrin binds NHERF2, coupling it to the actin cytoskeleton (359,360,442). The reduced level of P-ERM in podocytes of CLIC5^{-/-} mice (Figure 5.3-B), would predict that deletion of CLIC5 would also alter the association of NHERF2 with the cytoskeleton. WB analysis of kidney cortex fractions showed that substantial NHERF2 was observed in the detergent-insoluble, cytoskeletal fraction of kidney cortex lysates from wild-type mice, but in CLIC5^{-/-} mice, most of the NHERF2 remained in the soluble fraction. This finding

is consistent with the concept that CLIC5A-dependent ezrin phosphorylation leads to the association of NHERF2 with the cytoskeleton and that this association is disrupted in CLIC5^{-/-} mice (Figure 5.4).

5.2.3.3- *Reduced abundance and altered mobility of glomerular Podocalyxin in CLIC5^{-/-} mice.*

Podocalyxin interacts with both, P-Ezrin and NHERF2, and loss of this interaction is associated with podocalyxin hyperphosphorylation, and its retardation on SDS-PAGE gels (443). I therefore determined the podocalyxin abundance and SDS-PAGE mobility in glomerular lysates from CLIC5^{-/-} mice relative to control wild-type mice. WB analysis showed that the CLIC5^{-/-} glomerular podocalyxin abundance was reduced, and its mobility was retarded relative to podocalyxin in glomerular lysates from CLIC5^{+/+} mice (Figure 5.5-A). In addition, the co-localization of P-ERM with podocalyxin in glomeruli observed in CLIC5^{+/+} mice was largely lost in glomeruli of CLIC5^{-/-} mice (Figure 5.5-B). These findings suggest that CLIC5 stabilizes podocalyxin/NHERF2/ezrin protein complex most likely by regulating ERM phosphorylation and function *in vivo*. The findings also raise the possibility that the absence of CLIC5A could contribute to an increased susceptibility to glomerular injury and impaired kidney function.

5.2.4 Ultrastructural and functional abnormalities in glomeruli of CLIC5^{-/-} mice

The molecular abnormalities in the podocalyxin/NHERF2/ezrin protein complex associated with CLIC5 deficiency led us to explore any possible histological and ultrastructural abnormalities in CLIC5^{-/-} mice. Renal histology appeared normal by light microscopy in CLIC5^{+/+} and CLIC5^{-/-}. Mice ≤ 18 months of age. However, by TEM there was a clear, patchy broadening and effacement of podocyte foot processes in CLIC5^{-/-} compared to CLIC5^{+/+} mice (Figure 5.6-A). Morphometric analysis showed a significant reduction in the number of

podocytes foot processes / linear μm GBM in $\text{CLIC5}^{-/-}$ relative to $\text{CLIC5}^{+/+}$ (Figure 5.6-B). In the glomerular endothelium, the fenestrated portion appeared normal, but large vacuoles were observed in many glomerular endothelial cell bodies (Figure 5.6-C). Morphometric analysis showed a significant increase in vacuolar : endothelial cell area in $\text{CLIC5}^{-/-}$ relative to $\text{CLIC5}^{+/+}$ (Figure 5.6-D). These ultrastructural abnormalities were associated with a subtle increase in urinary albumin concentration in the $\text{CLIC5}^{-/-}$ mice based on western blot analysis with anti-albumin antibodies (Figure 5.6-C).

5.2.5 Increased susceptibility of $\text{CLIC5}^{-/-}$ mice to adriamycin-induced glomerular injury

5.2.5.1-Histological and ultrastructural characterization of ADR nephropathy in $\text{CLIC5}^{-/-}$ mice.

Adriamycin nephropathy is a well-established model of glomerular injury in rats and mice (444,445). The susceptibility of mice lacking CLIC5 to adriamycin-induced glomerular injury was evaluated. Three month-old, male $\text{CLIC5}^{+/+}$ and $\text{CLIC5}^{-/-}$ were injected intravenously with 10 mg/kg Adriamycin. Two months after adriamycin injection, the kidneys were removed, fixed in 10% buffered formalin, and embedded in paraffin. Paraffin sections (5 μm thick) were stained with hematoxylin & eosin (H&E) and Masson's trichrome stain. By light microscopy, H & E staining did not show any obvious differences between WT and $\text{CLIC5}^{-/-}$ Adriamycin-treated mice. In preliminary experiments done with two pairs of animals, there appears to be an increase in glomerulosclerosis in the $\text{CLIC5}^{-/-}$ but not $\text{CLIC5}^{+/+}$ mice as shown by trichrome staining (Figure 5.7-A), however the number of animals in this experiment need to be increased to determine whether this finding holds. Similarly, electron micrographs of ultrathin sections from $\text{CLIC5}^{-/-}$ and $\text{CLIC5}^{+/+}$ mice showed the marked effacement of podocyte foot processes in $\text{CLIC5}^{-/-}$ relative to $\text{CLIC5}^{+/+}$ mice (Figure 5.7-B). These findings suggest that CLIC5A may be

important in the resistance of podocytes against Adriamycin toxicity in mice, or they may indicate podocyte remodeling and repair after injury is defective in CLIC5^{-/-} mice.

5.2.5.2- Glomerular permselectivity in Adriamycin nephropathy in CLIC5^{-/-} mice.

To evaluate glomerular permselectivity after Adriamycin administration, urine samples were collected from conscious mice for two months. Amido black staining of SDS-PAGE membrane of urine samples from CLIC5^{+/+} and CLIC5^{-/-} mice showed that albuminuria starts to develop two weeks after injection of adriamycin and persist thereafter (Figure 5.8-A). WB analysis of urine samples three weeks after Adriamycin injection showed that albuminuria was observed in both CLIC5^{+/+} mice and their CLIC5^{-/-} littermates (Figure 5.8-B), but albuminuria was significantly greater (albumin:creatinine ratio 560 ± 135 vs. $1,691 \pm 350$ $\mu\text{g}/\text{mg}$, $P < 0.02$; $n = 5/\text{group}$, mean \pm SE) in the CLIC5^{-/-} mice compared to CLIC5^{+/+} controls (Figure 5.8-C). This finding is consistent with the severe ultrastructural abnormalities observed in the CLIC5^{-/-} and suggests that that CLIC5A deficiency enhances the vulnerability of glomerular podocytes to adriamycin-toxicity.

5.3 Discussion:

The data in this chapter show that the CLIC5A protein is highly expressed in renal glomerular podocytes and in glomerular endothelial cells. In podocyte foot processes, CLIC5A localizes to the apical membrane and is not found at the filtration slit or in the basal, GBM-anchoring domain. CLIC5A colocalizes with ezrin, NHERF2 and podocalyxin in podocytes, and podocalyxin coimmunoprecipitates with CLIC5A from glomerular lysates. In keeping with the idea that CLIC5A is a member of the podocalyxin/NHERF2/ezrin complex. In CLIC5^{-/-} mice, podocyte-associated P-ERM immunoreactivity is essentially absent, and total ezrin abundance is markedly reduced when compared to that in wild-type mice. Furthermore, when compared to CLIC5^{+/+} mice, the association of NHERF2 with the cytoskeleton, and the overall abundance of podocalyxin are markedly diminished in podocytes of the CLIC5^{-/-} mice. The absence of CLIC5 is also associated with visible broadening and effacement of podocyte foot processes, which becomes more severe in response to Adriamycin-induced glomerular injury. The CLIC5^{-/-} mice have microalbuminuria at baseline, and develop more severe albuminuria during the course of Adriamycin nephropathy when compared to their wild-type littermates. Together, these findings are consistent with the functions of CLIC5A described in COS-7 cells, where CLIC5A enhances ERM phosphorylation (Chapter 3). It seems likely that CLIC5A serves to activate ezrin phosphorylation at the apical plasma membrane of podocyte foot processes, thereby coupling NHERF2 and podocalyxin to cortical actin. I postulate that this process is important in maintaining the appropriate ultrastructure of glomerular podocytes.

Ezrin is abundant in developing and mature podocytes, and its distribution changes in response to podocyte injury (446). The localization of ezrin by immunogold TEM to the apical domain of podocyte foot processes (442), is similar to that observed here for CLIC5A (Figure

5.1-C). In podocytes, ezrin, together with the scaffold protein NHERF2 connects the cytoplasmic tail of podocalyxin to the actin cytoskeleton (360,442). This association between ezrin and podocalyxin is lost when the negative charges on podocalyxin are neutralized with protamine sulfate or removed by sialidase (360). Podocyte foot process effacement, which is observed under these conditions, is therefore associated with inactivation (and probably degradation) of ezrin and the uncoupling of podocalyxin and NHERF2 from the podocyte cytoskeleton. In keeping with the importance of podocalyxin in defining podocyte function, deletion of the podocalyxin gene in mice causes death within 24 hours of birth as a result of renal failure that is associated with podocyte foot processes effacement (361). Our results showed a reduced level and altered electrophoretic mobility of podocalyxin from glomerular lysates of CLIC5^{-/-} mice, similar to that observed for rat glomerular podocalyxin in the model of puromycin aminonucleoside (PAN)-mediated nephrosis (443).

The inter-dependence of ezrin and its intermediate adaptor proteins NHERF1 or NHERF2 is well established in the formation of cell-surface projections in epithelial cells. For example, the loss of ezrin results in reduced microvillus formation and mis-localization of NHERF1 in retinal epithelial cells (447), and the loss of NHERF1 results in ezrin depletion from the brush border of the kidney proximal tubule and small intestine epithelial cells (448). In podocytes, ezrin uses NHERF2 as an intermediate linker to podocalyxin. My observation that NHERF2 failed to be associated with the cytoskeleton in CLIC5^{-/-} mice, where phosphorylated ezrin was also reduced, is consistent with the dependence of NHERF2-cytoskeletal coupling on active ezrin, and the requirement of ezrin activation by CLIC5A in podocytes.

CLIC5A co-localizes with ezrin in glomerular podocyte foot processes (Figure 5.2-A), and with radixin at the base of cochlear and vestibular hair cell stereocilia (57,98,449). Deletion of

the CLIC5A protein in CLIC5^{-/-} in mice is associated with progressive loss of hair cell stereocilia and with a reduced number of podocyte foot processes in glomeruli (Figure 5.6-A). Furthermore, CLIC5A was originally identified in an interaction with ezrin-containing cytoskeletal protein complexes in human placental microvilli (28), and in COS-7 cells, and ectopic CLIC5A expression leads to ezrin activation, actin polymerization and the formation of cell-surface projections (Chapter 3). Taken together, the findings are consistent with a model in which CLIC5A is required for the highly localized activation of the ERM proteins radixin and ezrin and their association with actin, in turn organizing the specialized actin-based projections of hair cells and podocytes, respectively. In the absence of CLIC5A the structure and function of both, hair cell stereocilia and podocyte foot processes is impaired. Hence, it seems safe to conclude that CLIC5A and ezrin cooperate in regulating the membrane to cortical actin linkages required for proper morphology of podocyte foot processes.

In CLIC5^{-/-} mice the significant derangement of podocyte architecture was associated with only mild albuminuria at baseline, and the overall renal histology seemed normal even in aged CLIC5^{-/-} mice, even though the number of foot processes per unit GBM was reduced by almost 50% (Figure 5.6-B). These findings argue that the absence of CLIC5A, the associated reduction in ezrin expression, and the alteration in podocyte foot process architecture are not sufficient to substantially alter glomerular permselectivity, and that these abnormalities do not lead to obvious glomerular matrix remodeling over time. Although it has been proven that proteins forming the filtration slit diaphragm and those linking podocytes to the GBM are critical in maintaining glomerular protein permselectivity (300,311), our findings suggest that the ezrin-dependent apical membrane organization is less important in this function. While experiments exploring the abundance and regulation of slit diaphragm proteins in CLIC5A has not been undertaken, it

seems likely that the expression of nephrin, the Nephs and FATs as well as their association with intracellular binding and signaling partners is not altered in podocytes lacking CLIC5A. Nonetheless, the absence of CLIC5A and associated abnormalities in ezrin abundance and glomerular structure do confer greater susceptibility to Adriamycin-induced injury. Since the severity of albuminuria and the degree of foot process effacement seemed to worsen as a function of time after Adriamycin injection, it is tempting to speculate that podocyte remodeling after injury requires CLIC5A.

In addition to defective podocyte structure in the CLIC5^{-/-} mice, the glomerular capillary lumen was larger in CLIC5^{-/-} than in wild-type mice, the glomerular endothelial cell compartment was expanded, and many glomerular endothelial cells contained large vacuoles. The functional significance of these changes in glomerular endothelial cells is unclear. Certainly, while moesin is hyperphosphorylated in COS-7 cells expressing CLIC5A (Chapter 3), the absence of CLIC5A did not reduce ERM phosphorylation in glomerular endothelial cells (Figure 5.3). Hence, if CLIC5A regulates ERM phosphorylation in these cells, substitution of this role by other CLICs in CLIC5^{-/-} mice must be postulated. Excess glomerular endothelial cell vacuolization has been described in rats given VEGF antagonists (450,451). Since podocyte-derived VEGF is critical for glomerular endothelial cell differentiation (290,452), the possibility that podocytes of CLIC5^{-/-} mice produce less VEGF than controls will need to be investigated. Nonetheless, since glomerular endothelial fenestration was preserved, a major defect in podocyte VEGF synthesis seems unlikely.

It is of note that P-ERM was diminished only in podocytes and not in glomerular capillary endothelial cells of CLIC5^{-/-} mice, although CLIC5A is expressed by glomerular endothelial cells in wild-type mice and in culture (453). Therefore, a function of CLIC5A that does not involve

moesin in glomerular endothelial cells must also be considered. In this regard, a role for CLIC4 in endothelial cell tube formation in vitro has been described (48,49), and an angiogenesis defect has recently been reported in CLIC4^{-/-} mice (377). Furthermore, acidified vacuoles that appeared to be capillary lumen precursors were observed in three-dimensional cultures of endothelial cells from wild-type mice, and in endothelial cells from the CLIC4^{-/-} mice, vacuolar acidification was defective (377). Given the role of CLIC4 in endothelial cells, I considered whether CLIC5A immunofluorescence and immunogold labeling of glomerular ECs in this study could be due simply to cross-reactivity of the anti-CLIC5A antibody with CLIC4 in endothelial cells. This possibility seems unlikely given that the transcript-specific CLIC5A SAGE tag was first discovered in homogeneous cultures of glomerular endothelial cells (453). Furthermore, in CLIC5^{-/-} mice, the CLIC5A antibody showed no glomerular immunoreactivity at all. Glomerular endothelial cell vacuolization and endothelial cell compartment expansion phenotypes observed in the CLIC5^{-/-} mice is also consistent with previous finding which showed that disruption of the CLIC homolog (EXC)-4, normally associated with the plasma membrane of the excretory canal of *C. elegans*, results in expansion of luminal membrane and cystic enlargement of the canal (3). It is conceivable that the vacuoles observed in glomerular ECs of CLIC5^{-/-} mice are in some way related to disordered capillary lumen formation and that CLIC4 functionally substitutes for CLIC5 in glomerular endothelial cells in regard to moesin phosphorylation, since these two proteins share 76% homology at the amino acid level.

Since deletion of CLIC5 results in general absence of CLIC5A and CLIC5B, it might be argued that the abnormalities observed here are due to a nonspecific systemic effect. However, whereas ezrin is highly expressed in many epithelial cell types, including proximal tubule epithelial cells, and supports the formation of microvilli, CLIC5A expression is highly restricted

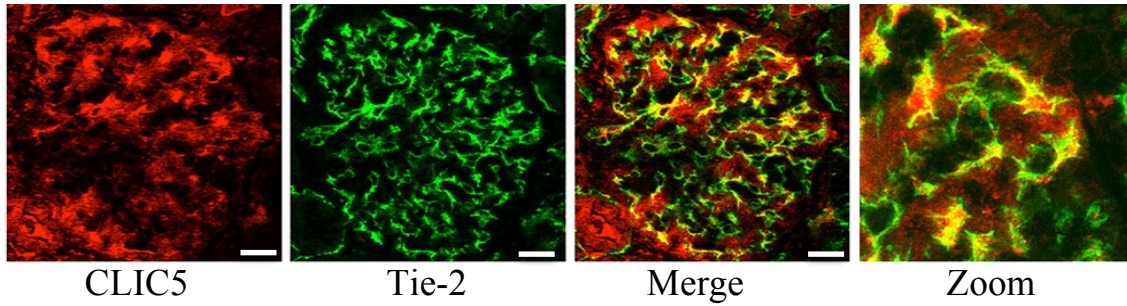
to only a few cell types, among them glomerular cells (439). Therefore, CLIC5A cannot be essential for ERM protein activation generally, but must regulate ERM protein function in relationship to other, highly specific processes that define the structure of hair cell stereocilia and podocytes. Still, since overexpression strongly activates ERM proteins even in cells that do not express CLIC5A at baseline (Chapters 3,4), and since CLIC1 and CLIC4 seem to mimic this effect, it seems likely that CLICs generally serve to activate ERM proteins but that each isoform has its specific functional target. The preliminary findings that CLIC1 and CLIC4 overexpression lead to enhanced ERM phosphorylation in COS-7 cells (Figure 3.7) would be consistent with the latter possibility. Nonetheless, to clearly demonstrate that the effects of CLIC5 on ezrin activation are specific for podocytes, it will be necessary to study either podocyte-specific deletion of CLIC5 or podocyte-specific rescue in CLIC5 transgenic mice.

In summary, my data support a functional role for CLIC5A in renal glomerular podocytes. *In vivo* CLIC5 plays a crucial role in maintaining the stability of podocalyxin/NHERF2/ezrin complex and its absence causes a marked reduction in abundance of podocalyxin, ezrin and P-ezrin as well as reduced association of NHERF2 with the cytoskeleton, leading to abnormal glomerular cell morphology and increased susceptibility to kidney injury (Figure 5.9). It remains to be determined whether the CLIC5 deficiency that leads to deafness in humans and is associated with reduced renal function (59) also leads to podocyte abnormalities. In addition, whether altered regulation of CLIC5A plays a role in diseases associated with podocyte effacement remains to be determined.

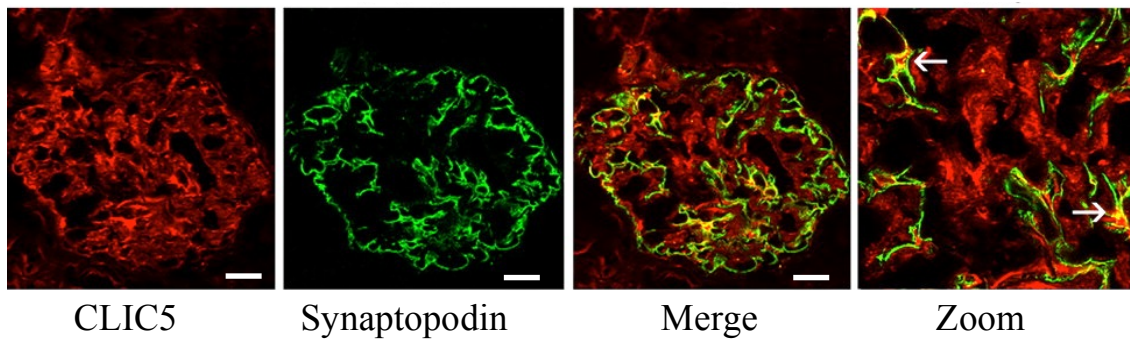
5.4 Figures

Figure 5.1

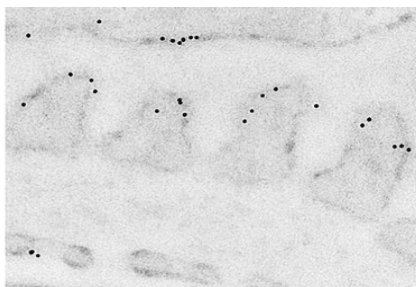
A



B



C



D

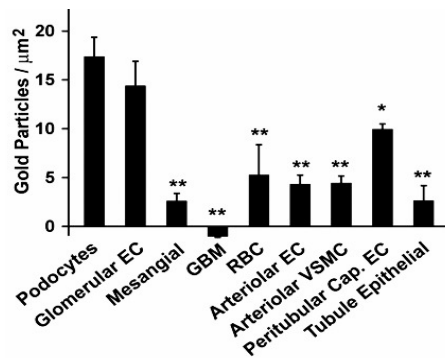
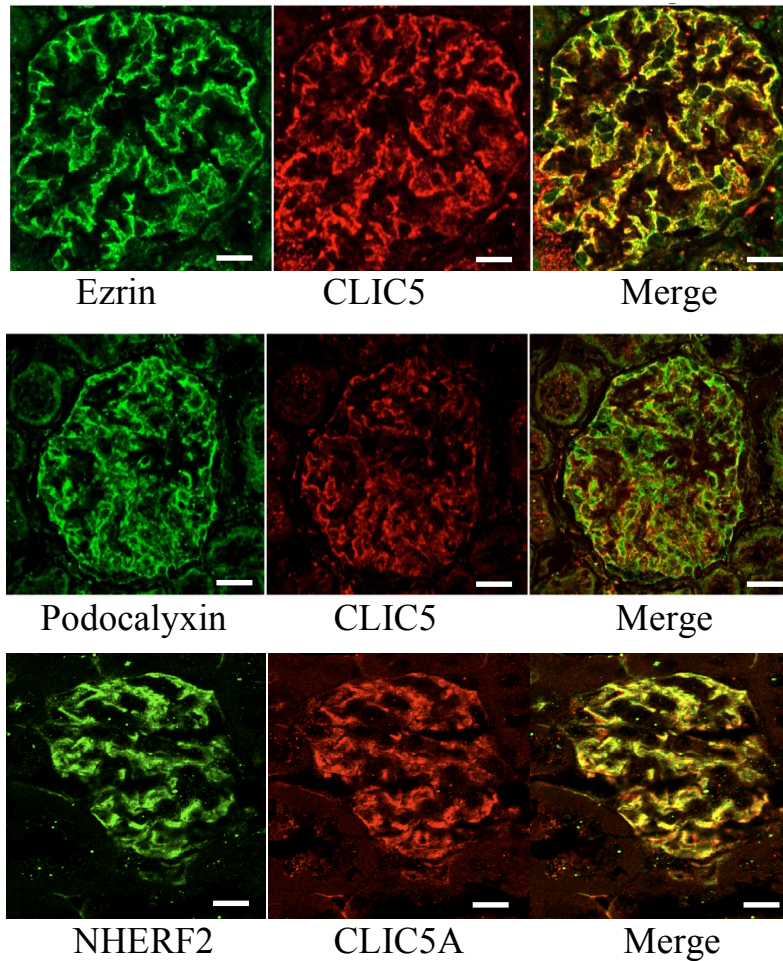


Figure 5.1. *CLIC5* protein expression in glomeruli. **A-** Confocal microscopy of frozen kidney section stained with antibodies against *CLIC5* (red) and endothelial marker Tie-2 (green) in human glomeruli. **B-** Confocal microscopy of frozen kidney section stained with antibodies against *CLIC5* (red) and podocytes foot processes marker Synaptopodin (green) in human glomeruli. White arrows: apparent *CLIC5* immunoreactivity in podocytes. **C-** *CLIC5* immunogold transmission electron microscopy (TEM) with *CLIC5* antibody in mouse kidney. **D-** Cell-associated gold particle density/background particle density. Scale bar = 10 μm

Figure 5.2

A



B

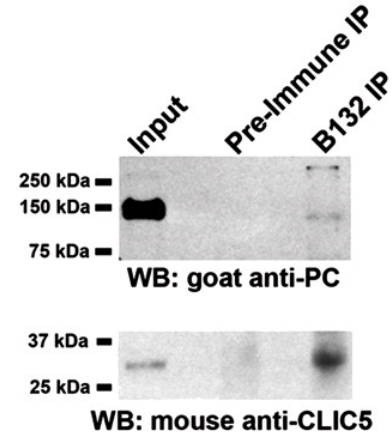


Figure 5.2. Glomerular CLIC5A is a component of the Ezrin-NHERF2-Podocalyxin complex. **A-** confocal immunofluorescence microscopy of human glomeruli co-stained with antibodies against (ezrin, podocalyxin and NHERF2) in green and CLIC5A in red. **B-** immunoprecipitation of CLIC5A followed by Western blot (WB) analysis with goat anti-podocalyxin (PC) or mouse anti-CLIC5 antibodies. Scale bar =10 μ m

Figure 5. 3

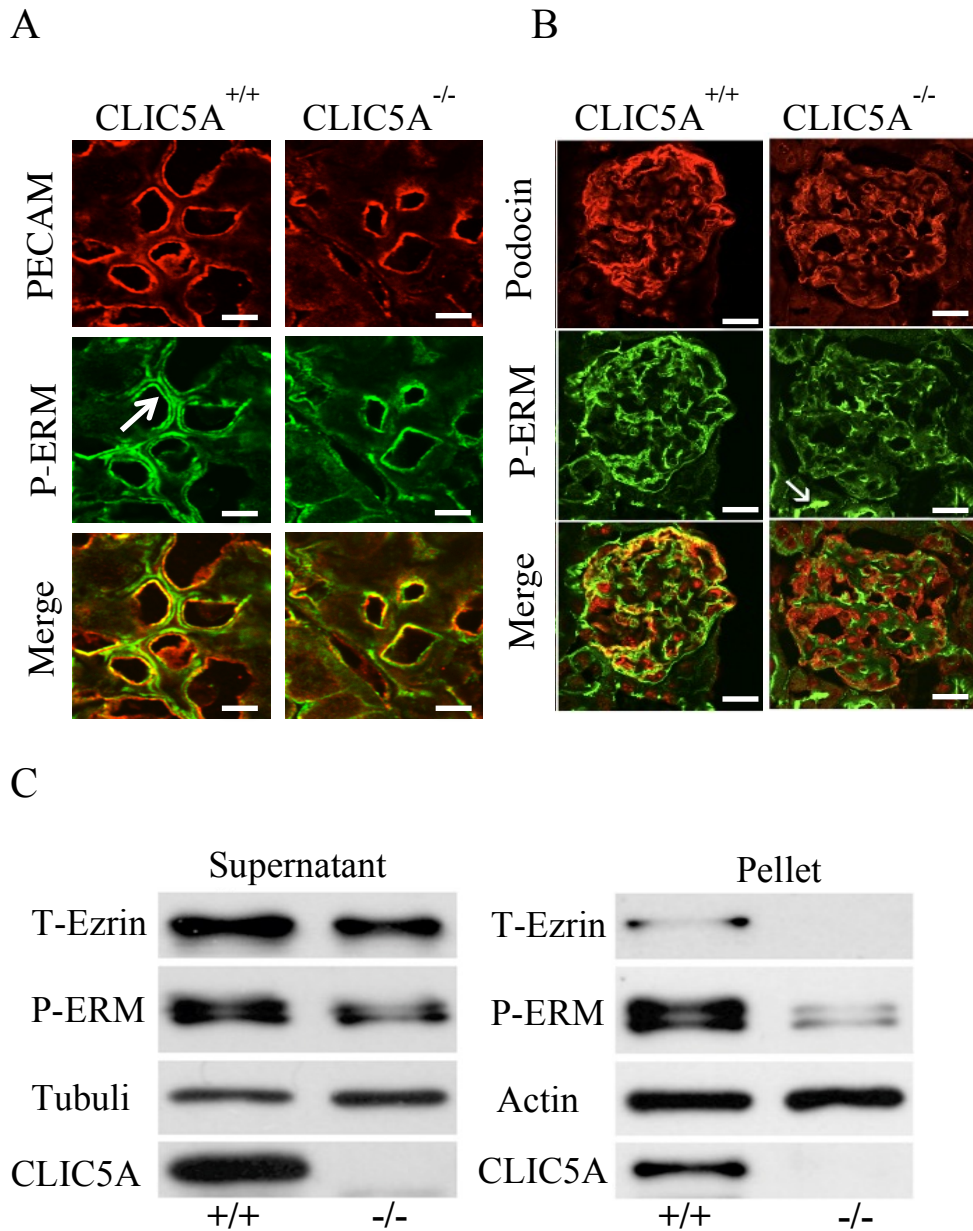


Figure 5.3. Reduced P-ERM and total ezrin abundance in glomeruli podocytes of CLIC5^{-/-} mice. Confocal-IF of TCA-fixed glomeruli from CLIC5^{+/+} and CLIC5^{-/-} mice. **A-** Goat anti-PECAM-1 and rabbit anti-P-ERM antibody. The white arrow shows a dual band of P-ERM labeling along a glomerular capillary loop. **B-** Goat anti-podocin and rabbit anti-P-ERM antibody. The white arrow shows preserved P-ERM in a proximal tubule. **C-** WB analysis of glomerular lysate from CLIC5^{+/+} and CLIC5^{-/-} mice. CLIC5 was observed in lysate and pellet from CLIC5^{+/+}, but not CLIC5^{-/-} mice. The P-ERM abundance was reduced in the supernatant and detergent insoluble fraction from glomeruli of CLIC5^{-/-} mice. Scale bar in A =10μm, and in B =20μm

Figure 5.4

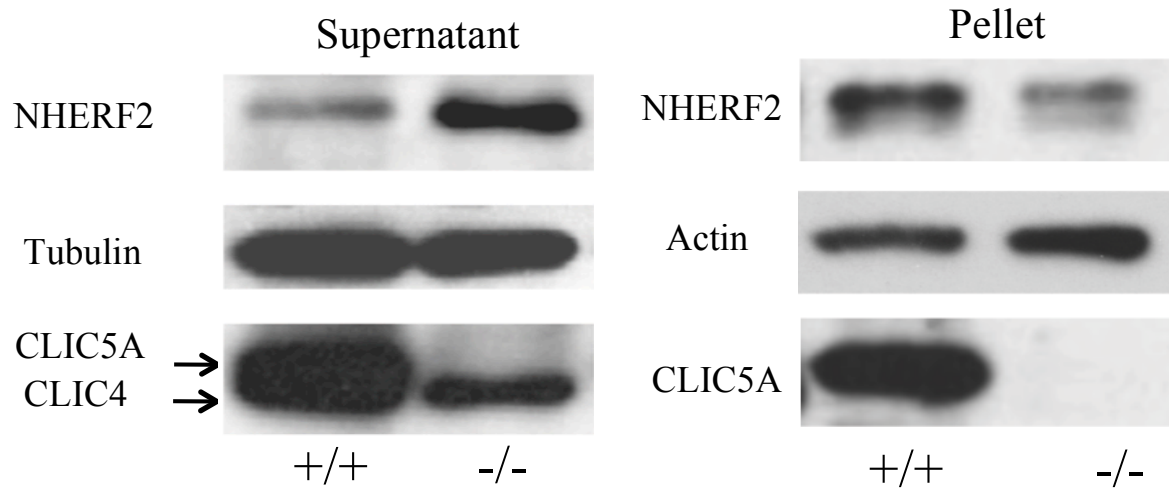


Figure 5.4. *CLIC5* deletion reduces *NHERF2* association with actin cytoskeletal fraction. Renal cortex from *CLIC5*^{+/+} and *CLIC5*^{-/-} mice was homogenized in Nonidet-40/Deoxycholate lysis buffer and then separated into soluble (supernatant) and insoluble (pellet) fractions followed by western blot analysis. In *CLIC5A*^{+/+} mice, substantial *NHERF2* was observed in the pellet, whereas most of *NHERF2* remained soluble in *CLIC5A*^{-/-} mice.

Figure 5.5

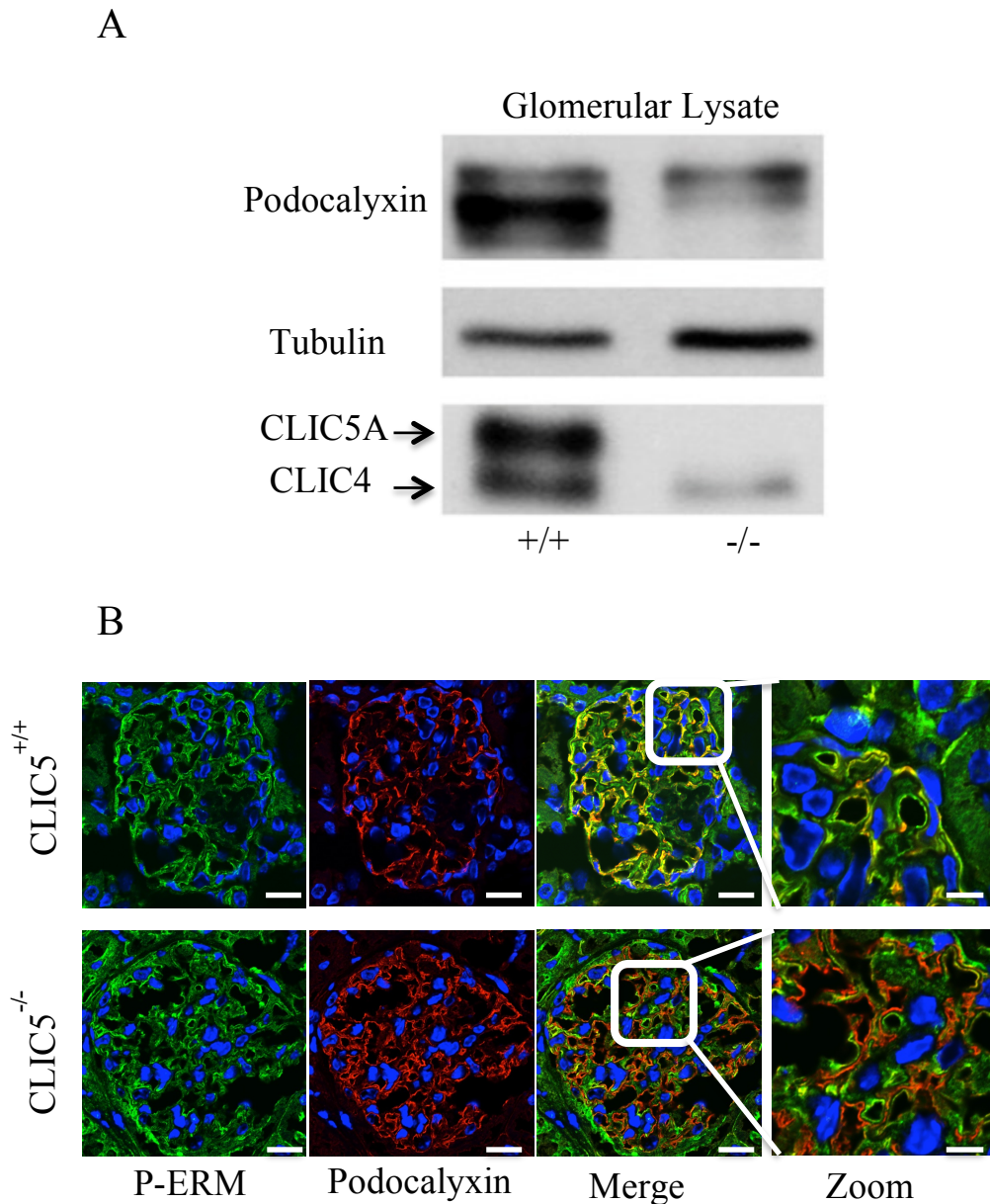


Figure 5.5. *CLIC5* deletion reduces and alters podocalyxin migration. **A-** Western blot analysis for podocalyxin in whole glomerular lysates from *CLIC5*^{+/+} and *CLIC5*^{-/-} mice. In *CLIC5*^{+/+} mice, podocalyxin migrated as a predominant ~150 kDa band, and a second band with slightly retarded mobility. In *CLIC5*^{-/-}, the predominant ~150 kDa band was not observed and only the more slowly moving band was observed. **B-** Confocal immunofluorescence microscopy for P-ERM (rabbit anti-phospho-Thr567 ezrin) and podocalyxin (goat anti-podocalyxin) in TCA-fixed renal glomeruli from *CLIC5*^{+/+} and *CLIC5*^{-/-} mice. P-ERM is present in glomeruli of both *CLIC5*^{+/+} and *CLIC5*^{-/-} mice, but co-localization of P-ERM with podocalyxin was substantially reduced in *CLIC5A* deficient, compared to wild-type mice. Scale bar =10μm

Figure 5.6

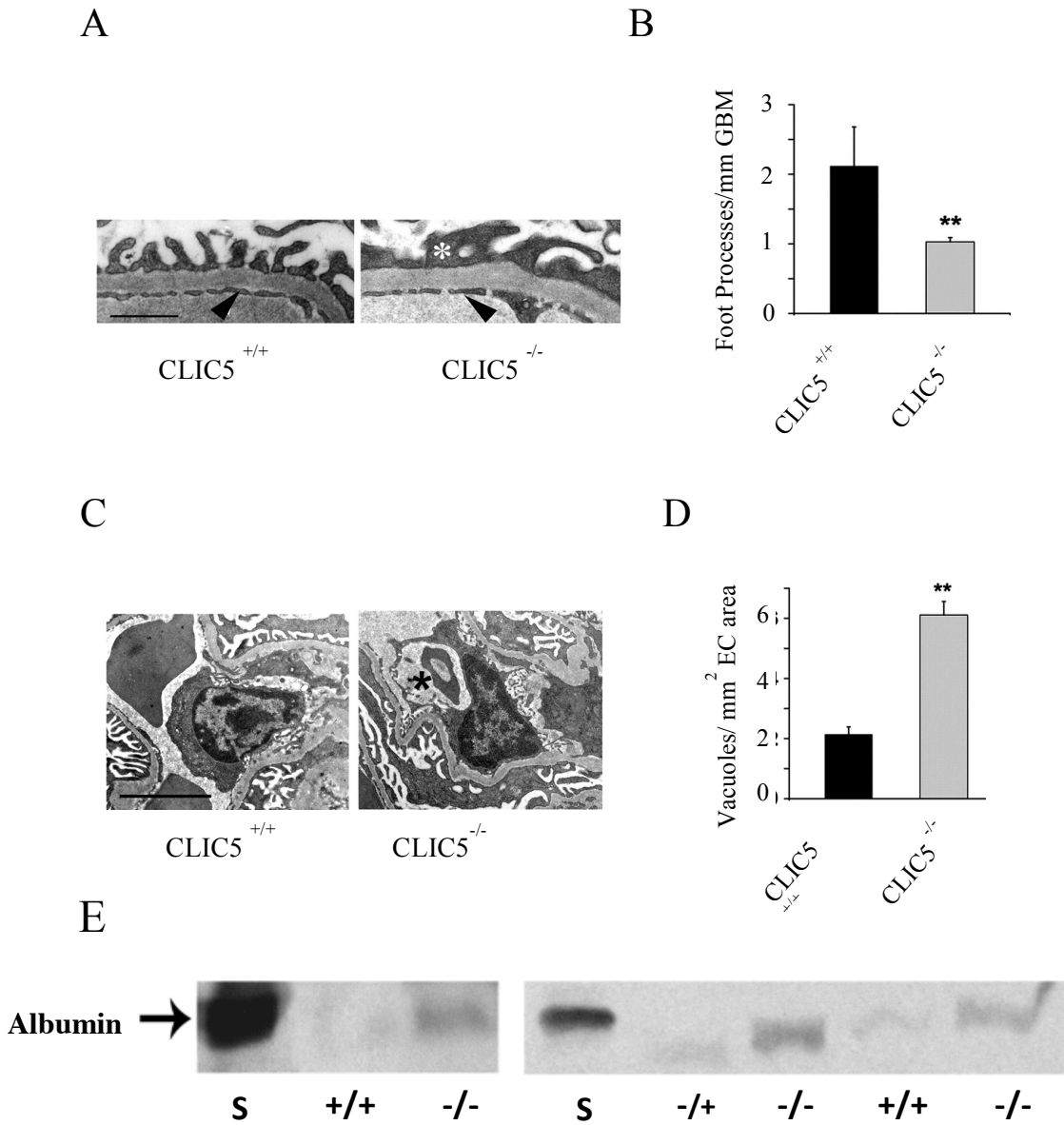
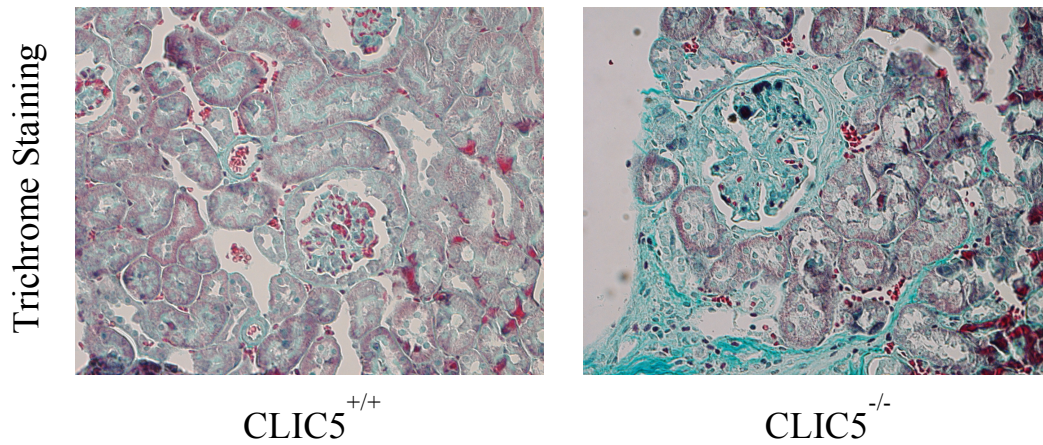


Figure 5.6. Abnormal glomerular ultrastructure and function in *CLIC5*^{-/-} mice. **A-** TEM appearance of the capillary wall of *CLIC5*^{+/+} and *CLIC5*^{-/-} mice. White asterisk shows a broadened foot process (scale bar, 0.5 μ m). **B-** The bar graph shows the quantification of foot process density in 8-mo-old *CLIC5*^{+/+} and *CLIC5*^{-/-} mice (means \pm SE; n = 4 mice/group, **P < 0.001). **C-** TEM of glomerular capillary endothelial cells from WT control and age-matched *CLIC5*^{-/-} mice. Black asterisk shows vacuolization of glomerular ECs (scale bar, 10 μ m). **D-** The bar graph shows the quantification of EC vacuoles/EC area (means \pm SE; n = 4 mice/group, **P < 0.01). **E-** Western blot analysis of mouse urine and serum with anti-albumin antibodies at baseline; 10 μ l of urine (20 mg/dl creatinine) was loaded per lane. +/+ : wild-type; +/- : heterozygous; -/- : homozygous mice. S stand for serum

Figure 5.7

A



B

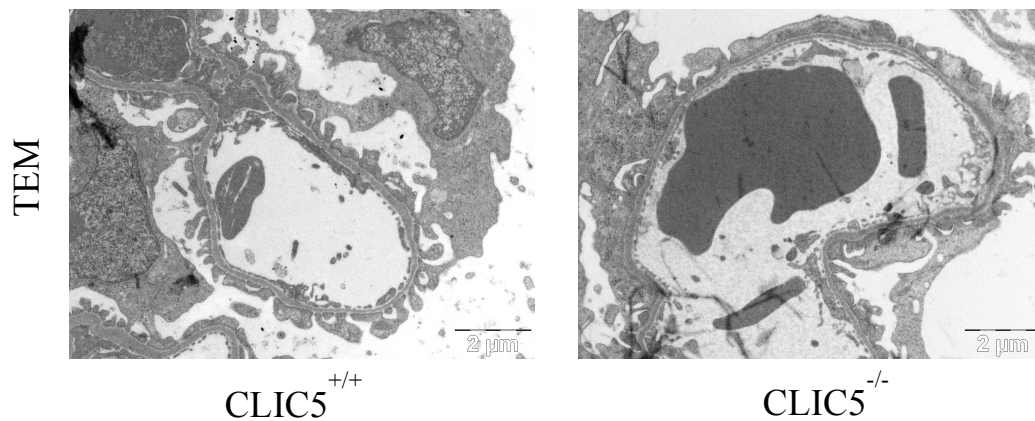


Figure 5.7. *CLIC5* deletion enhances susceptibility to glomerular injury as a result of ADR administration. **A-** Masson's trichrome stain of sections taken from CLIC5^{+/+} and CLIC5^{-/-} two months after ADR administration, showing increased collagen deposition in glomerulus of CLIC5^{-/-} relative to CLIC5^{+/+}. **B-** TEM micrographs of ultrathin sections taken from CLIC5^{+/+} and CLIC5^{-/-} 2 months after ADR administration showing increased effacement of podocyte foot processes of CLIC5^{-/-} relative to CLIC5^{+/+}.

Figure 5.8

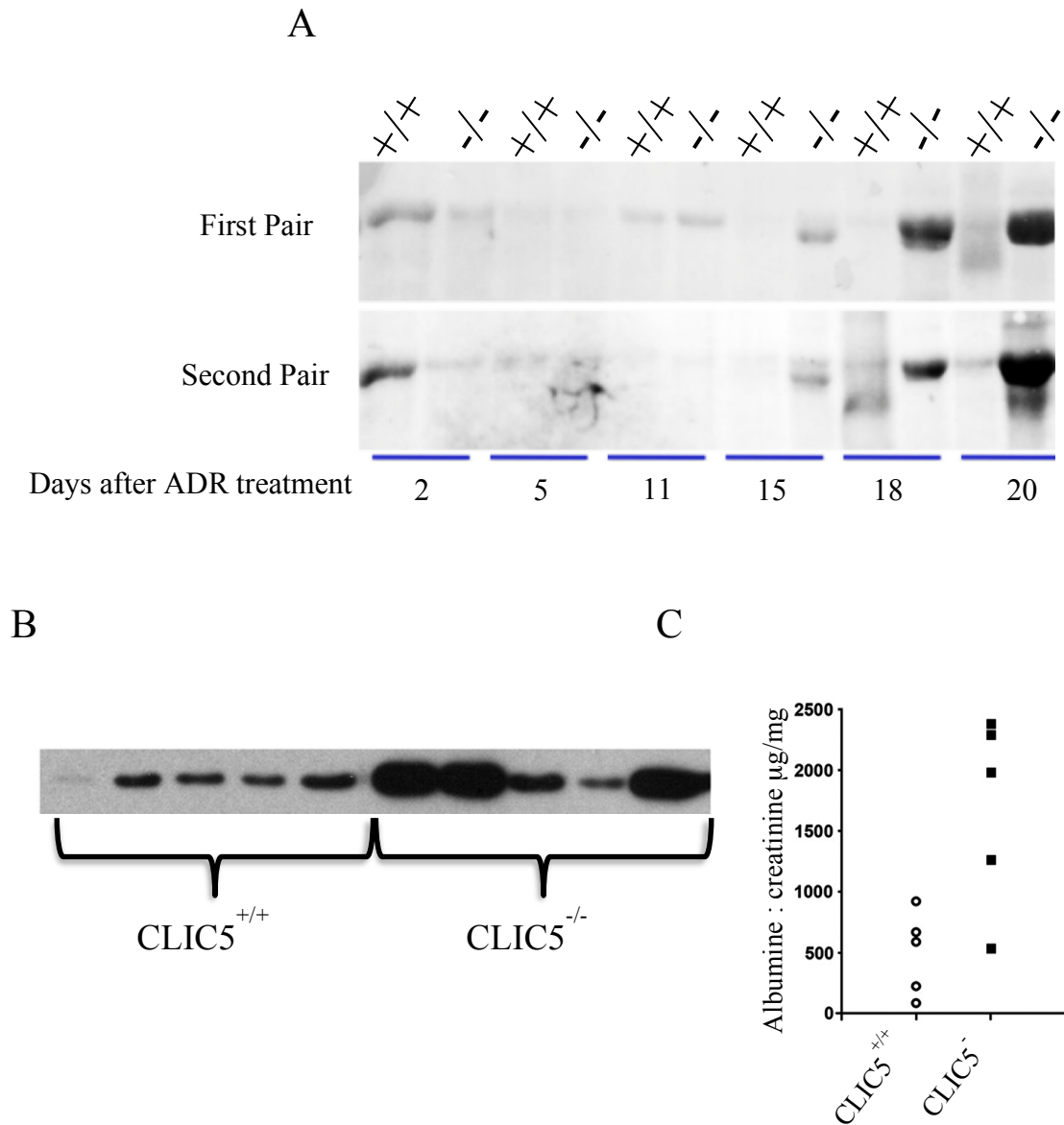


Figure 5.8. *CLIC5* deletion enhances susceptibility to glomerular injury. **A-** Amido black staining of SDS-PAGE membrane of mouse urine at several time points after ADR administration showing increased albumin leakage in *CLIC5*^{-/-} 3 weeks after ADR administration. All urine samples were normalized based on creatinine assay (20 mg/dl creatinine). **B-** Western blot analysis of mouse urine 3 weeks after adriamycin administration. Each lane represents urine from a separate mouse. All urine samples were normalized based on creatinine assay (20 mg/dl creatinine). **C-** Urine albumin was quantified densitometrically and expressed as the albumin/creatinine ratio. The difference between groups was significant ($P < 0.02$, unpaired t-test).

Figure 5.9

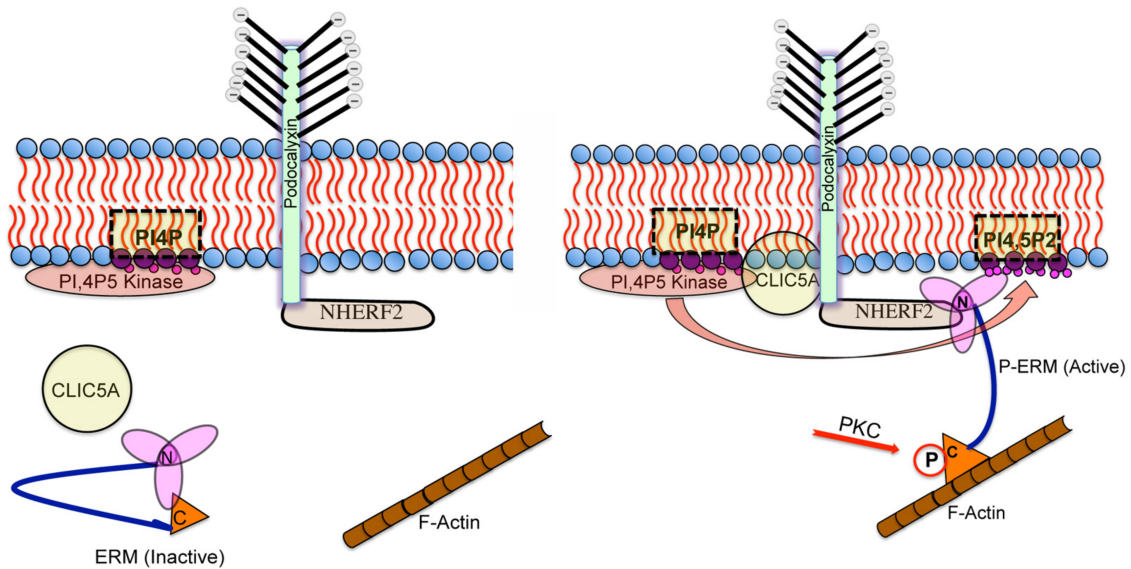


Figure 5.9. Schematic model of *CLIC5A* function in glomerular podocytes. It is postulated that the association of *CLIC5A* with the inner leaflet of the apical plasma membrane serves to promote clustered PI(4,5)P₂ generation. Ezrin binding to PI(4,5)P₂ in turn frees the ezrin C-terminus to bind actin and to promote ezrin phosphorylation. In the presence of *CLIC5A* the active form of ezrin couples the intracellular tail of podocalyxin to actin via NHERF2, a key determinant of the normal apical podocyte architecture

Chapter 6

General discussion and future directions

Chapter 6

General Discussion and Future Directions

6.1 General discussion

This thesis provides experimental evidence for a novel molecular mechanism that explains, at least in part, the functional relationship between the CLIC and ERM protein families. While previous studies had focused strongly on the putative (and controversial) ion-conducting properties of CLIC proteins, and only an association between CLIC and ERM proteins had been described, the work in this thesis shows that CLIC5A stimulates localized PI(4,5)P₂ generation by activating PI4P5 Kinases in the plasma membrane. In turn, PI(4,5)P₂ serves to bind and activate the ERM proteins ezrin and moesin, which control coupling of integral membrane proteins to cortical F-actin. Whereas the detailed function was dissected only for CLIC5A, my findings that CLIC1 and CLIC4, like CLIC5A, stimulate ERM phosphorylation suggest that this mechanism may hold generally for CLIC proteins.

In the final chapter of this thesis, I present data indicating that the mechanism of CLIC5A function observed in the simple cell-culture model, also holds *in vivo*. I was able to show that the CLIC5A is highly expressed in renal glomeruli, in keeping with previous reports of CLIC5A transcript enrichment in this capillary bed. In glomeruli CLIC5A localized to the apical membrane domain of podocyte foot processes, where it co-localized with podocalyxin, NHERF2 and ezrin. In CLIC5 deficient mice, glomerular podocyte ezrin phosphorylation was abrogated, and both ezrin and NHERF2 were found dissociated from the actin cytoskeleton. These molecular abnormalities are consistent with the mechanism uncovered in cells, where CLIC5A

stimulated ezrin phosphorylation and its associated with the cytoskeleton. I found that the number of podocyte foot processes in CLIC5A deficient mice was reduced by almost 50%, that the mice had a subtle glomerular wall permselectivity defect at baseline, and that they developed greater glomerular injury in response to Adriamycin than their wild-type littermates. The pathophysiologic changes in CLIC5 deficient mice suggest that podocyte remodeling and repair after injury is markedly abnormal.

The work so far leads me to postulate that CLIC5A acts to activate PI4P5- and/or PI5P4 kinase(s) at specific locations in the dorsal (apical) plasma membrane, resulting in an increased generation of PI(4,5)P2. The PI(4,5)P2 molecule then binds ezrin and facilitates its local phosphorylation and interaction with cortical actin and plasma membrane protein, forming dorsal actin-based projections. The data from CLIC5^{-/-} mice support a functional role for CLIC5 in renal glomerular podocytes. CLIC5A, through its association with the plasma membrane, either directly or indirectly activates PI4P5 kinase at the apical plasma membrane of podocyte foot processes which leads to the localized, clustered generation of PI(4,5)P2. In turn, PI(4,5)P2 serves as the docking site for inactive ezrin leading to its activation and the association of the ezrin with NHERF2/podocalyxin and the with cortical actin (Figure 5.9)

Taken together with the findings in Chapters 3 and 4, I therefore propose the following model to explain the mechanism of CLIC5A- stimulated ERM phosphorylation:

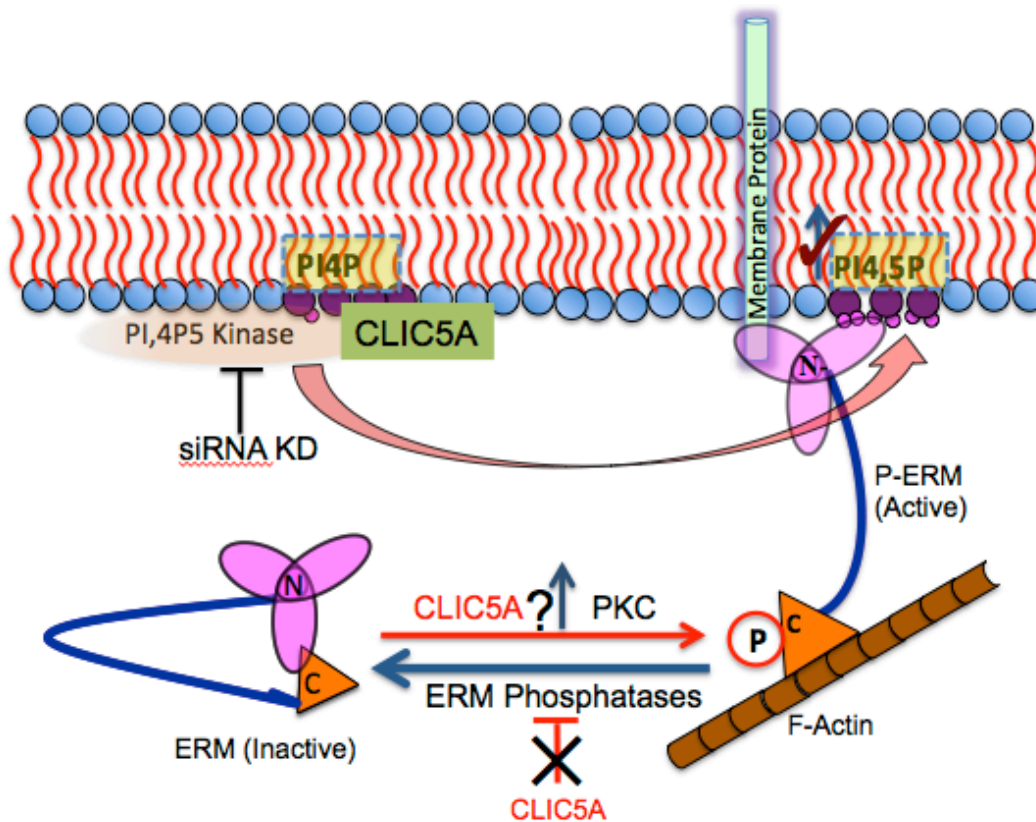


Figure 6.1 Schematic model of the mechanism of CLIC5A-stimulated ERM phosphorylation.

When CLIC5A is overexpressed in COS-7 cells it is associated with a dorsal PM and enhances ERM protein phosphorylation. The CLIC5A-stimulated ERM phosphorylation is most likely not due to the inhibition of ERM phosphatases but the activation of PI(4,5)P₂ generating kinases which enhances clustered PI(4,5)P₂ generation, subsequently ezrin activation and increased association with actin cytoskeleton.

6.2 Future Directions

6.2.1. Explore the nature of molecular and functional interaction between CLIC5A and PI(4,5)P2 generating kinases.

In COS-7 cells, I found that CLIC5A expression induced the accumulation of the PI(4,5)P2 reporter GFP- or RFP-PH-PLC in discrete dorsal PM patches. CLIC5A co-localized with the PI(4,5)P2 reporter and with its generating enzyme PI4P5K1 α . The ratio of apical PM: cytosolic GFP-PH-PLC was also much higher in CLIC5A expressing, than in control cells, in keeping with an increase in the local PI(4,5)P2 content. Since the localization of the PI(4,5)P2 reporter is, however only an indirect marker of PI(4,5)P2 content, future work will be needed to determine whether CLIC5A expression leads to an increase in the actual PI(4,5)P2 phospholipid content in the plasma membrane. This will require labeling and extraction of phospholipids, separation by thin layer chromatography or HPLC, to quantitatively determine PI(4,5)P2 abundance in the presence and absence of CLIC5A.

Similar to increased dorsal accumulation of PI(4,5)P2 reporter, CLIC5A overexpression also resulted in the redistribution of membrane potential reporter GFP-Kras. This finding raises the question whether clustering of the plasma membrane negative surface charge is due to clustering of PI(4,5)P2 or potentially aggregation of CLIC5A into larger heteromeric complexes, and whether CLIC5A itself, due to its acidic foot loop, may be responsible for the accumulation of negative charges in these discrete clusters. It is also possible that CLIC5A interacts with, or induces the formation of discrete lipid microdomains, particularly since we observe that it dissociates from the membrane when PLC is activated. In this regard, it is known that PI(4,5)P2 is not usually associated with cholesterol-rich membrane microdomains. It is conceivable that

CLIC5A, and perhaps CLIC proteins in general, define a distinct type of lipid domain that serves PI(4,5)P2-based signaling. Our findings predict that future studies will show CLIC5A and CLIC proteins not to be associated with cholesterol-rich membrane microdomains, and that cholesterol depletion will not disrupt PI(4,5)P2 and CLIC protein clustering. Instead, we postulate that CLICs define a unique PI(4,5)P2-containing area of phospholipid bilayers.

Activation of PLC with m-3M3FBS which depletes PI(4,5)P2, and siRNA knock down of endogenous PI4P5K1 α blocked CLIC5A-stimulated ezrin phosphorylation. Depletion of plasma membrane PI(4,5)P2 furthermore and caused the redistribution of GFP-CLIC5A and the PI(4,5)P2 reporter from the plasma membrane to the cytoplasm. These findings leave open the possibility that CLIC5A, and perhaps also other CLICs themselves bind PI(4,5)P2, which would generate a positive feed-forward loop. Since PLC activation results in IP3 and DAG generation, in turn activating PKC, the data are consistent with previous reports indicating that PKC activation itself is not sufficient to stimulate ERM phosphorylation. Furthermore, the data indicate that PKC activation itself also would not be sufficient to stimulate phosphorylation-dependent CLIC5A partitioning into the lipid bilayer. The data leave open the possibility that the PI(4,5)P2 reporter, and perhaps also ezrin, bind CLIC5A directly. Future studies using artificial phospholipid bilayers with defined PI(4,5)P2 content along with recombinant CLIC5A mutants in which negatively charged residues in the acidic foot loop are replaced with alanine would be able to define to what extent CLIC5A can bind the reporter and the N-terminus of ezrin. In this regard, it will be of great interest to determine whether silencing of PI4P5K1 α also leads to CLIC5A dissociation from the plasma membrane.

My findings indicate that PI(4,5)P2 generating kinases (PI4P5K α , PI4P5K β , PI5P4k α and PI4P5K β) and CLIC5A exist in the same complex (Figure 4.10) and CLIC5A and PI4P5K α

colocalize at the dorsal membrane. (Figure 4.9). CLIC5A overexpression results in localized clustering of PI(4,5)P2 at the apical membrane (Figure 4.4) where it co-localizes with CLIC5A (Figure 4.5) and increases PI(4,5)P2-dependent ERM phosphorylation (Figures 3.1, 3.2 & 3.3). I also showed that GST-CLIC5A specifically pulled all isoforms of HA-tagged PI(4,5)P2-generating kinases from cell lysates. These findings support an interaction, direct or indirect, of CLIC5A with the kinases and suggest that CLIC5A may act as a platform for the assembly of PI(4,5)P2 generating kinase complexes at the plasma membrane, similar to PI4P5K γ by Ap-2 (454) and PI4P5K α by Ajuba (455). It is furthermore very attractive to postulate that the acidic foot loop of CLIC5A mediates an interaction with the polybasic domain of the PI4P5- and PI5P4 kinases.

The targeting of PI4P5Ks to the inner leaflet of the plasma membrane is determined mainly by their substrate (PI4P). In addition to that, PI4P5K- α , - β , and - γ share a positively charged region on the protein surface that is essential also for their association with the negatively charged inner leaflet of the lipid bilayer (405). X-ray crystallography analysis of CLIC1 showed that CLIC1 has polyanionic foot loop located between helices 5 and 6 and this foot loop is believed to function in protein- protein interaction. Similar to CLIC1 all other members of CLIC family share a polyanionic “foot loop”(417-420), which may serve to bind directly or creating a localized cluster of PI4P5Ks. I found that CLIC5A N- and C-terminal deletion mutants remained diffuse in the cytoplasm and that PI4P5K1 α , associated with the dorsal plasma membrane even in the absence of CLIC5A. This piece of data indicates that CLIC5A is not required for the recruitment of the PI(4,5)P2 generating kinases to the phospholipid bilayer. However, since increased PI(4,5)P2 accumulation was only observed in the presence of full-length, membrane-associated CLIC5A the data furthermore suggest that CLIC5A must activate,

either directly or indirectly, the PI(4,5)P2 generating kinases

6.2.2. The potential role of CLIC1, CLIC4 and CLIC5 in the mechanism for ERM protein phosphorylation in glomerular endothelial cells

Immuno-gold TEM micrograph of kidney sections showed CLIC5A immunoreactivity in glomerular endothelial cells, surrounding their fenestrae (60), and preliminary data from our lab suggest that the loss of glomerular endothelial cell fenestrae in the DOCA/salt hypertension model is much greater in CLIC5^{-/-} compared to CLIC^{+/+} mice (Unpublished data).

In endothelial cells, the most abundant ERM protein is moesin (81). Moesin is present in glomerular endothelial cells *in vivo* where it is phosphorylated (Figure 5.3-A). CLIC1 and CLIC4 are expressed in cultured glomerular endothelial cells and in glomeruli and CLIC4 immunoreactivity co-localizes with moesin in glomerular endothelial cells in CLIC5^{-/-} mice (Unpublished data). Cultured bovine glomerular endothelial cells express CLIC5A at levels ~30 fold higher than aortic endothelial cells (380). *In vivo*, CLIC5A immunoreactivity was observed in glomerular endothelial cells and podocytes of CLIC5^{+/+} mice (Figure 5.1) but P-ERM in glomerular ECs persists when CLIC5 is deleted while P-ERM in podocytes is lost (Figure 5.3 A&B) (60). My preliminary data showed that similar to CLIC5A, CLIC1 and CLIC4 overexpression in COS-7 cells enhanced ERM phosphorylation (Figure 3.7). The most likely interpretation for these findings is that CLIC1 and CLIC4 may compensate for the loss of CLIC5A. Nonetheless, much more work will need to be done to define the role of CLIC5A, and the CLIC1 and CLIC4 proteins in glomerular endothelium. In fact, whether moesin-dependent actin cytoskeleton remodeling underlies the formation of fenestrae also has not been explored so far. For this work, it will be necessary to create mice in which CLIC5A, as well as CLIC4 and

CLIC1 are deleted specifically from endothelial cells, either singly or in combination, followed by ultrastructural characterization of the cells. The experiments in this direction will clarify whether CLIC5A can regulate ERM phosphorylation in glomerular endothelial cells, and whether CLIC4 or CLIC1 function similarly and can substitute for CLIC5A.

6.2.3. Mechanism(s) regulating the CLIC5A-plasma membrane association.

CLIC proteins can exist in the cytoplasm and at the PM (418,420) and individual CLICs can associate with the nucleus (9,456), mitochondria (456,457), the Golgi (458), endosomes/lysosomes (43) and macrophage phagosomes (37,44). Several publications show that CLICs can translocate from cytosolic to membrane compartments. Incorporation of soluble proteins into a membrane is not a common property in cell biology, however CLIC proteins can partition into lipid bilayer spontaneously similar other classes of proteins that have this ability including bacterial pore forming toxins (15), annexins and the Bcl-2 family of apoptotic proteins (16). The most important known regulators of CLICs translocation are the redox state of the molecule as well as pH (9,459-461). Under reducing conditions, CLIC1 form a soluble monomer with 3D structure identical to a GST fold, while under oxidizing conditions, it forms a non-covalent dimer, which is stabilized by an intramolecular disulphide bond (408). Studies using surface plasmon resonance (SPR) showed that human CLICs CLIC1 (4) and CLIC4 (17) and invertebrate CLIC-like proteins (Exc-4 and DmCLIC (4)) can bind to artificial lipid bilayers membranes in a concentration-dependent manner. Membrane binding of these CLIC and CLIC-like proteins enhanced with acidic pH and under oxidizing conditions (18). These data are consistent with the oxidation-mediated 3D structural changes observed in CLIC1 (408) and the conformational instability of CLIC1 at low pH values (462-465).

My experiments showed that CLIC5A associates selectively with the dorsal plasma membrane in COS-7 cells and is not found in the basal domain, even though these cells do not fully polarized. This is similar to the distribution in podocyte foot processes, where CLIC5A is expressed in a very polarized fashion, in the apical plasma membrane domain, away from the basal and lateral (slit diaphragm) domains. Furthermore, in COS-7 cells, CLIC5A rapidly dissociated from the plasma membrane when PI(4,5)P2 was depleted. Taken together, these findings suggest that there must be specific mechanism targeting CLIC5A to the apical (dorsal) plasma membrane in a reversible fashion. Since CLIC5A (and other CLICs) do not have signal peptides, and are not inserted into the membrane co-translationally, but spontaneously partition into lipid bilayers, it seems that they must either bind reversibly to integral membrane proteins that are present in these locations, or that the lipid composition at the apical (dorsal) domain dictates CLIC5A association with that specific domain. Future studies will be required to determine whether lipid composition is sufficient for apical membrane association, or whether binding to other membrane proteins is required. In the case of CLIC5A, which is expressed in such a restricted fashion, the most plausible protein partner is podocalyxin and potentially other members of the sialoglycoprotein family. Studies determining whether CLIC5A specifically interacts with podocalyxin, CD44 and other sialoglycoproteins will therefore be of great interest

To conclude, these future studies will determine whether CLIC5A and other CLICs directly bind and activate PI(4,5)P2 generating kinases, and to what degree the acidic foot loop is involved. The future work will define the role of CLICs in glomerular endothelial cells. In addition, the mechanisms that regulate reversible, polarized CLIC5A plasma membrane association will be defined. Since the CLIC proteins are widely expressed, this work will not only be pertinent for glomerular cell physiology, it should also help to unravel the general

functional role of CLICs in regulating cell-membrane protein interactions with cortical F-actin, and consequently the architecture of cells.

References

1. Cromer, B. A., Morton, C. J., Board, P. G., and Parker, M. W. (2002) From glutathione transferase to pore in a CLIC. *Eur Biophys J* **31**, 356-364
2. Ashley, R. H. (2003) Challenging accepted ion channel biology: p64 and the CLIC family of putative intracellular anion channel proteins (Review). *Molecular membrane biology* **20**, 1-11
3. Berry, K. L., Bulow, H. E., Hall, D. H., and Hobert, O. (2003) A *C. elegans* CLIC-like protein required for intracellular tube formation and maintenance. *Science* **302**, 2134-2137
4. Littler, D. R., Harrop, S. J., Brown, L. J., Pankhurst, G. J., Mynott, A. V., Luciani, P., Mandyam, R. A., Mazzanti, M., Tanda, S., Berryman, M. A., Breit, S. N., and Curmi, P. M. (2008) Comparison of vertebrate and invertebrate CLIC proteins: the crystal structures of *Caenorhabditis elegans* EXC-4 and *Drosophila melanogaster* DmCLIC. *Proteins* **71**, 364-378
5. Elter, A., Hartel, A., Sieben, C., Hertel, B., Fischer-Schliebs, E., Luttge, U., Moroni, A., and Thiel, G. (2007) A plant homolog of animal chloride intracellular channels (CLICs) generates an ion conductance in heterologous systems. *J Biol Chem* **282**, 8786-8792
6. Mizukawa, Y., Nishizawa, T., Nagao, T., Kitamura, K., and Urushidani, T. (2002) Cellular distribution of parchorin, a chloride intracellular channel-related protein, in various tissues. *American journal of physiology. Cell physiology* **282**, C786-795

7. Nishizawa, T., Nagao, T., Iwatsubo, T., Forte, J. G., and Urushidani, T. (2000) Molecular cloning and characterization of a novel chloride intracellular channel-related protein, parchorin, expressed in water-secreting cells. *J Biol Chem* **275**, 11164-11173
8. Qian, Z., Okuhara, D., Abe, M. K., and Rosner, M. R. (1999) Molecular cloning and characterization of a mitogen-activated protein kinase-associated intracellular chloride channel. *J Biol Chem* **274**, 1621-1627
9. Suh, K. S., Mutoh, M., Nagashima, K., Fernandez-Salas, E., Edwards, L. E., Hayes, D. D., Crutchley, J. M., Marin, K. G., Dumont, R. A., Levy, J. M., Cheng, C., Garfield, S., and Yuspa, S. H. (2004) The organellular chloride channel protein CLIC4/mtCLIC translocates to the nucleus in response to cellular stress and accelerates apoptosis. *J Biol Chem* **279**, 4632-4641
10. Harrop, S. J., DeMaere, M. Z., Fairlie, W. D., Reztsova, T., Valenzuela, S. M., Mazzanti, M., Tonini, R., Qiu, M. R., Jankova, L., Warton, K., Bauskin, A. R., Wu, W. M., Pankhurst, S., Campbell, T. J., Breit, S. N., and Curmi, P. M. (2001) Crystal structure of a soluble form of the intracellular chloride ion channel CLIC1 (NCC27) at 1.4-A resolution. *J Biol Chem* **276**, 44993-45000
11. Singh, H., and Ashley, R. H. (2006) Redox regulation of CLIC1 by cysteine residues associated with the putative channel pore. *Biophys J* **90**, 1628-1638
12. Murzin, A. G. (2008) Biochemistry. Metamorphic proteins. *Science* **320**, 1725-1726
13. Bryan, P. N., and Orban, J. (2010) Proteins that switch folds. *Current opinion in structural biology* **20**, 482-488
14. Jentsch, T. J., Stein, V., Weinreich, F., and Zdebik, A. A. (2002) Molecular structure and physiological function of chloride channels. *Physiol Rev* **82**, 503-568

15. Gouaux, E. (1997) Channel-forming toxins: tales of transformation. *Current opinion in structural biology* **7**, 566-573
16. Schendel, S. L., Montal, M., and Reed, J. C. (1998) Bcl-2 family proteins as ion-channels. *Cell Death Differ* **5**, 372-380
17. Littler, D. R., Assaad, N. N., Harrop, S. J., Brown, L. J., Pankhurst, G. J., Luciani, P., Aguilar, M. I., Mazzanti, M., Berryman, M. A., Breit, S. N., and Curmi, P. M. (2005) Crystal structure of the soluble form of the redox-regulated chloride ion channel protein CLIC4. *FEBS J* **272**, 4996-5007
18. Goodchild, S. C., Howell, M. W., Cordina, N. M., Littler, D. R., Breit, S. N., Curmi, P. M., and Brown, L. J. (2009) Oxidation promotes insertion of the CLIC1 chloride intracellular channel into the membrane. *European biophysics journal : EBJ* **39**, 129-138
19. Cromer, B. A., Gorman, M. A., Hansen, G., Adams, J. J., Coggan, M., Board, P. G., and Parker, M. W. (2007) Expression, purification, crystallization and preliminary X-ray diffraction analysis of chloride intracellular channel 2 (CLIC2). *Acta crystallographica. Section F, Structural biology and crystallization communications* **63**, 961-963
20. Duncan, R. R., Westwood, P. K., Boyd, A., and Ashley, R. H. (1997) Rat brain p64H1, expression of a new member of the p64 chloride channel protein family in endoplasmic reticulum. *J Biol Chem* **272**, 23880-23886
21. Singh, H., and Ashley, R. H. (2007) CLIC4 (p64H1) and its putative transmembrane domain form poorly selective, redox-regulated ion channels. *Molecular membrane biology* **24**, 41-52

22. Singh, H., Cousin, M. A., and Ashley, R. H. (2007) Functional reconstitution of mammalian 'chloride intracellular channels' CLIC1, CLIC4 and CLIC5 reveals differential regulation by cytoskeletal actin. *FEBS J* **274**, 6306-6316
23. Landry, D. W., Akabas, M. H., Redhead, C., Edelman, A., Cragoe, E. J., Jr., and Al-Awqati, Q. (1989) Purification and reconstitution of chloride channels from kidney and trachea. *Science* **244**, 1469-1472
24. Weber-Schurholz, S., Wischmeyer, E., Laurien, M., Jockusch, H., Schurholz, T., Landry, D. W., and al-Awqati, Q. (1993) Indanyloxyacetic acid-sensitive chloride channels from outer membranes of skeletal muscle. *J Biol Chem* **268**, 547-551
25. Suginta, W., Karoulias, N., Aitken, A., and Ashley, R. H. (2001) Chloride intracellular channel protein CLIC4 (p64H1) binds directly to brain dynamin I in a complex containing actin, tubulin and 14-3-3 isoforms. *Biochem J* **359**, 55-64
26. Landry, D. W., Akabas, M. A., Redhead, C., and al-Awqati, Q. (1990) Purification and reconstitution of epithelial chloride channels. *Methods Enzymol* **191**, 572-583
27. Redhead, C. R., Edelman, A. E., Brown, D., Landry, D. W., and al-Awqati, Q. (1992) A ubiquitous 64-kDa protein is a component of a chloride channel of plasma and intracellular membranes. *Proc Natl Acad Sci U S A* **89**, 3716-3720
28. Berryman, M., and Bretscher, A. (2000) Identification of a novel member of the chloride intracellular channel gene family (CLIC5) that associates with the actin cytoskeleton of placental microvilli. *Molecular biology of the cell* **11**, 1509-1521
29. Valenzuela, S. M., Martin, D. K., Por, S. B., Robbins, J. M., Warton, K., Bootcov, M. R., Schofield, P. R., Campbell, T. J., and Breit, S. N. (1997) Molecular cloning and expression of a chloride ion channel of cell nuclei. *J Biol Chem* **272**, 12575-12582

30. Tulk, B. M., and Edwards, J. C. (1998) NCC27, a homolog of intracellular Cl⁻ channel p64, is expressed in brush border of renal proximal tubule. *Am J Physiol* **274**, F1140-1149
31. Henriksen, K., Gram, J., Neutzsky-Wulff, A. V., Jensen, V. K., Dziegiel, M. H., Bollerslev, J., and Karsdal, M. A. (2009) Characterization of acid flux in osteoclasts from patients harboring a G215R mutation in ClC-7. *Biochem Biophys Res Commun* **378**, 804-809
32. Valenzuela, S. M., Mazzanti, M., Tonini, R., Qiu, M. R., Warton, K., Musgrove, E. A., Campbell, T. J., and Breit, S. N. (2000) The nuclear chloride ion channel NCC27 is involved in regulation of the cell cycle. *J Physiol* **529 Pt 3**, 541-552
33. Ulmasov, B., Bruno, J., Woost, P. G., and Edwards, J. C. (2007) Tissue and subcellular distribution of CLIC1. *BMC Cell Biol* **8**, 8
34. Chen, J. I., Hannan, N. J., Mak, Y., Nicholls, P. K., Zhang, J., Rainczuk, A., Stanton, P. G., Robertson, D. M., Salamonsen, L. A., and Stephens, A. N. (2009) Proteomic characterization of midproliferative and midsecretory human endometrium. *J Proteome Res* **8**, 2032-2044
35. Milton, R. H., Abeti, R., Averaimo, S., DeBiasi, S., Vitellaro, L., Jiang, L., Curmi, P. M., Breit, S. N., Duchon, M. R., and Mazzanti, M. (2008) CLIC1 function is required for beta-amyloid-induced generation of reactive oxygen species by microglia. *J Neurosci* **28**, 11488-11499
36. Setti, M., Savalli, N., Osti, D., Richichi, C., Angelini, M., Brescia, P., Fornasari, L., Carro, M. S., Mazzanti, M., and Pelicci, G. (2013) Functional Role of CLIC1 Ion

- Channel in Glioblastoma-Derived Stem/Progenitor Cells. *J Natl Cancer Inst* **105**, 1644-1655
37. Jiang, L., Salao, K., Li, H., Rybicka, J. M., Yates, R. M., Luo, X. W., Shi, X. X., Kuffner, T., Tsai, V. W., Husaini, Y., Wu, L., Brown, D. A., Grewal, T., Brown, L. J., Curmi, P. M., and Breit, S. N. (2012) Intracellular chloride channel protein CLIC1 regulates macrophage function through modulation of phagosomal acidification. *J Cell Sci* **125**, 5479-5488
38. Qiu, M. R., Jiang, L., Matthaei, K. I., Schoenwaelder, S. M., Kuffner, T., Mangin, P., Joseph, J. E., Low, J., Connor, D., Valenzuela, S. M., Curmi, P. M., Brown, L. J., Mahaut-Smith, M., Jackson, S. P., and Breit, S. N. (2010) Generation and characterization of mice with null mutation of the chloride intracellular channel 1 gene. *Genesis* **48**, 127-136
39. Jalilian, C., Gallant, E. M., Board, P. G., and Dulhunty, A. F. (2008) Redox potential and the response of cardiac ryanodine receptors to CLIC-2, a member of the glutathione S-transferase structural family. *Antioxidants & redox signaling* **10**, 1675-1686
40. Edwards, J. C., Tulk, B., and Schlesinger, P. H. (1998) Functional expression of p64, an intracellular chloride channel protein. *J Membr Biol* **163**, 119-127
41. Heiss, N. S., and Poustka, A. (1997) Genomic structure of a novel chloride channel gene, CLIC2, in Xq28. *Genomics* **45**, 224-228
42. Takano, K., Liu, D., Tarpey, P., Gallant, E., Lam, A., Witham, S., Alexov, E., Chaubey, A., Stevenson, R. E., Schwartz, C. E., Board, P. G., and Dulhunty, A. F. (2012) An X-linked channelopathy with cardiomegaly due to a CLIC2 mutation enhancing ryanodine receptor channel activity. *Human molecular genetics* **21**, 4497-4507

43. Dozynkiewicz, M. A., Jamieson, N. B., Macpherson, I., Grindlay, J., van den Berghe, P. V., von Thun, A., Morton, J. P., Gourley, C., Timpson, P., Nixon, C., McKay, C. J., Carter, R., Strachan, D., Anderson, K., Sansom, O. J., Caswell, P. T., and Norman, J. C. (2012) Rab25 and CLIC3 collaborate to promote integrin recycling from late endosomes/lysosomes and drive cancer progression. *Developmental cell* **22**, 131-145
44. Kim, K. H., Choi, B. K., Song, K. M., Cha, K. W., Kim, Y. H., Lee, H., Han, I. S., and Kwon, B. S. (2013) CR1g signals induce anti-intracellular bacterial phagosome activity in a chloride intracellular channel 3-dependent manner. *Eur J Immunol* **43**, 667-678
45. Howell, S., Duncan, R. R., and Ashley, R. H. (1996) Identification and characterisation of a homologue of p64 in rat tissues. *FEBS Lett* **390**, 207-210
46. Fernandez-Salas, E., Sagar, M., Cheng, C., Yuspa, S. H., and Weinberg, W. C. (1999) p53 and tumor necrosis factor alpha regulate the expression of a mitochondrial chloride channel protein. *J Biol Chem* **274**, 36488-36497
47. Chuang, J. Z., Milner, T. A., Zhu, M., and Sung, C. H. (1999) A 29 kDa intracellular chloride channel p64H1 is associated with large dense-core vesicles in rat hippocampal neurons. *The Journal of neuroscience : the official journal of the Society for Neuroscience* **19**, 2919-2928
48. Tung, J. J., Hobert, O., Berryman, M., and Kitajewski, J. (2009) Chloride intracellular channel 4 is involved in endothelial proliferation and morphogenesis in vitro. *Angiogenesis* **12**, 209-220
49. Bohman, S., Matsumoto, T., Suh, K., Dimberg, A., Jakobsson, L., Yuspa, S., and Claesson-Welsh, L. (2005) Proteomic analysis of vascular endothelial growth factor-induced endothelial cell differentiation reveals a role for chloride intracellular channel 4

- (CLIC4) in tubular morphogenesis. *The Journal of biological chemistry* **280**, 42397-42404
50. Fernandez-Salas, E., Suh, K. S., Speransky, V. V., Bowers, W. L., Levy, J. M., Adams, T., Pathak, K. R., Edwards, L. E., Hayes, D. D., Cheng, C., Steven, A. C., Weinberg, W. C., and Yuspa, S. H. (2002) mtCLIC/CLIC4, an organelular chloride channel protein, is increased by DNA damage and participates in the apoptotic response to p53. *Mol Cell Biol* **22**, 3610-3620
 51. Shukla, A., Malik, M., Cataisson, C., Ho, Y., Friesen, T., Suh, K. S., and Yuspa, S. H. (2009) TGF-beta signalling is regulated by Schnurri-2-dependent nuclear translocation of CLIC4 and consequent stabilization of phospho-Smad2 and 3. *Nat Cell Biol* **11**, 777-784
 52. Chuang, J. Z., Chou, S. Y., and Sung, C. H. (2010) Chloride intracellular channel 4 is critical for the epithelial morphogenesis of RPE cells and retinal attachment. *Mol Biol Cell* **21**, 3017-3028
 53. Edwards, J. C., Bruno, J., Key, P., and Cheng, Y. W. (2014) Absence of chloride intracellular channel 4 (CLIC4) predisposes to acute kidney injury but has minimal impact on recovery. *BMC nephrology* **15**, 54
 54. Edwards, J. C., Cohen, C., Xu, W., and Schlesinger, P. H. (2006) c-Src control of chloride channel support for osteoclast HCl transport and bone resorption. *J Biol Chem* **281**, 28011-28022
 55. Schlesinger, P. H., Blair, H. C., Teitelbaum, S. L., and Edwards, J. C. (1997) Characterization of the osteoclast ruffled border chloride channel and its role in bone resorption. *J Biol Chem* **272**, 18636-18643

56. Berryman, M., Bruno, J., Price, J., and Edwards, J. C. (2004) CLIC-5A functions as a chloride channel in vitro and associates with the cortical actin cytoskeleton in vitro and in vivo. *The Journal of biological chemistry* **279**, 34794-34801
57. Gagnon, L. H., Longo-Guess, C. M., Berryman, M., Shin, J. B., Saylor, K. W., Yu, H., Gillespie, P. G., and Johnson, K. R. (2006) The chloride intracellular channel protein CLIC5 is expressed at high levels in hair cell stereocilia and is essential for normal inner ear function. *The Journal of neuroscience : the official journal of the Society for Neuroscience* **26**, 10188-10198
58. Khan, S. Y., Ahmed, Z. M., Shabbir, M. I., Kitajiri, S., Kalsoom, S., Tasneem, S., Shayiq, S., Ramesh, A., Srisailpathy, S., Khan, S. N., Smith, R. J., Riazuddin, S., Friedman, T. B., and Riazuddin, S. (2007) Mutations of the RDX gene cause nonsyndromic hearing loss at the DFNB24 locus. *Human mutation* **28**, 417-423
59. Seco, C. Z., Oonk, A. M., Dominguez-Ruiz, M., Draaisma, J. M., Gandia, M., Oostrik, J., Neveling, K., Kunst, H. P., Hoefsloot, L. H., Del Castillo, I., Pennings, R. J., Kremer, H., Admiraal, R. J., and Schraders, M. (2014) Progressive hearing loss and vestibular dysfunction caused by a homozygous nonsense mutation in CLIC5. *European journal of human genetics : EJHG*
60. Wegner, B., Al-Momany, A., Kulak, S. C., Kozłowski, K., Obeidat, M., Jahroudi, N., Paes, J., Berryman, M., and Ballermann, B. J. (2010) CLIC5A, a component of the ezrin-podocalyxin complex in glomeruli, is a determinant of podocyte integrity. *Am J Physiol Renal Physiol* **298**, F1492-1503
61. Patrakka, J., and Tryggvason, K. (2010) Molecular make-up of the glomerular filtration barrier. *Biochemical and biophysical research communications* **396**, 164-169

62. Pierchala, B. A., Munoz, M. R., and Tsui, C. C. (2010) Proteomic analysis of the slit diaphragm complex: CLIC5 is a protein critical for podocyte morphology and function. *Kidney Int* **78**, 868-882
63. Edwards, J. C., and Kapadia, S. (2000) Regulation of the bovine kidney microsomal chloride channel p64 by p59fyn, a Src family tyrosine kinase. *J Biol Chem* **275**, 31826-31832
64. Friedli, M., Guipponi, M., Bertrand, S., Bertrand, D., Neerman-Arbez, M., Scott, H. S., Antonarakis, S. E., and Reymond, A. (2003) Identification of a novel member of the CLIC family, CLIC6, mapping to 21q22.12. *Gene* **320**, 31-40
65. Griffon, N., Jeanneteau, F., Prieur, F., Diaz, J., and Sokoloff, P. (2003) CLIC6, a member of the intracellular chloride channel family, interacts with dopamine D(2)-like receptors. *Brain research. Molecular brain research* **117**, 47-57
66. Crothers, J. M., Jr., Reenstra, W. W., and Forte, J. G. (1990) Ontogeny of gastric H(+)-K(+)-ATPase in suckling rabbits. *The American journal of physiology* **259**, G913-921
67. Conboy, J. (1987) Molecular cloning and characterization of the gene coding for red cell membrane skeletal protein 4.1. *Biorheology* **24**, 673-687
68. Chishti, A. H., Kim, A. C., Marfatia, S. M., Lutchman, M., Hanspal, M., Jindal, H., Liu, S. C., Low, P. S., Rouleau, G. A., Mohandas, N., Chasis, J. A., Conboy, J. G., Gascard, P., Takakuwa, Y., Huang, S. C., Benz, E. J., Jr., Bretscher, A., Fehon, R. G., Gusella, J. F., Ramesh, V., Solomon, F., Marchesi, V. T., Tsukita, S., Tsukita, S., Hoover, K. B., and et al. (1998) The FERM domain: a unique module involved in the linkage of cytoplasmic proteins to the membrane. *Trends in biochemical sciences* **23**, 281-282

69. Leto, T. L., and Marchesi, V. T. (1984) A structural model of human erythrocyte protein 4.1. *J Biol Chem* **259**, 4603-4608
70. Correas, I. (1991) Characterization of isoforms of protein 4.1 present in the nucleus. *Biochem J* **279 (Pt 2)**, 581-585
71. Delaunay, J. (1995) Genetic disorders of the red cell membrane. *Critical reviews in oncology/hematology* **19**, 79-110
72. Shi, Z. T., Afzal, V., Coller, B., Patel, D., Chasis, J. A., Parra, M., Lee, G., Paszty, C., Stevens, M., Walensky, L., Peters, L. L., Mohandas, N., Rubin, E., and Conboy, J. G. (1999) Protein 4.1R-deficient mice are viable but have erythroid membrane skeleton abnormalities. *J Clin Invest* **103**, 331-340
73. Walensky, L. D., Shi, Z. T., Blackshaw, S., DeVries, A. C., Demas, G. E., Gascard, P., Nelson, R. J., Conboy, J. G., Rubin, E. M., Snyder, S. H., and Mohandas, N. (1998) Neurobehavioral deficits in mice lacking the erythrocyte membrane cytoskeletal protein 4.1. *Current biology : CB* **8**, 1269-1272
74. Hamada, K., Shimizu, T., Matsui, T., Tsukita, S., and Hakoshima, T. (2000) Structural basis of the membrane-targeting and unmasking mechanisms of the radixin FERM domain. *The EMBO journal* **19**, 4449-4462
75. Pearson, M. A., Reczek, D., Bretscher, A., and Karplus, P. A. (2000) Structure of the ERM protein moesin reveals the FERM domain fold masked by an extended actin binding tail domain. *Cell* **101**, 259-270
76. Martin, M., Roy, C., Montcourrier, P., Sahuquet, A., and Mangeat, P. (1997) Three determinants in ezrin are responsible for cell extension activity. *Mol Biol Cell* **8**, 1543-1557

77. Roy, C., Martin, M., and Mangeat, P. (1997) A dual involvement of the amino-terminal domain of ezrin in F- and G-actin binding. *The Journal of biological chemistry* **272**, 20088-20095
78. Louvet-Vallee, S. (2000) ERM proteins: from cellular architecture to cell signaling. *Biology of the cell / under the auspices of the European Cell Biology Organization* **92**, 305-316
79. Bretscher, A., Edwards, K., and Fehon, R. G. (2002) ERM proteins and merlin: integrators at the cell cortex. *Nat Rev Mol Cell Biol* **3**, 586-599
80. Bretscher, A., Chambers, D., Nguyen, R., and Reczek, D. (2000) ERM-Merlin and EBP50 protein families in plasma membrane organization and function. *Annual review of cell and developmental biology* **16**, 113-143
81. Berryman, M., Franck, Z., and Bretscher, A. (1993) Ezrin is concentrated in the apical microvilli of a wide variety of epithelial cells whereas moesin is found primarily in endothelial cells. *Journal of cell science* **105 (Pt 4)**, 1025-1043
82. Franck, Z., Gary, R., and Bretscher, A. (1993) Moesin, like ezrin, colocalizes with actin in the cortical cytoskeleton in cultured cells, but its expression is more variable. *Journal of cell science* **105 (Pt 1)**, 219-231
83. Sato, N., Funayama, N., Nagafuchi, A., Yonemura, S., Tsukita, S., and Tsukita, S. (1992) A gene family consisting of ezrin, radixin and moesin. Its specific localization at actin filament/plasma membrane association sites. *Journal of cell science* **103 (Pt 1)**, 131-143
84. Tsukita, S., Hieda, Y., and Tsukita, S. (1989) A new 82-kD barbed end-capping protein (radixin) localized in the cell-to-cell adherens junction: purification and characterization. *J Cell Biol* **108**, 2369-2382

85. Pataky, F., Pironkova, R., and Hudspeth, A. J. (2004) Radixin is a constituent of stereocilia in hair cells. *Proceedings of the National Academy of Sciences of the United States of America* **101**, 2601-2606
86. Lankes, W. T., and Furthmayr, H. (1991) Moesin: a member of the protein 4.1-talin-ezrin family of proteins. *Proc Natl Acad Sci U S A* **88**, 8297-8301
87. Fievet, B., Louvard, D., and Arpin, M. (2007) ERM proteins in epithelial cell organization and functions. *Biochim Biophys Acta* **1773**, 653-660
88. McClatchey, A. I. (2003) Merlin and ERM proteins: unappreciated roles in cancer development? *Nature reviews. Cancer* **3**, 877-883
89. Niggli, V., and Rossy, J. (2008) Ezrin/radixin/moesin: versatile controllers of signaling molecules and of the cortical cytoskeleton. *The international journal of biochemistry & cell biology* **40**, 344-349
90. Fehon, R. G., McClatchey, A. I., and Bretscher, A. (2010) Organizing the cell cortex: the role of ERM proteins. *Nat Rev Mol Cell Biol* **11**, 276-287
91. Gatto, C. L., Walker, B. J., and Lambert, S. (2003) Local ERM activation and dynamic growth cones at Schwann cell tips implicated in efficient formation of nodes of Ranvier. *J Cell Biol* **162**, 489-498
92. Saotome, I., Curto, M., and McClatchey, A. I. (2004) Ezrin is essential for epithelial organization and villus morphogenesis in the developing intestine. *Developmental cell* **6**, 855-864
93. Li, W., and Crouch, D. H. (2000) Cloning and expression profile of chicken radixin. *Biochimica et biophysica acta* **1491**, 327-332

94. Amieva, M. R., Wilgenbus, K. K., and Furthmayr, H. (1994) Radixin is a component of hepatocyte microvilli in situ. *Exp Cell Res* **210**, 140-144
95. Henry, M. D., Gonzalez Agosti, C., and Solomon, F. (1995) Molecular dissection of radixin: distinct and interdependent functions of the amino- and carboxy-terminal domains. *The Journal of cell biology* **129**, 1007-1022
96. Sato, N., Yonemura, S., Obinata, T., Tsukita, S., and Tsukita, S. (1991) Radixin, a barbed end-capping actin-modulating protein, is concentrated at the cleavage furrow during cytokinesis. *The Journal of cell biology* **113**, 321-330
97. Kikuchi, S., Hata, M., Fukumoto, K., Yamane, Y., Matsui, T., Tamura, A., Yonemura, S., Yamagishi, H., Keppler, D., Tsukita, S., and Tsukita, S. (2002) Radixin deficiency causes conjugated hyperbilirubinemia with loss of Mrp2 from bile canalicular membranes. *Nature genetics* **31**, 320-325
98. Kitajiri, S., Fukumoto, K., Hata, M., Sasaki, H., Katsuno, T., Nakagawa, T., Ito, J., Tsukita, S., and Tsukita, S. (2004) Radixin deficiency causes deafness associated with progressive degeneration of cochlear stereocilia. *The Journal of cell biology* **166**, 559-570
99. Lankes, W., Griesmacher, A., Grunwald, J., Schwartz-Albiez, R., and Keller, R. (1988) A heparin-binding protein involved in inhibition of smooth-muscle cell proliferation. *Biochem J* **251**, 831-842
100. Amieva, M. R., and Furthmayr, H. (1995) Subcellular localization of moesin in dynamic filopodia, retraction fibers, and other structures involved in substrate exploration, attachment, and cell-cell contacts. *Exp Cell Res* **219**, 180-196

101. Doi, Y., Itoh, M., Yonemura, S., Ishihara, S., Takano, H., Noda, T., and Tsukita, S. (1999) Normal development of mice and unimpaired cell adhesion/cell motility/actin-based cytoskeleton without compensatory up-regulation of ezrin or radixin in moesin gene knockout. *J Biol Chem* **274**, 2315-2321
102. Turunen, O., Wahlstrom, T., and Vaheri, A. (1994) Ezrin has a COOH-terminal actin-binding site that is conserved in the ezrin protein family. *J Cell Biol* **126**, 1445-1453
103. Niggli, V., Andreoli, C., Roy, C., and Mangeat, P. (1995) Identification of a phosphatidylinositol-4,5-bisphosphate-binding domain in the N-terminal region of ezrin. *FEBS letters* **376**, 172-176
104. Tsukita, S., Oishi, K., Sato, N., Sagara, J., Kawai, A., and Tsukita, S. (1994) ERM family members as molecular linkers between the cell surface glycoprotein CD44 and actin-based cytoskeletons. *J Cell Biol* **126**, 391-401
105. Hirao, M., Sato, N., Kondo, T., Yonemura, S., Monden, M., Sasaki, T., Takai, Y., Tsukita, S., and Tsukita, S. (1996) Regulation mechanism of ERM (ezrin/radixin/moesin) protein/plasma membrane association: possible involvement of phosphatidylinositol turnover and Rho-dependent signaling pathway. *The Journal of cell biology* **135**, 37-51
106. Mori, T., Kitano, K., Terawaki, S., Maesaki, R., Fukami, Y., and Hakoshima, T. (2008) Structural basis for CD44 recognition by ERM proteins. *J Biol Chem* **283**, 29602-29612
107. Serrador, J. M., Nieto, M., Alonso-Lebrero, J. L., del Pozo, M. A., Calvo, J., Furthmayr, H., Schwartz-Albiez, R., Lozano, F., Gonzalez-Amaro, R., Sanchez-Mateos, P., and Sanchez-Madrid, F. (1998) CD43 interacts with moesin and ezrin and regulates its redistribution to the uropods of T lymphocytes at the cell-cell contacts. *Blood* **91**, 4632-4644

108. Takai, Y., Kitano, K., Terawaki, S., Maesaki, R., and Hakoshima, T. (2008) Structural basis of the cytoplasmic tail of adhesion molecule CD43 and its binding to ERM proteins. *Journal of molecular biology* **381**, 634-644
109. Yonemura, S., Hirao, M., Doi, Y., Takahashi, N., Kondo, T., Tsukita, S., and Tsukita, S. (1998) Ezrin/radixin/moesin (ERM) proteins bind to a positively charged amino acid cluster in the juxta-membrane cytoplasmic domain of CD44, CD43, and ICAM-2. *J Cell Biol* **140**, 885-895
110. Hamada, K., Shimizu, T., Matsui, T., Tsukita, S., Tsukita, S., and Hakoshima, T. (2001) Crystallographic characterization of the radixin FERM domain bound to the cytoplasmic tail of the adhesion protein ICAM-2. *Acta crystallographica. Section D, Biological crystallography* **57**, 891-892
111. Hamada, K., Shimizu, T., Yonemura, S., Tsukita, S., Tsukita, S., and Hakoshima, T. (2003) Structural basis of adhesion-molecule recognition by ERM proteins revealed by the crystal structure of the radixin-ICAM-2 complex. *The EMBO journal* **22**, 502-514
112. Heiska, L., Alftan, K., Gronholm, M., Vilja, P., Vaheri, A., and Carpen, O. (1998) Association of ezrin with intercellular adhesion molecule-1 and -2 (ICAM-1 and ICAM-2). Regulation by phosphatidylinositol 4, 5-bisphosphate. *The Journal of biological chemistry* **273**, 21893-21900
113. Denker, S. P., Huang, D. C., Orlowski, J., Furthmayr, H., and Barber, D. L. (2000) Direct binding of the Na⁺-H exchanger NHE1 to ERM proteins regulates the cortical cytoskeleton and cell shape independently of H⁺ translocation. *Mol Cell* **6**, 1425-1436

114. Reczek, D., Berryman, M., and Bretscher, A. (1997) Identification of EBP50: A PDZ-containing phosphoprotein that associates with members of the ezrin-radixin-moesin family. *J Cell Biol* **139**, 169-179
115. Reczek, D., and Bretscher, A. (1998) The carboxyl-terminal region of EBP50 binds to a site in the amino-terminal domain of ezrin that is masked in the dormant molecule. *J Biol Chem* **273**, 18452-18458
116. Terawaki, S., Maesaki, R., and Hakoshima, T. (2006) Structural basis for NHERF recognition by ERM proteins. *Structure* **14**, 777-789
117. Yun, C. H., Lamprecht, G., Forster, D. V., and Sidor, A. (1998) NHE3 kinase A regulatory protein E3KARP binds the epithelial brush border Na⁺/H⁺ exchanger NHE3 and the cytoskeletal protein ezrin. *J Biol Chem* **273**, 25856-25863
118. Zhang, M., Bohlsen, S. S., Dy, M., and Tenner, A. J. (2005) Modulated interaction of the ERM protein, moesin, with CD93. *Immunology* **115**, 63-73
119. Barret, C., Roy, C., Montcourrier, P., Mangeat, P., and Niggli, V. (2000) Mutagenesis of the phosphatidylinositol 4,5-bisphosphate (PIP(2)) binding site in the NH(2)-terminal domain of ezrin correlates with its altered cellular distribution. *J Cell Biol* **151**, 1067-1080
120. Yonemura, S., Matsui, T., Tsukita, S., and Tsukita, S. (2002) Rho-dependent and -independent activation mechanisms of ezrin/radixin/moesin proteins: an essential role for polyphosphoinositides in vivo. *Journal of cell science* **115**, 2569-2580
121. Canals, D., Roddy, P., and Hannun, Y. A. (2012) Protein phosphatase 1alpha mediates ceramide-induced ERM protein dephosphorylation: a novel mechanism independent of

- phosphatidylinositol 4, 5-biphosphate (PIP₂) and myosin/ERM phosphatase. *J Biol Chem* **287**, 10145-10155
122. Hao, J. J., Liu, Y., Kruhlak, M., Debell, K. E., Rellahan, B. L., and Shaw, S. (2009) Phospholipase C-mediated hydrolysis of PIP₂ releases ERM proteins from lymphocyte membrane. *J Cell Biol* **184**, 451-462
123. Fievet, B. T., Gautreau, A., Roy, C., Del Maestro, L., Mangeat, P., Louvard, D., and Arpin, M. (2004) Phosphoinositide binding and phosphorylation act sequentially in the activation mechanism of ezrin. *J Cell Biol* **164**, 653-659
124. Rasmussen, M., Alexander, R. T., Darborg, B. V., Mobjerg, N., Hoffmann, E. K., Kapus, A., and Pedersen, S. F. (2008) Osmotic cell shrinkage activates ezrin/radixin/moesin (ERM) proteins: activation mechanisms and physiological implications. *American journal of physiology. Cell physiology* **294**, C197-212
125. Hayashi, K., Yonemura, S., Matsui, T., and Tsukita, S. (1999) Immunofluorescence detection of ezrin/radixin/moesin (ERM) proteins with their carboxyl-terminal threonine phosphorylated in cultured cells and tissues. *J Cell Sci* **112 (Pt 8)**, 1149-1158
126. Matsui, T., Yonemura, S., Tsukita, S., and Tsukita, S. (1999) Activation of ERM proteins in vivo by Rho involves phosphatidyl-inositol 4-phosphate 5-kinase and not ROCK kinases. *Curr Biol* **9**, 1259-1262
127. Oshiro, N., Fukata, Y., and Kaibuchi, K. (1998) Phosphorylation of moesin by rho-associated kinase (Rho-kinase) plays a crucial role in the formation of microvilli-like structures. *J Biol Chem* **273**, 34663-34666

128. Shaw, R. J., Henry, M., Solomon, F., and Jacks, T. (1998) RhoA-dependent phosphorylation and relocalization of ERM proteins into apical membrane/actin protrusions in fibroblasts. *Molecular biology of the cell* **9**, 403-419
129. Gautreau, A., Louvard, D., and Arpin, M. (2000) Morphogenic effects of ezrin require a phosphorylation-induced transition from oligomers to monomers at the plasma membrane. *J Cell Biol* **150**, 193-203
130. Nakamura, F., Huang, L., Pestonjamas, K., Luna, E. J., and Furthmayr, H. (1999) Regulation of F-actin binding to platelet moesin in vitro by both phosphorylation of threonine 558 and polyphosphatidylinositides. *Molecular biology of the cell* **10**, 2669-2685
131. Chen, J., Cohn, J. A., and Mandel, L. J. (1995) Dephosphorylation of ezrin as an early event in renal microvillar breakdown and anoxic injury. *Proceedings of the National Academy of Sciences of the United States of America* **92**, 7495-7499
132. Kondo, T., Takeuchi, K., Doi, Y., Yonemura, S., Nagata, S., and Tsukita, S. (1997) ERM (ezrin/radixin/moesin)-based molecular mechanism of microvillar breakdown at an early stage of apoptosis. *J Cell Biol* **139**, 749-758
133. Matsui, T., Maeda, M., Doi, Y., Yonemura, S., Amano, M., Kaibuchi, K., Tsukita, S., and Tsukita, S. (1998) Rho-kinase phosphorylates COOH-terminal threonines of ezrin/radixin/moesin (ERM) proteins and regulates their head-to-tail association. *The Journal of cell biology* **140**, 647-657
134. Tran Quang, C., Gautreau, A., Arpin, M., and Treisman, R. (2000) Ezrin function is required for ROCK-mediated fibroblast transformation by the Net and Dbl oncogenes. *The EMBO journal* **19**, 4565-4576

135. Ng, T., Parsons, M., Hughes, W. E., Monypenny, J., Zicha, D., Gautreau, A., Arpin, M., Gschmeissner, S., Verveer, P. J., Bastiaens, P. I., and Parker, P. J. (2001) Ezrin is a downstream effector of trafficking PKC-integrin complexes involved in the control of cell motility. *EMBO J* **20**, 2723-2741
136. Pietromonaco, S. F., Simons, P. C., Altman, A., and Elias, L. (1998) Protein kinase C-theta phosphorylation of moesin in the actin-binding sequence. *The Journal of biological chemistry* **273**, 7594-7603
137. Simons, P. C., Pietromonaco, S. F., Reczek, D., Bretscher, A., and Elias, L. (1998) C-terminal threonine phosphorylation activates ERM proteins to link the cell's cortical lipid bilayer to the cytoskeleton. *Biochem Biophys Res Commun* **253**, 561-565
138. Shiue, H., Musch, M. W., Wang, Y., Chang, E. B., and Turner, J. R. (2005) Akt2 phosphorylates ezrin to trigger NHE3 translocation and activation. *J Biol Chem* **280**, 1688-1695
139. Baumgartner, M., Sillman, A. L., Blackwood, E. M., Srivastava, J., Madson, N., Schilling, J. W., Wright, J. H., and Barber, D. L. (2006) The Nck-interacting kinase phosphorylates ERM proteins for formation of lamellipodium by growth factors. *Proc Natl Acad Sci U S A* **103**, 13391-13396
140. Belkina, N. V., Liu, Y., Hao, J. J., Karasuyama, H., and Shaw, S. (2009) LOK is a major ERM kinase in resting lymphocytes and regulates cytoskeletal rearrangement through ERM phosphorylation. *Proceedings of the National Academy of Sciences of the United States of America* **106**, 4707-4712
141. ten Klooster, J. P., Jansen, M., Yuan, J., Oorschot, V., Begthel, H., Di Giacomo, V., Colland, F., de Koning, J., Maurice, M. M., Hornbeck, P., and Clevers, H. (2009) Mst4

- and Ezrin induce brush borders downstream of the Lkb1/Strad/Mo25 polarization complex. *Developmental cell* **16**, 551-562
142. Yang, H. S., Alexander, K., Santiago, P., and Hinds, P. W. (2003) ERM proteins and Cdk5 in cellular senescence. *Cell cycle* **2**, 517-520
143. Thuillier, L., Hivroz, C., Fagard, R., Andreoli, C., and Mangeat, P. (1994) Ligation of CD4 surface antigen induces rapid tyrosine phosphorylation of the cytoskeletal protein ezrin. *Cellular immunology* **156**, 322-331
144. Crepaldi, T., Gautreau, A., Comoglio, P. M., Louvard, D., and Arpin, M. (1997) Ezrin is an effector of hepatocyte growth factor-mediated migration and morphogenesis in epithelial cells. *The Journal of cell biology* **138**, 423-434
145. Jiang, W. G., Hiscox, S., Singhrao, S. K., Puntis, M. C., Nakamura, T., Mansel, R. E., and Hallett, M. B. (1995) Induction of tyrosine phosphorylation and translocation of ezrin by hepatocyte growth factor/scatter factor. *Biochemical and biophysical research communications* **217**, 1062-1069
146. Krieg, J., and Hunter, T. (1992) Identification of the two major epidermal growth factor-induced tyrosine phosphorylation sites in the microvillar core protein ezrin. *The Journal of biological chemistry* **267**, 19258-19265
147. Carreno, S., Kouranti, I., Glusman, E. S., Fuller, M. T., Echard, A., and Payre, F. (2008) Moesin and its activating kinase Slik are required for cortical stability and microtubule organization in mitotic cells. *J Cell Biol* **180**, 739-746
148. Hipfner, D. R., Keller, N., and Cohen, S. M. (2004) Slik Sterile-20 kinase regulates Moesin activity to promote epithelial integrity during tissue growth. *Genes Dev* **18**, 2243-2248

149. Hughes, S. C., and Fehon, R. G. (2006) Phosphorylation and activity of the tumor suppressor Merlin and the ERM protein Moesin are coordinately regulated by the Slik kinase. *J Cell Biol* **175**, 305-313
150. Chen, J., and Mandel, L. J. (1997) Unopposed phosphatase action initiates ezrin dysfunction: a potential mechanism for anoxic injury. *Am J Physiol* **273**, C710-716
151. Fukata, Y., Kimura, K., Oshiro, N., Saya, H., Matsuura, Y., and Kaibuchi, K. (1998) Association of the myosin-binding subunit of myosin phosphatase and moesin: dual regulation of moesin phosphorylation by Rho-associated kinase and myosin phosphatase. *J Cell Biol* **141**, 409-418
152. Hishiya, A., Ohnishi, M., Tamura, S., and Nakamura, F. (1999) Protein phosphatase 2C inactivates F-actin binding of human platelet moesin. *The Journal of biological chemistry* **274**, 26705-26712
153. Potter, D. A., Tirnauer, J. S., Janssen, R., Croall, D. E., Hughes, C. N., Fiacco, K. A., Mier, J. W., Maki, M., and Herman, I. M. (1998) Calpain regulates actin remodeling during cell spreading. *J Cell Biol* **141**, 647-662
154. Shcherbina, A., Bretscher, A., Kenney, D. M., and Remold-O'Donnell, E. (1999) Moesin, the major ERM protein of lymphocytes and platelets, differs from ezrin in its insensitivity to calpain. *FEBS Lett* **443**, 31-36
155. Speck, O., Hughes, S. C., Noren, N. K., Kulikauskas, R. M., and Fehon, R. G. (2003) Moesin functions antagonistically to the Rho pathway to maintain epithelial integrity. *Nature* **421**, 83-87

156. Molnar, C., and de Celis, J. F. (2006) Independent roles of Drosophila Moesin in imaginal disc morphogenesis and hedgehog signalling. *Mechanisms of development* **123**, 337-351
157. Kunda, P., Pelling, A. E., Liu, T., and Baum, B. (2008) Moesin controls cortical rigidity, cell rounding, and spindle morphogenesis during mitosis. *Current biology : CB* **18**, 91-101
158. Gobel, V., Barrett, P. L., Hall, D. H., and Fleming, J. T. (2004) Lumen morphogenesis in *C. elegans* requires the membrane-cytoskeleton linker erm-1. *Developmental cell* **6**, 865-873
159. Van Furden, D., Johnson, K., Segbert, C., and Bossinger, O. (2004) The *C. elegans* ezrin-radixin-moesin protein ERM-1 is necessary for apical junction remodelling and tubulogenesis in the intestine. *Dev Biol* **272**, 262-276
160. Takeuchi, K., Sato, N., Kasahara, H., Funayama, N., Nagafuchi, A., Yonemura, S., Tsukita, S., and Tsukita, S. (1994) Perturbation of cell adhesion and microvilli formation by antisense oligonucleotides to ERM family members. *The Journal of cell biology* **125**, 1371-1384
161. Bonilha, V. L., Finnemann, S. C., and Rodriguez-Boulan, E. (1999) Ezrin promotes morphogenesis of apical microvilli and basal infoldings in retinal pigment epithelium. *The Journal of cell biology* **147**, 1533-1548
162. Haas, M. A., Vickers, J. C., and Dickson, T. C. (2007) Rho kinase activates ezrin-radixin-moesin (ERM) proteins and mediates their function in cortical neuron growth, morphology and motility in vitro. *Journal of neuroscience research* **85**, 34-46

163. Pujuguet, P., Del Maestro, L., Gautreau, A., Louvard, D., and Arpin, M. (2003) Ezrin regulates E-cadherin-dependent adherens junction assembly through Rac1 activation. *Mol Biol Cell* **14**, 2181-2191
164. Takahashi, K., Sasaki, T., Mammoto, A., Takaishi, K., Kameyama, T., Tsukita, S., and Takai, Y. (1997) Direct interaction of the Rho GDP dissociation inhibitor with ezrin/radixin/moesin initiates the activation of the Rho small G protein. *J Biol Chem* **272**, 23371-23375
165. Hunter, K. W. (2004) Ezrin, a key component in tumor metastasis. *Trends in molecular medicine* **10**, 201-204
166. Gautreau, A., Pouillet, P., Louvard, D., and Arpin, M. (1999) Ezrin, a plasma membrane-microfilament linker, signals cell survival through the phosphatidylinositol 3-kinase/Akt pathway. *Proc Natl Acad Sci U S A* **96**, 7300-7305
167. Kuo, W. C., Yang, K. T., Hsieh, S. L., and Lai, M. Z. (2010) Ezrin is a negative regulator of death receptor-induced apoptosis. *Oncogene* **29**, 1374-1383
168. Allenspach, E. J., Cullinan, P., Tong, J., Tang, Q., Tesciuba, A. G., Cannon, J. L., Takahashi, S. M., Morgan, R., Burkhardt, J. K., and Sperling, A. I. (2001) ERM-dependent movement of CD43 defines a novel protein complex distal to the immunological synapse. *Immunity* **15**, 739-750
169. Delon, J., Kaibuchi, K., and Germain, R. N. (2001) Exclusion of CD43 from the immunological synapse is mediated by phosphorylation-regulated relocation of the cytoskeletal adaptor moesin. *Immunity* **15**, 691-701
170. Roumier, A., Olivo-Marin, J. C., Arpin, M., Michel, F., Martin, M., Mangeat, P., Acuto, O., Dautry-Varsat, A., and Alcover, A. (2001) The membrane-microfilament linker ezrin

is involved in the formation of the immunological synapse and in T cell activation.

Immunity **15**, 715-728

171. Hiscox, S., and Jiang, W. G. (1999) Ezrin regulates cell-cell and cell-matrix adhesion, a possible role with E-cadherin/beta-catenin. *J Cell Sci* **112 Pt 18**, 3081-3090
172. Martin, M., Andreoli, C., Sahuquet, A., Montcourrier, P., Algrain, M., and Mangeat, P. (1995) Ezrin NH₂-terminal domain inhibits the cell extension activity of the COOH-terminal domain. *The Journal of cell biology* **128**, 1081-1093
173. Sechi, A. S., and Wehland, J. (2000) The actin cytoskeleton and plasma membrane connection: PtdIns(4,5)P(2) influences cytoskeletal protein activity at the plasma membrane. *J Cell Sci* **113 Pt 21**, 3685-3695
174. Lamb, R. F., Roy, C., Diefenbach, T. J., Vinters, H. V., Johnson, M. W., Jay, D. G., and Hall, A. (2000) The TSC1 tumour suppressor hamartin regulates cell adhesion through ERM proteins and the GTPase Rho. *Nat Cell Biol* **2**, 281-287
175. Serrador, J. M., Alonso-Lebrero, J. L., del Pozo, M. A., Furthmayr, H., Schwartz-Albiez, R., Calvo, J., Lozano, F., and Sanchez-Madrid, F. (1997) Moesin interacts with the cytoplasmic region of intercellular adhesion molecule-3 and is redistributed to the uropod of T lymphocytes during cell polarization. *The Journal of cell biology* **138**, 1409-1423
176. Yonemura, S., Nagafuchi, A., Sato, N., and Tsukita, S. (1993) Concentration of an integral membrane protein, CD43 (leukosialin, sialophorin), in the cleavage furrow through the interaction of its cytoplasmic domain with actin-based cytoskeletons. *J Cell Biol* **120**, 437-449

177. Nobes, C. D., and Hall, A. (1995) Rho, rac, and cdc42 GTPases regulate the assembly of multimolecular focal complexes associated with actin stress fibers, lamellipodia, and filopodia. *Cell* **81**, 53-62
178. Martin, T. F. (1998) Phosphoinositide lipids as signaling molecules: common themes for signal transduction, cytoskeletal regulation, and membrane trafficking. *Annual review of cell and developmental biology* **14**, 231-264
179. Di Paolo, G., and De Camilli, P. (2006) Phosphoinositides in cell regulation and membrane dynamics. *Nature* **443**, 651-657
180. Janetopoulos, C., and Devreotes, P. (2006) Phosphoinositide signaling plays a key role in cytokinesis. *J Cell Biol* **174**, 485-490
181. Simonsen, A., Wurmser, A. E., Emr, S. D., and Stenmark, H. (2001) The role of phosphoinositides in membrane transport. *Curr Opin Cell Biol* **13**, 485-492
182. Takenawa, T., and Itoh, T. (2001) Phosphoinositides, key molecules for regulation of actin cytoskeletal organization and membrane traffic from the plasma membrane. *Biochimica et biophysica acta* **1533**, 190-206
183. Toker, A. (2002) Phosphoinositides and signal transduction. *Cellular and molecular life sciences : CMLS* **59**, 761-779
184. Jones, D. R., and Varela-Nieto, I. (1999) Diabetes and the role of inositol-containing lipids in insulin signaling. *Molecular medicine* **5**, 505-514
185. Logothetis, D. E., Petrou, V. I., Adney, S. K., and Mahajan, R. (2010) Channelopathies linked to plasma membrane phosphoinositides. *Pflugers Archiv : European journal of physiology* **460**, 321-341

186. Pendaries, C., Tronchere, H., Plantavid, M., and Payrastre, B. (2003) Phosphoinositide signaling disorders in human diseases. *FEBS Lett* **546**, 25-31
187. Hilgemann, D. W., and Ball, R. (1996) Regulation of cardiac Na⁺,Ca²⁺ exchange and KATP potassium channels by PIP₂. *Science* **273**, 956-959
188. Suh, B. C., and Hille, B. (2005) Regulation of ion channels by phosphatidylinositol 4,5-bisphosphate. *Current opinion in neurobiology* **15**, 370-378
189. Aikawa, Y., and Martin, T. F. (2003) ARF6 regulates a plasma membrane pool of phosphatidylinositol(4,5)bisphosphate required for regulated exocytosis. *The Journal of cell biology* **162**, 647-659
190. Gong, L. W., Di Paolo, G., Diaz, E., Cestra, G., Diaz, M. E., Lindau, M., De Camilli, P., and Toomre, D. (2005) Phosphatidylinositol phosphate kinase type I gamma regulates dynamics of large dense-core vesicle fusion. *Proc Natl Acad Sci U S A* **102**, 5204-5209
191. Halstead, J. R., van Rheenen, J., Snel, M. H., Meeuws, S., Mohammed, S., D'Santos, C. S., Heck, A. J., Jalink, K., and Divecha, N. (2006) A role for PtdIns(4,5)P₂ and PIP5K α in regulating stress-induced apoptosis. *Current biology : CB* **16**, 1850-1856
192. Mejillano, M., Yamamoto, M., Rozelle, A. L., Sun, H. Q., Wang, X., and Yin, H. L. (2001) Regulation of apoptosis by phosphatidylinositol 4,5-bisphosphate inhibition of caspases, and caspase inactivation of phosphatidylinositol phosphate 5-kinases. *J Biol Chem* **276**, 1865-1872
193. Saarikangas, J., Zhao, H., and Lappalainen, P. (2010) Regulation of the actin cytoskeleton-plasma membrane interplay by phosphoinositides. *Physiological reviews* **90**, 259-289

194. Chuang, D. M. (1989) Neurotransmitter receptors and phosphoinositide turnover. *Annual review of pharmacology and toxicology* **29**, 71-110
195. Hilgemann, D. W. (2007) Local PIP(2) signals: when, where, and how? *Pflugers Archiv : European journal of physiology* **455**, 55-67
196. Hokin, L. E., and Hokin, M. R. (1964) The Incorporation of ³²p from Triphosphate into Polyphosphoinositides (Gamma-³²p)Adenosine and Phosphatidic Acid in Erythrocyte Membranes. *Biochimica et biophysica acta* **84**, 563-575
197. Michell, R. H. (1975) Inositol phospholipids and cell surface receptor function. *Biochimica et biophysica acta* **415**, 81-47
198. Thompson, W., Strickland, K. P., and Rossiter, R. J. (1963) Biosynthesis of phosphatidylinositol in rat brain. *Biochem J* **87**, 136-142
199. Toker, A., and Cantley, L. C. (1997) Signalling through the lipid products of phosphoinositide-3-OH kinase. *Nature* **387**, 673-676
200. Berridge, M. J., Heslop, J. P., Irvine, R. F., and Brown, K. D. (1984) Inositol trisphosphate formation and calcium mobilization in Swiss 3T3 cells in response to platelet-derived growth factor. *Biochem J* **222**, 195-201
201. Berridge, M. J., and Irvine, R. F. (1984) Inositol trisphosphate, a novel second messenger in cellular signal transduction. *Nature* **312**, 315-321
202. Wenk, M. R., and De Camilli, P. (2004) Protein-lipid interactions and phosphoinositide metabolism in membrane traffic: insights from vesicle recycling in nerve terminals. *Proc Natl Acad Sci U S A* **101**, 8262-8269

203. Lassing, I., and Lindberg, U. (1988) Specificity of the interaction between phosphatidylinositol 4,5-bisphosphate and the profilin:actin complex. *Journal of cellular biochemistry* **37**, 255-267
204. Gilmore, A. P., and Burridge, K. (1996) Regulation of vinculin binding to talin and actin by phosphatidyl-inositol-4-5-bisphosphate. *Nature* **381**, 531-535
205. Shibasaki, Y., Ishihara, H., Kizuki, N., Asano, T., Oka, Y., and Yazaki, Y. (1997) Massive actin polymerization induced by phosphatidylinositol-4-phosphate 5-kinase in vivo. *J Biol Chem* **272**, 7578-7581
206. Kanaho, Y., Kobayashi-Nakano, A., and Yokozeki, T. (2007) The phosphoinositide kinase PIP5K that produces the versatile signaling phospholipid PI4,5P(2). *Biological & pharmaceutical bulletin* **30**, 1605-1609
207. Mao, Y. S., and Yin, H. L. (2007) Regulation of the actin cytoskeleton by phosphatidylinositol 4-phosphate 5 kinases. *Pflugers Archiv : European journal of physiology* **455**, 5-18
208. Loijens, J. C., and Anderson, R. A. (1996) Type I phosphatidylinositol-4-phosphate 5-kinases are distinct members of this novel lipid kinase family. *J Biol Chem* **271**, 32937-32943
209. Loijens, J. C., Boronenkov, I. V., Parker, G. J., and Anderson, R. A. (1996) The phosphatidylinositol 4-phosphate 5-kinase family. *Advances in enzyme regulation* **36**, 115-140
210. Oude Weernink, P. A., Schmidt, M., and Jakobs, K. H. (2004) Regulation and cellular roles of phosphoinositide 5-kinases. *European journal of pharmacology* **500**, 87-99

211. Kwiatkowska, K. (2010) One lipid, multiple functions: how various pools of PI(4,5)P(2) are created in the plasma membrane. *Cellular and molecular life sciences : CMLS* **67**, 3927-3946
212. Toliás, K. F., Hartwig, J. H., Ishihara, H., Shibasaki, Y., Cantley, L. C., and Carpenter, C. L. (2000) Type Ialpha phosphatidylinositol-4-phosphate 5-kinase mediates Rac-dependent actin assembly. *Current biology : CB* **10**, 153-156
213. Ishihara, H., Shibasaki, Y., Kizuki, N., Katagiri, H., Yazaki, Y., Asano, T., and Oka, Y. (1996) Cloning of cDNAs encoding two isoforms of 68-kDa type I phosphatidylinositol-4-phosphate 5-kinase. *J Biol Chem* **271**, 23611-23614
214. Doughman, R. L., Firestone, A. J., Wojtasiak, M. L., Bunce, M. W., and Anderson, R. A. (2003) Membrane ruffling requires coordination between type Ialpha phosphatidylinositol phosphate kinase and Rac signaling. *J Biol Chem* **278**, 23036-23045
215. Mellman, D. L., Gonzales, M. L., Song, C., Barlow, C. A., Wang, P., Kendzioriski, C., and Anderson, R. A. (2008) A PtdIns4,5P2-regulated nuclear poly(A) polymerase controls expression of select mRNAs. *Nature* **451**, 1013-1017
216. Coppolino, M. G., Dierckman, R., Loijens, J., Collins, R. F., Pouladi, M., Jongstra-Bilen, J., Schreiber, A. D., Trimble, W. S., Anderson, R., and Grinstein, S. (2002) Inhibition of phosphatidylinositol-4-phosphate 5-kinase Ialpha impairs localized actin remodeling and suppresses phagocytosis. *J Biol Chem* **277**, 43849-43857
217. Galiano, F. J., Ulug, E. T., and Davis, J. N. (2002) Overexpression of murine phosphatidylinositol 4-phosphate 5-kinase type Ibeta disrupts a phosphatidylinositol 4,5 bisphosphate regulated endosomal pathway. *Journal of cellular biochemistry* **85**, 131-145

218. Divecha, N., Roefs, M., Halstead, J. R., D'Andrea, S., Fernandez-Borga, M., Oomen, L., Saqib, K. M., Wakelam, M. J., and D'Santos, C. (2000) Interaction of the type Ialpha PIPkinase with phospholipase D: a role for the local generation of phosphatidylinositol 4, 5-bisphosphate in the regulation of PLD2 activity. *The EMBO journal* **19**, 5440-5449
219. Sasaki, J., Sasaki, T., Yamazaki, M., Matsuoka, K., Taya, C., Shitara, H., Takasuga, S., Nishio, M., Mizuno, K., Wada, T., Miyazaki, H., Watanabe, H., Iizuka, R., Kubo, S., Murata, S., Chiba, T., Maehama, T., Hamada, K., Kishimoto, H., Frohman, M. A., Tanaka, K., Penninger, J. M., Yonekawa, H., Suzuki, A., and Kanaho, Y. (2005) Regulation of anaphylactic responses by phosphatidylinositol phosphate kinase type I {alpha}. *J Exp Med* **201**, 859-870
220. Wang, Y., Chen, X., Lian, L., Tang, T., Stalker, T. J., Sasaki, T., Kanaho, Y., Brass, L. F., Choi, J. K., Hartwig, J. H., and Abrams, C. S. (2008) Loss of PIP5KIbeta demonstrates that PIP5KI isoform-specific PIP2 synthesis is required for IP3 formation. *Proc Natl Acad Sci U S A* **105**, 14064-14069
221. Doughman, R. L., Firestone, A. J., and Anderson, R. A. (2003) Phosphatidylinositol phosphate kinases put PI4,5P(2) in its place. *J Membr Biol* **194**, 77-89
222. Padron, D., Wang, Y. J., Yamamoto, M., Yin, H., and Roth, M. G. (2003) Phosphatidylinositol phosphate 5-kinase Ibeta recruits AP-2 to the plasma membrane and regulates rates of constitutive endocytosis. *J Cell Biol* **162**, 693-701
223. Lacalle, R. A., Peregil, R. M., Albar, J. P., Merino, E., Martinez, A. C., Merida, I., and Manes, S. (2007) Type I phosphatidylinositol 4-phosphate 5-kinase controls neutrophil polarity and directional movement. *J Cell Biol* **179**, 1539-1553

224. Chen, M. Z., Zhu, X., Sun, H. Q., Mao, Y. S., Wei, Y., Yamamoto, M., and Yin, H. L. (2009) Oxidative stress decreases phosphatidylinositol 4,5-bisphosphate levels by deactivating phosphatidylinositol- 4-phosphate 5-kinase beta in a Syk-dependent manner. *J Biol Chem* **284**, 23743-23753
225. Mao, Y. S., Yamaga, M., Zhu, X., Wei, Y., Sun, H. Q., Wang, J., Yun, M., Wang, Y., Di Paolo, G., Bennett, M., Mellman, I., Abrams, C. S., De Camilli, P., Lu, C. Y., and Yin, H. L. (2009) Essential and unique roles of PIP5K-gamma and -alpha in Fcgamma receptor-mediated phagocytosis. *The Journal of cell biology* **184**, 281-296
226. Schill, N. J., and Anderson, R. A. (2009) Two novel phosphatidylinositol-4-phosphate 5-kinase type I gamma splice variants expressed in human cells display distinctive cellular targeting. *Biochem J* **422**, 473-482
227. Ling, K., Doughman, R. L., Firestone, A. J., Bunce, M. W., and Anderson, R. A. (2002) Type I gamma phosphatidylinositol phosphate kinase targets and regulates focal adhesions. *Nature* **420**, 89-93
228. Di Paolo, G., Pellegrini, L., Letinic, K., Cestra, G., Zoncu, R., Voronov, S., Chang, S., Guo, J., Wenk, M. R., and De Camilli, P. (2002) Recruitment and regulation of phosphatidylinositol phosphate kinase type 1 gamma by the FERM domain of talin. *Nature* **420**, 85-89
229. Ishihara, H., Shibasaki, Y., Kizuki, N., Wada, T., Yazaki, Y., Asano, T., and Oka, Y. (1998) Type I phosphatidylinositol-4-phosphate 5-kinases. Cloning of the third isoform and deletion/substitution analysis of members of this novel lipid kinase family. *J Biol Chem* **273**, 8741-8748

230. Wang, Y. J., Li, W. H., Wang, J., Xu, K., Dong, P., Luo, X., and Yin, H. L. (2004) Critical role of PIP5KI γ 87 in InsP3-mediated Ca²⁺ signaling. *J Cell Biol* **167**, 1005-1010
231. Vasudevan, L., Jeromin, A., Volpicelli-Daley, L., De Camilli, P., Holowka, D., and Baird, B. (2009) The beta- and gamma-isoforms of type I PIP5K regulate distinct stages of Ca²⁺ signaling in mast cells. *J Cell Sci* **122**, 2567-2574
232. Powner, D. J., Payne, R. M., Pettitt, T. R., Giudici, M. L., Irvine, R. F., and Wakelam, M. J. (2005) Phospholipase D2 stimulates integrin-mediated adhesion via phosphatidylinositol 4-phosphate 5-kinase Igamma b. *Journal of cell science* **118**, 2975-2986
233. Ling, K., Bairstow, S. F., Carbonara, C., Turbin, D. A., Huntsman, D. G., and Anderson, R. A. (2007) Type I gamma phosphatidylinositol phosphate kinase modulates adherens junction and E-cadherin trafficking via a direct interaction with mu 1B adaptin. *The Journal of cell biology* **176**, 343-353
234. Wenk, M. R., Pellegrini, L., Klenchin, V. A., Di Paolo, G., Chang, S., Daniell, L., Arioka, M., Martin, T. F., and De Camilli, P. (2001) PIP kinase Igamma is the major PI(4,5)P(2) synthesizing enzyme at the synapse. *Neuron* **32**, 79-88
235. Nakano-Kobayashi, A., Yamazaki, M., Unoki, T., Hongu, T., Murata, C., Taguchi, R., Katada, T., Frohman, M. A., Yokozeki, T., and Kanaho, Y. (2007) Role of activation of PIP5Kgamma661 by AP-2 complex in synaptic vesicle endocytosis. *The EMBO journal* **26**, 1105-1116

236. Morgan, J. R., Di Paolo, G., Werner, H., Shchedrina, V. A., Pypaert, M., Pieribone, V. A., and De Camilli, P. (2004) A role for talin in presynaptic function. *J Cell Biol* **167**, 43-50
237. Wang, Y., Lian, L., Golden, J. A., Morrisey, E. E., and Abrams, C. S. (2007) PIP5KI gamma is required for cardiovascular and neuronal development. *Proc Natl Acad Sci U S A* **104**, 11748-11753
238. Di Paolo, G., Moskowitz, H. S., Gipson, K., Wenk, M. R., Voronov, S., Obayashi, M., Flavell, R., Fitzsimonds, R. M., Ryan, T. A., and De Camilli, P. (2004) Impaired PtdIns(4,5)P₂ synthesis in nerve terminals produces defects in synaptic vesicle trafficking. *Nature* **431**, 415-422
239. Narkis, G., Ofir, R., Landau, D., Manor, E., Volokita, M., Hershkowitz, R., Elbedour, K., and Birk, O. S. (2007) Lethal contractural syndrome type 3 (LCCS3) is caused by a mutation in PIP5K1C, which encodes PIPKI gamma of the phosphatidylinositol pathway. *Am J Hum Genet* **81**, 530-539
240. Condeelis, J. (2001) How is actin polymerization nucleated in vivo? *Trends in cell biology* **11**, 288-293
241. Small, J. V., Stradal, T., Vignat, E., and Rottner, K. (2002) The lamellipodium: where motility begins. *Trends in cell biology* **12**, 112-120
242. Ren, X. D., Bokoch, G. M., Traynor-Kaplan, A., Jenkins, G. H., Anderson, R. A., and Schwartz, M. A. (1996) Physical association of the small GTPase Rho with a 68-kDa phosphatidylinositol 4-phosphate 5-kinase in Swiss 3T3 cells. *Mol Biol Cell* **7**, 435-442
243. Oude Weernink, P. A., Schulte, P., Guo, Y., Wetzel, J., Amano, M., Kaibuchi, K., Haverland, S., Voss, M., Schmidt, M., Mayr, G. W., and Jakobs, K. H. (2000)

- Stimulation of phosphatidylinositol-4-phosphate 5-kinase by Rho-kinase. *J Biol Chem* **275**, 10168-10174
244. Chatah, N. E., and Abrams, C. S. (2001) G-protein-coupled receptor activation induces the membrane translocation and activation of phosphatidylinositol-4-phosphate 5-kinase I alpha by a Rac- and Rho-dependent pathway. *J Biol Chem* **276**, 34059-34065
245. Aikawa, Y., and Martin, T. F. (2005) ADP-ribosylation factor 6 regulation of phosphatidylinositol-4,5-bisphosphate synthesis, endocytosis, and exocytosis. *Methods Enzymol* **404**, 422-431
246. Honda, A., Nogami, M., Yokozeki, T., Yamazaki, M., Nakamura, H., Watanabe, H., Kawamoto, K., Nakayama, K., Morris, A. J., Frohman, M. A., and Kanaho, Y. (1999) Phosphatidylinositol 4-phosphate 5-kinase alpha is a downstream effector of the small G protein ARF6 in membrane ruffle formation. *Cell* **99**, 521-532
247. Martin, A., Brown, F. D., Hodgkin, M. N., Bradwell, A. J., Cook, S. J., Hart, M., and Wakelam, M. J. (1996) Activation of phospholipase D and phosphatidylinositol 4-phosphate 5-kinase in HL60 membranes is mediated by endogenous Arf but not Rho. *J Biol Chem* **271**, 17397-17403
248. Itoh, T., Ishihara, H., Shibasaki, Y., Oka, Y., and Takenawa, T. (2000) Autophosphorylation of type I phosphatidylinositol phosphate kinase regulates its lipid kinase activity. *J Biol Chem* **275**, 19389-19394
249. Ling, K., Doughman, R. L., Iyer, V. V., Firestone, A. J., Bairstow, S. F., Mosher, D. F., Schaller, M. D., and Anderson, R. A. (2003) Tyrosine phosphorylation of type I gamma phosphatidylinositol phosphate kinase by Src regulates an integrin-talin switch. *J Cell Biol* **163**, 1339-1349

250. Moritz, A., Westerman, J., de Graan, P. N., and Wirtz, K. W. (1992) Phosphatidylinositol 4-kinase and phosphatidylinositol-4-phosphate 5-kinase from bovine brain membranes. *Methods Enzymol* **209**, 202-211
251. Jarquin-Pardo, M., Fitzpatrick, A., Galiano, F. J., First, E. A., and Davis, J. N. (2007) Phosphatidic acid regulates the affinity of the murine phosphatidylinositol 4-phosphate 5-kinase-Ibeta for phosphatidylinositol-4-phosphate. *J Cell Biochem* **100**, 112-128
252. Tisher, C., and Madsen, K. (1991) *The Kidney* Saunders Company, Philadelphia, USA
253. Ling, F. D. (1990) *Anatomy*, 3ed ed., People Health Press, Beijing- China
254. Herrera, G. A. (2006) Plasticity of mesangial cells: a basis for understanding pathological alterations. *Ultrastructural pathology* **30**, 471-479
255. Leveen, P., Pekny, M., Gebre-Medhin, S., Swolin, B., Larsson, E., and Betsholtz, C. (1994) Mice deficient for PDGF B show renal, cardiovascular, and hematological abnormalities. *Genes & development* **8**, 1875-1887
256. Soriano, P. (1994) Abnormal kidney development and hematological disorders in PDGF beta-receptor mutant mice. *Genes & development* **8**, 1888-1896
257. Ballermann, B. J. (2005) Glomerular endothelial cell differentiation. *Kidney international* **67**, 1668-1671
258. Nagai, T., Yokomori, H., Yoshimura, K., Fujimaki, K., Nomura, M., Hibi, T., and Oda, M. (2004) Actin filaments around endothelial fenestrae in rat hepatic sinusoidal endothelial cells. *Medical electron microscopy : official journal of the Clinical Electron Microscopy Society of Japan* **37**, 252-255

259. Deen, W. M., Lazzara, M. J., and Myers, B. D. (2001) Structural determinants of glomerular permeability. *American journal of physiology. Renal physiology* **281**, F579-596
260. Saborio, P., and Scheinman, J. (1998) Genetic renal disease. *Curr Opin Pediatr* **10**, 174-183
261. Smeets, H. J., Knoers, V. V., van de Heuvel, L. P., Lemmink, H. H., Schroder, C. H., and Monnens, L. A. (1996) Hereditary disorders of the glomerular basement membrane. *Pediatr Nephrol* **10**, 779-788
262. Paulsson, M. (1992) Basement membrane proteins: structure, assembly, and cellular interactions. *Critical reviews in biochemistry and molecular biology* **27**, 93-127
263. Kallunki, P., and Tryggvason, K. (1992) Human basement membrane heparan sulfate proteoglycan core protein: a 467-kD protein containing multiple domains resembling elements of the low density lipoprotein receptor, laminin, neural cell adhesion molecules, and epidermal growth factor. *J Cell Biol* **116**, 559-571
264. Hassell, J. R., Robey, P. G., Barrach, H. J., Wilczek, J., Rennard, S. I., and Martin, G. R. (1980) Isolation of a heparan sulfate-containing proteoglycan from basement membrane. *Proc Natl Acad Sci U S A* **77**, 4494-4498
265. Haraldsson, B., Nystrom, J., and Deen, W. M. (2008) Properties of the glomerular barrier and mechanisms of proteinuria. *Physiol Rev* **88**, 451-487
266. Hudson, B. G., Tryggvason, K., Sundaramoorthy, M., and Neilson, E. G. (2003) Alport's syndrome, Goodpasture's syndrome, and type IV collagen. *The New England journal of medicine* **348**, 2543-2556
267. Kuhn, K. (1995) Basement membrane (type IV) collagen. *Matrix Biol* **14**, 439-445

268. Groffen, A. J., Veerkamp, J. H., Monnens, L. A., and van den Heuvel, L. P. (1999) Recent insights into the structure and functions of heparan sulfate proteoglycans in the human glomerular basement membrane. *Nephrol Dial Transplant* **14**, 2119-2129
269. Abrahamson, D. R., Hudson, B. G., Stroganova, L., Borza, D. B., and St John, P. L. (2009) Cellular origins of type IV collagen networks in developing glomeruli. *J Am Soc Nephrol* **20**, 1471-1479
270. Colognato, H., and Yurchenco, P. D. (2000) Form and function: the laminin family of heterotrimers. *Developmental dynamics : an official publication of the American Association of Anatomists* **218**, 213-234
271. Miner, J. H., and Yurchenco, P. D. (2004) Laminin functions in tissue morphogenesis. *Annual review of cell and developmental biology* **20**, 255-284
272. Miner, J. H. (2005) Building the glomerulus: a matricentric view. *J Am Soc Nephrol* **16**, 857-861
273. Kreidberg, J. A., and Symons, J. M. (2000) Integrins in kidney development, function, and disease. *Am J Physiol Renal Physiol* **279**, F233-242
274. Denzer, A. J., Schulthess, T., Fauser, C., Schumacher, B., Kammerer, R. A., Engel, J., and Rugg, M. A. (1998) Electron microscopic structure of agrin and mapping of its binding site in laminin-1. *The EMBO journal* **17**, 335-343
275. Noakes, P. G., Miner, J. H., Gautam, M., Cunningham, J. M., Sanes, J. R., and Merlie, J. P. (1995) The renal glomerulus of mice lacking s-laminin/laminin beta 2: nephrosis despite molecular compensation by laminin beta 1. *Nature genetics* **10**, 400-406
276. Groffen, A. J., Rugg, M. A., Dijkman, H., van de Velden, T. J., Buskens, C. A., van den Born, J., Assmann, K. J., Monnens, L. A., Veerkamp, J. H., and van den Heuvel, L. P.

- (1998) Agrin is a major heparan sulfate proteoglycan in the human glomerular basement membrane. *The journal of histochemistry and cytochemistry : official journal of the Histochemistry Society* **46**, 19-27
277. Noonan, D. M., Fulle, A., Valente, P., Cai, S., Horigan, E., Sasaki, M., Yamada, Y., and Hassell, J. R. (1991) The complete sequence of perlecan, a basement membrane heparan sulfate proteoglycan, reveals extensive similarity with laminin A chain, low density lipoprotein-receptor, and the neural cell adhesion molecule. *J Biol Chem* **266**, 22939-22947
278. Kanwar, Y. S., Danesh, F. R., and Chugh, S. S. (2007) Contribution of proteoglycans towards the integrated functions of renal glomerular capillaries: a historical perspective. *Am J Pathol* **171**, 9-13
279. Stow, J. L., Sawada, H., and Farquhar, M. G. (1985) Basement membrane heparan sulfate proteoglycans are concentrated in the laminae rarae and in podocytes of the rat renal glomerulus. *Proc Natl Acad Sci U S A* **82**, 3296-3300
280. Raats, C. J., van den Born, J., Bakker, M. A., Oppers-Walgreen, B., Pisa, B. J., Dijkman, H. B., Assmann, K. J., and Berden, J. H. (2000) Expression of agrin, dystroglycan, and utrophin in normal renal tissue and in experimental glomerulopathies. *Am J Pathol* **156**, 1749-1765
281. Tamsma, J. T., van den Born, J., Bruijn, J. A., Assmann, K. J., Weening, J. J., Berden, J. H., Wieslander, J., Schrama, E., Hermans, J., Veerkamp, J. H., and et al. (1994) Expression of glomerular extracellular matrix components in human diabetic nephropathy: decrease of heparan sulphate in the glomerular basement membrane. *Diabetologia* **37**, 313-320

282. Murdoch, A. D., Liu, B., Schwarting, R., Tuan, R. S., and Iozzo, R. V. (1994) Widespread expression of perlecan proteoglycan in basement membranes and extracellular matrices of human tissues as detected by a novel monoclonal antibody against domain III and by in situ hybridization. *The journal of histochemistry and cytochemistry : official journal of the Histochemistry Society* **42**, 239-249
283. Pyke, C., Kristensen, P., Ostergaard, P. B., Oturai, P. S., and Romer, J. (1997) Proteoglycan expression in the normal rat kidney. *Nephron* **77**, 461-470
284. Mayer, U., Nischt, R., Poschl, E., Mann, K., Fukuda, K., Gerl, M., Yamada, Y., and Timpl, R. (1993) A single EGF-like motif of laminin is responsible for high affinity nidogen binding. *The EMBO journal* **12**, 1879-1885
285. Aumailley, M., Wiedemann, H., Mann, K., and Timpl, R. (1989) Binding of nidogen and the laminin-nidogen complex to basement membrane collagen type IV. *Eur J Biochem* **184**, 241-248
286. Fox, J. W., Mayer, U., Nischt, R., Aumailley, M., Reinhardt, D., Wiedemann, H., Mann, K., Timpl, R., Krieg, T., Engel, J., and et al. (1991) Recombinant nidogen consists of three globular domains and mediates binding of laminin to collagen type IV. *The EMBO journal* **10**, 3137-3146
287. Kriz, W., Elger, M., Mundel, P., and Lemley, K. V. (1995) Structure-stabilizing forces in the glomerular tuft. *J Am Soc Nephrol* **5**, 1731-1739
288. Kriz, W., Hackenthal, E., Nobiling, R., Sakai, T., Elger, M., and Hahnel, B. (1994) A role for podocytes to counteract capillary wall distension. *Kidney Int* **45**, 369-376
289. Kriz, W., Kretzler, M., Provoost, A. P., and Shirato, I. (1996) Stability and leakiness: opposing challenges to the glomerulus. *Kidney Int* **49**, 1570-1574

290. Eremina, V., Sood, M., Haigh, J., Nagy, A., Lajoie, G., Ferrara, N., Gerber, H. P., Kikkawa, Y., Miner, J. H., and Quaggin, S. E. (2003) Glomerular-specific alterations of VEGF-A expression lead to distinct congenital and acquired renal diseases. *The Journal of clinical investigation* **111**, 707-716
291. Korhonen, M., Ylanne, J., Laitinen, L., and Virtanen, I. (1990) The alpha 1-alpha 6 subunits of integrins are characteristically expressed in distinct segments of developing and adult human nephron. *J Cell Biol* **111**, 1245-1254
292. Adler, S. (1992) Characterization of glomerular epithelial cell matrix receptors. *Am J Pathol* **141**, 571-578
293. Regele, H. M., Fillipovic, E., Langer, B., Poczewki, H., Kraxberger, I., Bittner, R. E., and Kerjaschki, D. (2000) Glomerular expression of dystroglycans is reduced in minimal change nephrosis but not in focal segmental glomerulosclerosis. *J Am Soc Nephrol* **11**, 403-412
294. Kerjaschki, D., Sharkey, D. J., and Farquhar, M. G. (1984) Identification and characterization of podocalyxin--the major sialoprotein of the renal glomerular epithelial cell. *J Cell Biol* **98**, 1591-1596
295. Rodewald, R., and Karnovsky, M. J. (1974) Porous substructure of the glomerular slit diaphragm in the rat and mouse. *J Cell Biol* **60**, 423-433
296. Kreidberg, J. A. (2000) Functions of alpha3beta1 integrin. *Curr Opin Cell Biol* **12**, 548-553
297. Rahilly, M. A., and Fleming, S. (1992) Differential expression of integrin alpha chains by renal epithelial cells. *J Pathol* **167**, 327-334

298. Kreidberg, J. A., Donovan, M. J., Goldstein, S. L., Rennke, H., Shepherd, K., Jones, R. C., and Jaenisch, R. (1996) Alpha 3 beta 1 integrin has a crucial role in kidney and lung organogenesis. *Development* **122**, 3537-3547
299. Kanasaki, K., Kanda, Y., Palmsten, K., Tanjore, H., Lee, S. B., Lebleu, V. S., Gattone, V. H., Jr., and Kalluri, R. (2008) Integrin beta1-mediated matrix assembly and signaling are critical for the normal development and function of the kidney glomerulus. *Dev Biol* **313**, 584-593
300. Pozzi, A., Jarad, G., Moeckel, G. W., Coffa, S., Zhang, X., Gewin, L., Eremina, V., Hudson, B. G., Borza, D. B., Harris, R. C., Holzman, L. B., Phillips, C. L., Fassler, R., Quaggin, S. E., Miner, J. H., and Zent, R. (2008) Beta1 integrin expression by podocytes is required to maintain glomerular structural integrity. *Developmental biology* **316**, 288-301
301. Has, C., Sparta, G., Kiritsi, D., Weibel, L., Moeller, A., Vega-Warner, V., Waters, A., He, Y., Anikster, Y., Esser, P., Straub, B. K., Hausser, I., Bockenhauer, D., Dekel, B., Hildebrandt, F., Bruckner-Tuderman, L., and Laube, G. F. (2012) Integrin alpha3 mutations with kidney, lung, and skin disease. *N Engl J Med* **366**, 1508-1514
302. Jarad, G., Pippin, J. W., Shankland, S. J., Kreidberg, J. A., and Miner, J. H. (2011) Dystroglycan does not contribute significantly to kidney development or function, in health or after injury. *Am J Physiol Renal Physiol* **300**, F811-820
303. Hamano, Y., Grunkemeyer, J. A., Sudhakar, A., Zeisberg, M., Cosgrove, D., Morello, R., Lee, B., Sugimoto, H., and Kalluri, R. (2002) Determinants of vascular permeability in the kidney glomerulus. *J Biol Chem* **277**, 31154-31162

304. Hjalmarsson, C., Johansson, B. R., and Haraldsson, B. (2004) Electron microscopic evaluation of the endothelial surface layer of glomerular capillaries. *Microvasc Res* **67**, 9-17
305. Jeansson, M., and Haraldsson, B. (2006) Morphological and functional evidence for an important role of the endothelial cell glycocalyx in the glomerular barrier. *American journal of physiology. Renal physiology* **290**, F111-116
306. Rostgaard, J., and Qvortrup, K. (2002) Sieve plugs in fenestrae of glomerular capillaries--site of the filtration barrier? *Cells Tissues Organs* **170**, 132-138
307. Tryggvason, K., and Wartiovaara, J. (2001) Molecular basis of glomerular permselectivity. *Curr Opin Nephrol Hypertens* **10**, 543-549
308. Foo, S. S., Turner, C. J., Adams, S., Compagni, A., Aubyn, D., Kogata, N., Lindblom, P., Shani, M., Zicha, D., and Adams, R. H. (2006) Ephrin-B2 controls cell motility and adhesion during blood-vessel-wall assembly. *Cell* **124**, 161-173
309. Holthofer, H., Ahola, H., Solin, M. L., Wang, S., Palmén, T., Luimula, P., Miettinen, A., and Kerjaschki, D. (1999) Nephritin localizes at the podocyte filtration slit area and is characteristically spliced in the human kidney. *Am J Pathol* **155**, 1681-1687
310. Ruotsalainen, V., Ljungberg, P., Wartiovaara, J., Lenkkeri, U., Kestila, M., Jalanko, H., Holmberg, C., and Tryggvason, K. (1999) Nephritin is specifically located at the slit diaphragm of glomerular podocytes. *Proc Natl Acad Sci U S A* **96**, 7962-7967
311. Kestila, M., Lenkkeri, U., Mannikko, M., Lamerdin, J., McCready, P., Putaala, H., Ruotsalainen, V., Morita, T., Nissinen, M., Herva, R., Kashtan, C. E., Peltonen, L., Holmberg, C., Olsen, A., and Tryggvason, K. (1998) Positionally cloned gene for a novel

- glomerular protein--nephrin--is mutated in congenital nephrotic syndrome. *Molecular cell* **1**, 575-582
312. Tryggvason, K. (1999) Unraveling the mechanisms of glomerular ultrafiltration: nephrin, a key component of the slit diaphragm. *J Am Soc Nephrol* **10**, 2440-2445
313. Ahvenainen, E. K., Hallman, N., and Hjelt, L. (1956) Nephrotic syndrome in newborn and young infants. *Ann Paediatr Fenn* **2**, 227-241
314. Hallman, N., Norio, R., and Rapola, J. (1973) Congenital nephrotic syndrome. *Nephron* **11**, 101-110
315. Huttunen, N. P., Hallman, N., and Rapola, J. (1976) Glomerular basement membrane antigens in congenital and acquired nephrotic syndrome in childhood. *Nephron* **16**, 401-414
316. Tryggvason, K., and Kouvalainen, K. (1975) Number of nephrons in normal human kidneys and kidneys of patients with the congenital nephrotic syndrome. A study using a sieving method for counting of glomeruli. *Nephron* **15**, 62-68
317. Tryggvason, K. (1978) Morphometric studies on glomeruli in the congenital nephrotic syndrome. *Nephron* **22**, 544-550
318. Autio-Harmainen, H., and Rapola, J. (1981) Renal pathology of fetuses with congenital nephrotic syndrome of the Finnish type. A qualitative and quantitative light microscopic study. *Nephron* **29**, 158-163
319. Rapola, J. (1981) Renal pathology of fetal congenital nephrosis. *Acta pathologica et microbiologica Scandinavica. Section A, Pathology* **89**, 63-64
320. Patrakka, J., Kestila, M., Wartiovaara, J., Ruotsalainen, V., Tissari, P., Lenkkeri, U., Mannikko, M., Visapaa, I., Holmberg, C., Rapola, J., Tryggvason, K., and Jalanko, H.

- (2000) Congenital nephrotic syndrome (NPHS1): features resulting from different mutations in Finnish patients. *Kidney Int* **58**, 972-980
321. Ruotsalainen, V., Patrakka, J., Tissari, P., Reponen, P., Hess, M., Kestila, M., Holmberg, C., Salonen, R., Heikinheimo, M., Wartiovaara, J., Tryggvason, K., and Jalanko, H. (2000) Role of nephrin in cell junction formation in human nephrogenesis. *Am J Pathol* **157**, 1905-1916
322. Lahdenkari, A. T., Lounatmaa, K., Patrakka, J., Holmberg, C., Wartiovaara, J., Kestila, M., Koskimies, O., and Jalanko, H. (2004) Podocytes are firmly attached to glomerular basement membrane in kidneys with heavy proteinuria. *J Am Soc Nephrol* **15**, 2611-2618
323. Putaala, H., Soinen, R., Kilpelainen, P., Wartiovaara, J., and Tryggvason, K. (2001) The murine nephrin gene is specifically expressed in kidney, brain and pancreas: inactivation of the gene leads to massive proteinuria and neonatal death. *Human molecular genetics* **10**, 1-8
324. Rantanen, M., Palmen, T., Patari, A., Ahola, H., Lehtonen, S., Astrom, E., Floss, T., Vauti, F., Wurst, W., Ruiz, P., Kerjaschki, D., and Holthofer, H. (2002) Nephrin TRAP mice lack slit diaphragms and show fibrotic glomeruli and cystic tubular lesions. *J Am Soc Nephrol* **13**, 1586-1594
325. Jones, N., Blasutig, I. M., Eremina, V., Ruston, J. M., Bladt, F., Li, H., Huang, H., Larose, L., Li, S. S., Takano, T., Quaggin, S. E., and Pawson, T. (2006) Nck adaptor proteins link nephrin to the actin cytoskeleton of kidney podocytes. *Nature* **440**, 818-823
326. Verma, R., Wharram, B., Kovari, I., Kunkel, R., Nihalani, D., Wary, K. K., Wiggins, R. C., Killen, P., and Holzman, L. B. (2003) Fyn binds to and phosphorylates the kidney slit diaphragm component Nephrin. *J Biol Chem* **278**, 20716-20723

327. Harita, Y., Kurihara, H., Kosako, H., Tezuka, T., Sekine, T., Igarashi, T., Ohsawa, I., Ohta, S., and Hattori, S. (2009) Phosphorylation of Nephrin Triggers Ca²⁺ Signaling by Recruitment and Activation of Phospholipase C- γ 1. *J Biol Chem* **284**, 8951-8962
328. Qin, X. S., Tsukaguchi, H., Shono, A., Yamamoto, A., Kurihara, H., and Doi, T. (2009) Phosphorylation of nephrin triggers its internalization by raft-mediated endocytosis. *J Am Soc Nephrol* **20**, 2534-2545
329. Boute, N., Gribouval, O., Roselli, S., Benessy, F., Lee, H., Fuchshuber, A., Dahan, K., Gubler, M. C., Niaudet, P., and Antignac, C. (2000) NPHS2, encoding the glomerular protein podocin, is mutated in autosomal recessive steroid-resistant nephrotic syndrome. *Nat Genet* **24**, 349-354
330. Roselli, S., Gribouval, O., Boute, N., Sich, M., Benessy, F., Attie, T., Gubler, M. C., and Antignac, C. (2002) Podocin localizes in the kidney to the slit diaphragm area. *Am J Pathol* **160**, 131-139
331. Roselli, S., Heidet, L., Sich, M., Henger, A., Kretzler, M., Gubler, M. C., and Antignac, C. (2004) Early glomerular filtration defect and severe renal disease in podocin-deficient mice. *Molecular and cellular biology* **24**, 550-560
332. Liu, G., Kaw, B., Kurfis, J., Rahmanuddin, S., Kanwar, Y. S., and Chugh, S. S. (2003) Nephrin and nephrin interaction in the slit diaphragm is an important determinant of glomerular permeability. *J Clin Invest* **112**, 209-221
333. Neumann-Haefelin, E., Kramer-Zucker, A., Slanchev, K., Hartleben, B., Noutsou, F., Martin, K., Wanner, N., Ritter, A., Godel, M., Pagel, P., Fu, X., Muller, A., Baumeister, R., Walz, G., and Huber, T. B. (2010) A model organism approach: defining the role of

- Neph proteins as regulators of neuron and kidney morphogenesis. *Human molecular genetics* **19**, 2347-2359
334. Wang, H., Lehtonen, S., Chen, Y. C., Heikkila, E., Panula, P., and Holthofer, H. (2012) Neph3 associates with regulation of glomerular and neural development in zebrafish. *Differentiation* **83**, 38-46
335. Ihalmo, P., Palmén, T., Ahola, H., Valtonen, E., and Holthofer, H. (2003) Filtrin is a novel member of nephrin-like proteins. *Biochem Biophys Res Commun* **300**, 364-370
336. Sellin, L., Huber, T. B., Gerke, P., Quack, I., Pavenstadt, H., and Walz, G. (2003) NEPH1 defines a novel family of podocin interacting proteins. *FASEB J* **17**, 115-117
337. Barletta, G. M., Kovari, I. A., Verma, R. K., Kerjaschki, D., and Holzman, L. B. (2003) Nephrin and Neph1 co-localize at the podocyte foot process intercellular junction and form cis hetero-oligomers. *J Biol Chem* **278**, 19266-19271
338. Gerke, P., Sellin, L., Kretz, O., Petraschka, D., Zentgraf, H., Benzing, T., and Walz, G. (2005) NEPH2 is located at the glomerular slit diaphragm, interacts with nephrin and is cleaved from podocytes by metalloproteinases. *J Am Soc Nephrol* **16**, 1693-1702
339. Ihalmo, P., Schmid, H., Rastaldi, M. P., Mattinzoli, D., Langham, R. G., Luimula, P., Kilpikari, R., Lassila, M., Gilbert, R. E., Kerjaschki, D., Kretzler, M., and Holthofer, H. (2007) Expression of filtrin in human glomerular diseases. *Nephrol Dial Transplant* **22**, 1903-1909
340. Yaoita, E., Kurihara, H., Yoshida, Y., Inoue, T., Matsuki, A., Sakai, T., and Yamamoto, T. (2005) Role of Fat1 in cell-cell contact formation of podocytes in puromycin aminonucleoside nephrosis and neonatal kidney. *Kidney Int* **68**, 542-551

341. Ciani, L., Patel, A., Allen, N. D., and French-Constant, C. (2003) Mice lacking the giant protocadherin mFAT1 exhibit renal slit junction abnormalities and a partially penetrant cyclopia and anophthalmia phenotype. *Molecular and cellular biology* **23**, 3575-3582
342. Inoue, T., Yaoita, E., Kurihara, H., Shimizu, F., Sakai, T., Kobayashi, T., Ohshiro, K., Kawachi, H., Okada, H., Suzuki, H., Kihara, I., and Yamamoto, T. (2001) FAT is a component of glomerular slit diaphragms. *Kidney Int* **59**, 1003-1012
343. Stevenson, B. R., Siliciano, J. D., Mooseker, M. S., and Goodenough, D. A. (1986) Identification of ZO-1: a high molecular weight polypeptide associated with the tight junction (zonula occludens) in a variety of epithelia. *J Cell Biol* **103**, 755-766
344. Fanning, A. S., Ma, T. Y., and Anderson, J. M. (2002) Isolation and functional characterization of the actin binding region in the tight junction protein ZO-1. *FASEB J* **16**, 1835-1837
345. Huber, T. B., Schmidts, M., Gerke, P., Schermer, B., Zahn, A., Hartleben, B., Sellin, L., Walz, G., and Benzing, T. (2003) The carboxyl terminus of Neph family members binds to the PDZ domain protein zonula occludens-1. *J Biol Chem* **278**, 13417-13421
346. Reiser, J., Kriz, W., Kretzler, M., and Mundel, P. (2000) The glomerular slit diaphragm is a modified adherens junction. *Journal of the American Society of Nephrology : JASN* **11**, 1-8
347. Radice, G. L., Ferreira-Cornwell, M. C., Robinson, S. D., Rayburn, H., Chodosh, L. A., Takeichi, M., and Hynes, R. O. (1997) Precocious mammary gland development in P-cadherin-deficient mice. *J Cell Biol* **139**, 1025-1032
348. Dustin, M. L., Olszowy, M. W., Holdorf, A. D., Li, J., Bromley, S., Desai, N., Widder, P., Rosenberger, F., van der Merwe, P. A., Allen, P. M., and Shaw, A. S. (1998) A novel

- adaptor protein orchestrates receptor patterning and cytoskeletal polarity in T-cell contacts. *Cell* **94**, 667-677
349. Lehtonen, S., Ora, A., Olkkonen, V. M., Geng, L., Zerial, M., Somlo, S., and Lehtonen, E. (2000) In vivo interaction of the adapter protein CD2-associated protein with the type 2 polycystic kidney disease protein, polycystin-2. *J Biol Chem* **275**, 32888-32893
350. Shih, N. Y., Li, J., Cotran, R., Mundel, P., Miner, J. H., and Shaw, A. S. (2001) CD2AP localizes to the slit diaphragm and binds to nephrin via a novel C-terminal domain. *Am J Pathol* **159**, 2303-2308
351. Saleem, M. A., Ni, L., Witherden, I., Tryggvason, K., Ruotsalainen, V., Mundel, P., and Mathieson, P. W. (2002) Co-localization of nephrin, podocin, and the actin cytoskeleton: evidence for a role in podocyte foot process formation. *Am J Pathol* **161**, 1459-1466
352. Kim, J. M., Wu, H., Green, G., Winkler, C. A., Kopp, J. B., Miner, J. H., Unanue, E. R., and Shaw, A. S. (2003) CD2-associated protein haploinsufficiency is linked to glomerular disease susceptibility. *Science* **300**, 1298-1300
353. Huber, T. B., Hartleben, B., Kim, J., Schmidts, M., Schermer, B., Keil, A., Egger, L., Lecha, R. L., Borner, C., Pavenstadt, H., Shaw, A. S., Walz, G., and Benzing, T. (2003) Nephrin and CD2AP associate with phosphoinositide 3-OH kinase and stimulate AKT-dependent signaling. *Molecular and cellular biology* **23**, 4917-4928
354. Li, C., Ruotsalainen, V., Tryggvason, K., Shaw, A. S., and Miner, J. H. (2000) CD2AP is expressed with nephrin in developing podocytes and is found widely in mature kidney and elsewhere. *Am J Physiol Renal Physiol* **279**, F785-792
355. Somlo, S., and Mundel, P. (2000) Getting a foothold in nephrotic syndrome. *Nature genetics* **24**, 333-335

356. Dekan, G., Gabel, C., and Farquhar, M. G. (1991) Sulfate contributes to the negative charge of podocalyxin, the major sialoglycoprotein of the glomerular filtration slits. *Proc Natl Acad Sci U S A* **88**, 5398-5402
357. Takeda, T., Go, W. Y., Orlando, R. A., and Farquhar, M. G. (2000) Expression of podocalyxin inhibits cell-cell adhesion and modifies junctional properties in Madin-Darby canine kidney cells. *Mol Biol Cell* **11**, 3219-3232
358. Miettinen, A., Dekan, G., and Farquhar, M. G. (1990) Monoclonal antibodies against membrane proteins of the rat glomerulus. Immunochemical specificity and immunofluorescence distribution of the antigens. *Am J Pathol* **137**, 929-944
359. Schmieder, S., Nagai, M., Orlando, R. A., Takeda, T., and Farquhar, M. G. (2004) Podocalyxin activates RhoA and induces actin reorganization through NHERF1 and Ezrin in MDCK cells. *Journal of the American Society of Nephrology : JASN* **15**, 2289-2298
360. Takeda, T., McQuistan, T., Orlando, R. A., and Farquhar, M. G. (2001) Loss of glomerular foot processes is associated with uncoupling of podocalyxin from the actin cytoskeleton. *The Journal of clinical investigation* **108**, 289-301
361. Doyonnas, R., Kershaw, D. B., Duhme, C., Merkens, H., Chelliah, S., Graf, T., and McNagny, K. M. (2001) Anuria, omphalocele, and perinatal lethality in mice lacking the CD34-related protein podocalyxin. *The Journal of experimental medicine* **194**, 13-27
362. Pavenstadt, H., Kriz, W., and Kretzler, M. (2003) Cell biology of the glomerular podocyte. *Physiological reviews* **83**, 253-307

363. Smoyer, W. E., Mundel, P., Gupta, A., and Welsh, M. J. (1997) Podocyte alpha-actinin induction precedes foot process effacement in experimental nephrotic syndrome. *Am J Physiol* **273**, F150-157
364. Honda, K., Yamada, T., Endo, R., Ino, Y., Gotoh, M., Tsuda, H., Yamada, Y., Chiba, H., and Hirohashi, S. (1998) Actinin-4, a novel actin-bundling protein associated with cell motility and cancer invasion. *J Cell Biol* **140**, 1383-1393
365. Kos, C. H., Le, T. C., Sinha, S., Henderson, J. M., Kim, S. H., Sugimoto, H., Kalluri, R., Gerszten, R. E., and Pollak, M. R. (2003) Mice deficient in alpha-actinin-4 have severe glomerular disease. *J Clin Invest* **111**, 1683-1690
366. Mundel, P., Heid, H. W., Mundel, T. M., Kruger, M., Reiser, J., and Kriz, W. (1997) Synaptopodin: an actin-associated protein in telencephalic dendrites and renal podocytes. *J Cell Biol* **139**, 193-204
367. Asanuma, K., Yanagida-Asanuma, E., Faul, C., Tomino, Y., Kim, K., and Mundel, P. (2006) Synaptopodin orchestrates actin organization and cell motility via regulation of RhoA signalling. *Nat Cell Biol* **8**, 485-491
368. Asanuma, K., Kim, K., Oh, J., Giardino, L., Chabanis, S., Faul, C., Reiser, J., and Mundel, P. (2005) Synaptopodin regulates the actin-bundling activity of alpha-actinin in an isoform-specific manner. *J Clin Invest* **115**, 1188-1198
369. Faul, C., Donnelly, M., Merscher-Gomez, S., Chang, Y. H., Franz, S., Delfgaauw, J., Chang, J. M., Choi, H. Y., Campbell, K. N., Kim, K., Reiser, J., and Mundel, P. (2008) The actin cytoskeleton of kidney podocytes is a direct target of the antiproteinuric effect of cyclosporine A. *Nat Med* **14**, 931-938

370. Rops, A. L., van der Vlag, J., Jacobs, C. W., Dijkman, H. B., Lensen, J. F., Wijnhoven, T. J., van den Heuvel, L. P., van Kuppevelt, T. H., and Berden, J. H. (2004) Isolation and characterization of conditionally immortalized mouse glomerular endothelial cell lines. *Kidney international* **66**, 2193-2201
371. Bonilha, V. L., Rayborn, M. E., Saotome, I., McClatchey, A. I., and Hollyfield, J. G. (2006) Microvilli defects in retinas of ezrin knockout mice. *Experimental eye research* **82**, 720-729
372. Erwig, L. P., McPhillips, K. A., Wynes, M. W., Ivetic, A., Ridley, A. J., and Henson, P. M. (2006) Differential regulation of phagosome maturation in macrophages and dendritic cells mediated by Rho GTPases and ezrin-radixin-moesin (ERM) proteins. *Proceedings of the National Academy of Sciences of the United States of America* **103**, 12825-12830
373. Grune, T., Reinheckel, T., North, J. A., Li, R., Bescos, P. B., Shringarpure, R., and Davies, K. J. (2002) Ezrin turnover and cell shape changes catalyzed by proteasome in oxidatively stressed cells. *FASEB journal : official publication of the Federation of American Societies for Experimental Biology* **16**, 1602-1610
374. Ivetic, A., and Ridley, A. J. (2004) Ezrin/radixin/moesin proteins and Rho GTPase signalling in leucocytes. *Immunology* **112**, 165-176
375. Csontos, C., Czikora, I., Bogatcheva, N. V., Adyshev, D. M., Poirier, C., Olah, G., and Verin, A. D. (2008) TIMAP is a positive regulator of pulmonary endothelial barrier function. *Am J Physiol Lung Cell Mol Physiol* **295**, L440-450
376. Barreiro, O., Yanez-Mo, M., Serrador, J. M., Montoya, M. C., Vicente-Manzanares, M., Tejedor, R., Furthmayr, H., and Sanchez-Madrid, F. (2002) Dynamic interaction of

- VCAM-1 and ICAM-1 with moesin and ezrin in a novel endothelial docking structure for adherent leukocytes. *J Cell Biol* **157**, 1233-1245
377. Ulmasov, B., Bruno, J., Gordon, N., Hartnett, M. E., and Edwards, J. C. (2009) Chloride intracellular channel protein-4 functions in angiogenesis by supporting acidification of vacuoles along the intracellular tubulogenic pathway. *The American journal of pathology* **174**, 1084-1096
378. Tung, J. J., and Kitajewski, J. (2010) Chloride intracellular channel 1 functions in endothelial cell growth and migration. *Journal of angiogenesis research* **2**, 23
379. Chalothorn, D., Zhang, H., Smith, J. E., Edwards, J. C., and Faber, J. E. (2009) Chloride intracellular channel-4 is a determinant of native collateral formation in skeletal muscle and brain. *Circ Res* **105**, 89-98
380. Sengoelge, G., Luo, W., Fine, D., Perschl, A. M., Fierlbeck, W., Haririan, A., Sorensson, J., Rehman, T. U., Hauser, P., Trevick, J. S., Kulak, S. C., Wegner, B., and Ballermann, B. J. (2005) A SAGE-based comparison between glomerular and aortic endothelial cells. *Am J Physiol Renal Physiol* **288**, F1290-1300
381. Zhu, L., Liu, Y., and Forte, J. G. (2005) Ezrin oligomers are the membrane-bound dormant form in gastric parietal cells. *American journal of physiology. Cell physiology* **288**, C1242-1254
382. Zhu, L., Zhou, R., Mettler, S., Wu, T., Abbas, A., Delaney, J., and Forte, J. G. (2007) High turnover of ezrin T567 phosphorylation: conformation, activity, and cellular function. *American journal of physiology. Cell physiology* **293**, C874-884

383. Nakamura, F., Amieva, M. R., and Furthmayr, H. (1995) Phosphorylation of threonine 558 in the carboxyl-terminal actin-binding domain of moesin by thrombin activation of human platelets. *The Journal of biological chemistry* **270**, 31377-31385
384. Huang, L., Wong, T. Y., Lin, R. C., and Furthmayr, H. (1999) Replacement of threonine 558, a critical site of phosphorylation of moesin in vivo, with aspartate activates F-actin binding of moesin. Regulation by conformational change. *The Journal of biological chemistry* **274**, 12803-12810
385. Yonemura, S., Tsukita, S., and Tsukita, S. (1999) Direct involvement of ezrin/radixin/moesin (ERM)-binding membrane proteins in the organization of microvilli in collaboration with activated ERM proteins. *J Cell Biol* **145**, 1497-1509
386. Zhu, L., Hatakeyama, J., Chen, C., Shastri, A., Poon, K., and Forte, J. G. (2008) Comparative study of ezrin phosphorylation among different tissues: more is good; too much is bad. *American journal of physiology. Cell physiology* **295**, C192-202
387. Condeelis, J., Hall, A., Bresnick, A., Warren, V., Hock, R., Bennett, H., and Ogihara, S. (1988) Actin polymerization and pseudopod extension during amoeboid chemotaxis. *Cell motility and the cytoskeleton* **10**, 77-90
388. Mitchison, T. J., and Cramer, L. P. (1996) Actin-based cell motility and cell locomotion. *Cell* **84**, 371-379
389. Small, J. V., Herzog, M., and Anderson, K. (1995) Actin filament organization in the fish keratocyte lamellipodium. *The Journal of cell biology* **129**, 1275-1286
390. Pollard, T. D., and Cooper, J. A. (1986) Actin and actin-binding proteins. A critical evaluation of mechanisms and functions. *Annual review of biochemistry* **55**, 987-1035

391. Carlier, M. F. (1998) Control of actin dynamics. *Current opinion in cell biology* **10**, 45-51
392. Vandekerckhove, J., and Vancompernelle, K. (1992) Structural relationships of actin-binding proteins. *Current opinion in cell biology* **4**, 36-42
393. Bretscher, A. (1999) Regulation of cortical structure by the ezrin-radixin-moesin protein family. *Curr Opin Cell Biol* **11**, 109-116
394. Mangeat, P., Roy, C., and Martin, M. (1999) ERM proteins in cell adhesion and membrane dynamics: Authors' correction. *Trends in cell biology* **9**, 289
395. Marion, S., Hoffmann, E., Holzer, D., Le Clainche, C., Martin, M., Sachse, M., Ganeva, I., Mangeat, P., and Griffiths, G. (2011) Ezrin promotes actin assembly at the phagosome membrane and regulates phago-lysosomal fusion. *Traffic* **12**, 421-437
396. Desjardins, M., Celis, J. E., van Meer, G., Dieplinger, H., Jahraus, A., Griffiths, G., and Huber, L. A. (1994) Molecular characterization of phagosomes. *The Journal of biological chemistry* **269**, 32194-32200
397. Yao, X., Cheng, L., and Forte, J. G. (1996) Biochemical characterization of ezrin-actin interaction. *The Journal of biological chemistry* **271**, 7224-7229
398. Defacque, H., Egeberg, M., Habermann, A., Diakonova, M., Roy, C., Mangeat, P., Voelter, W., Marriott, G., Pfannstiel, J., Faulstich, H., and Griffiths, G. (2000) Involvement of ezrin/moesin in de novo actin assembly on phagosomal membranes. *The EMBO journal* **19**, 199-212
399. Berryman, M., Gary, R., and Bretscher, A. (1995) Ezrin oligomers are major cytoskeletal components of placental microvilli: a proposal for their involvement in cortical morphogenesis. *J Cell Biol* **131**, 1231-1242

400. Roch, F., Polesello, C., Roubinet, C., Martin, M., Roy, C., Valenti, P., Carreno, S., Mangeat, P., and Payre, F. (2010) Differential roles of PtdIns(4,5)P₂ and phosphorylation in moesin activation during *Drosophila* development. *Journal of cell science* **123**, 2058-2067
401. Newton, A. C. (1995) Protein kinase C: structure, function, and regulation. *The Journal of biological chemistry* **270**, 28495-28498
402. Yeung, T., Terebiznik, M., Yu, L., Silvius, J., Abidi, W. M., Philips, M., Levine, T., Kapus, A., and Grinstein, S. (2006) Receptor activation alters inner surface potential during phagocytosis. *Science* **313**, 347-351
403. Niggli, V. (2001) Structural properties of lipid-binding sites in cytoskeletal proteins. *Trends Biochem Sci* **26**, 604-611
404. Divecha, N. (2010) Lipid kinases: charging PtdIns(4,5)P₂ synthesis. *Curr Biol* **20**, R154-157
405. Fairn, G. D., Ogata, K., Botelho, R. J., Stahl, P. D., Anderson, R. A., De Camilli, P., Meyer, T., Wodak, S., and Grinstein, S. (2009) An electrostatic switch displaces phosphatidylinositol phosphate kinases from the membrane during phagocytosis. *J Cell Biol* **187**, 701-714
406. Newton, A. C. (2003) Regulation of the ABC kinases by phosphorylation: protein kinase C as a paradigm. *Biochem J* **370**, 361-371
407. Parekh, D. B., Ziegler, W., and Parker, P. J. (2000) Multiple pathways control protein kinase C phosphorylation. *EMBO J* **19**, 496-503
408. Littler, D. R., Harrop, S. J., Fairlie, W. D., Brown, L. J., Pankhurst, G. J., Pankhurst, S., DeMaere, M. Z., Campbell, T. J., Bauskin, A. R., Tonini, R., Mazzanti, M., Breit, S. N.,

- and Curmi, P. M. (2004) The intracellular chloride ion channel protein CLIC1 undergoes a redox-controlled structural transition. *J Biol Chem* **279**, 9298-9305
409. Goodchild, S. C., Howell, M. W., Cordina, N. M., Littler, D. R., Breit, S. N., Curmi, P. M., and Brown, L. J. (2009) Oxidation promotes insertion of the CLIC1 chloride intracellular channel into the membrane. *Eur Biophys J*
410. Valenzuela, S. M., Alkhamici, H., Brown, L. J., Almond, O. C., Goodchild, S. C., Carne, S., Curmi, P. M., Holt, S. A., and Cornell, B. A. (2013) Regulation of the membrane insertion and conductance activity of the metamorphic chloride intracellular channel protein CLIC1 by cholesterol. *PLoS One* **8**, e56948
411. Landry, D., Sullivan, S., Nicolaides, M., Redhead, C., Edelman, A., Field, M., al-Awqati, Q., and Edwards, J. (1993) Molecular cloning and characterization of p64, a chloride channel protein from kidney microsomes. *J Biol Chem* **268**, 14948-14955
412. Kunz, J., Wilson, M. P., Kisseleva, M., Hurley, J. H., Majerus, P. W., and Anderson, R. A. (2000) The activation loop of phosphatidylinositol phosphate kinases determines signaling specificity. *Molecular cell* **5**, 1-11
413. Burden, L. M., Rao, V. D., Murray, D., Ghirlando, R., Doughman, S. D., Anderson, R. A., and Hurley, J. H. (1999) The flattened face of type II beta phosphatidylinositol phosphate kinase binds acidic phospholipid membranes. *Biochemistry* **38**, 15141-15149
414. Cromer, B. A., Gorman, M. A., Hansen, G., Adams, J. J., Coggan, M., Littler, D. R., Brown, L. J., Mazzanti, M., Breit, S. N., Curmi, P. M., Dulhunty, A. F., Board, P. G., and Parker, M. W. (2007) Structure of the Janus protein human CLIC2. *J Mol Biol* **374**, 719-731

415. Littler, D. R., Brown, L. J., Breit, S. N., Perrakis, A., and Curmi, P. M. (2010) Structure of human CLIC3 at 2 Å resolution. *Proteins* **78**, 1594-1600
416. Rameh, L. E., Toliás, K. F., Duckworth, B. C., and Cantley, L. C. (1997) A new pathway for synthesis of phosphatidylinositol-4,5-bisphosphate. *Nature* **390**, 192-196
417. Peter, B., Ngubane, N. C., Fanucchi, S., and Dirr, H. W. (2013) Membrane mimetics induce helix formation and oligomerization of the chloride intracellular channel protein 1 transmembrane domain. *Biochemistry* **52**, 2739-2749
418. Jiang, L., Phang, J. M., Yu, J., Harrop, S. J., Sokolova, A. V., Duff, A. P., Wilk, K. E., Alkhamici, H., Breit, S. N., Valenzuela, S. M., Brown, L. J., and Curmi, P. M. (2013) CLIC proteins, ezrin, radixin, moesin and the coupling of membranes to the actin cytoskeleton: A smoking gun? *Biochim Biophys Acta*
419. Goodchild, S. C., Angstrom, C. N., Breit, S. N., Curmi, P. M., and Brown, L. J. (2011) Transmembrane extension and oligomerization of the CLIC1 chloride intracellular channel protein upon membrane interaction. *Biochemistry* **50**, 10887-10897
420. Littler, D. R., Harrop, S. J., Goodchild, S. C., Phang, J. M., Mynott, A. V., Jiang, L., Valenzuela, S. M., Mazzanti, M., Brown, L. J., Breit, S. N., and Curmi, P. M. (2010) The enigma of the CLIC proteins: Ion channels, redox proteins, enzymes, scaffolding proteins? *FEBS Lett* **584**, 2093-2101
421. Koss, M., Pfeiffer, G. R., 2nd, Wang, Y., Thomas, S. T., Yerukhimovich, M., Gaarde, W. A., Doerschuk, C. M., and Wang, Q. (2006) Ezrin/radixin/moesin proteins are phosphorylated by TNF- α and modulate permeability increases in human pulmonary microvascular endothelial cells. *J Immunol* **176**, 1218-1227

422. Payraastre, B., Nievers, M., Boonstra, J., Breton, M., Verkleij, A. J., and Van Bergen en Henegouwen, P. M. (1992) A differential location of phosphoinositide kinases, diacylglycerol kinase, and phospholipase C in the nuclear matrix. *The Journal of biological chemistry* **267**, 5078-5084
423. Boronenkov, I. V., Loijens, J. C., Umeda, M., and Anderson, R. A. (1998) Phosphoinositide signaling pathways in nuclei are associated with nuclear speckles containing pre-mRNA processing factors. *Molecular biology of the cell* **9**, 3547-3560
424. Mundel, P., and Shankland, S. J. (2002) Podocyte biology and response to injury. *Journal of the American Society of Nephrology : JASN* **13**, 3005-3015
425. Asanuma, K., and Mundel, P. (2003) The role of podocytes in glomerular pathobiology. *Clinical and experimental nephrology* **7**, 255-259
426. Faul, C., Asanuma, K., Yanagida-Asanuma, E., Kim, K., and Mundel, P. (2007) Actin up: regulation of podocyte structure and function by components of the actin cytoskeleton. *Trends in cell biology* **17**, 428-437
427. Goldberg, S., Harvey, S. J., Cunningham, J., Tryggvason, K., and Miner, J. H. (2009) Glomerular filtration is normal in the absence of both agrin and perlecan-heparan sulfate from the glomerular basement membrane. *Nephrology, dialysis, transplantation : official publication of the European Dialysis and Transplant Association - European Renal Association* **24**, 2044-2051
428. Utriainen, A., Sormunen, R., Kettunen, M., Carvalhaes, L. S., Sajanti, E., Eklund, L., Kauppinen, R., Kitten, G. T., and Pihlajaniemi, T. (2004) Structurally altered basement membranes and hydrocephalus in a type XVIII collagen deficient mouse line. *Human molecular genetics* **13**, 2089-2099

429. Satchell, S. C., and Tooke, J. E. (2008) What is the mechanism of microalbuminuria in diabetes: a role for the glomerular endothelium? *Diabetologia* **51**, 714-725
430. Kanwar, Y. S., Linker, A., and Farquhar, M. G. (1980) Increased permeability of the glomerular basement membrane to ferritin after removal of glycosaminoglycans (heparan sulfate) by enzyme digestion. *The Journal of cell biology* **86**, 688-693
431. Miner, J. H. (2012) The glomerular basement membrane. *Experimental cell research* **318**, 973-978
432. Zenker, M., Aigner, T., Wendler, O., Tralau, T., Muntefering, H., Fenski, R., Pitz, S., Schumacher, V., Royer-Pokora, B., Wuhl, E., Cochat, P., Bouvier, R., Kraus, C., Mark, K., Madlon, H., Dotsch, J., Rascher, W., Maruniak-Chudek, I., Lennert, T., Neumann, L. M., and Reis, A. (2004) Human laminin beta2 deficiency causes congenital nephrosis with mesangial sclerosis and distinct eye abnormalities. *Human molecular genetics* **13**, 2625-2632
433. Deen, W. M. (2004) What determines glomerular capillary permeability? *The Journal of clinical investigation* **114**, 1412-1414
434. Chen, Y. M., Zhou, Y., Go, G., Marmorstein, J. T., Kikkawa, Y., and Miner, J. H. (2013) Laminin beta2 gene missense mutation produces endoplasmic reticulum stress in podocytes. *Journal of the American Society of Nephrology : JASN* **24**, 1223-1233
435. Mundel, P., and Kriz, W. (1995) Structure and function of podocytes: an update. *Anatomy and embryology* **192**, 385-397
436. Kerjaschki, D. (2001) Caught flat-footed: podocyte damage and the molecular bases of focal glomerulosclerosis. *The Journal of clinical investigation* **108**, 1583-1587

437. Oh, J., Reiser, J., and Mundel, P. (2004) Dynamic (re)organization of the podocyte actin cytoskeleton in the nephrotic syndrome. *Pediatric nephrology* **19**, 130-137
438. Welsh, G. I., and Saleem, M. A. (2012) The podocyte cytoskeleton--key to a functioning glomerulus in health and disease. *Nature reviews. Nephrology* **8**, 14-21
439. Nystrom, J., Fierlbeck, W., Granqvist, A., Kulak, S. C., and Ballermann, B. J. (2009) A human glomerular SAGE transcriptome database. *BMC nephrology* **10**, 13
440. Chabardes-Garonne, D., Mejean, A., Aude, J. C., Cheval, L., Di Stefano, A., Gaillard, M. C., Imbert-Teboul, M., Wittner, M., Balian, C., Anthouard, V., Robert, C., Segurens, B., Wincker, P., Weissenbach, J., Doucet, A., and Elalouf, J. M. (2003) A panoramic view of gene expression in the human kidney. *Proceedings of the National Academy of Sciences of the United States of America* **100**, 13710-13715
441. He, L., Sun, Y., Patrakka, J., Mostad, P., Norlin, J., Xiao, Z., Andrae, J., Tryggvason, K., Samuelsson, T., Betsholtz, C., and Takemoto, M. (2007) Glomerulus-specific mRNA transcripts and proteins identified through kidney expressed sequence tag database analysis. *Kidney international* **71**, 889-900
442. Orlando, R. A., Takeda, T., Zak, B., Schmieder, S., Benoit, V. M., McQuistan, T., Furthmayr, H., and Farquhar, M. G. (2001) The glomerular epithelial cell anti-adhesin podocalyxin associates with the actin cytoskeleton through interactions with ezrin. *Journal of the American Society of Nephrology : JASN* **12**, 1589-1598
443. Fukasawa, H., Obayashi, H., Schmieder, S., Lee, J., Ghosh, P., and Farquhar, M. G. (2011) Phosphorylation of podocalyxin (Ser415) Prevents RhoA and ezrin activation and disrupts its interaction with the actin cytoskeleton. *The American journal of pathology* **179**, 2254-2265

444. Okuda, S., Oh, Y., Tsuruda, H., Onoyama, K., Fujimi, S., and Fujishima, M. (1986) Adriamycin-induced nephropathy as a model of chronic progressive glomerular disease. *Kidney international* **29**, 502-510
445. Wang, Y., Wang, Y. P., Tay, Y. C., and Harris, D. C. (2000) Progressive adriamycin nephropathy in mice: sequence of histologic and immunohistochemical events. *Kidney international* **58**, 1797-1804
446. Hugo, C., Nangaku, M., Shankland, S. J., Pichler, R., Gordon, K., Amieva, M. R., Couser, W. G., Furthmayr, H., and Johnson, R. J. (1998) The plasma membrane-actin linking protein, ezrin, is a glomerular epithelial cell marker in glomerulogenesis, in the adult kidney and in glomerular injury. *Kidney international* **54**, 1934-1944
447. Bonilha, V. L., Rayborn, M. E., Bhattacharya, S. K., Gu, X., Crabb, J. S., Crabb, J. W., and Hollyfield, J. G. (2006) The retinal pigment epithelium apical microvilli and retinal function. *Advances in experimental medicine and biology* **572**, 519-524
448. Morales, F. C., Takahashi, Y., Kreimann, E. L., and Georgescu, M. M. (2004) Ezrin-radixin-moesin (ERM)-binding phosphoprotein 50 organizes ERM proteins at the apical membrane of polarized epithelia. *Proceedings of the National Academy of Sciences of the United States of America* **101**, 17705-17710
449. Shearer, A. E., Hildebrand, M. S., Bromhead, C. J., Kahrizi, K., Webster, J. A., Azadeh, B., Kimberling, W. J., Anousheh, A., Nazeri, A., Stephan, D., Najmabadi, H., Smith, R. J., and Bahlo, M. (2009) A novel splice site mutation in the RDX gene causes DFNB24 hearing loss in an Iranian family. *American journal of medical genetics. Part A* **149A**, 555-558

450. Advani, A., Kelly, D. J., Advani, S. L., Cox, A. J., Thai, K., Zhang, Y., White, K. E., Gow, R. M., Marshall, S. M., Steer, B. M., Marsden, P. A., Rakoczy, P. E., and Gilbert, R. E. (2007) Role of VEGF in maintaining renal structure and function under normotensive and hypertensive conditions. *Proceedings of the National Academy of Sciences of the United States of America* **104**, 14448-14453
451. Sugimoto, H., Hamano, Y., Charytan, D., Cosgrove, D., Kieran, M., Sudhakar, A., and Kalluri, R. (2003) Neutralization of circulating vascular endothelial growth factor (VEGF) by anti-VEGF antibodies and soluble VEGF receptor 1 (sFlt-1) induces proteinuria. *The Journal of biological chemistry* **278**, 12605-12608
452. Eremina, V., Baelde, H. J., and Quaggin, S. E. (2007) Role of the VEGF--a signaling pathway in the glomerulus: evidence for crosstalk between components of the glomerular filtration barrier. *Nephron. Physiology* **106**, p32-37
453. Sengoelge, G., Luo, W., Fine, D., Perschl, A. M., Fierlbeck, W., Haririan, A., Sorensson, J., Rehman, T. U., Hauser, P., Trevick, J. S., Kulak, S. C., Wegner, B., and Ballermann, B. J. (2005) A SAGE-based comparison between glomerular and aortic endothelial cells. *American journal of physiology. Renal physiology* **288**, F1290-1300
454. Kahlfeldt, N., Vahedi-Faridi, A., Koo, S. J., Schafer, J. G., Krainer, G., Keller, S., Saenger, W., Krauss, M., and Haucke, V. (2010) Molecular basis for association of PIPKI gamma-p90 with clathrin adaptor AP-2. *J Biol Chem* **285**, 2734-2749
455. Kisseleva, M., Feng, Y., Ward, M., Song, C., Anderson, R. A., and Longmore, G. D. (2005) The LIM protein Ajuba regulates phosphatidylinositol 4,5-bisphosphate levels in migrating cells through an interaction with and activation of PIPKI alpha. *Mol Cell Biol* **25**, 3956-3966

456. Yang, J. Y., Jung, J. Y., Cho, S. W., Choi, H. J., Kim, S. W., Kim, S. Y., Kim, H. J., Jang, C. H., Lee, M. G., Han, J., and Shin, C. S. (2009) Chloride intracellular channel 1 regulates osteoblast differentiation. *Bone* **45**, 1175-1185
457. Berryman, M. A., and Goldenring, J. R. (2003) CLIC4 is enriched at cell-cell junctions and colocalizes with AKAP350 at the centrosome and midbody of cultured mammalian cells. *Cell Motil Cytoskeleton* **56**, 159-172
458. Shanks, R. A., Larocca, M. C., Berryman, M., Edwards, J. C., Urushidani, T., Navarre, J., and Goldenring, J. R. (2002) AKAP350 at the Golgi apparatus. II. Association of AKAP350 with a novel chloride intracellular channel (CLIC) family member. *J Biol Chem* **277**, 40973-40980
459. Malik, M., Jividen, K., Padmakumar, V. C., Cataisson, C., Li, L., Lee, J., Howard, O. M., and Yuspa, S. H. (2012) Inducible NOS-induced chloride intracellular channel 4 (CLIC4) nuclear translocation regulates macrophage deactivation. *Proc Natl Acad Sci U S A* **109**, 6130-6135
460. Malik, M., Shukla, A., Amin, P., Niedelman, W., Lee, J., Jividen, K., Phang, J. M., Ding, J., Suh, K. S., Curmi, P. M., and Yuspa, S. H. (2010) S-nitrosylation regulates nuclear translocation of chloride intracellular channel protein CLIC4. *J Biol Chem* **285**, 23818-23828
461. Ponsioen, B., van Zeijl, L., Langeslag, M., Berryman, M., Littler, D., Jalink, K., and Moolenaar, W. H. (2009) Spatiotemporal Regulation of Chloride Intracellular Channel protein CLIC4 by RhoA. *Mol Biol Cell*

462. Legg-E'silva, D., Achilonu, I., Fanucchi, S., Stoychev, S., Fernandes, M., and Dirr, H. W. (2012) Role of arginine 29 and glutamic acid 81 interactions in the conformational stability of human chloride intracellular channel 1. *Biochemistry* **51**, 7854-7862
463. Achilonu, I., Fanucchi, S., Cross, M., Fernandes, M., and Dirr, H. W. (2012) Role of individual histidines in the pH-dependent global stability of human chloride intracellular channel 1. *Biochemistry* **51**, 995-1004
464. Stoychev, S. H., Nathaniel, C., Fanucchi, S., Brock, M., Li, S., Asmus, K., Woods, V. L., Jr., and Dirr, H. W. (2009) Structural dynamics of soluble chloride intracellular channel protein CLIC1 examined by amide hydrogen-deuterium exchange mass spectrometry. *Biochemistry* **48**, 8413-8421
465. Fanucchi, S., Adamson, R. J., and Dirr, H. W. (2008) Formation of an unfolding intermediate state of soluble chloride intracellular channel protein CLIC1 at acidic pH. *Biochemistry* **47**, 11674-11681

Appendices

1. Predicted phosphorylation sites for CLIC5A.

Threonine predictions

Name	Pos	Context	Score	Pred
Sequence	2	---MTDSAT	0.155	.
Sequence	6	TDSATANGD	0.012	.
Sequence	52	VFNVTTVDL	0.200	.
Sequence	53	FNVTTVDLK	0.213	.
Sequence	70	LAPGTHPPF	0.263	.
Sequence	76	PPFLTFNGD	0.248	.
Sequence	83	GDVKTDVNK	0.050	.
Sequence	95	FLEETLTPE	0.322	.
Sequence	97	EETLTPEKY	0.879	*T*
Sequence	113	RESNTAGID	0.096	.
Sequence	129	YIKNTKQQN	0.076	.
Sequence	142	ERGLTKALK	0.546	*T*
Sequence	154	DYLNTPLE	0.797	*T*
Sequence	164	IDANTCGED	0.600	*T*
Sequence	182	GDELTLADC	0.184	.
Sequence	212	PAEMTGLWR	0.373	.
Sequence	228	RDEFTNTCA	0.048	.
Sequence	230	EFTNTCAAD	0.162	.

Tyrosine predictions

Name	Pos	Context	Score	Pred
Sequence	101	TPEKYPKLA	0.727	*Y*
Sequence	125	KFSAYIKNT	0.575	*Y*
Sequence	151	KLDDYLNTP	0.970	*Y*
Sequence	202	VAKKYRNYD	0.190	.
Sequence	205	KYRNYDIPA	0.119	.
Sequence	217	GLWRYLKNA	0.057	.
Sequence	222	LKNAYARDE	0.235	.
Sequence	241	IELAYADVA	0.970	*Y*

Predicted phosphorylation sites for CLIC5A. <http://www.cbs.dtu.dk/services/NetPhos/>

2. Ethics approval for animal use protocol



UNIVERSITY OF ALBERTA

ETHICS APPROVAL FOR ANIMAL USE PROTOCOL

THE ANIMAL CARE AND USE COMMITTEE: HEALTH SCIENCES

Has reviewed and approved the protocol application entitled:

GLOMERULAR ENDOTHELIAL CELL DEVELOPMENT & DIFFERENTIATION

Title

D 398/06/09

Category of Invasiveness Protocol Number

Submitted by:

Dr. Barbara Ballermann Dr. Valerie Luyckx

Name of Principal Investigator Co-Investigator(s)

And found the proposed protocol involving animals to meet the standards of the Canadian Council on Animal Care (CCAC), and the proposed facilities in which the animals will be housed and used to comply with the CCAC requirements.

Mouse 288

Rat 27

Species Number of Animals Approved

Signature of ACUC: Health Sciences Chair

July 1, 2008 – June 30, 2009

Start Date End Date

Recommended wording to accompany publications completed by Principal Investigators at the University of Alberta
All animal studies were conducted in accordance with the Canadian Council on Animal Care Guidelines and Policies with approval from the
Animal Care and Use Committee: Health Sciences for the University of Alberta.

Animal Care and Use Committee: Health Sciences

218 Campus Tower, 8625-112 Street, Edmonton, AB T6G 2E1 Canada • Phone: 780-492-5322 • Fax: 780-492-9429

3. Ethics approval for the use of human samples

Health Research Ethics Board

213 Heritage Medical Research Centre
University of Alberta, Edmonton, Alberta T6G 2S2
p.780.492.9724 (Biomedical Panel)
p.780.492.6302 (Health Panel)
p.780.492.0439
p.780.492.0839
t.780.492.7803

ETHICS APPROVAL FORM

Date: January 2008

Name(s) of Principal Investigator(s): Dr. Barbara Ballermann

Department: Medicine

Title: Identification of highly expressed glomerular endothelial genes using Serial Analysis of Gene Expression (SAGE) and localization of gene transcripts/proteins.

The Health Research Ethics Board (Biomedical Panel) has reviewed the file on this project, for which all documentation is currently up to date. The research has been found to be acceptable within the limitations of human experimentation.

Specific Comments: This is the annual re-approval and is valid for one year. Next year, a few weeks prior to its expiration, a Progress Report will be sent to you for completion. If no major issues are identified, your approval will be renewed for another year.

For studies where investigators must obtain informed consent, signed copies of the consent form must be retained, as should all study related documents, so as to be available to the HREB on request. They should be kept for the duration of the project and for at least seven years following its completion. In the case of clinical trials approved under Division 5 of the Food and Drug Regulations of Health Canada, study records must be retained for 25 years.



S.K.M. Kimber, MD, FRCPC
Chair, Health Research Ethics Board
Biomedical Panel

Issue #6196

